STUDIES ON PEROXIREDOXIN ANTIOXIDANT SYSTEM FROM *CANDIDATUS* LIBERIBACTER ASIATICUS

Ph.D. THESIS

by

ANAMIKA SINGH

DEPARTMENT OF BIOTECHNOLOGY
INDIAN INSTITUTE OF TECHNOLOGY ROORKEE
ROORKEE-247 667 (INDIA)
July, 2015

STUDIES ON PEROXIREDOXIN ANTIOXIDANT SYSTEM FROM *CANDIDATUS* LIBERIBACTER ASIATICUS

A THESIS

Submitted in partial fulfilment of the
Requirements for the award of the degree
of

DOCTOR OF PHILOSOPHY

in

BIOTECHNOLOGY

by

ANAMIKA SINGH

DEPARTMENT OF BIOTECHNOLOGY
INDIAN INSTITUTE OF TECHNOLOGY ROORKEE
ROORKEE-247 667 (INDIA)
July, 2015

INDIAN INSTITUTE OF TECHNOLOGY ROORKEE
ROORKEE

CANDIDATE'S DECLARATION

I hereby certify that the work which is being presented in the thesis entitled, **"STUDIES ON PEROXIREDOXIN ANTIOXIDANT SYSTEM FROM *CANDIDATUS* LIBERIBACTER ASIATICUS"** in partial fulfilment of the requirements for the award of the degree of Doctor of Philosophy and submitted in the Department of Biotechnology of the Indian Institute of Technology Roorkee, Roorkee is an authentic record of my own work carried out during the period from December, 2009 to July, 2015 under the supervision of Dr. Ashwani Kumar Sharma, and Dr. Pravindra Kumar, Associate professor, Department of Biotechnology, Indian Institute of Technology Roorkee, Roorkee.

The matter presented in this thesis has not been submitted by me for the award of any other degree to this or any other institute.

(ANAMIKA SINGH)

This is to certify that the above statement made by the candidate is correct to the best of our knowledge.

Dated: (Ashwani Kumar Shrama) (Supervisor) (Pravindra Kumar) (Supervisor)

The PhD Viva-Voce Examination of **Ms. Anamika Singh**, Research Scholar has been held on…….

Chairman SRC **External Examiner**

This is to certify that the student has made all the corrections in the thesis.

Supervisor **Head of the Department**

ABSTRACT

Structure-function studies endow with influential insight on biological systems

Proteins are requisite to life as we know it. Proteins are polymers constructed from 20 different amino acids. Proteins execute their functions due to their capability to bind to diverse macromolecules distinctively and ability to form different strong interactions with them. They are involved in virtually all cell functions. Along with their many important roles, they provide structure (e.g. collagen), transport (e.g. haemoglobin) and catalytic power (e.g. catalase) for biological systems and are fine-tuned to be highly specific for their function. It is well established that for all proteins, both their structure and dynamics are intimately tied to their function. Thus protein structure and dynamics are fundamental components for building our foundation of biochemistry. Thus the field of structural biology is broad to understand the structure-function relationships of proteins. Two powerful tools to examine structure-function relationships are the harmonizing biophysical techniques of macromolecular X-ray crystallography and nuclear magnetic resonance (NMR). X-ray crystallography provides atomic resolution structures that allow us to see well-defined positions of atoms. These "pictures" show us what a protein's structure looks like. While NMR can be used to solve protein structure, NMR's strength is in its ability to probe enzyme motions (dynamics) and changes in local environment with per-residue resolution. These two techniques, along with many other macromolecular biophysics tools (e.g. fluorescence, circular dichroism, mass spectrometry, isothermal titration calorimetry, surface Plasmon resonance) provide complementary information that helps to create a detailed picture of a protein's structure and dynamics that can be interpreted to understand its function.

Nearly 2.7 billion years ago, the introduction of molecular oxygen (O_2) into our atmosphere, resulted in the reactive oxygen species (ROS) as unwelcome companions in the ecosystem. Although they control many different processes in plants, their toxic nature is also capable of injuring cells. Oxidative stress is an uncompleted battle between highly reactive free radicals and the systems designed to soften their effects. When free radicals are winning this battle, oxidative damage occurs. ROS react with cell biomolecules, leading to organelle dysfunction. Oxidative stress may be seen to start at the molecular level, with a direct interaction between free radicals and a protein, a lipid, carbohydrates, or nucleic acids. Indeed certain diseases results because of failure to respond to these damaging consequences, causing damage both locally or systemically.

Oxidative stress is a foremost problem for whichever organisms that uses oxygen as an electron acceptor. Because, as incomplete reduction of oxygen to water can yield reactive oxygen species (ROS) such as the superoxide anion (O_2^-), hydrogen peroxide (H_2O_2), and the hydroxyl radical ($^{\bullet}HO$) ions. Build up of these highly reactive species can lead to damage to proteins, nucleic acids, and membranes. ROS are also produced by the immune system to kill invading microbes. Therefore, an ability to combat these compounds is a key to the survival of bacterial pathogens in the environment and the host exerted via their antioxidant systems.

In the present work, proteins of antioxidant system were cloned purified and characterized from genomic DNA of *Candidatus* Liberibacter asiaticus (CLA) which includes Bacterioferritin comigratory protein; 1-Cys Prxs and thioredoxin. These proteins revealed multiple functions which may have strong impact in relation to its biotechnology applications. The CLa-BCP characterized from CLA showed DNA-binding, in-vitro antioxidant and peroxidase activities against varied peroxide substrates. The cloning of gene revealed a 471bp bp ORF encoding a polypeptide of 157 amino acid residues which included the N-terminal his-tagged with a calculated molecular mass of 19.670 kDa. The protein was cloned in pET-TEV expression vector. The variant form of CLa-BCP after introduction of non-conserved cysteine at 77^{th} position, CLa-BCP_{S77C} by site directed mutagenesis also purified and characterized. It also exhibited DNA-binding, in-vitro antioxidant and peroxidase activities against varied peroxide substrates. The thesis has been divided into three chapters.

Chapter 1 reviews the literature describing about plant defense against microbes' invasion which summarizes the reactive oxygen species (ROS), reactive nitrogen species (RNS) network and counter antioxidant network prevalent in microorganism to combat the oxidative stress. An array of antioxidant machinery present in microorganism to counteract the deleterious effect of ROS includes non-enzymatic and enzymatic antioxidants. Enzymatic antioxidants include superoxide dismutase, catalase, cytochrome c peroxidases, and alkyl hydroperoxide-reductase (AhpC). BCPs (Bacterioferritin comigartory proteins) are least characterized subfamily of (AhpC) Prx family which is also played an important role in detoxifying hydroperoxides.

Chapter 2 describes the cloning, expression, purification of 1-Cys Prxs CLa-BCP and its biochemical characterization along with the cloning of its reductant partner CLa-TrxA. The cloning and sequence analysis revealed that CLa-BCP is 1-cys Prx protein having single peroxidatic key cysteine residue (CpSH) without resolving cysteine (C_RSH). The purification of CLa-BCP and its variant CLa-BCP_{S77C} was accomplished using two step purification

method employing Ni-NTA affinity and size exclusion chromatography. The purified protein showed a single band in both and non-reducing condition depicting the predominance of monomers of 19.6 kDa. The purified CLa-BCP when applied to size exclusion chromatography column showed a single peak corresponding to dimeric species. Gel filtration describes its concentration dpendent oligomeric nature; possess dimers with predominant monomeric species. An introduction of cysteine residue replacing 77^{th} serine residue in α3 helix (CLa-BCP_{S77C}) results into intermolecular disulfide bonds revealing its dimeric nature. The reductant partner Thioredoxin (CLa-TrxA) was successfully cloned, expressed and purified to its homogeneity. The SDS-PAGE analysis showed that it forms dimer but predominantly monomeric in nature. The purified protein exhibited peroxiredoxin, DNA-binding and *in-vitro* antioxidant activities also. Both showed a strong ROS scavenging activity towards breast cancer (MCF-7) and mouse mesenchymal stem cells (C3H10t1/2) cell lines. The cell viability was estimated by MTT assay towards Adenocarcinoma breast cancer cells (MCF7), Fibroblast-like cell line (COS7) indicated the protective effect of the protein against hydrogen peroxide mediated cell killing. Both CLa-BCP and CLa-BCP_{S77C} showed DNA-binding capability resulting in protection from oxidative nicking of supercoiled DNA.

Chapter 3 describes the biophysical characterization of CLa-BCP and CLa-$BCP_{S77C,}$ preliminary crystallization of CLa-BCP and *in-silico* analysis regarding its versatility in function. Secondary structure analysis by CD showed that both proteins are quite ordered in its reduced form. CD at different temperature showed that CLa-BCP quite steady even at higher temperature like 90°C and maintains its β sheet structure. Intrinsic fluorescence studies at different pH demonstrated the conformational stability of protein. During crystallization, initially CLa-BCP crystals were poor-quality inter grown sea urchin like crystals. Addition of low percentage agarose results into well ordered crystals. While mounting crystals, crystals when kept in low ethylene glycol followed by annealing results into better diffraction. Thus for better diffraction of BCP crystals perquisite were very low percentage of ethylene glycol and annealing. The frozen crystal diffracted X-rays to 2.4 Å resolution using the Cu rotating-anode generator. Analysis of crystal symmetry and recorded diffraction patterns specified that the CLa-BCP crystal belongs to monoclinic space group type C2 having unit-cell parameters a= 92.226, b= 151.9440, c= 139.4940 A °, α= γ=90°, β= 108.7140. The amino acid sequence comparisons and phylogenetic analysis of CLa-BCP showed significant homology to BCPs family proteins (both 1-Cys and 2-Cys) from different pathogenic bacterium but higher similarity with bacterial AhpCs. Model has been built on the basis of amino acid sequence that substantiates its α/β structure predominantly β structure and sites for catalysis.

In summary, our studies confirm that peroxiredoxins; Prxs family proteins are multifaceted proteins which not only involve in detoxification of peroxides but potent scavenger of ROS precluding DNA from oxidative damage. Many proteins of this family have been shown to possess more than one function which includes redox regulation, antioxidant defence and signalling of different organisms. The proposed work will certainly enhance our understanding in terms of specificity and mechanism of action of these antioxidant enzymes from CLA and will lead to the development of effective inhibitor molecules to control citrus greening as well as contribute towards understanding the significance of free radical scavenging therapy for several diseases.

ACKNOWLEDGEMENTS

Before writing my final acknowledgement I would like to share my thoughts. After finishing my thesis writing I was about to write my feelings, memories which I have shared here and outside this environment. Because I know, no one is going to read your "whole" thesis besides your mentor, examiner and of course yourself. Your dear ones always look forward to see your acknowledgement and look for their names only☺. So I thought I should mention each and every person who played a very important role in my life not only professionally but more importantly emotionally. Because these are your emotions which always make you do something extraordinary not for yourself but for them who believe in you more than yourself.

Before acknowledging anyone in this thesis I dedicated it to my "MAA" and to her dreams. She was the one who always dreamt of seeing me to become "Dr." more precisely would say that this "Dr." Prefix before my name. Now, when her dreams are really coming true she is not with me to enjoy this precious moment. But I am sure she is seeing me and partying for sure above with our almighty god☺. A special thanks to my family. Words are not enough to express how grateful I am to my bhaiya, bhabhi and especially my sisters for all of the sacrifices that they've made on my behalf. Big thanks to my bhaiya who never questioned me for anything he gave as much time I wanted. He never complained, trusted me all through my journey and always said "do whatever you want to do" in your life. I think it's because of his attitude only that I am able to do what I did. As I belong to a very large family with five sisters, Badi di, Neelam di, Shalini di, Juhi di and Parul di. I want to acknowledge each of them. Because each of them had played a major role in my life in every respect they can be. Whenever I felt bad, depressed, low in energy or running out of money it's my sisters who always presented me everything as a gift, I still have someone to turn to and not all alone. Their spiritual support is also indispensable to sustain me to complete this thesis. Without their support, strength and trust in me I would not be able to accomplish what I achieved today. It's all their efforts and guidance that proves out be blessing for me. I owe everything to them including all my nieces and nephews who constantly giving me proud moments that I am doing exceptionally great without knowing a single thing about my work.

My Ph.D. started with very ups and down, but there is one person after my mom who was always beside me and pushed me forward. She is the one who critics me, encourages me, helped me in every possible way she can do. She is my strength, my Best Friend, my life support and most importantly my frustration bearer "Jassi". Without you my thesis would not

be possible. This thesis is the result of Jassi's efforts and my family support that were always there when I really needed.

At this moment of accomplishment, I would like to give special thanks to my guide, supervisor Dr. Ashwani Kumar Sharma for his erudite guidance, encouraging attitude and cool behavior. I thank him for his patience, kind nature, for many fruitful discussions and also for rectifying my mistakes many times. Not only this he is the one who allowed me to do my work on my own pace without pressurising much. And to my co-guide Dr. Pravindra Kumar, I particular thank him for considering me being a part of his research group. A big thanks for all his valuable advice even though not knowing much about my work, but helping me out trying very hard for me to get some good crystals. For all his constructive criticism and his belief that I can do better still even if nothing is going out to work.

I owe a great deal of appreciation and gratitude to Dr. Partha Roy for providing me to use cell culture facility. I want to acknowledge Dr. Kiran Ambatipudi for his understanding, encouragement and personal attention for my "MS experiments" and a very healthy discussion throughout. My thanks are due to Narender Kumar and Dr. Swati Srivasatava for their valuable suggestions and untried help during cell line work. I am much indebted to both of them for their valuable advice and precious times to read my work.

I feel overwhelmed in thanking to Prof. Partha Roy (Present) and Prof. R. Prasad (Former) Head, Department of Biotechnology for providing necessary facilities, support and cooperation in the Department. I would also like to acknowledge Dr. Ramesh Chandra Head, Institute Instrumentation Centre and Dr. Pravindra Kumar for providing Macromolecular Crystallographic Unit facilities. I gratefully acknowledge the help rendered from time to time by the members of my Student Research Committee (SRC) Prof. R.P. Singh, Prof. R Prasad (Internal member) and Dr. M.R. Maurya (External member) for their helpful suggestions and comments during my progress report presentations and scholarly suggestions, prudent admonitions and immense interest that have made this task a success. I am courteous to the honourable faculty members, Prof. G.S. Randhawa, Dr. Shailly Tomar, Dr. Ranjana Pathania, Dr. Vikas Pruthi, Dr. Naveen Navani, Dr. Bijan Choudhury, Dr. Sanjoy Ghosh, Dr. Maya Nair for their support and encouragement.

My thanks go in particular to Dr. P.Selva Kumar with whom I started this work and his help. I want to give my warm appreciation and big thanks to Dr. Prabhat PS Tomar. He was the one here in IITR who always there beside me during the happy and hard moments to push me and motivate me. He always helped me even though I was not working with him. I owe

gratitude to, Dr. Girijesh Patel, Dr. Deepankar Galoth who willingly devoted so much time in giving guidance to me.

My warm appreciation is due to all the Ph.D. students of my lab, Dr. Saurabh, Dr. Navneet, Mr. Bibekananda, Ms. Nidhi, Ms. Preeti Verma, Mr. Pranav, Mr. Vishvajeet, Mr. Rahul, Mr. Ashish, Mr. Hrishikesh, Mr.Akhilesh, Mr. Amit, Mr.Virendra, Mr. Ravi and Mr. Vivek for their sincere efforts, amiable attitude and cooperation while working in lab. I am very much indebted to my juniors for providing a stimulating and fun-filled environment especially Rajat, Raman, Gunjan, Vishvajeet and Pooja. A special thanks to Pooja for giving her time from tight schedule and all her efforts in correcting my thesis and respect to all of them for their, encouragement, support, and understanding. I warm thanks to Mr.Umesh for editing my final draft. Friends are always most valuable asset anyone can treasure and this list is incomplete without acknowledging, Sonali who was the source of inspiration for me who taught me many things. She always pushes me to do my things on time. My special appreciation goes to all my friends Rajbala, Varinder, Shailza, Pooja, Soumita, Sapna, Niyati who made my stay in IITR, a memorable one for their constant love, care and moral support, friendship and encouragement. Because beside your Ph.D., you have another world and friends played very important part in life in their own way like outing, late night fun, shopping, keeping lunch and dinner when you are not able to make it in time. I want give my love to my sweetest friend Pallavi who came very late precisely in my last phase of Ph.D. but she turns out be my lovable friend. She is the one whose priority was that I had my breakfast, lunch, dinner in time and be healthy so that I can complete in time. I never felt home sick only because of their loving and caring attitude. Outside this campus there are lot people who do so much for me in every aspect say research and no research. My school and Grad and Post Grad friends who always made me realise that I am doing great, thanks to you all Shreya Di, Devesh, Ani, Harsh, Arshpreet, Ayan ,Prachi, Pratip, Saurabh, Ajit, Chetu, Ankur, Anubhav, Hari, Sakshi, Dilip and Nishu.

Also to be acknowledged with love and appreciation in the memorable concern, affection and care from my seniors and juniors Dr. Rajini Salunke, Dr. Nidhi Pareek, Dr. Preeti, Dr. Satya Tapas, Dr. Pradeep, Dr. Megha, Dr. Shilpi, Mr. Madhu, Ms. Aanchal, Ms. Neha, Mr. Harvijay, Mr. Rajesh, Ms. Benazir, Ms. Anjali, Mr. Shailendra Singh Khichi, Mr. Tamogan, Mr. Atin, Mr. Snehashish and many others. I would like to mention all the technical and office staff of the Biotechnology Department in particular Mr. Ved Pal Singh Saini our "Saini sir" for all instrument technical error things and small small things happening day to day basis. We always look forward for "Saini sir" without his help things would not be that much

smooth. Besides him Mr. Subhash Jain, Mrs. Shashi Prabha, Mr. Lokesh, Mr.Yogendar Valthare, Mr.Rajesh Pal and "Anil ji". I would like to special thank to Mr.Ajit and Mr.Vikas for supplying me chemical requirements on time.

Lastly, I will be delighted to say a big thanks to my parents, for giving birth to me at the first place. I pleased to thank my brother and my sisters for their never ending encouragement throughout my PhD tenure and lifting up my spirits whenever I felt low. I take this opportunity to sincerely acknowledge the Department of Biotechnology (DBT), Government of India, Pune, for providing financial assistance in the form of Senior Research Fellowship making me to work calmly.

Finally, I thanks to God for my life through all tests in the past years.

(*Anamika Singh*)

LIST OF PUBLICATIONS

- **Anamika Singh,** Purushotham Selvakumar, Akhilesh Saraswat, Prabhat PS Tomar, Manisha Mishra, Pradhyumna K Singh, Ashwani Kumar Sharma. Characterization and cloning of an 11S globulin with hemagglutination activity from *Murraya paniculata*. ***Protein and Peptide Letters*** (2015) 22, 750-761

- Prabhat Pratap Singh Tomar, Kumar Nikhil, **Anamika Singh**, Purushotham Selvakumar, Partha Roy, Ashwani Kumar Sharma. Characterization of anticancer, DNase and antifungal activity of pumpkin 2S albumin. ***Biochemical and biophysical research communications*** (2014) 448: 349-354

- **Anamika Singh**, Narendra Kumar, Prabhat PS Tomar, Sumit Bhose, Dilip Ghosh, Partha Roy, Ashwani K. Sharma. Characterization of a DNA binding 1-Cys peroxiredoxin from *Candidatus* Liberibacter asiaticus (CLA). ***(In communication)***

- **Anamika Singh**, Pravindra Kumar and Ashwani K. Sharma. Crystallization and initial X-ray diffraction data of Bacterioferritin Comigratory Protein, 1 Cys Peroxiredoxin 2.4Å from *Candidatus* Liberibacter asiaticus (CLA): addition of agarose improved the quality of the crystals. ***(In preparation)***

WORKSHOPS/CONFERENCE ATTENDED AND POSTER PRESENTATION

- Presented a poster at **International Conference on Biomolecular Forms and Functions "A celebration of 50 years of the Ramachandran Map"** held at Indian Institute of Sciences, Bangalore, India from 8-11 January, 2013.

- Delivered an oral talk on Characterization and cloning of an 11S globulin with hemagglutination activity from *Murraya paniculata* at '**42nd National Seminar on Crystallography and International workshop on application of X- ray diffraction for drug discovery**' at New Delhi.

- Attended International workshop on Application of X-ray diffraction for drug discovery held at Jawahar Lal University, New Delhi, India from 21-23 November, 2013.

- Presented a poster entitled "Structural and biochemical study of peroxiredoxin from *Candidatus* Liberibacter Asiaticus" at '**INDO-US international conference/ workshop on recent advances in structural biology & drug discovery'** held in IIT Roorkee, Roorkee from October 9-11, 2014.

GENES SUBMITTED TO NCBI DATABASE

MPG (11Sglobulin) gene submitted from Murraya *paniculata* having accession no. KJ508183

LIST OF ABBREVIATIONS USED

˚C	Degree Centigrade
Å	Angstrom
BCP	Bacterioferritin Comigratory Protein
βME	Betamercaptoethanol
bp	Base pair
CD	Circular Dichroism
CLas	Candidatus Liberibacter asiaticus
COS7	Fibroblast-like cell line
C3H10T1/2	Mouse mesenchymal stem cells
CO_2	Carbon dioxide
Da	Daltons
DCF-DA	2', 7' dichloro dihydrofluorescein diacetate
Dimedone	5, 5-dimethyl-1, 3 cyclohexanedione
DMEM	Dulbecco's Modified Eagle's medium
DMSO	Dimethyl Sulfoxide
DNA	Deoxyribose nucleic acid
dNTPs	Deoxy nucleotide tri phosphates
DTNB	5,5'-dithiobis(2-nitrobenzoate)
DTPA	Diethylenetriamine pentaacetic acid
DTT	1, 4-dithio-D-threitol
E. coli	Escherichia coli
EDTA	Ethylenediaminetetracetic acid
e.g	For example
et.al	et alia
eq	Equivalence
Fe $(NH_4)(SO_4)_2$	Ferrous ammonium sulphate
$FeCl_3$	Iron chloride
g	Gram
h	Hours
HCl	Hydrocholride
Hepes	2-[4-(2-hydroxyethyl) piperazin-1-yl] ethanesulfonic acid
HLB	Huanlongbing
HMW	High Molecular Weight
H_2O_2	Hydrogen Peroxide
H_2SO_4	Sulphuric acid
IPTG	Isopropyl β-D-thiogalactoside
ITC	Isothermal Titration Calorimatory
K	Kelvin
kDa	Kilo Daltons

LB	Luria Bertani
LMW	Low Molecular Weight
M	Molar
MCF-7	Adenocarcinoma breast cancer cells
mg	milligram
min	Minute
ml	Millilitre
mM	Millimolar
MTT	3-(4,5-dimethylthiazol-2-yl)-2,5-diphenyltetrazolium bromide
NaCl	Sodium Chloride
NaOH	Sodium hydroxide
NCBI	National Center for Biotechnology Information
Nde	Neisseria denitrificans
Ni-NTA	Nickel-nitrilotriacetic acid
NBD-Cl	7-chloro-4-nitrobenzo-2-oxa-1, 3-diazole
nm	Nanometer
NMR	Nuclear magnetic resonance
NRCC	National Research Centre for Citrus
PCR	Polymerase chain reaction
PDB	Protein Data Bank
Pvt Ltd	Private Limited
rDNA	Ribosomal deoxyribose nucleic acid
RNA	Ribose nucleic acid
ROS	Reactive Oxygen Species
rpm	Revolutions per minute
s	Seconds
SDS-PAGE	Sodium dodecyl sulfate polyacrylamide gel electrophoresis
TEV	Tobacco etch virus
TNB	2-nitro-5-thiobenzoate
TrxA	Thioredoxin
t-H_20_2	Tertiary butyl hydrogen peroxide
USA	United States of America
UV	Ultra-violet
Xho	Xanthomonas holcicola
α	Alpha
β	Beta
Ɛ	Molar extinction coefficient
γ	Gamma
µg	Microgram
µl	Microlitre
µM	Micromolar

Table of Contents

INTRODUCTION

Plants are exposed to an array of biotic and abiotic influences under natural environment. These external factors can lead to the imbalance of critically important cellular metabolic activities and therefore can eventually affect plant growth, their development, and reproduction as well. The fundamental mechanisms of these effects are predominantly based on disturbances in the redox and osmotic state. The redox effect often results from an enhancement of electron transfer thereby to the generation of reactive oxygen species (ROS) [325]. Plant cells are chiefly prone to these systems-especially due to their photosynthetic capacity, their aerobic existence.

In case of plant system, metabolism under optimal conditions leads to the formation of ROS, as electron seepage from electron transport chains within the different organelles and in membranes [12] (for review see Apel and Hirt, 2004). Plants live in constantly changing environment triggered by altered biotic and abiotic conditions can boost ROS generation which creates an additional oxidative threat [255]. ROS play a dual role in cell metabolism since they facilitate oxidative damage and are important in signal transduction processes. Therefore a tight control of these reactive species in every cellular compartment is of utmost importance [77]. The metabolic performances in a plant cell are flawlessly regulated to follow biosynthetic pathways. Besides the tightly regulated mechanism in plant cell, even if the plant growth continues to deteriorates than what could be the reason behind it? In our case of study, it surveyed that citrus plants defoliation or drastic decrement in growth because of unculturable pathogen *Candidatus* Liberibacter asiaticus (CLA) infection. So we focussed on that protein machinery which plays role in anti ROS mechanisms, which might makes this pathogen to combat the ROS generation, a first line of defense mechanism of plants.

Citrus Huanglongbing (HLB) or citrus greening worldwide including India is the most vicious citrus pathosystem which causes huge economic losses to the citrus industry [35, 36]. *Candidatus* Liberibacter asiaticus (CLA), an unculturable gram negative phloem-limited bacterium is the associated causal agent of the disease which is transmitted by the Asian citrus psyllid, *Diaphorina citri* [169]. CLA mostly infects the rutaceae family plants includes *Murraya Koenigi*, *Murraya paniculata* but other non- rutaceae family members as well. Because of its unculturable attributes results into difficulty in characterization experimentally. Even though through computational analysis of the CLA proteome provided a basis for establishing the mechanism and designing treatment strategies towards its control. There have

been reports for designing effective anti-microbial through proteome research through computational analysis [1, 110, 347]. Thus effective strategies to control CLA could include the development of inhibitor molecules/antimicrobials against the CLA proteins critical in bacterial survival through proteome and *in-silico* analysis. Earlier in our lab we have purified and characterized a miraculin like protein (MLP) from *M. Koenigi* which has been shown to express constitutively in seeds has been characterized [109, 329, 330, 337, 338]. MLPs have been reported to possess protease inhibitory and antifungal properties [338, 373]. It has been reported that MLPs get over expressed during CLA infection [95]. We have purified a globulin protein from *Murraya paniculata* [342] one of the host for CLA. An important component of the evolved complex antioxidant system of CLA, Bacterioferritin comigratory protein (BCP), a Prx protein being in focus of the present work which could be an important target for developing antimicrobial by obstructing the antioxidant system of bacterium. There can be many proteins/protein systems critical for survival of organisms which can be targeted for development of inhibitors/antimicrobials. The experiments conducted and data presented in this thesis provide an analysis of peroxidase mechanisms, biochemical properties of protein deciphering its DNA binding properties and antioxidant activity in-vitro in order to better understand the physiological role of CLa-BCP *in-vitro*. The biophysical aspect of CLa-BCP and CLa-BCP_{S77C} in order to understand the conformational changes that protein undergoes. The crystallization of CLa-BCP in the presence of agarose improves the crystal quality. Gene analysis shed light on binding of substrate and reductant partner and over all conformation primarily present in CLa-BCP. In summary derived from these data, focusing on the overall role of CLa-BCP in CLA oxidative stress defense and how it compares to other peroxiredoxins in its subfamily.

LITERATURE REVIEW

1.1 CITRUS GREENING DISEASE

Citrus greening is one of the most destructive diseases of citrus, debilitating the productive capacity of citrus trees all over the world. In China, it is called huanglongbing (HLB) or the yellow dragon disease because of the blotchy yellow leaf mottle that it causes. Leaves of infected plants also become hardened and curl outward. After infection the fruit retains its green color at the navel end when mature, therefore termed as "citrus greening disease". HLB caused by a phloem-limited fastidious prokaryotic gram negative α-proteobacterium *Candidatus* Liberibacter asiaticus that is yet to be cultured. Citrus Huanglongbing (HLB) or citrus greening, associated with '*Candidatus* Liberibacter spp., based on its 16S rRNA gene sequence [169]. The genus "*Candidatus*" is for "non-culturable" bacteria proposed by Murray and Schleifer [267]. Afterwards the trivial name "Liberobacter" means ("liber" for bark and bacter for bacterium), given to this new subgroup of α proteobacterium organisms. This disease is transmitted by *Diaphorina citri* kuwayama as a carrier (Hemiptera: Psyllidae). *Diaphorina citri* acquires the greening bacterium while feeding on infected phloem [159].

Host Range

As bacterium resides onto phloem cells of the plant and transmitted by vector psyllidae who is also flourished in plants. Thus two types of plants are of significance in referring to probable hosts for HLB. First class of plant that nurtures the psyllid vectors and second class includes plant in which the bacterial pathogen can replicate. HLB has a broad host range along with the diverse species of citrus. It is largely destructive to sweet orange (*Citrus sinensis*) and Mandarin orange (*C. reticulata*), but it furthermore damages sour orange (*C. aurantium*), pommelo (*C. maxima*), lemon (*C. limon*) and grapefruit (*C. X paradisi*) [36, 128, 205, 236, 372]. HLB ultimately is fatal to susceptible citrus trees, so early detection and removal of infected trees is important for disease management. Unluckily, citrus trees often showed no symptoms for years before the common signs of HLB, including yellowing and mottling of leaf veins and misshapen green-colored fruit, are noticeable [124]. The most preferred hosts of psyllidae *D. citri* are *Murraya paniculata* (Orange jasmine and mock orange) [21] and *Citrus aurantifolia* [128] even though it possibly will be able to feed on numerous citrus species and closely related species. *M. paniculata* is most preferable host of psyllids as confirmed by field observation and laboratory studies but yet not clear that whether it will serve as substitute host for Liberibacters [160, 386, 409]. From various studies, it has been showed that plants of non-Rutaceae family could also be host for *Ca.* L. spp. , and showed

that transmission of all species to periwinkle plants is possible by dodder (Cuscutaceae family) [112]. Another example [94] such as yellow shoots on *Pithecellobium lucidum,* a non-member of Rutaceae family reported the presence of HLB symptoms.

Figure 1.1 adopted from book entitled "Asian Citrus"

Prevalence of HLB disease Worldwide and in INDIA

The disease is widespread in most areas of citrus-growing Asian countries, Africa, Brazil and Florida. HLB was foremost observed in China [412]. This disease is widely spread in Africa due to '*Candidatus* Liberibacter africanus*'* infection vectored through African citrus psyllid *Trioza erytreae*. In March 2004, symptoms of citrus HLB, were recognized on sweet orange trees near the city of Araraquara in Sa˜o Paulo State (SPS), Brazil [66, 85]. HLB caused by the gram-negative bacterium *Candidatus* Liberibacter asiaticus (*Ca.* L. asiaticus) [113] was confirmed in southern Florida in 2005 [34, 127]. Along with Liberibacter sp. affecting citrus industry worldwide, a new Liberibacter species was discovered. It was named as '*Candidatus* Liberibacter solanacearum', associated with the emerging 'zebra chip' disease of potatoes in the U.S. and tomatoes in New Zealand [230]. Though strongly related to '*Ca.* L. asiaticus',

even though '*Ca.* L. solanacearum' it was associated with HLB disease and not found in Asian citrus psyllids as well [228]. Worldwide, HLB is spread throughout in China, eastern and southern Africa, the Indian subcontinent, Madagascar, Mauritius, Reunion, the Saudi Arabian peninsula and Southeast Asia.

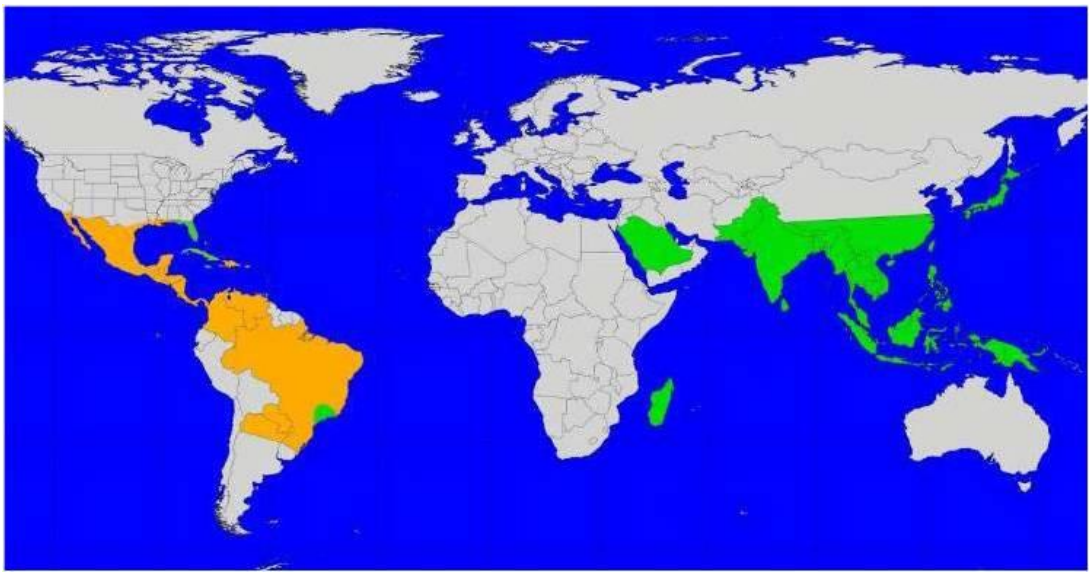

Figure 1.2 showing the prevalnace of HL disease world wide

Both the psyllid and HLB disease

Asian citrus psyllid, but not the disease Figure Illustration by G.H.Montez

Among Asian countries India occupies 6th rank in the fabrication of citrus fruits thus citrus industry turns out to be the 3rd chief fruit industry in India. As a result citrus engross a central place in the horticultural wealth and to Indian economy as well. The inhabitant place of major citrus species is the North East region of India. In India, orange (santra or mandarin), sweet orange (mosambi, or satgudi) and lime/lemon are of industrial magnitude among the range of citrus fruits grown. The most cultivable location for citrus fruits prevalent in India, are mainly Maharashtra, Andhra Pradesh, Punjab, Karnataka, Uttaranchal, Bihar, Orissa, Assam and Gujarat. Before knowing about HLB disease, in the 18th Century the citrus disease was discovered termed as "citrus dieback" by Roghoji Bhonsale. Later detected by Bonavia in 1988 in Assam [63]. In 1963, Capoor stated that citrus plants were acutely suffered from assured disorders ensuing in "low production, slow death, twig dieback, and sudden wilting" [45] along with observation of Asana (1958). Both stated that, "dieback in citrus is not a specific disease" [19] and "dieback was merely a symptom picture", and numerous issues were suggested to describe this dieback [45]. The major cause was *Citrus Tristeza Virus* (CTV) as undoubtedly proved by the Virus Research Center at Poona [45, 380]. While in the

Coorg region, north of Mysore, where the most pronounced symptom of the disease is the characteristic mottling of leaves according to Asana (1958) they have speculated that HLB might have been involved which was later confirmed in mottled Coorg mandarin leaves by positive dot blot hybridisation [379]. The same feature was observed for "greening" in South Africa (1965), and for "Huanglongbing" [156] in China and indicated that dieback was "caused by the virus responsible for greening disease of citrus in South Africa" [156, 247, 248]. In due course, Capoor and co-workers verified the presence of HLB following in Asian psylla, *D. citri* responsible for transmitting the HLB pathogen at the virus Research Center at Poona [46]. At last, Bové and co-workers, in 1971, the HLB bacterium was detected in a sweet orange seedling, when was infected with *D. citri* nymphs experimentally with the "Poona" strain of HLB [37, 221].

Distribution of CLA in an infected plant

With the help of two techniques the distribution and movement of the HLB pathogen in the infected citrus tree has been done which includes conventional polymerase chain reaction (PCR) and real-time PCR targeting the putative DNA polymerase and 16S rDNA sequence of '*Ca.* Liberibacter asiaticus respectively. From this approach it was seen that CLA was distributed mainly in bark tissue, leaf midrib, roots and different floral and fruit parts, leaving the endosperm and embryo of infected citrus trees. The disease causes extensive economic losses to the citrus industry throughout the world by shortening the life span of infected trees. Along with trees, fruit from HLB-infected trees are "small, lopsided, poorly colored, and contain aborted seeds". The juice from affected fruit is also having high level of acids with pungent smell due to which fruits became of no commercial value. Although cultivation of this bacterium on complex media have been reported [328], the fact still remains that CLA are at present largely unculturable in the majority of laboratories worldwide. Current chemical and biological controls reduce *D. Citri* populations [155, 252, 307, 317], but may not be sufficient to eliminate all HLB transmission. Current strategies and followed methods still lagging behind in stopping the HLB spread and its control.

At present no control strategies developed to control HLB obstructing it to spread to new citrus-fabrication areas. The most probable reason behind is late appearance of symptoms after its infection. Thus the direct strategy is to avoid trees from becoming infected by removing the infected tree and diminishing the psyllid population. A blend of penicillin and streptomycin is being researched to be effective in eliminating or restraining the CLAs bacterium providing an effective therapeutic control [410]. Along with that a range of

antibiotics like Ampicillin, Carbenicillin, Penicillin, Cefalexin, Rifampicin and Sulfadimethoxine are found to be highly effective in eradicating or to hold back of CLAs infection and might be prospective candidates for controlling citrus HLB [409]. "CaliforniaCitrusThreat.Org" has well documented the affected region and their effective measures towards eradication of HLB disease. It was found that for pysllid infection one of the protective measures to be taken includes application of foliar and systemic insecticides. But yet again these treatments will negatively affect the many of the natural enemies which are much needed for other pest control. As a result of which bioremediation is becomes of utmost importance which uses naturally occurring organisms utilize to break down hazardous substances into less toxic or non toxic substances. There are many research groups focussing on bioremediation to some extent relieve the deleterious effect of these chemicals treatments by mending microorganism's pathways [26, 27, 256]. Some reports have mentioned the effect of these treatments on antioxidant system of microorganisms and their adaptability towards these treatments. Because of which controlling the bacterium infection will become more challenging. Thus may be some other approaches that can be holding true for controlling HLB. It involves targeting essential proteins for survival by designing the potential inhibitor leads against these proteins to weaken the protein function. There are quite a lot of vital proteins from many pathogenic bacteria are potential targets for developing anti-bacterial drugs [165, 214, 215]. Beside that there are several reports from other pathogenic bacteria which are come up with plausible solution to combat disease [216, 217, 269].

Distribution of genes in CLA genome

Genome of CLA has been sequenced successfully in 2009 [86], verified and computational analyses of the whole proteome has been done to a large extent shed light onto the mechanisms of the disease which could lead to the development of treatment strategies. The major metabolic pathways and enzyme reactions envisaged from the CLA genome sequence were mapped onto established metabolic pathways thus summarized here in table:

Functional class and categories		'Candidatus Liberibacter asiaticus' genome				
		No. of genes	% of total	Correlation[a]	% in *Wolbachia* AE017321	% in α-proteobacteria[b]
Information storage and processing						
J	Translation, ribosomal structure & biogenesis	123	10.83	–	13.91	4.31
K	Transcription	29	2.55	+	2.07	5.69
L	DNA replication, recombination, repair	75	6.60	–	6.21	4.36
Cellular processes						
D	Cell division and chromosome partitioning	13	1.14	–	1.03	0.71
V	Defense mechanisms	5	0.44	No	0.23	0.97
O	Postranslational modification	47	4.14	No	5.86	3.24
M	Cell envelope biogenesis, outer membrane	57	5.02	No	3.79	4.34
P	Inorganic ion transport and metabolism	25	2.20	No	4.02	4.79
U	Intracellular trafficking and secretion	7	0.62	No	3.33	1.78
N	Cell motility	51	4.49	+	0.11	1.18
T	Signal transduction	18	1.59	+	1.15	3.70
Metabolism						
F	Nucleotide transport and metabolism	44	3.87	–	4.25	1.61
G	Carbohydrate transport and metabolism	23	2.02	No	2.76	4.90
E	Amino acid transport and metabolism	48	4.23	No	4.37	8.18
H	Coenzyme metabolism	53	4.67	No	3.79	2.97
I	Lipid metabolism	33	2.90	No	2.99	3.54
C	Energy production and conversion	62	5.46	+	7.82	5.15
Q	Secondary metabolite transport and metabolism	8	0.71	+	1.26	2.80
Poorly characterized						
R	General function prediction only	69	6.07	No	7.24	10.62
S	Function unknown	46	4.05	No	3.56	6.06
	Not in COG	300	26.4		20.23	19.03
		1,136	100.00		100.00	100.00

[a] The expected positive (+), negative (–), or no correlation (No) of genome size with the number of genes in each COG assignment category (Konstantinidis and Tiedje 2004).

[b] Representative small (940 genes encoded by 1.08 Mb) α-Proteobacteria genome.

Figure 1.3 Summary of COG (Clusters of Orthologous Groups) database assignments by functional category. Genes responsible in defence mechanism, involved in detoxification of by product of aerobic respiration highlighted in rectangular box.

This has enabled researchers to study CLA proteins *in-vitro* via a heterologous expression of the recombinant proteins. From such experiments, the function of a hypothetical ADP/ ATP translocase has been verified [375] and a moderate inhibitor of the predicted secA gene product has been identified [3, 4]. Besides this 137 'CLA' proteins classified as transporter proteins. Briefly, 'CLA' contains all 14 genes that typically encode NADH dehydrogenase subunits [A-N], a major component of the respiratory electron transport chain. The 'CLA' genome does not have homologs for the cytochrome bc1 complex (EC 1.10.2.2), cytochrome c oxidase, the cbb3-type (EC 1.9.3.1), or the cytochrome bd complex even though all 4 cytochrome O ubiquinol oxidase subunits [I to IV] have been identified. This is interesting because α-Proteobacteria (the class containing 'CLA') typically employ cytochrome c oxidases as terminal oxidases, whereas γ-Proteobacteria (the class containing *E. coli* and *Xylella fastidiosa*) employ quinol oxidases [103]. In contrast to *E. coli*, which has two terminal oxidases [10], the respiratory complex of 'CLA' resembles that of the citrus

pathogen *Xylella fastidiosa* [30], with one active terminal oxidase. Through microarray analysis it was suggested that there was no notable expression of defense-related genes in the early stages after CLAs infection in citrus [5, 192]. Besides that CLAs could inhibit the host defense. It was validated by reporting a gene encoding a salicylate hydroxylase constitutively expressed in planta in comparison to psyllid. It converts salicylic acid (SA) into catechol [377] in CLAs infection responsible for resistance suppression. Thus a role impart by SA is in plant defenses against pathogens for basal defense and acquired systemic resistance [350]. While because of highly expressed Salicylate hydroxylase in plants, destroys plant defenses by degrading SA [378] which could be used by CLAs as one of the strategy against plant defense responses [368, 369] which ultimately leads to the down-regulation of defense-related genes in CLAs infected citrus [5, 192]. As there are other plant defenses do exist in plants like production of reactive oxygen species (ROS/RNS) produced as by products of their respiratory mechanism. Some reports have reported the control of plant defense mechanism and regulation of pathogenesis caused by microorganisms [72, 181, 201]. The CLA genome shown to have genes involved in detoxification of respiratory by products induced by these plants defence mechanism. It includes putative oxidoreductase, quinone oxidoreductase, oxidoreductase, DSBA, putative FAD-dependent oxidoreductase, super oxide dismutase (SOD) and BCP/PRXQ having gene identifiers (CLIBASIA_00285, CLIBASIA_00875, CLIBASIA_01110, CLIBASIA_01810, CLIBASIA_03240, CLIBASIA_01910 and CLIBASIA_00485) (Fig. 1.4).

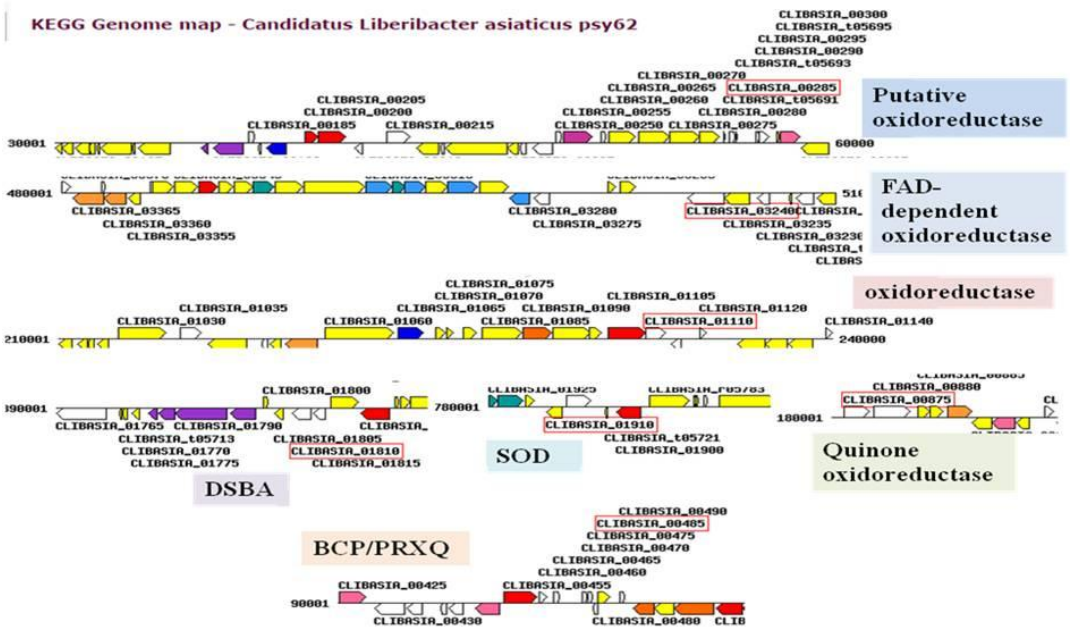

Figure 1.4 Graphical representations of genes involved in detoxification of respiratory burst and their genome location.

1.2 REACTIVE OXYGEN SPECIES (ROS) AND REACTIVE NITROGEN SPECIES (RNS) – THEIR MECHANISM AND SITES OF GENERATION

All aerobic organisms are uncovered to the risk of partially reduced oxygen species which is mostly described as Reactive Oxygen Species (ROS). ROS are highly reactive and participate in free radical reactions that cause damage to DNA, proteins and lipids (reviewed in Finkel and Holbrook 2000) [98]. The most dreadful damage caused by ROS for biological orchestra makes them to be a foundation of the free radical theory of aging. As proposed by Denham Harman in the 1950s, this theory states that organisms age because cells accumulate free radical damage over time [136, 265]. The build up of oxidative damages is held to be responsible for many general age-related conditions including cancer, diabetes, arthritis, degenerative diseases such as Parkinson's, Alzheimer's disease and atherosclerosis [341].

Reactive Oxygen Species (ROS)

Oxygen in the atmosphere and water is required for sustaining aerobic life on Earth. However, aerobic organism must cope with adverse effects of oxygen. ROS are a consequence of oxygen metabolism. Most ROS are generated as by-products during mitochondrial electron transport and are formed as necessary intermediates of metal catalyzed oxidation reactions. The sequential reduction of oxygen through the addition of electrons leads to the formation of a number of ROS including: superoxide; hydrogen peroxide; hydroxyl radical; hydroxyl ion; and nitric oxide.

ROS generation from molecular oxygen occurs via two distinct mechanisms. On the one hand physical activation can take place by the transfer of energy. This is mediated by photosensitizers like e.g. chlorophyll, which are able to harvest light energy and subsequently energise O_2 to the considerably more reactive form singlet oxygen ($^1O_2$) [364]. On the other hand, chemical activation occurs via the transfer of electrons to dioxygen, leading in dependence on the number of transferred electrons to the successive generation of superoxide anion radical ($O_2^{\cdot-}$), hydrogen peroxide (H_2O_2), and hydroxyl radical (•OH) [82]. The hydroxyl radical can be generated in the presence of catalytic redox active metal ions by an interaction of O_2 with H_2O_2 or stochiometric metal oxidation [210].

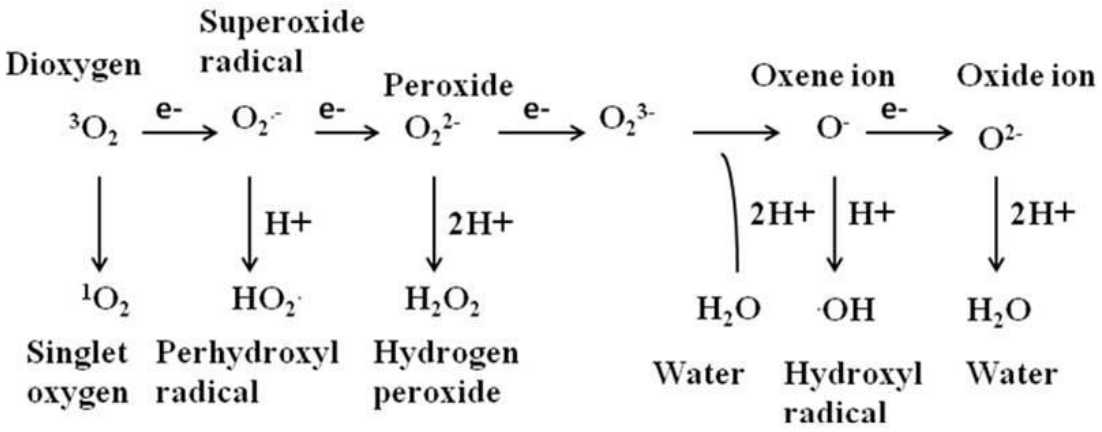

Figure 1.5 Generation of different types of reactive oxygen species from ground state dioxygen.

The partially reduced oxygen derivatives exhibit a advanced reactivity towards various cellular composites than molecular oxygen itself thereby causing oxidative damage when generated in excess [18].

Superoxide is the first reduction product of ground state oxygen and could be subjected to both oxidation and reduction reactions. It is able to react with some molecules to produce other reactive species or may be dismutated to H_2O_2 spontaneously or enzymatically [17]. Chemical and physiochemical studies suggest that superoxide anion radical are relatively inert for a molecule with an unpaired electron, because its chief reaction is its own dismutation. The generation of hydroxyl radical (•OH) in the presence of H_2O_2 through metal-catalysed generation is the most deleterious effects of the superoxide anion radical [104].

Hydrogen peroxide is the product of superoxide (O_2•-) dismutation reaction, could not be considered as a free radical though can acts as oxidant or reductant in many reactions. Its toxicity is mostly exerted via oxidation of thiol groups. H_2O_2 is very diffusible as compared to superoxide ions and it can directly inactivate susceptible enzymes with their lower concentration. Because of these properties, it has been considered as a common signalling molecule regulating many biological developments and triggering plants responses to a variety of environmental stresses. Nevertheless, at higher concentrations, i.e. 10µM and higher, H_2O_2 is capable of can oxidizing the cysteine and methionine residues of the enzymes such as Cu/Zn-SOD and Fe-SOD and can inactivate them [335]. The main risk enforced by both O_2•- , H_2O_2 is their ability to generate highly reactive hydroxyl radicals [257].

Hydroxyl radical (•OH) is the most reactive molecule among the different reactive oxygen intermediates. It in a highly indiscriminate way attacks the first available substrate at its site

of generation and therefore has the potential to inflict extensive damage [325]. Hydrogen peroxide and O_2•- can produce •OH, a highly damaging ROS. The oxidizing potential of hydrogen peroxide with ferrous salts is the foundation of Fenton reaction responsible for generation of •OH as the oxidizing species.

$Fe^{2+} + H_2O_2 \longrightarrow Fe^{3+} + OH^- + \bullet OH$ (Fenton reaction)

The hydroxyl radical is the most effective ROS species in the cells for oxidation of various molecules. It is remarkably destructive, acts as near diffusion limit rates and capable of damaging known biological molecules including protein, DNA/RNA, carbohydrates and lipids. There is no enzymatic mechanism to scavenge •OH, accordingly, its excessive generation usually leads to cell death [257].

Organic hydroperoxide (ROOH), basically formed by radical reactions with cellular components such as lipids and nucleobases.

O_2, singlet oxygen and $ONOO^-$, peroxynitrite, formed in a rapid reaction between O_2•- and NO•. It is lipid soluble and similar in reactivity to hypochlorous acid. Protonation forms peroxynitrous acid, which can undergo homolytic cleavage to form hydroxyl radical and nitrogen dioxide.

Reactive Nitrogen Species (RNS)

To complete the depiction of reactive intermediates within the network of oxidative stress and signal transduction pathways, another kind of reactive species need to be mentioned: the reactive nitrogen species (RNS) [295]. Their major compound nitic oxide (NO) exists in three interchangeable forms according to the gain or loss of electrons, namely the gaseous free radical ($NO^{\cdot}$), the nitrosonium cation (NO^+) and the nitroxyl radical (NO^-) [396]. Due to its characteristics as a free radical, NO has a short half life of just a few seconds and typically reacts with O_2 upon formation of nitrogen dioxide (NO_2), which rapidly degrades to nitrite and nitrate within an aqueous environment [273, 274]. Alternatively, NO may be rapidly converted to peroxynitrite ($ONOO^{\cdot}$) by reacting with $O_2^{\cdot\cdot}$, if both generation sites are in very close proximity [404]. $ONOO^-$ itself is an extremely short lived RNS with a half life of less than 10ms *in-vivo* and a high potential to damage cellular compounds [78, 408]. In contrast to the just described rapid conversions in an oxygen-rich environment, NO could also be shown to remain considerably more stable upon hypoxic conditions, allowing for long-distance transport of this molecule [404].

1.2.1 CONSEQUENCES OF ROS AND RNS FORMATION

The long-term presence of even a small amount of the peroxides is a risk to cells because of their conversion into the toxic radicals thereby damaging cellular components. As briefly mentioned before, ROS are assigned a dual function not only in damage development upon oxidative stress but also as signalling molecules [77]. If produced in high concentrations, ROS oxidise different macromolecules within the cell in an uncontrolled manner. Detrimental ROS effects on DNA are many; they include deletions, mutations or translocations, single strand breakage and cross-linking also. Also within proteins, there are different sites particularly prone to damage via ROS; oxidation of different amino acids such as tyrosine, cysteine, methionine and histidine results in cross-linking events [348] which consequently cause degradation of the affected proteins [105]. Furthermore, ROS can oxidize unsaturated fatty acids in membranes. Such generation of lipid peroxides impairs membrane functions with the concomitant loss of membrane integrity [38]. Thus, the modification of DNA, proteins and lipids may cause cellular dysfunction and ultimately induce cell death [29, 325, 363]. ROS were traditionally considered as harmful, although in recent years, it could be shown that they have an important role in a variety of signal transduction pathways. ROS exhibiting differential regulatory mechanisms on the level of transcription, translation or post translational processes and are able to adapt biotic and abiotic stress response, growth and hormone signalling, as well as development and programme cell death (PCD) [12, 211, 296, 367].

Production of •OH radical close to DNA could lead to reacting with DNA bases or the deoxyribosyl backbone of DNA to produce damaged bases or strand breaks. It has been proposed that the extent of DNA strand breaking by •OH is governed by the accessible surface areas of the hydrogen atoms of the DNA backbone. The hydroxyl radical is known to react with all components of the DNA molecule damaging both the purine and pyrimidine bases and also the deoxyribose backbone. It has been estimated that one human cell is exposed to approximately 1.5×10^5 oxidative hits a day from hydroxyl radicals and other such reactive species. High concentrations of ROS cause cell death or even necrosis, the effects of ROS on cell proliferation occurred exclusively at low or transient concentrations of radicals. Low concentrations of superoxide radical and hydrogen peroxide in fact stimulate proliferation and enhanced survival in a wide variety of cell types. Apoptosis and cancer are opposed phenomena, but ROS have been widely reported to play a key role in both. Although the mechanism involved is still controversial redox status and/or hydrogen peroxide have both

been proposed as critical factors [318, 358]. In addition, induction of carcinogenesis has been clearly linked to oxidative DNA damage [254].

The removal of H_2O_2 in cells is mediated predominantly by a collection of antioxidant enzymes like catalase, glutathione peroxidase (GPX) and Prxs. Glutathione peroxidase (EC 1.11.1.19) catalyses the reduction of a variety of hydro peroxides (ROOH and H_2O_2) using GSH, thereby protecting mammalian cells against oxidative damage and also by reducing cellular lipid hydro peroxides [183]. As a protective mechanism, cells express antioxidant enzymes such as Mn-SOD, Cu, Zn-SOD and GPX. Antioxidant enzymes can antagonize initiation and promotion phases of carcinogenesis and they are reduced in many malignancies. Observations of various types of cancer, present a possible link between decreased activities of antioxidant enzymes and increased levels of hydroxylated DNA base, due to oxidative damage. Mn-SOD is reduced in a variety of tumour cells and has been proposed to be a new type of tumour suppressor gene. Biochemical and clinical studies indicate that antioxidant therapy may be useful in the treatment of several diseases [331].

1.3 AN ANTIOXIDATIVE DEFENSE SYSTEM

Under nonstress conditions, there is a harmony between generation rate and scavenging ROS. Under various stress conditions, however, this harmony is perturbed and results into a rise in cellular ROS levels. To lessen oxidative damage to tissues, biological systems have equipped with many protective systems to get rid of ROS which includes range of biological catalyst commonly defined as enzymes i.e. superoxide dismutase (SODs), catalase (CAT), glutathione peroxidase (GPX, GSH), glutathione reductase (GR), ascorbate peroxidase (APX) and peroxiredoxins (Prxs) (Figure 1.6). A number of oxidoreducatses which participates in chlorophyll metabolism, a part of antioxidant defense in plant were also being characterized structurally [91, 204, 351]. Despite their dominant role, Prxs are less well known than the other components of this system. All these enzymes in general convert hydrogen peroxide to water, for protection against damaging ROS. These enzymes job is to sustain a balanced redox state in the cell to keep it hale and hearty.

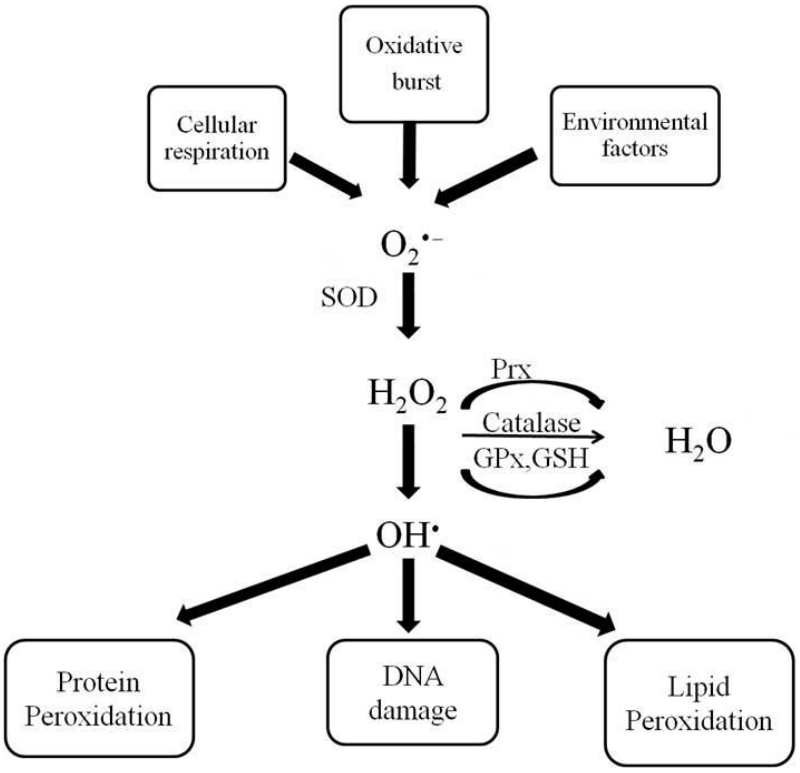

Figure 1.6 An overview of ROS their potential effects and detoxification system

1.3.1 DETOXIFICATION OF ROS-THE ANTIOXIDATIVE SYSTEM OF MICROORGANISM

Bacterial pathogens survive under two exclusively diverse conditions, to be exact, their natural environment and in their hosts. Microorganisms have advanced to perform optimally in their normal habitat by virtue of which they can attain very high growth rates under ideal conditions. Growth of most known microorganisms is however, restricted to more restrained circumstances and a shift to unfavourable surroundings imposes a cellular stress depending on their severity, can kill the microorganism. Bacterial pathogens have evolved extremely sophisticated mechanisms for sensing external conditions. For an enhanced perceptive of the host-parasite interaction it is advantageous to outline the bacterial functions that are specifically expressed under *in-vivo* conditions and to assign their role in the pathogenesis. Pathogenic bacteria do secrete many virulence factors including proteins as well to invade host immune system imparting the pathogenicity with some toxins responsible for disease development [33, 135, 333, 334].

Generally microorganisms cannot grow if they are exposed to oxygen levels that significantly exceed from their local habitats. The basis of this phenomenon is not straight away, in fact the molecular oxygen does not damage amino acids, carbohydrates, lipids, or nucleic acids

directly- in short, the basic molecules from which organism are made. So, why oxygen is toxic? In 1954, Gershman et al. proposed that the problem was not oxygen per se, but rather the partially reduced forms into which it might be converted within cells [118, 119]. Hydrogen peroxide (H_2O_2) is continuously formed by the autoxidation of redox enzymes in aerobic cells and it also enters from the environment, where it can be generated both by chemical processes and by the on purpose actions of competing organisms. It is very astonishing and puzzling to discover that organisms encode so countless enzymes that can degrade H_2O_2. In eukaryotes and higher organisms especially the presence of multiple scavengers might be endorsed to isoform-dependent compartmentalization within organelles or to tissue-specific expression patterns. This statement obviously does not hold true for bacteria, thus forcing researchers to look more narrowly. In considering each of the proposed scavenging enzymes, we will need to weigh up two things: whether its physiological job is undeniably to degrade H_2O_2; and, if so, what special role the enzyme plays that the other scavengers do not accomplish. Indeed, organisms universally contain enzymes that are devoted to the scavenging of superoxide, hydrogen peroxide. Defenses in opposition to oxidative damage comprise peroxide detoxifying enzyme as an essential constituents.

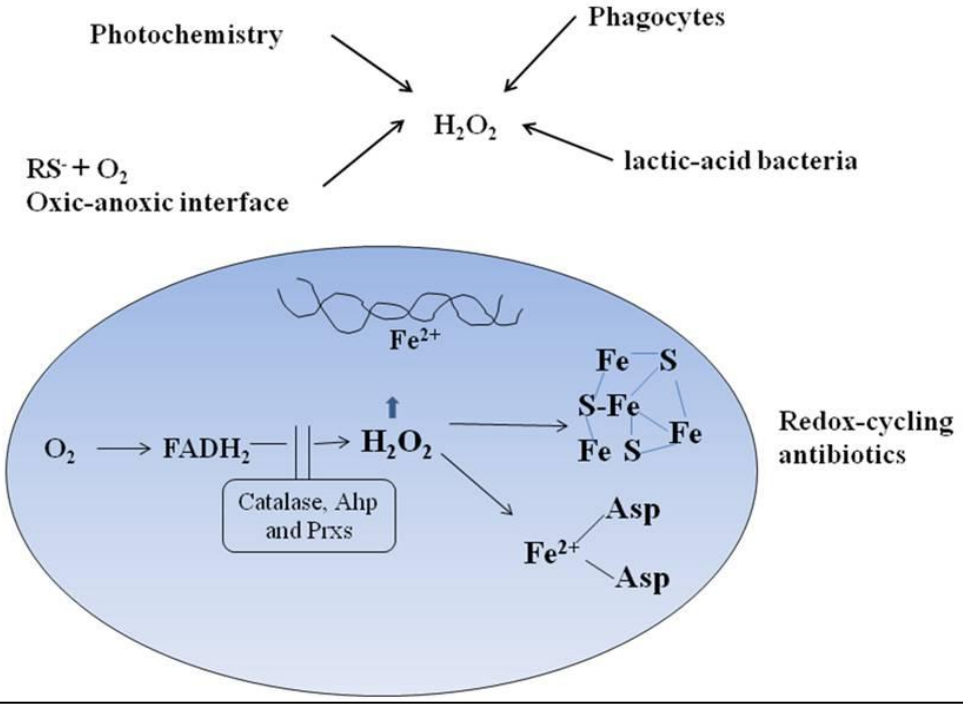

Figure 1.7 Bacteria can be exposed to extracellular H_2O_2 by photochemical reduction of O_2, respiratory burst of phagocytes, lactic acid bacteria, redox reactions and thiol/metal oxidations that occur at oxic-anoxic interface. Endogenously H_2O_2 is steadily formed through oxidation of flavoenzymes or by redox-cycling antibiotics. The H_2O_2 damages DNA employing the Fenton reaction and disables dehydratases that contain iron-sulfur cluster and non-redox mononuclear enzymes that contain iron.

To defend against the lethality of ROS, nature has armed microorganisms with a range of antioxidant proteins. Antioxidant defense system, which prevents oxidative damage by scavenging ROS, could be an important target for development of antimicrobials. For to understand how bacteria deal with with oxidative stress, it is imperative to recognize the enzymes involved in H_2O_2 degradation. To avoid redox imbalance and oxidative DNA damage, a wide array of enzymatic and non-enzymatic antioxidant defenses exists includes both non-enzymatic and enzymatic proteins. Molecules are non-enzymatic antioxidants such as NADPH and NADH pools, β-carotene, ascorbic acid, α-tocopherol and glutathione (GSH).

In 1900, Oscar Loew reported a protein in higher organisms that degrades hydrogen peroxide (H_2O_2) to oxygen and water:

$$H_2O_2 + H_2O_2 \longrightarrow O_2 + 2H_2O$$

During this time only few proteins were known he defined this enzyme as ‘‘catalase”, afterwards discovered in lower organisms as well like bacteria. Catalase (CAT) protein family are involved in H_2O_2 detoxification. These heme-containing enzymes are ubiquitous among aerobic eukaryotes and as well microorganisms. Catalase are localised in peroxisomes but exhibit different tissue specific distribution. As part of the first line of defence, catalase is a powerful enzyme which dismutates H_2O_2 to H_2O and molecular oxygen [326],[401]. The nature of their cofactor distinguishes catalases into heme and non-heme (or manganese) catalases. Catalases further defined as monofunctional catalases with catalytic activity only and bifunctional catalases with both catalytic and peroxidatic activities thus also termed as catalase–peroxidases. Monofunctional catalases are the earliest known bacterial catalases [65, 139] and are almost found among both aerobic and anaerobic bacteria. Bifunctional catalases are scarce; until November 2011, 435 catalase–peroxidase sequences were deposited in the peroxibase data set [294].

Besides catalase there was other H_2O_2 degrading proteins defined as peroxidases. They are defined due to their ability to reduce rather than disproportionate H_2O_2:

$$RH_2 + H_2O_2 \longrightarrow R + 2H_2O$$

Peroxidases are just as efficient as catalase, falls into two categories: thiol-based peroxidases and non-thiol peroxidases. The thiol-based peroxidases are also termed as peroxiredoxins. The selenium containing peroxidases discovered in 1957 defined as glutathione peroxidases (GPx) but did not get a lot notice until the 1970s [101]. Glutathione peroxidase also catalyzes the degradation of hydrogen peroxide along with organic peroxides to alcohols. Five variants of glutathione peroxidases (GPx-1 - GPx-5) are known in mammals to date. GPx-5 is the only

known non selenium containing peroxidase. They have all in common, that they detoxify hydroperoxides at the expense of NADPH via glutathione (GSH) and glutathione reductase, with the exception of GPx-3, which additionally uses glutaredoxin and thioredoxin (Trx).

Superoxide dismutases (SOD) are also one of the enzymes that catalyze the reaction along with catalases in higher organisms. The enzyme is responsible for conversion of two superoxide anions into a molecule of hydrogen peroxide (H_2O_2) and oxygen (O_2) (Eq. 1). In the peroxisomes of eukaryotic cells, the enzyme catalase converts H_2O_2 to water and oxygen, and thus completes the detoxification initiated by SOD (Eq. 2).

Eq. 1 $2\ O_2^- + 2H^+ \longrightarrow H_2O_2 + O_2$

Eq. 2 $2\ H_2O_2 \longrightarrow 2\ H_2O + O_2$

The family of SODs is subdivided according to the kind of metal co-factor utilised by the enzyme, which may be Cu/Zn, Fe or Mn as well as based on sub cellular localisation [6]. There is extensive range of additional enzymes are also being proposed to fulfil the similar roles. It includes thiol peroxidase (Tpx), Bacterioferritin Comigratory Protein (BCP), Glutathione Peroxidase (GPx), Cytochrome C Peroxidase, Thioredoxin Reductase (TrxR) and Rubrerythrins. These enzymes are capable of degrading H_2O_2 in vitro, but their role in *in-vivo* still unclear. These antioxidant enzymes could be responsible for reducing apoptosis by scavenging free radical ions generated during oxidative stress.

Escherichia coli have served as a model system for studies of oxidative stress, formerly because of its genetic tractability. A more definite advantage is that if this facultative anaerobe is maintained in an anaerobic environment, workers can engineer mutations that adequately interrupt oxidative defences that are lethal all through aerobic growth. During bacterial defense responses studies on treatment with hydrogen peroxide and cumene hydroperoxide, Bruce Ames's group identified mutant bacteria (*oxyR1* and *oxyR2* from *Salmonella typhimurium* and *Escherichia coli,* respectively) against peroxide stress [62]. The OxyR protein is a transcription factor found in many bacteria, including the model bacterium *E. coli*. Other bacteria use the PerR repressor as an alternative H_2O_2 sensor in place of OxyR [140, 224]. The PerR regulon detailed in *Bacillus subtilis*; showed to include a peroxidase (Ahp), catalase (KatA) and iron-sequestering protein (MrgA). These findings results into the identification of 2 chief proteins, AhpF and AhpC, as a novel NAD(P)H-dependent peroxide reductase system with activity toward such bulky alkyl and aromatic hydroperoxides such as t-butyl hydroperoxide and cumene hydroperoxide [62, 167, 355, 361]. As sequence information for AhpC, the "protector protein" (subsequently designated thiol-specific antioxidant, or TSA) and a number of other homologues of diverse or unknown functions

became available, the recognition of these proteins as a family of cysteine-based peroxidases expressed in a wide range of organisms led to their designation as “peroxiredoxins” or Prxs. AhpC belongs to a large family of enzymes known as the peroxiredoxins, which are present in both eukaryotes and prokaryotes with AhpC being the most widely studied. The identification of Prxs family members has greatly expanded over the last decade and includes not only representatives from every branch of the phylogenetic tree, but also multiple homologues (Prxs I through VI) in mammals with apparently diverse roles not only in oxidant stress protection, but also in differentiation, apoptosis and proliferation.

1.4 PEROXIREDOXINS

Peroxiredoxin (Prxs or PRDX) proteins (EC 1.11.1.15) are ubiquitous families of highly expressed, thioredoxin scaffold enzymes. Prxs, one of the principal non-heme peroxidases, exhibits catalytic activity toward hydrogen peroxide, peroxynitrite, and various organic hydroperoxides substrates that is endowed by reactive “Cysteine” residues for reduction of peroxides. Peroxiredoxin is more appropriate to symbolize the super family of peroxidases that utilize cysteine as the primary site of oxidation during the reduction of peroxides. While peroxi- indicates the nature of the substrate reduced, -redoxin rhymes with thioredoxin and glutaredoxin, which also contain redox-sensitive cysteine that undergo oxidation-reduction cycles during protein function (Fig. 1.8). These Prxs family members are located in the cytosol, mitochondria, peroxisomes or plasma, which are all sites of ROS production [106]. Prxs have received considerable attention in recent years as a new expanding family of thiol-specific antioxidant proteins [49, 51]. Prxs are evolutionary old proteins present in prokaryotes, archaea and eukaryotes and thus comprise members throughout all kingdoms [146, 401] and emerged out as dominant antioxidant enzymes that reduce and detoxified hydrogen peroxide, organic hydroperoxides and peroxinitrite [40, 146, 186, 303] having reaction rate can range upto10^{7}–10^{8} M^{-1} s^{-1} [71, 244, 287].

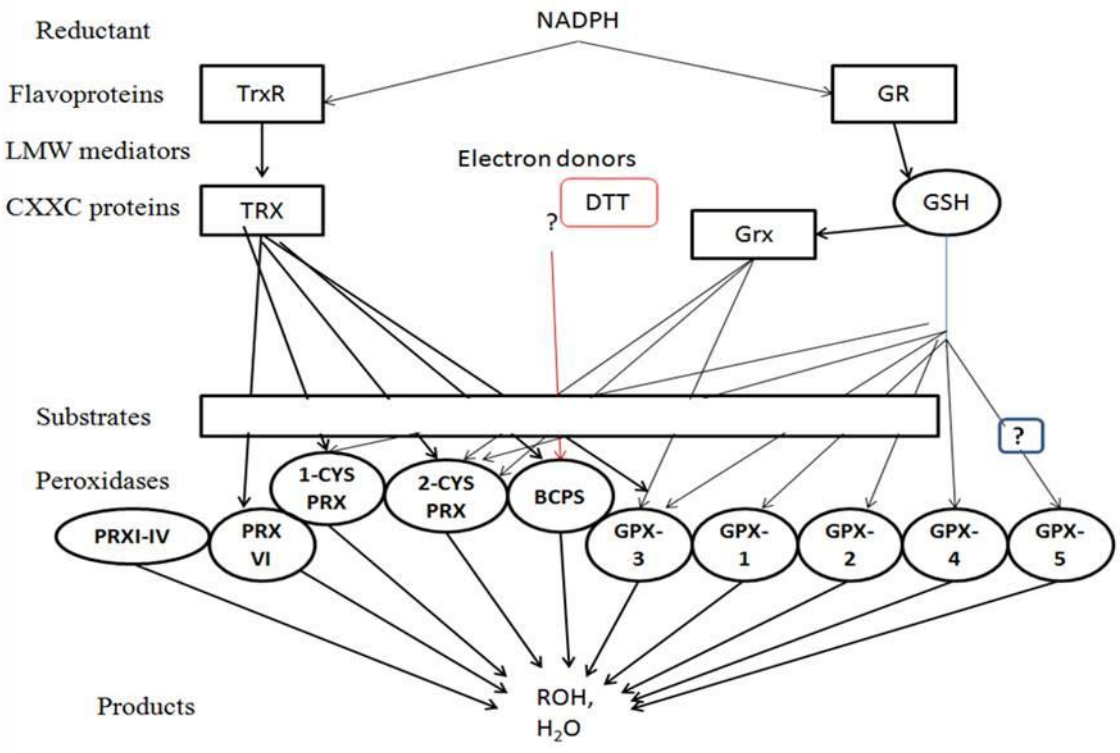

Figure 1.8 An overview of thiol-mediated hydroperoxide detoxification carried out by peroxiredoxin in different organisms including mammals. Homologous proteins are shown in circles. TrxR, Thioredoxin-reductase; GR, glutathione reductase; TRX, Thioredoxin; Grx, glutaredoxin; DTT, Dithioltriol PRX, peroxiredoxin; GPX, glutathione peroxidase; BCPS, Bacterioferritin Co- migratory Proteins.

The over oxidized forms of Prxs, which are catalytically inactive against peroxides [407], have an additional role in hydrogen peroxide signaling in eukaryotes, however the mechanism is unclear. Given their dominance and their involvement in both antioxidant defense and signalling pathways, it is not surprising that Prxs have been associated with cell proliferation, differentiation and apoptotic pathways and linked with several different types of cancer [52, 199, 283, 405, 406]. Due to the widespread connection of Prxs to multiple cancers, it has been proposed that profiling and manipulation of Prxs levels in cancer patients may be a promising new approach towards improving cancer treatments [166]. Since the first characterisation of a member of this protein family is yeast *Saccharomyces cerevisiae* [50], a constantly rising number of Prxs were identified and a broad spectrum of functions could be assigned to these proteins.

1.4.1 Universal features of the Peroxiredoxin catalytic cycle

A general scheme and the components involved in the Prx-catalyzed reduction of peroxides are shown in Figure 6. The reducing equivalents for the peroxide reduction come from

NAD(P)H (step 1). Two other enzymes are needed to complete the electron transfer to the peroxide substrate: a thioredoxin reductase (TrxR) or TrxR-like protein and a thioredoxin (Trx) or Trx-like protein [278, 303]. A disulfide exchange reaction is involved in the transfer of electrons between TrxR and Trx and then between Trx and the Prx (steps 2 and 3). The Prx, which is reduced in step ***3***, uses two catalytic cysteines for peroxide detoxification: the peroxidatic cysteine (S_p in Figure 6) directly reduces the peroxide substrate (step 4) and the resolving cysteine (S_R in Figure 6) forms a disulfide with the peroxidatic cysteine [186] step 5.

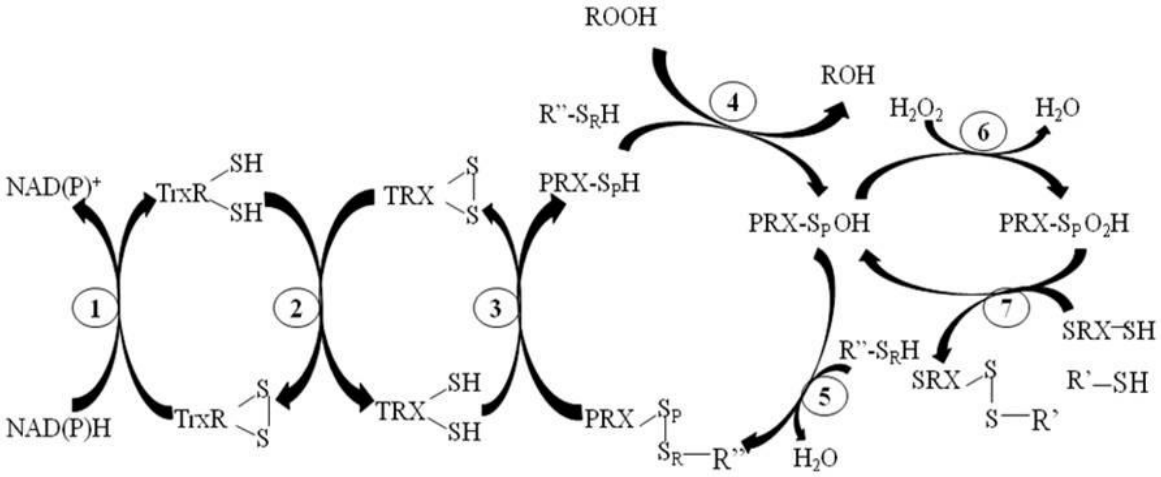

Figure 1.9 General Reaction mechanism employed by PRX system for the reduction of peroxides. NAD(P)H, a TrxR-like protein and a TRX-like protein are required for the reduction of peroxide substrates. In many bacteria, the TrxR and TRX activities are combined in one protein called AhpF. S_p and S_R represent the sulphur atoms of the peroxidatic and resolving Cysteines, respectively. Over oxidation to S_pO_2H in eukaryotic Prxs is associated with hydrogen peroxide signalling events and this form of the enzyme can be "resurrected" by sulfiredoxin (SRX) in ATP-dependent

In *Salmonella typhimurium* and many other bacteria, the TrxR-like and Trx-like proteins are combined in one protein called AhpF [303]. AhpF is a three domain protein; the FAD binding domain and NADH/SS domain work together to accomplish the TrxR-like activity while the N-terminal domain (NTD) has Trx-like activity and interacts directly with the Prx. In AhpF, an intramolecular disulfide exchange occurs in step ***2*** to reduce the NTD. Studies on the NTD showed that it is made up of two fused Trx-folds, with only one of the folds retaining an active site CXXC motif [303, 313, 400].

1.4.2 Scope and purposes

Peroxiredoxin are now distinguished as the super family of peroxidases to be precise significant in cellular signalling pathways and antioxidant defences equally [394]. Through in progress work to reveal the Prxs's functions along with various tremendous reviews [100] brief our present perceptive of different facets of Prxs. It includes covalent variations [13], signalling [129]. Besides that Prxs significance in organisms for instance yeast [75], plants [84], mitochondria [70] and *Caenorhabditis elegans* [288]. In totality enzymes functionality streams straight from structure thus structural data formulates decisive inputs in elucidating the Prxs role in respect to its antioxidant and cellular signalling roles. Prxs emerge from a common antecedent along with range of redox proteins, which are known to have a characteristics thioredoxin (Trx) fold [69, 203].

1.4.3 Classification of Peroxiredoxins

The nomenclature associated with Prxs family protein with time becoming quite confusing. For example, within Prx1 subfamily, protein naming as follows Prx1, Prx2, Prx3, Prx4, TXNPx, TryP, AhpC and 2-Cys. Second example, like thiol peroxidase which is not just represents Prxs but also used to assign Tpx subfamily. Furthermore the categorisation of Prxs on the basis of presence of key Cysteine residues into 1-Cys and 2-Cys [401] adds to more ambiguity since different types of Prxs are known to belongs to more than one subfamily, reflecting divergent self-governing evolutionary sources. Prxs have been classified into two groups, 2-Cys Prx and 1-Cys Prx, based on the mechanism of catalysis. The 2-Cys Prx group can be further divided into "typical 2-Cys Prx" and "atypical 2-Cys Prx", according to the localization of the additional Cysteine involved in catalysis. The "typical and atypical 2-Cys" naming refers to the Prxs having resolving Cys residue (C_R) in the C-terminal helix and atypical referring to all other 2-Cys Prxs which known to have different location of C_R. All groups share a common initial step of catalysis; the oxidation of a conserved reactive cysteine (the so-called peroxidatic cysteine) to a sulfenic acid intermediate (Cys-SOH) with the reduction of the hydroperoxide substrate to the correspondent alcohol. The fate of the sulfenic acid intermediate is distinct among the Prx groups. In typical 2-Cys Prx enzymes, the sulfenic acid reacts with a second cysteine residue located in the C terminus of the other subunit (the so-called resolving cysteine), resulting in the formation of an intermolecular disulfide bond. In contrast, the resolution reaction in atypical 2-Cys Prx enzymes occurs inside the same subunit, resulting in an intramolecular disulfide bond formation. The 1-Cys Prx enzymes do not contain a resolving cysteine, and their sulfenic acid cysteine is stabilized by polypeptide

backbone present at the active site micro-environment. The catalytic cycle is completed when disulfide or sulfenic acid is reduced. Bioinformatically it has been observed that all Prx enzymes contain a conserved cysteine residue in the N-terminal region that is the primary site of oxidation by H_2O_2 termed as peroxidatic Cys (C_P). In case of Trx, the second Cys in the CXXC motif is the one which reacts directly with the peroxides [102].

Cysteine (Cys, C) is an amino acid that contains a side chain thiol (SH) group. Cysteine residue is known to play a central role in peroxiredoxin activity through formation of different structure on reaction with hydrogen peroxide as shown below. It has been seen that cysteine plays an important role in the folding (and hence structure) and stability of some proteins through the formation of disulfide bonds.

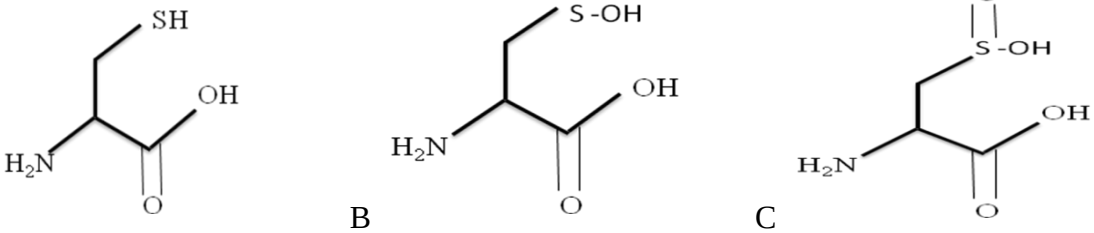

A B C

The chemical structure of the amino acid Cysteine in the thiol (A) sulfenic acid (B) and sulfinic acid form (C).

The thiol group is important in the detection of hydrogen peroxide. The rate of reaction between the protein thiol group and hydrogen peroxide is very important in redox signalling. The two most important factors in the reactivity of the thiol group is the ability of the cysteine residue to be deprotonated to the thiolate anion (eq. 1.3) and how accessible this thiol group is.

$$\text{Protein-SH} \rightleftharpoons \text{Protein-S}^- + \text{H}^+ \qquad (1.3)$$

As mentioned before, peroxiredoxins (Prxs) constitute a superfamily of non-heme containing peroxidases [84]. During catalysis, the active site cysteine is over oxidized to cysteine sulfinic acid. In contrast the general belief that oxidation to the sulfinic state is an irreversible process in cells, studies on over oxidized Prxs species proposed a mechanism by which the catalytically active thiol form can be recovered. This reaction mechanism termed as sulfinic reduction but, ATP-dependent a slow process specific to 2-Cys Prx isoforms. This reversible over oxidation may represent an adaptation unique to eukaryotic cells that accommodates the intracellular messenger function of H_2O_2, but experimental validation of such speculation is yet to come.

1.4.4 Conformational agility of Peroxiredoxins

Approximately more than 60% Prxs structures solved so far from different organisms wrap up the assortment between members of this super family. In most cases Prxs shown to posses packed in, globular protein structure with Trx fold [69] with possible variations of loop size and length of N- and C-terminal region.

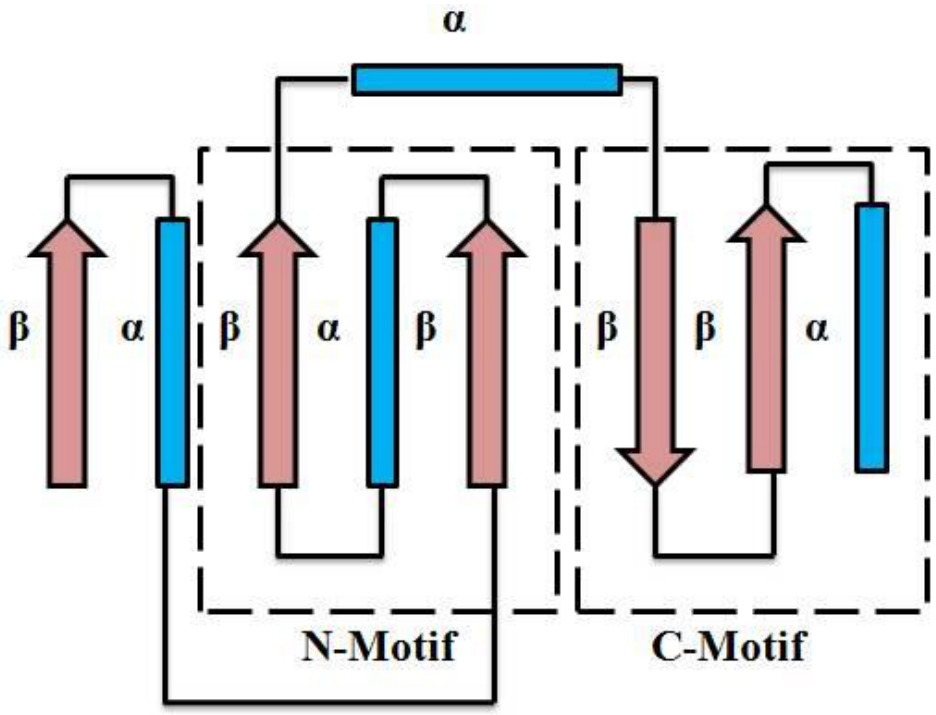

Figure 1.10 The arrangement of secondary structure elements (α helices and β sheets) mostly present in proteins with a thioredoxin like fold. The region corresponding to the thioredoxin fold is indicated with a dashed line; the active site of proteins with a Thioredoxin like fold is shown with a bar.

The structurally conserved, probable-core structure of Prxs comprises 7 beta-sheets (β1-β7) with 5 alpha-helices (α1-α5). The central β-sheet twist structured by 5 β-sheets along with 1 alpha helix and 2 β-sheets with the backbone of 3 α-helices; look alike cradle which holds α2 helix like a baby. The α1 is universally is a 3_{10}-helix in ~50 % of the known Prx structures. The commonly conserved active peroxidatic cysteine C_P residue found to be in helix α2 which is necessarily engaged in the locally unfolding of helix requisite for catalysis. Although α2 also known to have conformational changes during unfolding for each one of the members of the subfamily. It has been shown that the cradle around α2 is extremely vital in stabilization of "fully Folded" and" local Unfolded" conformations, and also assisting the toggle involving both the conformations. In case of Tpx subfamily, a bend in α2 is pursued by an extra one or two turns of the helix. Although the positioning of α5 is also begins in the approximate same

position in all structures, but varies in length from two to five turns. The numbering of secondary structure elements is not universal in all cases. The numbering of secondary structure elements is different cited in some publications, because of the presence of extra elements which is not conserved throughout the entire family. For instance, α1 is a 3_{10}-helix (the helix containing the C_P referred as α1), while in Tpx subfamily, an insertion of two β-strands at the N-terminal end changes the remaining strands numbering. The residues like Pro, Thr, and C_P are strictly conserved within universally conserved **P**XXX**T**XX**C**$_P$ sequence motif among subfamilies without gaps remarks the catalytic effectiveness is very much sensitive due to the inevitability of these key residues. The loop having conserved residues along with catalytic Cys residue termed as the C_P-loop. This is the region that go through structural transformation in catalysis of the Prx1 proteins [399]. The importance of Thr residues in the C_P loop have an evolutionary standpoint, instead of contributing only ~3% replacing first Cys in CXXC motif of a Trx-like ancestral protein [102], indicating that the positioning of Thr residue is essential for both the Prx and Trx catalysis, nevertheless with an altered function [69].

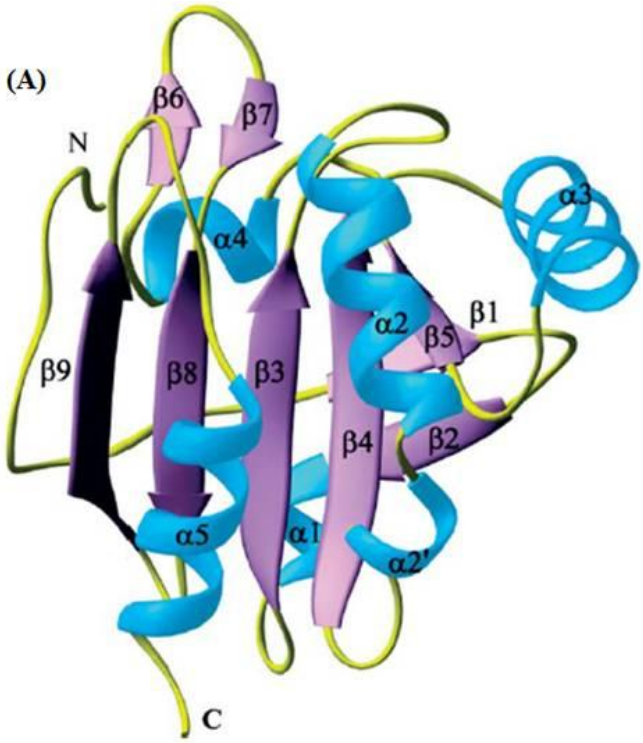

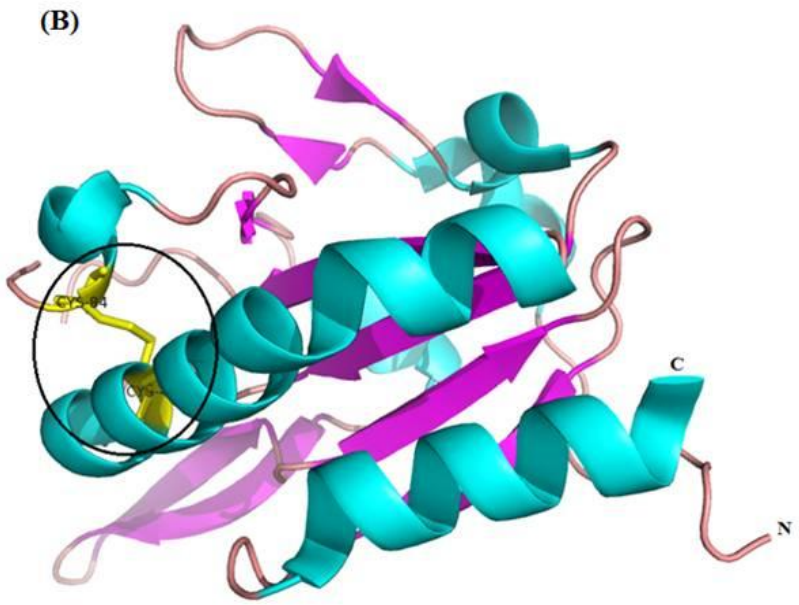

Figure 1.11 (A) The 1-Cys AhpE monomer (pdb id:1XVW**)** showed as a ribbon diagram. Secondary structural elements are labelled, with the N and C termini. (B)The 2-Cys Prx from *Xanthomonas campestris* AhpC **(**pdb id 3GKK**)** shown as a ribbon diagram, intramolecular disulfide bond formation between C_P and C_R present on same chain encircled and the N and C termini are indicated.

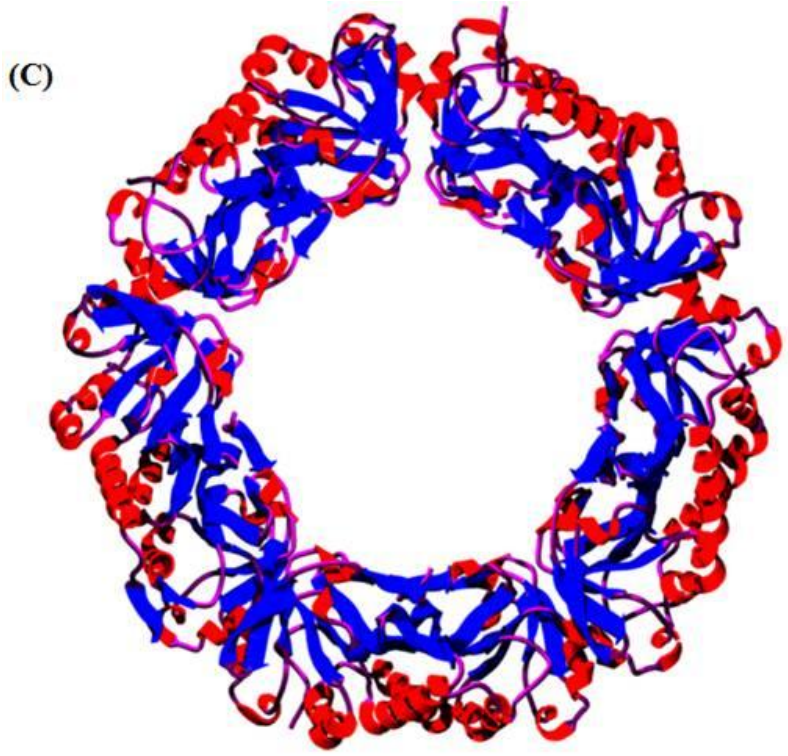

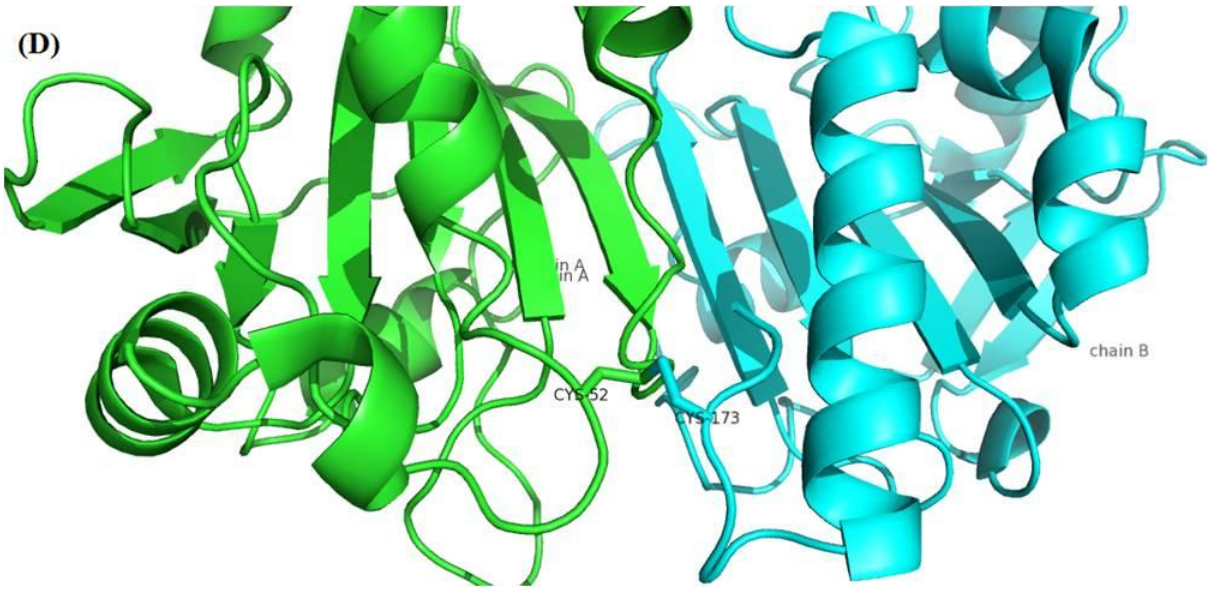

Figure 1.11 (C) Structure of AhpC, a bacterial 2-Cysteine peroxiredoxin from *Salmonella typhimurium* PDB id*:* 1YEX intermolecular redox-active disulfide center. (D) Mammalian 2-Cys peroxiredoxin, HBP23 (PDB code 1QQ2) intermolecular disulfide formation between the chains A and B by Cp (52) and C_R (173).

Theoretically as four key Prx catalytic residues appear on a single chain, thus Prxs could be monomeric. On the other hand, BCP subfamily is one of the Prxs subfamily known to be active as monomer for example monomeric Prx of the C-type bacterioferritin comigratory protein and PrxQ. Though Tpxs were designate preferentially as monomers [59], but now functions as dimers [24, 129]. In principle 2-Cys Prxs including all other Prxs are obligate dimers, tends to form high molecular weight oligomer structures holding solitary two types of dimer edges. The two distinctive dimer interfaces that explained so far in Prxs are classified as the A and B-type dimers [323]. A-type dimers refers to alternate dimers formed by union of corresponding parts of the two β with the loops former α-helices. B-type dimers refer to β-type dimers formed by interfaces at the β-sheets in a head-to-tail manner. It displays intermolecular disulfide bonds formation or stays reduced.

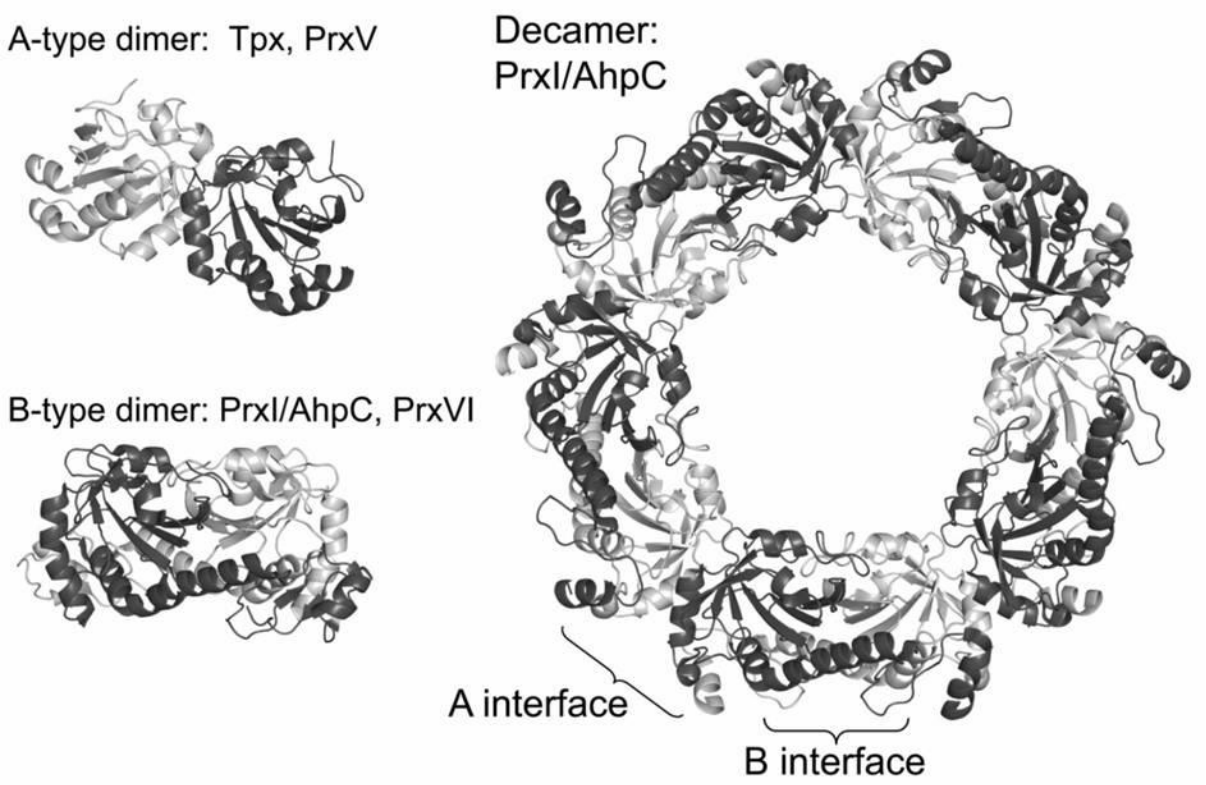

Fig 1.12 Oligomeric interfaces and quanternary structures of Prxs. Dimerization of Prx subunits can take place through two different types of interfaces. The A-type interface (as detected in Tpx and Prx5 subfamily members), or the B-type interface forms by β sheets to form an extended sheet (as observed for PrxI/AhpC and Prx6 subfamilies). Some members of the PrxI/AhpC and Prx6 subfamilies also form decameric, or less commonly dodecameric or octameric, structures built from B-type dimers through interaction at their A-type interfaces. Figure adopted from Hall et al. ANTIOXIDANTS & REDOX SIGNALING Volume 15, Number 3, 2011 [130].

With a large number of experimental designs which slowly emerging out to address the functionality of Prxs oligomerization for knowing the various *in-vivo* roles of redox-dependent attribute of Prxs. Increasing evidence indicates that atypical 2-Cys Prxs also undergo protein–protein interactions with functional implications possibly with the lower polymerization degree (dimers, tetramers and hexamers) in comparison with typical 2-Cys Prxs (decamers and HMW species). In atypical Prxs dimerization is of A-type interfaces [87, 186]. 1-Cys Prx is less characterized subfamily with the information gathered from literature not sufficient to propose the substantial function of their oligomerization. Although it has been cited that diversified group of 1-Cys Prx constitutes an array of proteins having one or more Cys with distinct reaction mechanisms. Series of crystal structures come up with the proposed oligomeric state of 1-Cys Prxs in spite of being predominantly monomeric in nature.

It includes for ex. human recombinant 1-Cys Prx (hORF6) structure which was resolved as a dimer [58] whereas monomeric and dimeric species seen in solution via gel filtration [402]. The 1-Cys Prx dimerization is solely endorsed to non-covalent interactions. Another from Toxoplasma gondii (Tg-Prx2) which is unique along with the 1-Cys Prx group both in reference to oligomerization behaviour and enzymatic reaction mechanism [79]. Oligomerisation property of 1-Cys Prxs from mycobacterium (AhpE-1XVW) has also been deciphered [227]. A recent 1-Cys Prx oligomerization study of PrxQ-A1 from *S. elongatus* which separated as monomer during SEC [352]. Even though oligomerization is broadly acknowledged feature of Prxs, still its *in-vivo* and physiological significance is to a certain extent understood but not fully.

Peroxiredoxins (Prxs) undergoes major redox-dependent conformational changes. The components of Prxs system have been already discussed. In brief, all Prxs employ common catalytic mechanism which uses a conserved peroxidatic Cys (C_P), to reduce peroxides directly. Catalysis carried out with three main steps includes: first peroxidation, second resolution and third recycling which requires local conformational changes. Thus, the conformational changes occur during catalytic cycle is being discussed further. The reaction commences by means of the substrate binding in the active site (FF conformation) in which the enzyme has a fully formed peroxide-binding active site. When attacked by substrates like peroxides, either sulfur or oxygen atom of C_P is being attacked and reacts, this step known as peroxidation. This step results into release of the corresponding alcohol (or water), commonly when sulphur atom being used it forms sulfenic acid (S_POH) an oxidized C_P reaction intermediate. Prxs known to react with range of substrates like H_2O_2, alkyl hydroperoxides and peroxynitrite [146, 203, 371, 401]. Resolution involves the resolving thiol (S_RH). This S_RH can be present either on the Prx itself (as most prevalent in 2-Cys mechanism) or on some other protein molecule (as in case of 1-Cys mechanism). The resolving thiol then reacts with S_POH and forms disulfide ($-S_P-S_R-$) which results into release of a water molecule. The S_POH moiety needs to be free in order to attack thus necessitates the fully folded conformation change which involves the local unfolding of the active site from FF to LU transition (Fig 1.13). Protein locks in LU conformation and preventing the FF conformation to be reform. Thus where recycling step occurs, which involves the disulfide reduction by means of another small molecule for the regeneration of free thiols S_PH and S_RH. These small molecules include Trx or Trx-like protein or single domain like AhpF in case of bacterial enzymes [302, 400] intended for many Prxs. After the disulfide bond reduction the FF active

site refolds because of which Prx is undergoes catalatyic cycle from LU to FF transition (Fig. 1.13).

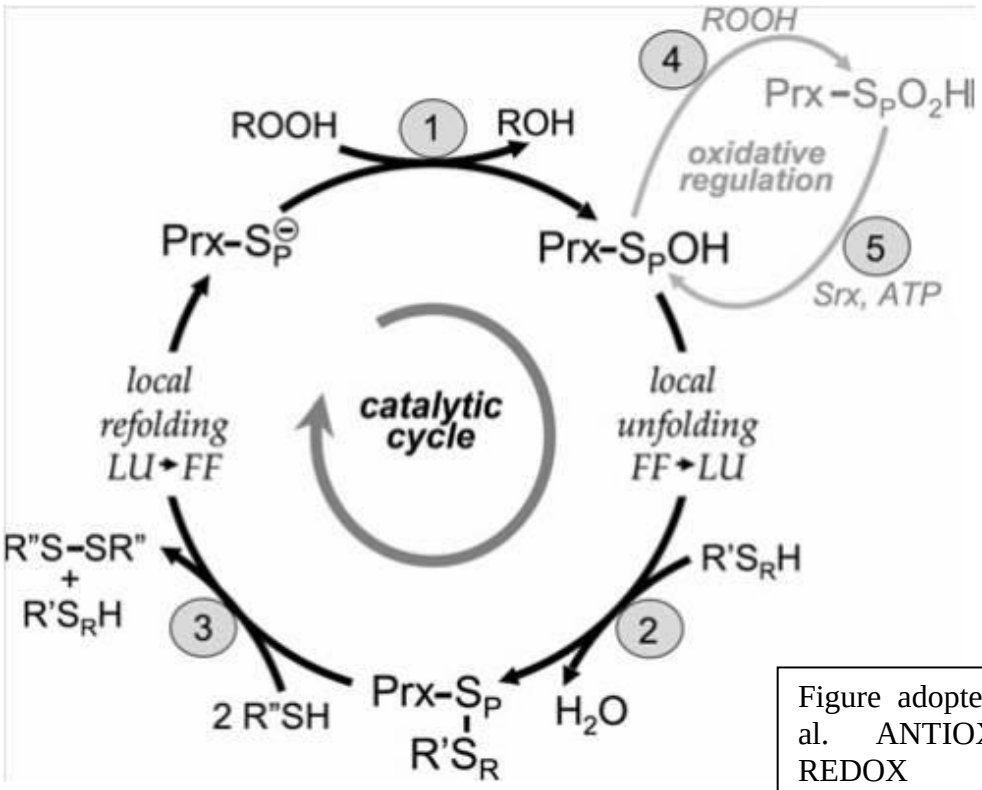

Figure adopted from Hall et al. ANTIOXIDANTS & REDOX SIGNALING Volume 15, Number 3, 2011

Figure 1.13 "Two distinct protein conformations are involved in the cycle: FF (fully folded active-site intact) and LU (locally unfolded, disulfide between the C_P and the C_R)". The "S_P" denotes the sulfur atom of the C_P. Proteins, like Trx and AhpF, have been denoted as R´´ in step 3. Oxidative regulation (gray, steps 4 and 5) is seen in sensitive, eukaryotic floodgate-type 2-Cys Prxs. Inactivation of the Prx by over oxidation of the C_P (step 4) is peroxide dependent. The inactivated form can be rescued through an ATP-dependent reaction catalyzed by sulfiredoxin (Srx) (step 5).

1.4.5 Human peroxiredoxins

The relevance of Prxs enzymes is accentuated by their abundance and involvement in multiple cellular processes [84, 297, 357]. Their importance becomes particularly noticeable in context of the causative participation of ROS in various diseases described for the mammalian/human system, ranging from neurodegenerative disease like Parkinson's or Alzheimer's and neuroinflammatory disorders e.g. Multiple sclerosis to cancer [376]. In addition to their effective role in antioxidative defence during various diseases [191, 270, 298,

411], Prxs are also involved in different signal transduction processes, as for a case in apoptosis and cell viability [53, 397]. These research findings nicely demonstrate the relevant importance of this protein family in vertebrates. Many organisms produce more than one isoform, including at least six Prxs identified in mammalian cells (PrxI - PrxVI) [146, 401]. Mammalian six isoforms of Prxs are further divided into three subgroups (2-Cys, atypical 2-Cys, and 1-Cys) based on the number and position of Cys residues involved in catalysis. In turn, the classes are divided into six subclasses: PrxI, PrxII, PrxIII, PrxIV (2-Cys), PrxV (atypical 2-Cys) and PrxVI (1-Cys). PrxI is 22 kDa, is abundant in human tissues [52, 180], and is localized in both the nucleus and cytosol in the cell. PrxI is involved in antioxidant protection of erythrocytes. For instance, mice with a PrxI knockout develop hemolytic anemia [164] and display a 15% decrease in lifespan [275]. Likewise, a decreased PrxII expression makes cells sensitive to apoptosis. Knockout mice displayed signs of hemolytic anemia and are more prone to develop hematopoietic tumors. PrxIII, localized in mitochondria is also involved in antioxidant protection of cells. A decrease in PrxIII levels leads to morphological alterations in mitochondria, a mitochondrial mass reduction and changes in membrane potential [398]. PrxIV occurs not only within cells, but also in the intercellular space and protects endothelial cells from extracellular ROS. The reduced form is capable of binding to the cell surface, while the oxidized form loses this capability. PrxV is an atypical 2-Cys peroxiredoxin and differs in catalytic mechanism, structure and intracellular localization from other enzymes of the family. PrxV is a monomeric protein and has one conserved Cys (Cys48) and two additional Cys residues in positions 73 and 152. Cys48 and Cys152 form an intramolecular disulfide bond as the peroxidative Cys is oxidized. An increase in PrxV expression was observed in pathology [202]. PrxVI belongs to 1-Cys peroxiredoxins and has one Cys at 47^{th} position. PrxVI is found in all tissues, but its content is the highest in the olfactory epithelium, tracheal and bronchial epithelium, gastrointestinal tract, oral cavity, liver and pancreatic cells. Water soluble secreted PrxVI was first isolated to purity from rat olfactory epithelium [299, 300]. Through biochemical studies it was shown that PrxVI is capable of neutralizing both organic and inorganic peroxides in the presence of certain thiols, and its protective role exerted due to its peroxidase activity [286]. The enzyme reduces alkyl hydroperoxides and phospholipid peroxides in addition to hydrogen peroxide. PrxVI utilises its active site Cys residue for catalytic reactions; moreover, does not use thioredoxin as a reducer in disparity to PrxI–PrxV. There were other reductant known to act as redox partner for PrxVI like glutathione, dehydrolipoic acid and cyclophilin. [56], while there is still no data on the physiological reducers of the protein. PrxVI exerts a therapeutic effect in treating burns

of the upper respiratory tract and healing of incised wounds [285]. Knockout mice devoid of PrxVI are viable, but have a higher sensibility to oxidative stress, in particular, hyperoxia [265]. The importance of human Prxs enzymes comes from the fact that they are capable of protecting cellular components by eliminating low levels of peroxides which are the outcome of normal cellular metabolism. Other oxidoreducatse proteins from mammals are also characterized; a part of redox signalling implicated their role in apoptosis [8, 108, 172, 356].

1.4.6 Plant Peroxiredoxins

The prevalence of H_2O_2 implicating their role in ABA-signalling protein, role of redox in regulating immunophilin is well being studied [121, 122, 346]. The prevalence of Peroxiredoxins (Prx) in higher eukaryotic organism is also well extensively studied. Prxs are known to be the essential elements of antioxidant defense system for dithiol-disulfide redox regulatory network of the plant and cyanobacterial cell. Plant peroxiredoxins broadly classified into 4 subgroups: 2-Cys Prx, 1-Cys Prx, type II Prx and PrxQ. Based on sequence, structure similarities and positions of conserved cysteinyl residues the Prx family can be divided in six groups, named A, B, C, D, E and F [146, 281, 282]. According to the more commonly used nomenclature, the A-type corresponds to the (typical) 2-CysPrx, the B-type to the (typical) 1-Cys Prx, the C-type to PrxQ, and the D-type to type II peroxiredoxins (PrxII) [281]. PrxQ and PrxII also are termed atypical 2-Cys Prx [146]. Group E includes homologous bacterial peroxidases and group F encodes archaea homologs. Among six groups, group A to D are the most common and conserved one in higher plants for example, the genome of *A. Thaliana* encodes genes for each of the four types of Prx [152, 153]. The localisation of Prxs in higher plants summarizes typically contain at least one plastid 2-Cys Prx, one nucleo-cytoplasmic 1- Cys Prx, one chloroplast PrxQ and one each of cytosolic, mitochondrial, and plastidic type II Prx. It exhibited a high sequence similarity to bacterial AhpC and the human and yeast thioredoxin-dependent peroxidase TPx [22]. Type II Prxs were simultaneously identified in yeast [175] and Chinese cabbage (*Brassica campestris*) [60], in the latter during a random sequencing project on flower bud-specific cDNA clones. Prx Q constitutes the fourth group of Prx that was most recently cloned from plants [206]. The N-terminal sequence of the 17-kDa protein from *Sedum lineare* showed similarity to the bacterioferritin comigrating protein (BCP) from *E. coli* and was named Sl-Prx Q.

1.4.7 Bacterial Peroxiredoxins

In bacteria also, the Prxs are indispensable; some pathogenic bacteria rely wholly on a Prx-based antioxidant defense response against oxidative stress. Prxs are universally dispersed and are found in the majority of the pathogenic bacteria. Mechanistic and structural studies of these bacterial proteins have delineated the linkage between redox state, oligomeric state, conformational changes and peroxidase activity for the peroxiredoxins. Through the available genomic sequence information majority of bacterial Prxs have been identified recently and functional studies have been conducted for enlightening the importance of this class of antioxidant enzymes. Prxs proteins are among the 10 most abundant cellular proteins prevalent in *Escherichia coli* [235], and in other bacteria, Prxs were characterized as species-specific antigens. In 1988 a thiol-specific antioxidant, TSA, was first identified in yeast as an enzyme that could protect glutamine synthetase from metal-catalyzed oxidation during dithiothreitol/ $Fe^{2}+/O_2$ exposure [193]. A thiol peroxidase, AhpC, was isolated from *Salmonella typhimurium* in 1989, was characterized as a member of the OxyR H_2O_2-stress regulon [362]. Identifications of other peroxiredoxins have followed; these enzymes appear to be more prevalent than catalase, being expressed in almost all bacteria. The few exceptions include *Streptococcus pneumoniae, Rhodobacter capsulatus, Rhodobacter sphaeroides, Borrelia spp., and Bartonella spp*.

1.4.7.1 Alkyl hydroperoxide reductase (Ahp)

The alkyl hydroperoxide reductase system consists of two cytoplasmic proteins AhpC (thiol peroxidase) and AhpF (flavoreductase) were first discovered in *Salmonella typhimurium* [167]. The homologues of Ahps are found throughout the aerobic and anaerobic biota. AhpC contains two conserved cysteines, Cys46 and Cys165. Cys46 is present in the N-terminal region and lies in a conserved VCP motif present ubiquitously in AhpC and other proposed thiol-based peroxidases. The *Mycobacterium tuberculosis* AhpC differs from other well characterized AhpC proteins in having three cysteine residues rather than one or two. An assortment of bacteria expresses a flavoprotein, AhpF NADH:disulfide oxidoreductase activity that acts as a disulfide reductase to recover the bacterial peroxiredoxin, AhpC, during catalysis by restoring the disulfide in AhpC to its reduced form [167, 303]. It includes three domains: an FAD-binding domain, an NADH-binding domain with a thiol/disulfide redox active center, and a thioredoxin-like domain [31]. The reducing partner for AhpC from *Helicobacter pylori* and *Mycobacterium tuberculosis* is Trx/Trx reductase system [25], and AhpD in mycobacterial species [40] as reducing partner, AhpF is absent [25, 81]. The number

of bacterial AhpC members which are characterized biochemically comparatively less *Streptococcus mutans* [143, 304] *Amphibacillus xylanus* [200, 277, 278] *Thermus aquaticus* [237, 366] *Clostridium pasteurianum* [308], *Chromatium gracile* [382], and *Mycobacterium* tuberculosis [40, 41, 54, 55, 144]. Kinetically it has been shown that AhpC were most active enzyme and able to quickly degrade low doses of H_2O_2 (<20 μM) as compare to known catalases. Substantial information pertaining to the biological importance of Prxs has also been achieved by genetic approaches, including disruption of the chromosomally-encoded structural genes from different pathogenic microorganisms *Escherichia coli, Salmonella typhimurium* [97, 126, 327, 353, 355], *Bacillus subtilis* [11, 42, 137], *Helicobacter pylori* [242, 289], *Staphylococcus aureus* [15], *Xanthomonas campestris* [238, 258, 259], *Streptococcus mutans, Streptococcus pyogenes* [198], *Bacteriodes fragilis* [314, 315] *and Mycobacterium* including *M. tuberculosis, M. leprae, M. bovis, M. smegmatis, M. aurum* and M. *Bovis* [81, 83, 141, 339, 345, 391, 392]. A recent study of NADH-dependent *t*-butyl hydroperoxide reductase activity in a number of diverse bacterial strains come up with the conclusion that, different levels of the two (or more) proteins involved in the peroxidase system expressed by the various organisms, possessed the ability to catalyze the reaction [280]. Other peroxidases are also being identified, characterized widely expressed in bacteria, but our understanding is much less complete. These include bacterioferritin comigratory protein (BCP) and thiol peroxidase (Tpx).

1.5 BACTERIOFERRITIN COMIGRATORY PROTEINS (BCP)

Bacterioferritin comigratory proteins (BCPs) were originally named for their propensity to comigrate with bacterioferritin proteins and was first discovered in *Escherichia coli* [9, 272]. *E.coli* BCP, a putative bacterial member of the TSA/AhpC family, was characterized as a thiol peroxidase. Biochemically it has been observed that recombinant E. coli BCP reacts with t-butyl hydroperoxide and linoleic hydroperoxide along with H_2O_2, depicting its actual role might be in reduction of an organic hydroperoxide [176]. Lipid peroxidation is well-established in eukaryotic organisms, but biological sources of organic hydroperoxides are not known in bacteria. The primary sequence suggested a resemblance to AhpC, and biochemical assays confirmed its ability to react with H_2O_2. The similarity of primary structure between bacterioferritin comigratory protein (BCP) and the TSA/AhpC family suggested that BCP could be another new member of the family. Still, the function of BCP has not been yet elucidated despite of the wide distribution of BCP in most pathogenic bacteria including

Haemophilus influenzae, *Helicobactor pylori*, and *Mycobacterium tuberculosis*. The biological importance of this protein, from the studies from different pathogenic bacteria *H. pylori, Campylobacter jejuni, and Porphyromonas gingivalis* showed that bcp mutant cells become hypersensitive towards varied peroxide substrates and eventually leads to cell impairment upon aeration [20, 41, 176, 182, 387, 388]. Recent studies in *Helicobacter pylori* have linked BCP with bacterial pathogenicity, and shown to contribute significantly to the ability of the bacteria to colonize the host's stomach. So is BCP an authentic scavenger of peroxides? BCP homologues are present in both gram-positive and gram-negative bacteria. BCP is a model for a set of proteins that exhibit thiol-dependent peroxidase activities *in-vitro* but whose *in-vivo* functions is ambiguous. BCPs constitute a group of antioxidant enzymes that exhibit thiol-dependent peroxidase activities in vitro widely distributed. Beside majority of the BCP subfamily members are of bacterial origin, BCPs known to belong to archaea and eukaryotes as well. The plant homologues of BCPs are defined as PrxQ. PrxQ from phytopathogenic bacterium *Xylella fastidiosa* (XfPrxQ) which is the etiological agent of various plant diseases has also been characterized [154, 290]. *In-silico* analysis of Prxs have been facilitated recently with upcoming structures of BCPs, sequence variations and biochemical studies define the extensive diversification among the subfamily members yet resembles to ancestral protein from which Prxs are diverged out. BCPs has been defined as the most diverse subfamily of Prxs and designated as 'C' group by Hoffmann et.al, 2002 [146]. The BCP subfamily was further reclassified for clarification in nomenclature wise into an alpha-group and βeta-group. The α-group known to possess the canonical C_PXXXXC_R motif and follows the 2-Cys Prxs mechanism while β-group without C_R functions as 1-Cys Prxs by Wakita et al. [384]. With the new more sequences, this nomenclature is unsatisfactory for relating the whole subfamily. The predicted amino acid sequence of BCP possesses the conserved catalytic triad common to the BCP subfamily of Prx's. From known biophysical facts it has been seen that BCPs differ in their oligomerisation pattern based due to the occurrence or position of the C_R. A-type dimerisation mostly seen for BCPs following both the 1-Cys or 2-Cys mechanisms, but depends upon the two distinctive locations of the C_R. For members that exhibit 2-Cys mechanism, the C_R generally resides in α2, towards C-terminal to C_P (C_PXXXXC_R) motif in most of the members. The probability of C_R in α3 position with the typical CXXXC motif is very less (~7%) for example in thiol peroxidase Tpx subfamily. There are many protein structure known for the BCP subfamily, representing five different Prxs. Current research established the role of the first cysteine being the catalytic peroxidatic

cysteine in all the members of this protein family. The functionality of the second cysteine is still controversial and necessitates further exploration. Being so much common to several bacterial pathogens the role of BCPs regarding their role in conferring ROS resistance during pathogenesis is less defined or little information present so far. Some of the examples make an attempt to define its role in pathogenesis taking an example of *Coxiella burnetii* gram-negative, obligate intracellular bacterial pathogen resides within the acidified lysosome-like compartment of the host cell termed a parasitophorous vacuole. It was shown that *Coxiella* BCP binds DNA and likely serves to detoxify endogenous hydroperoxide by products of *Coxiella*'s metabolism during intracellular replication [142]. Another example of *Camylobacter jejuni* in which BCPs showed to play an essential function in protection against oxygen-induced oxidative stress [20]. Biochemically it was observed that *H. Pylori* BCP plays a compelling role in capable of host colonization [388]. Interestingly, BCP expression was induced in the bacterium *Frankia* sp. during the formation of symbiosis with the plant, *Alnus glutinosa* [134].

Tpx, Thiol peroxidase was denoted thiol-specific antioxidant (TSA) in early literature [193]. It was discovered as a factor in *Saccharomyces cerevisiae* cell lysates that could protect glutamine synthetase from H_2O_2 [194]. Subsequently, Cha et al. isolated and characterized a homologous protein from periplasmic fractions of *E. coli* [47], was initially designated as p20 and later defined as thiol peroxidase. Tpx also contains a conserved Cysteine residue in its N-terminal region like Ahp, thiol peroxidase; on the other hand, they are not homologs at the sequence level. Thiol peroxidases from various bacteria showed conservation of peroxidatic cysteine residue at Cys61 position (numbering based on *E. coli* thiol peroxidase), and upon exposure to H_2O_2 these residues form an intramolecular disulfide bond [24]. Mutations studies indicated that mutant of Cys61 eliminate its peroxidatic activity [24, 415]. Crystal structures have been solved in both reduced and oxidized state [59, 132]. The physiological reductant electron donor for Tpx is unknown. On the other hand biochemically in vitro peroxidase activity of Tpx with H_2O_2, t-butyl hydroperoxide, cumene hydoperoxide and linoleic acid hydroperoxide has been achieved using dithiothreitol as an electron donor [48]. The localization of thiol peroxidases has been doubtful, as it was first isolated from *E. coli* after osmotic shock; it seemed likely to be a periplasmic protein. It may emerge to have a function that was distinct from that of the cytoplasmic Ahp system. However, it has been observed that thiol peroxidases from *E. coli* and other bacteria do not exhibit N-terminal signal sequences when analyzed by SignalP 4.0 software, while on the other hand researchers subsequently identified *E. coli* thiol peroxidase in cytoplasmic fractions [359]. The presence

of tpx homologs in Gram-positive bacteria further supports its cytoplasmic localization. The effective concentration of thiol peroxidase quietly (2- to 3-fold) induced by aeration in *E. coli* [190, 196]. Overall, the state of knowledge of Tpx function is similar to that of BCP. The enzyme activity can be demonstrated *in-vitro* under non-physiological stressful conditions, but neither the expression pattern nor genomic context suggests its physiological role.

1.5.1 Functional cysteine in BCPs/Prxs proteins

Encompassed by the four Prxs classes, class 1 is the primitive form of Prxs from which other three classes derived. Beside the absence of resolving Cysteine the peroxidatic Cysteine undergoes in catalytic cycle by reacting with hydroperoxides substrates by forming intermediate sulfenic acid (Cp-SOH). However, the resulting Cp-SOH does not form a disulphide because of absence of another Cys-SH close by. Research information regarding the resolution of the sulfenic acid in 1-Cys Prxs is very limited and stills an open question to decipher. There are though various non physiological small molecule electron donors been drawn in the role which includes glutathione, lipoic acid, cyclophilin, ascorbate and DTT [225, 243, 260, 266]. The 1-Cys Prx members ubiquitous in a variety of species including archaea, yeast, nematode, plant and mammals [49, 185]. GSH has been suggested to be the physiological donor for 1-Cys Prx [99, 107]. The physiological electron donor is not well characterized till date for this subclass of Prxs.

1-Cys Prxs are antioxidant enzymes uses strictly conserved cysteine for catalyzing the reduction of hydroperoxides into alcohols. The sequence identity among these 1-Cys Prxs subgroup members is more than 60 percent, while among human 1-Cys Prx and the four human 2-Cys Prx (Prx I to IV) enzymes is less than 30%.

Second class includes both typical and atypical 2-Cys Prxs. In the typical 2-Cys peroxiredoxins, a second cysteinyl residue, termed as the resolving Cysteine, involved in intersubunit disulfide bond formation during the course of catalysis. In 2-Cys Prxs, the C_P-SOH reacts with a second cysteine residue, the so-called resolving cysteine (C_RSH), forming a stable disulfide bond (C_P-S-S-C_R), which is then reduced by one of the cell-specific disulfide oxidoreductases, completing the catalytic cycle. These oxidoreductases include physiological electron donors like thioredoxin- thioredoxin reductase, glutaredoxin-glutaredoxin reductase and several others like glutathione-glutathione reductase. Based on the positioning of resolving cysteine the 2-Cys Prxs were further subdivided into either typical or atypical classes. In typical 2-Cys-Prxs, the C_PSH reacts with a C_RSH residue located in the C-terminal domain of another subunit within a homodimer. The typical 2-Cys Prxs are obligate

dimers, which contain two identical active sites. The atypical 2-Cys Prxs enzymes are functionally monomeric but shown to have the same basic mechanism as typical 2-Cys Prxs, except positioning of the resolving cysteine is, in most cases, located on the same polypeptide chain as the peroxidatic cysteine. Thus, resolution of the intermediate sulfenic acid (Cys-S_POH) results in an intramolecular disulfide bond. All atypical 2-Cys peroxidases use thioredoxin as an electron donor to reduce the disulfide and complete the catalytic cycle. In addition, it has been verified that 2-Cys Prxs can be converted into 1-Cys Prxs by mutation of the resolving cysteine, suggesting some intrinsic mechanistic compliance within the super family. In Kinetoplastida, comprising the medically important parasites *Trypanosoma brucei*, *T. cruzi* and *Leishmania* species, 2-Cys peroxiredoxins described shown to catalyze reduction of peroxides by the specific thiol trypanothione using tryparedoxin, a thioredoxin-related protein, as an immediate electron donor [43].

1.5.2 Thioredoxin and Thioredoxin reductase system

Thioredoxin (Trx), together with thioredoxin reductase (TrxR) and NADPH constitutes the thioredoxin system, an effective antioxidant system was discovered by Peter Reichard and co-workers in 1964 as a hydrogen donor for enzymatic synthesis of cytidine deoxyribonucleoside diphosphate by ribonucleotide reductase from *Escherichia coli* [223]. The amino acid sequence of *E. coli* Trx1 with 108 residues was determined in 1968 [147] demonstrating the universally conserved active site –Cys-Gly-Pro-Cys-. Initially role of Trx imparted as reducing substrate of ribonucleotide reductase(RNR) [148], in catalyzing *de novo* synthesis of 2′-deoxyribonucleotides from corresponding ribonucleotides as a result of which implicated be involved in DNA replication and repair (reviewed in recent times [151]). Additionally, Trx systems play vital roles in virus infection, the immune response, and cell death via interaction with thioredoxin-interacting protein as per say like Prxs. Trxs ordinarily designated as family of small reductases (~12 kDa) proteins, whose main role in redox reactions by means of dithiol–disulfide switch using two redox active Cys residues separated by two other amino acid residues (a CXXC active site motif). Trxs are universally distributed from prokaryotes to eukaryotes including humans with comprehensive functions. Trx is ubiquitously present in bacteria, where as other antioxidant proteins like the glutathione (GSH) antioxidant system or catalase (CAT) are absent in some specific gram-negative, -positive bacteria such as *H.pylori*, *M.tuberculosis*, *B. subtilis*, *Bacteroides fragilis* and *Lactobacillus casei* [93, 276, 316, 332, 365, 374]. Because of its ubiquitous presence makes the Trx system indispensable for cellular thiol/disulfide equilibrium and endurance under

oxidative stress in several bacteria. Taking an example, the absence of a GSH-Grx system in some pathogenic bacteria such as *Helicobacter pylori*, *Mycobacterium tuberculosis*, and *Staphylococcus aureus* makes the bacterial Trx system vital for endurance under oxidative stress. This presents a prospect to eradicate these bacteria by targeting the TrxR-Trx system. A recent review article on thioredoxin system very nicely points out the importance of thioredoxin system and their relevance [240]. The mechanism of action employ by Trx system includes transfer of electrons to thiol-dependent peroxidases (peroxiredoxins) to eliminate ROS and RNS with a rapid reaction rate. In general, the enzyme works by taking electrons from NADPH and via TrxRs these are transferred to the active site of Trx, which is the common disulfide reductase. TrxRs are high molecular weight selenoenzymes, together with the glutathione- glutaredoxin (Grx) system (NADPH, glutathione reductase, GSH, and Grx) in conjuction with Trxs monitors the cellular redox environment. In difference, bacterial TrxRs are LMW enzymes refer to their structure and catalytic mechanisms distinctively from mammalian TrxR. The foremost function of Trxs is to reduce the disulfide bonds in proteins [149]. The detailed general reaction mechanism employ by Trx antioxidant system in: the reaction proceeds through two steps. In first step, the thiol group of N-terminal Cys residue of a Trx attacks the disulfide bond of the target protein to release free thiol to form a disulfide bond. In second step, the thiol group of the C- terminal Cys residue of the thioredoxin disrupts the disulfide bond in the thioredoxin–protein complex to reduce the target protein. The thioredoxin is then oxidized which is enzymatically reduced in a NADPH-dependent reaction by thioredoxin reductase (TrxR), a flavoprotein in Trx antioxidant system. In plants, 20 thioredoxin isoforms were identified [251] and classified according to the differences in primary structure into Trx*f*, Trx*h*, Trx*m*, Trx*o*, Trx*x* and Trx*y* groups. By sequence comparison with other known thioredoxin sequences showed that thioredoxins *m*, *x* and *y* are of a prokaryotic origin [226, 322], whereas thioredoxins *f, h* and *o* are of a eukaryotic origin [222]. In case of *E. coli*, the genome codes two thioredoxins, Trx-1 and Trx-2, and one thioredoxin reductase. Where it has been identified that Trx-1 efficiently reduces phosphoadenosine phosphosulfate reductases [212] and methionine sulfoxide reductase [340]. The human genome encodes two Trx genes; one is cytosolic thioredoxin (Trx-1) and a mitochondrial thioredoxin precursor (Trx-2) and occurs in single copies and has two genes for thioredoxin reductases, cytosolic TrxR1 [116] and mitochondrial TrxR [115]. The vertebrate genome codes for several thioredoxin homologs: SpTrx1 [179]; SpTrx2 [321]; and Picot, which consists of two thioredoxin-like domains, two glutaredoxin-like domains, and one Trp14 domain [177, 395]. From Knockout experiments it has been established that devoid of

Trx-1mice die in early embryo development [245], signifying that mammalian Trx-1 and Trx-2 are vital and cannot be replaced by other reductases[67, 284] . One of the significant endogenous molecules to interact with Trx is thioredoxin interacting protein (TXNIP, TBP2, VDUP1), which is a negative regulator of Trx function [279]. The basic structure of Trx forms from 5 β-strands forming the internal core and 4 α-helices along with a short stretch of helix surround the central β-sheets outlines a reactive fold commonly termed as Thioredoxin fold. The active site disulfide is located after the β2-sheet and forms the N-terminal portion of α2 [88]. A lot of crucial enzymes in the thiol-dependent antioxidant system have this thioredoxin fold structure, such as glutaredoxin [96], peroxiredoxin [401] and glutathione peroxidase [219]. The thioredoxin fold of the proteins determines the positioning of the N-terminal Cys of the catalytic site in the immediate vicinity of the other Cys residue. Besides Thioredoxin system, some other indispensible systems present which function like Thioredoxin systems and serves as a backup for each other. It includes glutathione a system comprises of glutaredoxin-glutaredoxin reductase and glutathione reductase for example the presence of the GSH-Grx system in *E. coli* provides a strong backup for the Trx system. Infact, Grx was discovered by investigation of the substitutes to reduce RNR in a Trx-deficient mutant [148, 151]. In mammalian cells the GSH system is a major thiol-dependent antioxidant system which participates in the defense against oxidative stress via the efficient removal of various ROS by glutathione peroxidase [39, 292]. It has been described that GSH system together with Grxs can also regulate protein function by reversible protein S-glutathionylation under oxidative stress [231, 253]. In spite of the fact that the Trx and GSH systems have various extending functions, they do work in parallel in most cases. Of late compiled evidences showed that there is to a great extent cross-talk between the two systems. The glutaredoxin system was first discovered in *Escherichia coli* in 1976 as a dithiol hydrogen donor system for ribonucleotide reductase in the absence of thioredoxin 1 (Trx-1) [161] . Glutaredoxins are also thiol oxidoreductases which functions in catalyzing various SH-dependent thiol–disulfide exchange reactions. These thiol exchange reactions, includes glutathionylation and deglutathionylation of proteins; transformations of ribonucleotide reductases; and reduction of dehydroascorbates and arsenates. Glutaredoxins known to play a role in FeS homeostasis [231, 241]. This system also follows the same reaction mechanism as that of Thioredoxin system in which electrons are transferred consecutively from NADPH to glutathione reductase, glutathione, and then to one of the known glutaredoxins (Grx-1, Grx-2, and Grx-3). In brief, till date there is plentiful information regarding the functions of Trx and TrxR have been experimentally deciphered in quite lots of biological systems. Besides

detoxification of peroxides utilizing several enzymes involved it is pretty evident that it involves in maintaining DNA integrity as a "genetic material". These systems involved in the improvement of oxygen metabolism and defense against oxidative stress with the emergent concealed physiological functions together with the use of redox signalling oxidants like hydrogen peroxide and nitric oxide. Thus involved in redox signalling also by supervising the activities of many transcription factors[150, 232].

Thioredoxin reductases (TR, TrxR) (EC 1.8.1.9) are the dimeric enzyme known to reduce Thioredoxin (Trx)[268], functions as a homodimers. Each monomer contains a FAD prosthetic group, a NADPH binding domain and an active site containing a redox-active disulfide bond [145]. In general TrxR belongs to flavoproteins family of pyridine nucleotide-disulfide oxidoreductases which possess the N-terminal active site motif CVNVGC includes glutathione reductase(GR), trypanothione reductase (TryR), mercuric reductase and lipoamide dehydrogenase [14, 145]. The catalytic reaction carried out by TrxR via catalyzing the NADPH-dependent reduction of the substrate by transferring electrons from NADPH via FAD active site disulfide to "oxidized thioredoxin (Trx-S2) to give a dithiol in reduced thioredoxin (Trx-$(SH)_2$)".

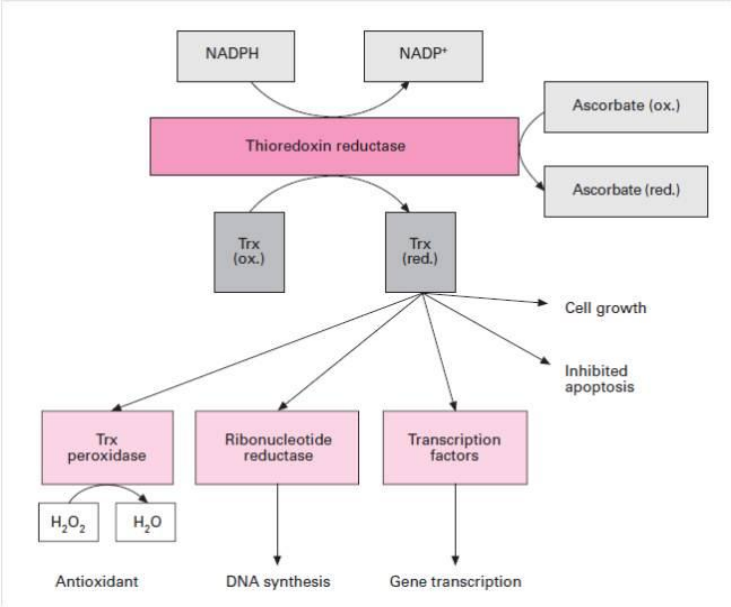

Figure 1.14 "Reactions and functions of TrxR in the cell": TrxR utilizes NADPH to catalyse the conversion of oxidized Trx (ox.) into reduced Trx (red.), and to reduce the oxidized forms of ascorbate into reduced ascorbate. Reduced Trx provides reducing equivalents to (i) Trx peroxidase, which breaks down H_2O_2 to water, (ii) ribonucleotide reductase, which reduces ribonucleotides to deoxyribonucleotides for DNA synthesis, and (iii) transcription factors, which leads to their increased binding to DNA and altered gene transcription. In addition, Trx increases cell growth and inhibits apoptosis. Fig taken from review article [268].

Two classes of thioredoxin reductase have been identified and evolved independently. First class includes a HMW (MW = ~55,000) type containing a selenocysteine residue in its active site found in higher eukaryotes including humans [390]. Second class comprises of a LMW (MW = ~ 35,000) type described in archaea, bacteria and other eukarya [145]. There is ~20% sequence identity between two classes of TrxR in its primary sequence where they can consistently aligned [145]. Three TrxR isozymes expressed in mammalian cells, TrxR1 (cytosolic), TrxR2 (mitochondrial), TrxR3 (testis-specific thioredoxin glutathione reductase) [68, 239]. Both TrxR1 and TrxR2 contain FAD and NADPH binding domains and an interface domain, whereas TrxR3 contains an extra Grx domain in the N-terminus besides FAD and NADPH binding domains. On the whole structures of mammalian TrxRs are similar to those of GR [57, 413]. The structure of low Mr TrxRs is quite distinctive as they possess only an active site-containing CXXC motif, instead of an N-terminal CVNVGC active site motif and another C-terminal active site as observed in high Mr TrxRs. Low Mr TrxRs have FAD and NADPH binding domains, but be deficient in the interface domain. The active site is located in the NADPH binding domain, not in the FAD binding domain. The two globular domains are linked by a two-stranded β-sheet. The extensively studied thioredoxin reductase is from *Escherichia coli* [262]. The structural features of TrxR from *E. coli* with a high specificity for its homologous Trx are also typical for TrxR from prokaryotes, lower eukaryotes like yeast or plants [76, 218, 264, 385]. Research on Trx and TrxR in the course of efforts in many laboratories global covers enormous areas of biomedicine. There are more than ~6100 references in pubmed demonstrating the importance of thioredoxin system in varied organisms. There several implication and role have been described for Thioredoxin systems and pertaining their role in many fields like a check in cell growth [23, 114], role in p53 activity [301],protection against oxidative stress , ascorbate recycling[44, 246], auto immune diseases [344]. Recently in *M. tuberculosis* mycoredoxin-1 (*Mt*Mrx1) acting in combination with mycothiol and mycothiol disulfide reductase (MR), as a biologically significant reducing system for *Mt*AhpE is elucidated [158].

In summary, Peroxiredoxin (Prx) plays an important role in the regulation of peroxide and protect organisms from peroxide induce oxidative damage. Therefore, they constitute an important antioxidant defense system of aerobic organisms. Also, they are involved in hydrogen peroxide signaling pathway. There are two aspects to the proposed study. One is to develop antimicrobials against CLA to control citrus greening and second is to illuminate the significance of free radical scavengers in the remedy of numerous diseases. A detailed

biochemical and structure analysis of these enzymes along with their reductase partner will enhance our understanding of structure function relationship and will lead to the development of effective inhibitor molecules against these enzymes and their efficacies will be established on infected plants under controlled conditions. Another importance outcome of structure-function analysis of Prx enzymes will be to elucidate their role in multiple cellular processes and signalling thereby develops strategies like for protection against hydrogen peroxide induced DNA damages. Structure-function studies of mutant enzymes will establish the role of catalytic residues and substrate specificities in peroxidase activity against various peroxides.

2. CLONING, EXPRESSION, PURIFICATION OF 1-CYS PRXS CLA-BCP AND ITS BIOCHEMICAL CHARACTERIZATION ALONG WITH THE CLONING OF ITS REDUCTANT PARTNER CLA-TRXA.

2.1 INTRODUCTION

Citrus Huanglongbing (HLB), a deleterious disease caused by unculturable gram negative α-proteobacterium *Candidatus* Liberibacter asiaticus (CLA) that infects citrus plants, causes extensive economic losses to the citrus industry worldwide [123, 168]. The first line of defense mechanism against the invasion of microorganisms is the production of reactive oxygen species (ROS) that includes hydrogen peroxide, peroxynitrite and organic hydroperoxides by host system constitute oxidative stress. ROS are highly reactive and participate in free radical reactions that cause damage to DNA, proteins and lipids [133, 354]. In addition, induction of carcinogenesis has been clearly linked to oxidative DNA damage [254]. Evidences that apoptosis can be induced by ROS are provided by studies in which mediators of apoptosis, induce intracellular production of ROS or are inhibited by the addition of antioxidants. Although the mechanism involved is still controversial redox status and/or hydrogen peroxide have both been proposed as critical factors [318, 358]. Owing to their dual role in both oxidative stress and signal transduction pathways, the firm control of ROS is of utmost importance.

To lessen oxidative damage to tissues, biological systems have equipped with many protective systems that get rid of ROS which includes an array of enzymes i.e. superoxide dismutase (SODs), catalase (CAT), glutathione peroxidase (GPX, GSH), glutathione reductase (GR), ascorbate peroxidase (APX), and peroxiredoxins (Prxs). Peroxiredoxins (Prxs) super family are thiol-specific antioxidant proteins known to play a major role in ROS detoxification [49, 51]. They exhibit peroxidase activity against varied hydroperoxides using thioredoxin and other thiol-containing reducing agents as an electron donor [40, 146, 303]. There have been several classifications for Prxs protein on the basis of their reactive cysteine key residue commonly termed as peroxidatic cysteine (C_PSH) and non conserved resolving cysteine (C_RSH) into 1-Cys and 2-Cys Prxs. 2-Cys Prxs further subdivided into two groups, typical or atypical types based on the location of the resolving cysteine (C_RSH) residue. Typical and atypical 2-Cys Prxs forms intermolecular or intramolecular disulfide bond respectively. Whereas 1-Cys Prx members with no or inactive C_RSH, found in a varied species but less well characterized [49, 185]. Bacterioferritin comigratory protein (BCPs), a

member of Prxs super family were originally named for their propensity to comigrate with bacterioferritin proteins initially discovered in *E. coli* [272]. BCP has been defined as the most diverse subfamily of Prxs and designated as 'C' group by Hoffmann et.al,2002 [146]. It has been further reclassified by Wakita et.al,2007 [384] into α and β-group having characteristic conserved C_pXXXXC_R motif and no C_R respectively. The biological importance of BCPs, from different pathogenic bacteria, showed that bcp mutant cells become hypersensitive towards varied peroxide substrates and eventually leads to cell impairment upon aeration [20, 41, 182, 388]. It has been cited earlier that Prxs have been associated with cell proliferation, differentiation and apoptotic pathways, and has been implicated as DNA binding protein as well [52, 142, 199]. Ellman's reagent or 5,5'-dithiobis(2-nitrobenzoate) (DTNB) is a symmetrical aryl disulfide which readily undergoes the thiol-disulfide interchange reaction in the presence of a free thiol:

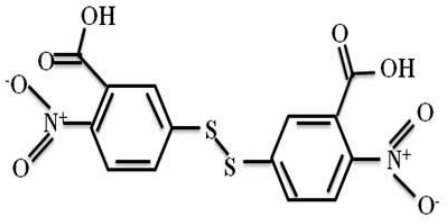

Ellman's reagent or 5,5'-dithiobis(2-nitrobenzoate)

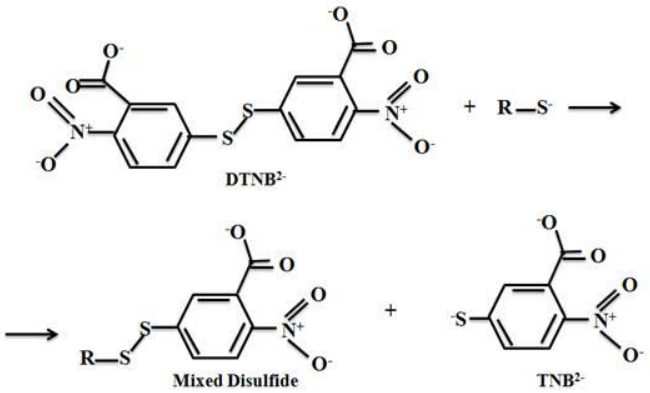

The TNB dianion has a relatively intense absorbance at 412nm compared to both disulfides thus can be used to assess the number of thiols present [90]. There are fluorogenic substrates known to detect H_2O_2, the most important ROS in regards to mitogenic stimulation or cell cycle regulation. They have been used in conjunction with horseradish peroxidase (HRP) enzyme to produce intensely fluorescent products [360]. Despite the fact that the list is quite extensive, the commonly used substrates include diacetyldichloro-fluorescein [306], "homovanillic acid" [320], and "Amplex® Red" [414]. The DCF-DA dye is quite explored one in determining the levels of H_2O_2. The diacetate form, H_2DCFDA and its acetomethyl

ester H_2DCFDA-AM are taken up by cells which then cleaved by non-specific cellular esterase resulting in a charged compound considered to be shut in inside the cell. Oxidation of non-flourogenic form H_2DCF by ROS converts the molecule into highly fluorescent form 2', 7' dichloro dihydrofluorescein (DCF), which can be easily monitored by their fluorescent intensity.

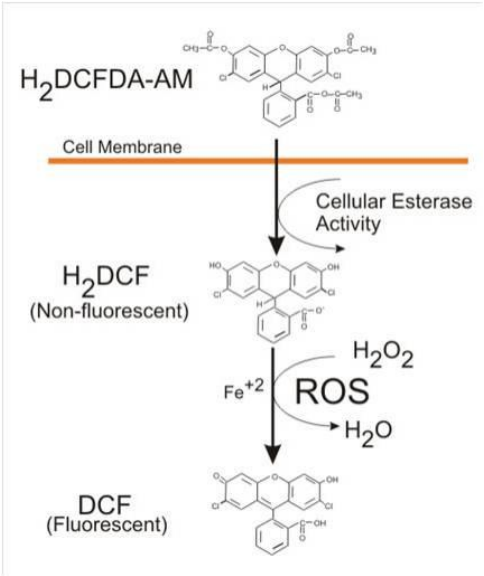

Figure adopted from application guide "an introduction to ROS" by Paul Held [138].

The capacity of phytopathogenic bacteria to multiply in host plant tissues may be due, in part, to the ability of these organisms to detoxify H_2O_2. The genome analysis of CLA showed that it possesses many genes for protection against oxidative stress. Development of effective anti microbial compounds targeting critical proteins of CLA is necessary. In this chapter we have cloned, expressed, purified, and characterized a 1-Cys peroxiredoxin BCP (CLa-BCP) from CLA. Further, its variant form, where a resolving cysteine has been introduced (CLa-BCP_{S77C}), was characterized. Peroxidase assays of both wild type and mutant form showed their ability to act on varied peroxide substrates. To the best of our knowledge this is first report of 1-Cys Prxs; BCPs to have an intracellular reactive oxygen species scavenging activity using DCF-DA dye method. Cell line based assays have shown the involvement of protein in the defense against induced H_2O_2 stress. It has been cited in literature that ROS involves in DNA lesions, so here we have shown the DNA protection activity against hydrogen peroxide.

2.2 MATERIALS AND METHODS

2.2.1. Materials

The Ni-NTA resin, BSA and SDS-PAGE reagents were purchased from Sigma-Aldrich (St Louis, MO, USA). Amicon ultra concentrator, Millex syringe filters were from Millipore Corporation, Billerica, MA. Dialysis membrane with 3500 Da cutoff was from Pierce, Rockford, USA. Hiload Superdex 200 16/60 columns were from GE Healthcare. *Taq* DNA polymerase was purchased from Promega (Madison, WI, USA). The expression vector pET28-C and rosetta BL21 lacZY derivates *E. coli* cells were purchased from Novagen Inc. Madison, WI, USA. The pET-TEV vector variant of pET28-C was provided by Dr. Shailly Tomar. Restriction enzymes, phusion high-fidelity DNA polymerase, dNTPs mix were purchased from New England Biolab Inc. Plasmid purification, gel elution; DNA clean and concentrator kit were purchased from Zymo Research (USA). All other chemicals used were of analytical grade. Hydrogen peroxide was purchased from Rankem. 1, 4-dithio-D-threitol (DTT), Diethylenetriamine pentaacetic acid (DTPA), Cumene hydroperoxide, DMEM low glucose and antibiotic mix ("100U/ml of penicillin, 100µg/ml streptomycin") purchased from (Himedia, India). Tertiary-butyl hydroperoxide (TBHP) were purchased from Sigma-Aldrich. 5, 5′-dithiobis (2-nitrobenzoic acid) (DTNB) was purchased from Cayman chemicals. All cell culture reagents and fluorescent probe DCF-DA were purchased from GIBCO (Invitrogen, USA). Adenocarcinoma breast cancer cells (MCF-7), Fibroblast-like cell line (COS7) and mouse mesenchymal stem cells (C3H10T1/2) were all obtained from National Centre for Cell Science (NCCS) Pune, India. 96-well plates were from Corning (NY, USA).

2.2.2 Genomic DNA

The CLA genomic DNA was provided by Dr. Dilip Ghosh from National Research Centre for citrus, Nagpur obtained from HLB infected sweet orange plants (*Citrus sinensis*) at Nagpur. The presence of CLA genomic DNA was confirmed by 2 CLA specific primers OI1/OI2c provided corresponding to 450bp and 1160bp amplicon sizes to confirm the presence of the genomic DNA [170].

2.2.3 Primer designing

The BCP primers were designed for optimal fragment 157 amino acid coded CLa-BCP, a 1-Cys Prxs Protein. The forward possessing NdeI restriction site and reverse possessing XhoI restriction site primer sequences are as follows:

BCP forward-5'-AATACATATGACATCTTTATCTGTGGGAGAC-'3 (NdeI)

BCP Reverse-5'-AATACTCGAGTTATTGTTTTAAGGATTTTACC-'3 (XhoI)

2.2.4 PCR conditions

For CLa-BCP gene amplifications PCR reaction was

DNA template /vector	01.0 µg
5X reaction buffer	10.0 µl
Forward primer (20pmol/µl)	01.0 µl
Reverse primer (20pmol/µl)	01.0 µl
25mM dNTPs	02.0 µl
2000U/ ml Phusion	00.5 µl
Total reaction volume	50.0 µl

And the conditions were initial denaturation at 94 °C for 4 min and rest programs includes 94 °C for 1 min/54.5 °C for 1 min / 72 °C for 1 min repeated for 30 cycles, followed by extension at 72 °C for 10 min.

2.2.5 Elution of DNA from agarose gel

Amplified PCR products were purified from 1% agarose gel using a gel elution kit from Zymo research. In brief, agarose gel slice containing DNA fragment was cut out with clean scalpel. Gel Sample was dissolved in gel solubiliser at 50 °C with intermittent mixing for 5 minutes. Complete dissolved gel solution was loaded on to the silica column provided with the kit and centrifuged. The column was washed with the wash buffer twice and eluted with the 50µl of elution solution. The concentration measurement of eluted product was done spectrophotometrically by taking an Abs at 260nm.

2.2.6 Cloning of CLa-BCP in pET-TEV vector system having TEV protease site

Amplified product of CLa-BCP and pET-TEV vector was digested with the *Nde*I and *Xho*I restriction enzymes. The total reaction mixture was as follows:

DNA template /vector	1.0 µg
10x reaction buffer	5.0 µl
10 unit/µl *Nde*I	1.0 µl
10 unit/µl *Xho*I	1.0 µl
100x BSA	0.5 µl
H_2O up to	50.0 µl

The above mentioned reaction mixture was incubated at 37 °C for 3h. Then the digested DNA got purified by low melting agarose using gel extraction kit as previously described for eluting amplified product.

The ligation of digested CLa-BCP gene and pET-TEV vector was done by DNA ligase. Briefly, the digested CLa-BCP DNA and pET-TEV vector has been ligated in 10µl of reaction mixture which contains 1 unit of DNA ligase. The reaction mixture contained:

10X Ligation buffer	1.0 µl
Vector	50.0 ng
BCP insert	250 ng
T4 DNA ligase (400CE/µl)	1.0 µl
Sterile nuclease free H_2O up to	10.0 µl

The ligation reaction was incubated at 22 °C for overnight in Thermocycler. The ligated product was used to transform XL-Blue host cell to confirm the successful cloning. The resulting transformed cells were plated onto the agar plates containing 30µg/ml of kanamycin. The cloning of insert into expression vector was verified by PCR by using gene specific primers of CLa-BCP followed by restriction digestion of cloned plasmid.

2.2.7 Sequencing of pET-TEV- CLa-BCP

The cloned pET-TEVCLa-BCP sequenced for assessment of the in frame ligation of gene into vector and mutations of the cloned gene from Eurofin, Banglore, India.

2.2.8. Site directed mutagenesis of CLa-BCP to introduce resolving Cysteine

A mutant of the wild type (CLa-BCP_{S77C}) with resolving cysteine was created by site-directed mutagenesis. The amplification was carried out using pET-TEV-CLa-BCP vector as template with forward (5'-CAGATTCTATCGCATGCCATAAAAATTTCAC-'3) and reverse (5'-GTGAAATTTTTTATGGCATGCGATAGAATCTG-'3), primers. The resulting plasmids (pET-TEV-BCP_{S77C}) were confirmed by sequencing and used for transforming E. coli rossetta, a BL-21 strain.

2.2.9 Recombinant CLa-BCP protein over expression in E. coli cells and purification

The recombinant expression vector pET-TEV having CLa-BCP insert, was transformed into the competent *E. coli* host cells rosetta. The plates were allowed to grow at 37 °C on Luria-Bertani (LB) agar plate supplemented with kanamycin (30µg/ml). A single colony of each generated strain was inoculated in LB medium (10ml) containing 0.1mg of kanamycin/ml and

grown overnight at 37 °C. The secondary culture was then done by transferring to 1 litre of fresh LB medium containing kanamycin and cultured further until the A600 (OD) reached to 0.6–0.8. The expression of the recombinant protein was then induced by the addition of 0.2mM isopropyl 1-thio-β-D-galactopyranoside, and growth was maintained at 16 °C for five hours. The cells were pelleted down by centrifugation, stored at ⁻20 °C. Frozen cells were suspended in start buffer (20mM Tris-HCl buffer (pH 8.8), containing 0.5M sodium chloride, 5mM imidazole, and 2mM phenylmethyl sulfonyl fluoride) and disrupted by sonication. The supernatants clarified by centrifugation were loaded onto a nickel affinity column (Ni-NTA column) from Sigma-Aldrich that had been equilibrated with start buffer. The conditions of His-tagged protein purification were optimized according instructions specified in manual. Then the purified protein from affinity column subjected to size exclusion chromatographic sephadex200 desalting columns (GE Healthcare) for removal of excess imidazole. Purified proteins were stored in 20mM Tris-HCl buffer (pH 8.8) in its reduced form. Protein concentrations were determined spectrophotometrically at 280nm. The extinction coefficients for reduced CLa-BCP protein including His-tag sequence (ε_{280}=18,450 M^{-1} cm^{-1}) were calculated using the ProtParam tool available on line [117].

2.2.10 SDS-PAGE analysis and molecular mass determination

Purified protein was analysed under both reducing and non-reducing conditions on a 12% SDS-PAGE gel according to the method of Laemmli [220]. The relative molecular mass of CLa-BCP was determined by performing SDS-PAGE with molecular weight standards under reducing condition. The molecular weight standards used were 97.4 kDa, Phosphorylase B; 66 kDa, Bovine serum albumin; 43 kDa, Ovalbumin; 29 kDa, carbonic anhydrase; 20.1 kDa, soybean trypsin inhibitor and 14.3 kDa, lysozyme. The Protein bands were visualized by staining with 0.15% Coomassie brilliant blue R-250.

2.2.11 Sequence analysis and multiple sequence alignment

Homologous sequences were identified using the BLAST search tool blastp program (URL-http://blast.ncbi.nlm.nih.gov) by taking non-redundant (nr) database and protein data base (PDB) [7] at the NCBI web site (http://www.ncbi.nlm.nih.gov/). All the sequences were aligned to understand evolutionary relationship between the similar sequences and conserved amino acid, by using online server using ClustalW Web server (http://www.ebi.ac.uk/Tools/msa/clustalw2/) taking default parameters.

2.3. CLONING OF REDUCTANT PARTNER THIOREDOXIN CLA-TRXA

2.3.1 Primer designing

The reductant partner for CLa-BCP, a Prxs protein; Thioredoxin, CLa-TrxA gene (GenBankTM accession number GenBank: EXU78407.1, originally annotated as TrxA gene) was also amplified by PCR using genomic DNA of the CLA strain as template. The Trx primers were designed for optimal fragment 107 amino acid coded CLa-TrxA protein. The forward possessing NdeI restriction site and reverse possessing XhoI restriction site primer sequences were as follows:

Forward 5'-AATACATATGATGAGTGCATTAAAAG-'3 (NdeI)

Reverse 5'-GGCGCTCGAGTCATTATACTCGGGATAATATC-'3 (XhoI)

2.3.2 PCR conditions

For CLa- TrxA gene amplifications PCR reaction mixture was:

DNA template /vector	01.0 µg
5X reaction buffer	10.0 µl
Forward primer	01.0 µl
Reverse primer	01.0 µl
25mM dNTPs	02.0 µl
2000U/ ml Phusion	0.5 µl
Total reaction volume	50.0 µl

And the conditions were 94°C (4 min), 94°C (1 min)/ 61°C (40 sec) / 72°C (1 min) for 30 cycles, followed by 72°C (10 min).

2.3.3 Elution of DNA from agarose gel

PCR products were purified from 1% agarose gel using a gel elution kit from Zymo research. In brief, agarose gel slice containing DNA fragment was cut out with clean scalpel. Sample was incubated at 50 °C after adding gel solubiliser. Complete solution of tube was loaded on to the silica column provided with the kit and centrifuged. The column was washed with the wash buffer twice and eluted with the 50µl of elution solution. The concentration measurement of eluted product was assessed either by measuring optical density on a spectrophotometer or by visualizing on an agarose gel.

2.3.4 Cloning of CLa-TrxA in pET-TEV vector system having TEV protease site

Amplified product of CLa-TrxA and pET-TEV vector was digested with the *Nde*I and *Xho*I restriction enzymes. The total reaction mixture contained:

DNA template /vector	1.0 µg
10x reaction buffer	5.0 µl
10 unit/µl *Nde*I	1.0 µl
10 unit/µl *Xho*I	1.0 µl
100x BSA	0.5 µl
H_2O up to	50.0 µl

The above reaction mixture was incubated at 37 °C for three hours. The digested DNA was purified by low melting agarose using gel extraction kit as previously described in this chapter. The ligation of digested CLa-TrxA gene and pET-TEV vector was done in 10µl of reaction mixture. Briefly, the digested CLa-TrxA DNA and pET-TEV vector has been ligated in 10µl of reaction mixture which contains 1 unit of DNA ligase. The reaction mixture contained following components:

10X Ligation buffer	1.0 µl
Vector	50.0 ng
CLa- TrxA insert	250 ng
T4 DNA ligase (400CE/µl)	01.0 µl
Sterile nuclease free H_2O up to	10.0 µl

The ligation reaction was incubated at 22 °C for overnight in Thermocycler. The ligated product was used to transform XL-Blue host cell to confirm the successful cloning. The transformed cells were plated onto the agar plates containing 30µg/ml of kanamycin. The presence of insert was verified by PCR by using gene specific primers of CLa-TrxA and isolated plasmid as a template and also by restriction digestion.

2.3.5 Recombinant CLa-TrxA protein over expression in *E. coli* cells and purification

The recombinant expression vector pET-TEV having CLa-TrxA insert, was transformed into the competent *E. coli* BL-21 (DE3) host cells. The plates were allowed to grow at 37 °C on Luria-Bertani (LB) agar plate supplemented with kanamycin (30µg/ml). A single colony of each generated strain was inoculated in LB medium (10 ml) containing 0.1mg of kanamycin/ml and grown overnight at 37 °C. The secondary culture was then done by transferring to 1 litre of fresh LB medium containing kanamycin and cultured further until the A600 reached to 0.6–0.8. The over expression of the recombinant protein was accomplished

by the addition of 0.2mM isopropyl 1-thio-β-D-galactopyranoside, and growth was maintained at 16 °C. After overnight incubation, cells were harvested by centrifugation and stored at ⁻20 °C. Frozen cells were suspended in start buffer (20mM Tris-HCl buffer pH 8.0), containing 0.3M sodium chloride, 5mM imidazole, and 2mM phenylmethyl sulfonyl fluoride and disrupted by sonication. The supernatants clarified by centrifugation were loaded onto a nickel affinity column (Ni-NTA column) from Sigma-Aldrich that had been equilibrated with start buffer. The conditions of His-tagged protein purification were optimized according to the manufacturer's instructions.

Protein concentrations were determined spectrophotometrically at 280 nm. The extinction coefficients for CLa-TrxA protein (ε_{280}=18,115 M^{-1} cm^{-1}) and (ε_{280}=17,990 M^{-1} cm^{-1} assuming all Cys residues are reduced) were calculated using the ProtParam tool available on line[117].

2.3.6 SDS-PAGE analysis and molecular mass determination

Purified protein was analysed under both reducing and non-reducing conditions on a 12% SDS-PAGE gel according to the method of Laemmli [220]. The relative molecular mass of CLa-TrxA was determined by performing SDS-PAGE with molecular weight standards under reducing condition. The molecular weight standards used were 97.4 kDa, Phosphorylase B; 66 kDa, Bovine serum albumin; 43 kDa, Ovalbumin; 29 kDa, carbonic anhydrase; 20.1 kDa, soybean trypsin inhibitor and 14.3 kDa, lysozyme. The Protein bands were visualized by staining with 0.15% Coomassie brilliant blue R-250.

2.4 DETERMINATION OF FREE THIOL CONTENT OF BOTH CLA-BCP AND CLA-BCP$_{S77C}$ PROTEIN

Free sulfhydryl concentration in both Cla-BCP and CLa-BCP$_{S77C}$ in its reduced form was estimated spectrophotometrically at 412 nm using DTNB [310], Ellman cited values ranging from 11,400 to 14,150 M^{-1} cm^{-1} for TNB^{2-} depending upon the buffer, chaotropic agent used in a reaction mixture. DTNB; 5, 5'-dithiobis (2-nitrobenzoate) is a symmetrical aryl disulfide which readily undergoes the thiol-disulfide interchange reaction in the presence of a free thiol. The TNB dianion has a relatively intense absorbance at 412 nm compared to both disulfides. DTT standards were made (0, 5, 10, 15, 20, and 30μM). Both CLa-BCP and CLa-BCP$_{S77C}$ were pre-reduced with reducing agent 2mM βME followed by dialysis against buffer 20mm Tris-HCl pH 8.0 and buffer 20mm Tris-HCl pH 8.8 respectively and with 5.0 eq of natural

reductant partner thioredoxin, TrxA. All thiol assays were done in 1.0 mL volumes containing adequate protein to give A412 values between 0.5 and 1.0. The stoichiometry of the reaction was calculated by using the extinction coefficient of 14150 M^{-1} cm^{-1}. The presented values were representatives of three replicate assays.

2.5 PEROXIREDOXIN ACTIVITY ASSAY WITH XYLENOL ORANGE ASSAY

BCPs, involved in peroxide detoxification thus detoxification ability of CLa-BCP towards hydrogen peroxide substrate was determined by utilizing the xylenol orange reagent (see table 2.1). This assay is based on the basic principle, which includes complex formation of the dye xylenol orange with the peroxide substrate that can be measured spectrophotometrically at 560 nm. The procedure adopted for determining the remaining concentration of hydroperoxide was from [154]. In the first reaction, the activity of CLa-BCP was determined by following the decrease of A560 in dependence on the amount of protein present in 0.1ml of reaction mixture. The peroxidase reaction of wild-type CLa-BCP protein was started by the addition of hydroperoxide (100μM). After incubation of the reaction at 37 °C for about 20 minutes, 0.9 ml of xylenol orange reagent (mentioned in table 2.1) was added and concentration of remaining peroxide was determined by measuring the absorbance at 560 nm. The value was corrected for background reduction of the substrate in the absence of the CLa-BCP. The assay typically contained 2mM DTT, 1mM azide, 0.1mM diethylenetriaminepentaacetic acid (DTPA) and 100μM of peroxide in 20mM Tris-HCl (pH 8.8). The working reagent was routinely calibrated against solutions of H_2O_2 with known concentrations.

Remaining hydroperoxide concentration in simple words its consumption due to the enzymatic reaction was determined by subtracting the non enzymatic reaction that occurs in the absence of protein from the reaction that occurs in the presence of protein. To identify the formation of sulfenic acid intermediate of protein S-OH group while reacting with hydroperoxide. The same reaction was started with 200 μM of hydrogen peroxide, in which protein was pre-treated with 1000 eq of dimedone, a sulfenic acid modifying agent.

Tab. 2.1 Components of xylenol orange reagent

The components of the working reagent containing the dye xylenol orange were added in the depicted order.

Component

4mM butylated hydroxytoluene

250mM H_2SO_4 (pH -1.6)

2.5mM Fe (NH4)(SO4)2

1.25mM Xylenol orange

2.6 DTT-LINKED PEROXIDASE ASSAY

The dithiothreitol (DTT)-linked peroxidise activity of purified CLa-BCP and CLa-BCP_{S77C} was performed, with slight modifications, as described by Atack et al. [20]. The first reaction was carried out with different hydrogen peroxide (H_2O_2) concentration keeping CLa-BCP concentration constant i.e. 1µM. The whole reaction volume was of 1ml containing 20µl of 0.1M DTT, 5.3µl of 188µM of CLa-BCP, 2 µl of 0.5M EDTA and varying concentration of the substrate from 100mM stock concentration in 20mM Tris-HCl (pH 8.8) buffer at room temperature. The blank was done with reaction buffer without H_2O_2, DTT and recombinant CLa-BCP by taking absorbance spectra at 310 nm. The negative control was done with reaction buffer in the absence of CLa-BCP. Finally the reaction was commenced by addition of different H_2O_2 concentration and absorbance spectras were recorded at 310 nm. Second set of reaction was carried out by taking effective concentration of substrate H_2O_2 (2mM),1mM EDTA, 2mM DTT and 1µM of CLa-BCP in 20mM Tris-HCl (pH 8.8) buffer.

The similar reactions were carried out with other peroxides like cumene hydroperoxide, tertiary-butyl hydroperoxide (TBHP). The same procedure was adopted for CLa-BCP_{S77C} protein reaction volume change according to the stock concentration of purified protein. Experiments were done in triplicate to avoid ambiguity of the experimental approach and results as well.

2.7 DNA PROTECTION ASSAYS

The ability of CLa-BCP and CLa-BCP_{S77C} to protect super coiled plasmid DNA against oxidative damage was assayed by a slightly modified method of Hicks et al [142]. The super coiled plasmid DNA pBR322 (100ng) was used for carrying out the peroxide mediated DNA nicking assay. The reaction volume was 20µl, firstly the protein (8µM) was pre incubated with super coiled DNA and then H_2O_2 was added (final concentration of 6mM). The reaction was incubated for 90 min at 37°C. Positive control was 100ng of pBR322, second control reaction was DNA treated with H_2O_2. Finally all the reactions were stopped by addition of DNA loading buffer and visualized by electrophoresis on ethidium bromide-stained 1.0% (wt/vol) agarose gels. A DNA super coiling assay based on thiol dependent metal catalyzed

oxidation system was also performed as described by Rho et al [309]. The pBR322 DNA (100ng) was mixed treated with 1µl of 0.1M DTT (working 5mM DTT), 3 µl of 0.01M $FeCl_3$ (15µM $FeCl_3$), and 5 µl of 80µM (20µM working concentration) of protein in 0.02 M Hepes-NaOH (pH 7.0) buffer, and incubated for 30 min at 37 °C. The reaction was stopped by adding 2µl of 0.5M EDTA to a final concentration of 50mM. For positive control, EDTA was added prior to starting the reaction. Reactions were directly analyzed by agarose gels electrophoresis using ethidium bromide-stained 1.0% (wt/vol) gel. Control experiments were done in the absence of protein, only DNA, DNA with H_2O_2.

2.8. PROTECTION AGAINST APOPTOSIS

2.8.1. Cell culture and treatment

The cell lines were grown in DMEM low glucose supplemented with 10% heat inactivated fetal bovine serum and 1% antibiotic mix (100 U/ml of penicillin and 100 µg/ml streptomycin) at 37 °C in incubator with a humidified atmosphere of 5% CO_2. The cells were then challenged with different H_2O_2 concentrations ranging from 0.5 to 100µM for 16 hours and then examined for cell viability using MTT assay. Accordingly, 100µM concentration of H_2O_2 was selected for this study.

2.8.2. Cell viability assay

The cell viability was assessed by MTT assay, which is a test of normal metabolic status of cells [263]. In brief, both COS7 and MCF7 cells were plated at seeding density of 5×10^3 in 96-well plates in 200µl of medium and grown under a humidified atmosphere. When the cells attained proper confluency, they were treated with various concentrations of recombinant protein, both wild type and mutant form (20µl of 1mg/ml), and further incubated for 30 min. Then, 100µM of H_2O_2 was added to the cell culture medium, and incubated for another 24 h at 37°C. Cultures were then assayed by the addition of 20µl of 10mg/ml MTT followed by, incubating it for another 4 h at 37 °C. The MTT-containing medium was then aspirated, and 100 µl of DMSO was added to solubilise the water insoluble formazon and the absorbances were determined on a FLUOstar optima microplate reader (BMG Labtech, Germany) at 570 nm. The optical density of the formazan generated in the control cells was considered to represent 100% viability. The data are expressed as mean percentages of the viable cells versus the respective control.

2.8.3. Determination of intracellular ROS by DCFH-DA

The intercellular ROS scavenging activity of protein was carried out using an oxidant-sensitive fluorescent probe DCF-DA(2′, 7′-dichloro-dihydrofluorescein diacetate) [403]. DCF-DA is hydrolyzed by intracellular esterase and converted to non-fluorescent DCFH which then oxidized to highly fluorescent DCF. DCFH-DA method was followed for the detection of intracellular ROS as previously described by Rosenkranz et.al., 1992 [319]. Briefly, the C3H10t1/2 and MCF-7 cells were seeded in 48-well plates at a concentration of 1 × 10^5 cells/ml. After 16 h, the cells were then treated with effective concentrations of the recombinant protein (1 µM), and incubated at 37°C under a humidified atmosphere. After 30 min, 100 µM H_2O_2 was added, and the cells were incubated for an additional 30 min. Finally, (DCFH-DA at a concentration of 5µg/ml) was introduced to the cells. Images from control and treated groups were observed under fluorescent microscope (Axiovert 25, Zeiss, Germany). Fluorescent intensities of images from three independent experiments were quantified using image-J software (NIH, USA).

2.9 RESULTS AND DISCUSSION

2.9.1 PCR amplification of BCP gene from genomic DNA

Genomic DNA template has been also used to amplify the CLa-BCP gene, using gene specific primers with restriction sites. A 471bp fragment of CLa-BCP gene (Fig 2.1) encodes a 157 amino acid protein.

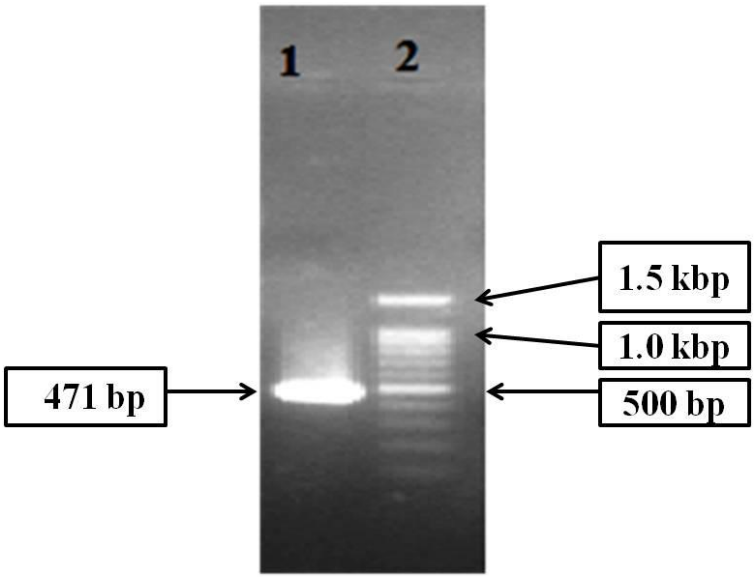

Figure 2.1: Agarose gel electrophoresis Lane1- PCR amplification of CLa-BCP**,** Lane2-100bp marker

2.9.2 Cloning confirmation

The inframe cloning of CLa-BCP gene was done by restriction digestion and ligation into expression pET-TEV vector. The colonies obtained through antibiotic selection plates were verified for the presence of positive clones by PCR and restriction digestion (Fig 2.2).

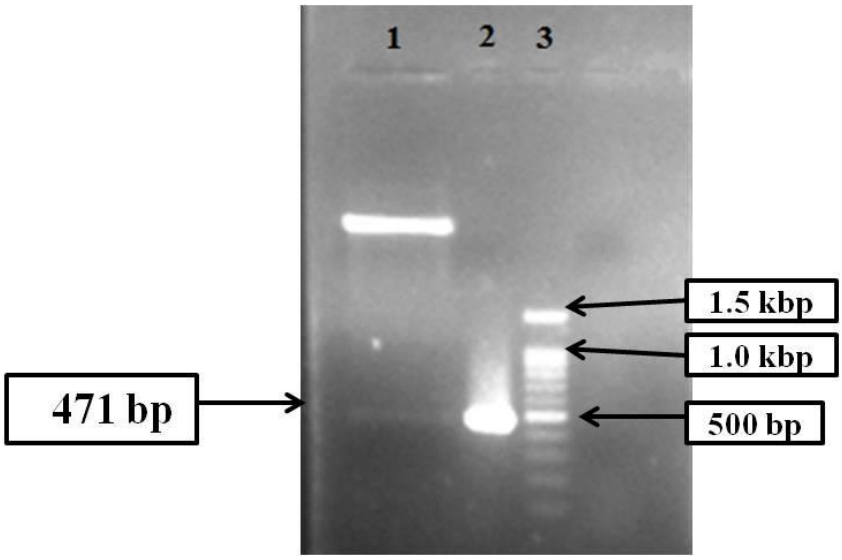

Figure 2.2: Agarose gel electrophoresis Lane1- restriction digestion of pET TEV - CLa-BCP plasmid, Lane 2- PCR amplification from pET TEV - CLa-BCP plasmid, Lane 3- DNA ladder.

2.9.3 Deduced sequence of cloned CLa-BCP and mutant CLa-BCP$_{S77C}$

The deduced sequence was having single cysteine in case of wild type CLa-BCP plasmid. A non-conserved Cys has been introduced at 77th position replacing serine to create a BCP mutant (Fig 2.3).

```
1           MTSLSVGDKAPHFVLPSNDEQEISLLALGGSKIVLYFYPKDDTSGCTAEAINFSSLKADF 60
CLa-BCP     MTSLSVGDKAPHFVLPSNDEQEISLLALGGSKIVLYFYPKDDTSGCTAEAINFSSLKADF 60
            ************************************************************

1           DEESTILIGISPDSIASHKKFHQKHNLSITLLADESKEVLKSYDVWKEKSMFGKKYMGVV 120
CLa-BCP      DEESTILIGISPDSIASHKKFHQKHNLSITLLADESKEVLKSYDVWKEKSMFGKKYMGVV 120
            ************************************************************

1           RTTFLIDEKGIIAQIWKPVTLKNHAQSVLKMVKSLKQ 157
CLa-BCP      RTTFLIDEKGIIAQIWKPVTLKNHAQSVLKMVKSLKQ 157
            *************************************
```

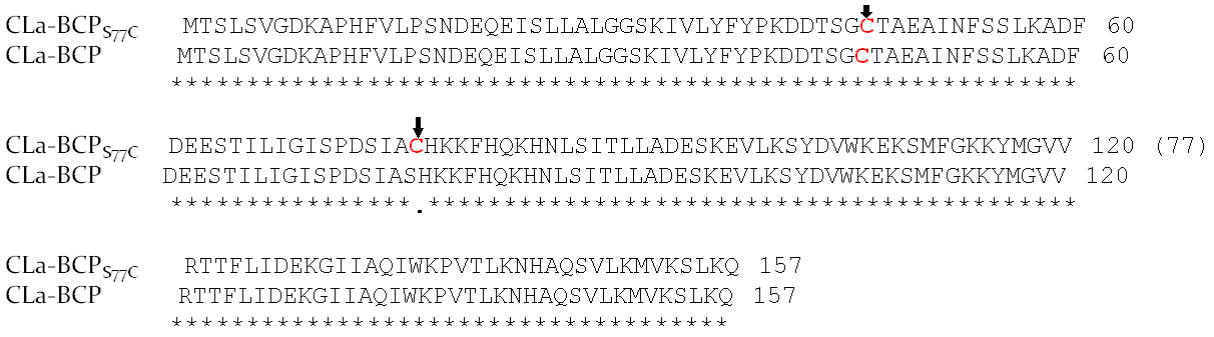

Figure 2.3: Deduced sequence after cloning into expression vector 1 represents the annotated sequence of BCP in database where CLa-BCP and CLa-BCP$_{S77C}$ are the cloned sequence and mutated sequence respectively after site directed mutagenesis. Bold arrow indicates the key "C" cysteine residue and their position.

2.9.4 Recombinant protein over expression and purification of CLa-BCP and CLa-BCP$_{S77C}$

The *E.coli* Rosetta cells with CLa-BCP plasmid were transformed, induced by IPTG and kept at 18 °C for 5hours at 200 rpm. The purification of both CLa-BCP and CLa-BCP$_{S77C}$ was achieved in two steps by affinity Ni-NTA followed by gel filtration chromatography. The purity was confirmed on a 12% SDS-PAGE gel. A single band corresponding to approximately 19.6 kDa, under both reducing and non-reducing SDS-PAGE, was observed for CLa-BCP (Fig. 2.4 A). A single peak around 70-80 ml was seen for CLa-BCP (10mg/ml) when subjected to gel filtration column Superdex 200. This depicts its oligomeric conformation when extrapolated on the basis of molecular weight standards (Fig. 2.4 B). However when run on non-reducing SDS-PAGE showed single band at ~19.6 kDa in both reducing and oxidizing conditions. Thus oligomeric conformation of CLa-BCP is quite confusing. Therefore a lower concentration of protein (5mg/ml) when loaded onto gel filtration column gave a peak around 95-110 ml which correspond to its monomeric nature (Fig. 2.4 C). Thus one thing is clear that, the protein undergoes oligomerisation in a concentration dependent manner. At higher concentration it tends to form oligomers, this phenomenon is observed while carrying out the experiment like ITC (data not shown).

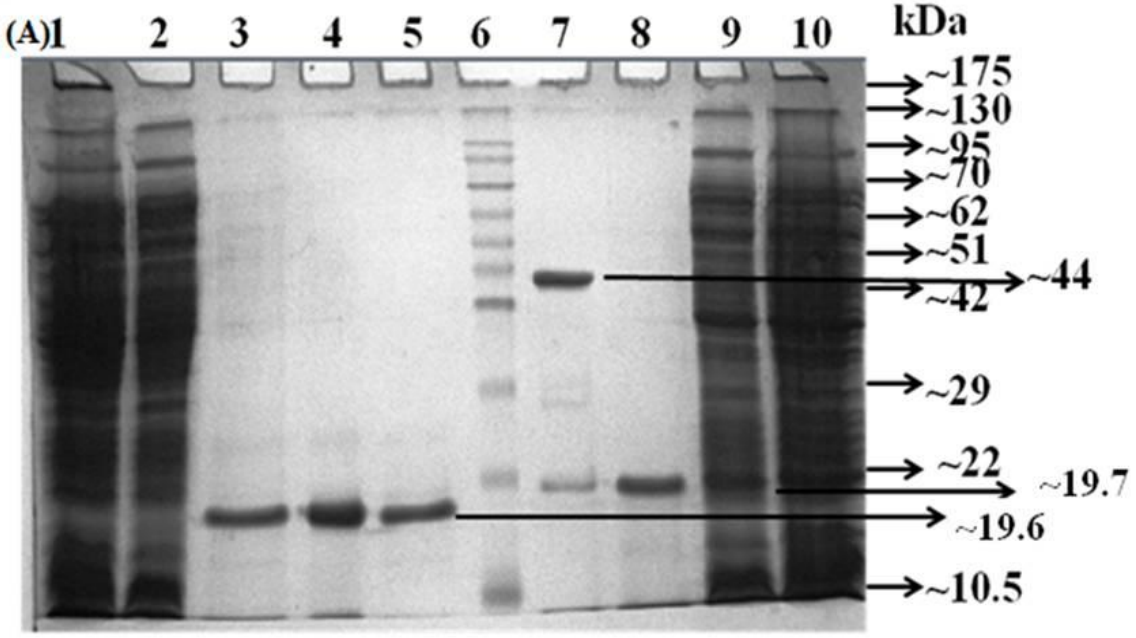
(A)1
2
3
4
5
6
7
8
9
10
kDa
~175
~130
~95
~70
~62
~51
~44
~42
~29
~22
~19.7
~19.6
~10.5

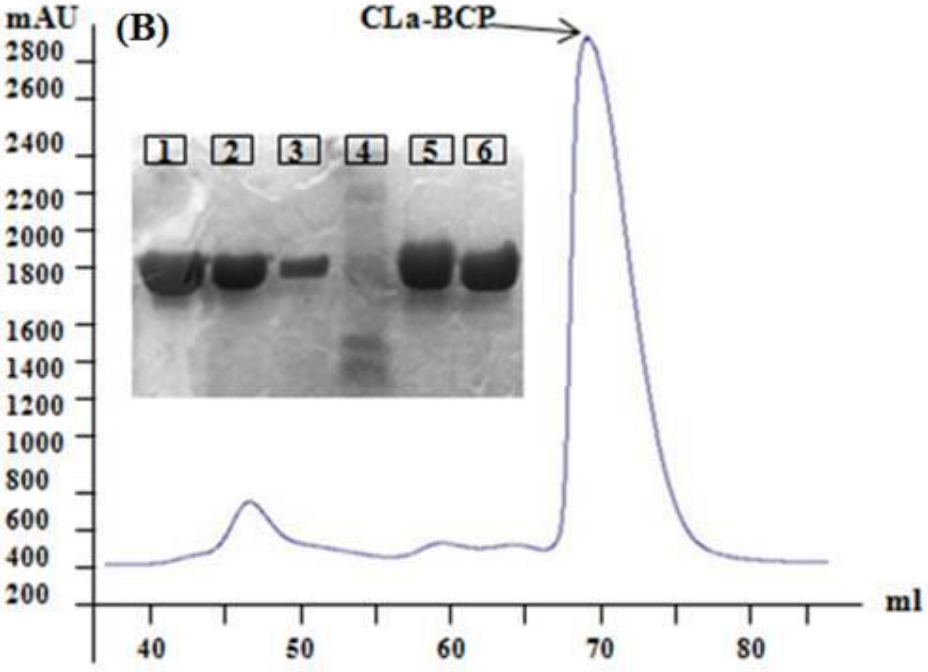
mAU
(B)
CLa-BCP
2800
2600
2400
2200
2000
1800
1600
1400
1200
1000
800
600
400
200
1
2
3
4
5
6
ml
40
50
60
70
80

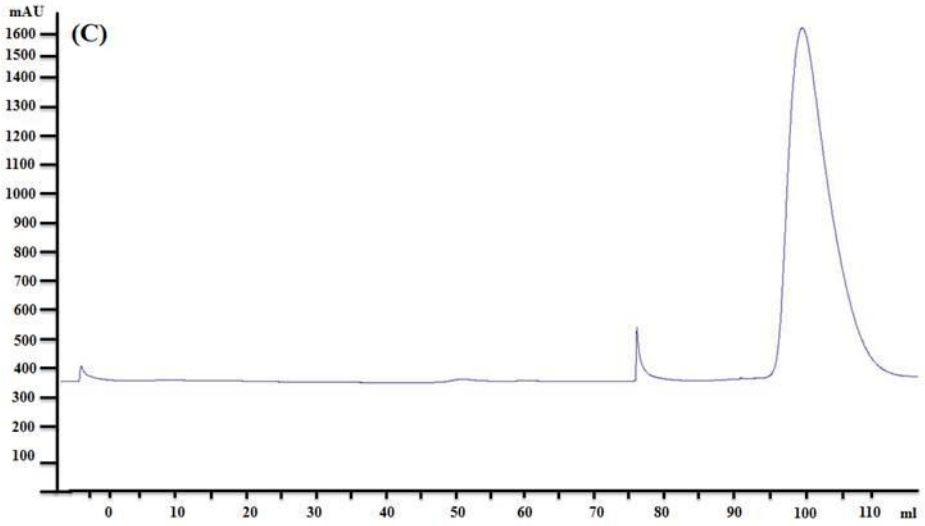

Figure 2.4: Purification profile of both CLa-BCP and mutant CLa-BCP_{S77C}. (A) SDS-PAGE gel of protein purification of both CLa-BCP (lane 1-5) and mutant CLa-BCP_{S77C} (lane 7-10). Purified CLa-BCP in reduced condition (lane 3, 4) and in non-reducing condition (lane 5) was monomeric. While CLa-BCP_{S77C} in non-reducing condition (lane 7) confirms the presence of disulfide bond and in reduced condition (lane 8) showed single band. (B) Gel filtration profile of CLa-BCP fractions of major peak in reducing (lane 1-3), molecular weight marker (lane 4) and in non-reducing condition and oxidizing conditions (lane 5, 6) respectively. (C) Gel filtration profile of CLa-BCP (5mg/ml).

In initial purification experiments of mutant CLa-BCP_{S77C}, it has been observed that CLa-BCP_{S77C} in its native form tends to aggregates and degrades gradually, while in reduced form it is quite stable. A single band around 21 kDa was observed under reducing condition while an increase intensity of 44 kDa band was seen under non-reducing condition suggesting the fact that intermolecular disulfide bond formation takes place (Fig. 2.4 A). During dimer formation, an increase intensity of ~44 kDa band and a reduced intensity of 21 kDa band was observed. It suggests that mutant protein undergoes oligomerisation with predominance of dimeric species. During purification experiments, it has been observed that CLa-BCP_{S77C} protein in its native form tends to aggregates, but when subjected to gel filtration column showed anomalous peaks merging with each other (Fig 2.5 A). All the monomeric, dimeric species peaks tends to merge with each other and undergoes aggregation thus showing a major peak around 45 ml which was close to void volume of the column. In order to avoid the aggregation of the protein, the purification and gel filtration was carried out in the buffer containing 10mM βME. The reduced gel filtration profile showed a single peak 90-100 ml depicting the monomeric species in reduced condition of dimeric protein (Fig 2.5 B). Introduction of C-terminal cysteine might be acting as resolving cysteine or not and resulting mutant CLa-BCP_{S77C} may follows typical or atypical 2-Cys Prxs mechanism need to be deciphered.

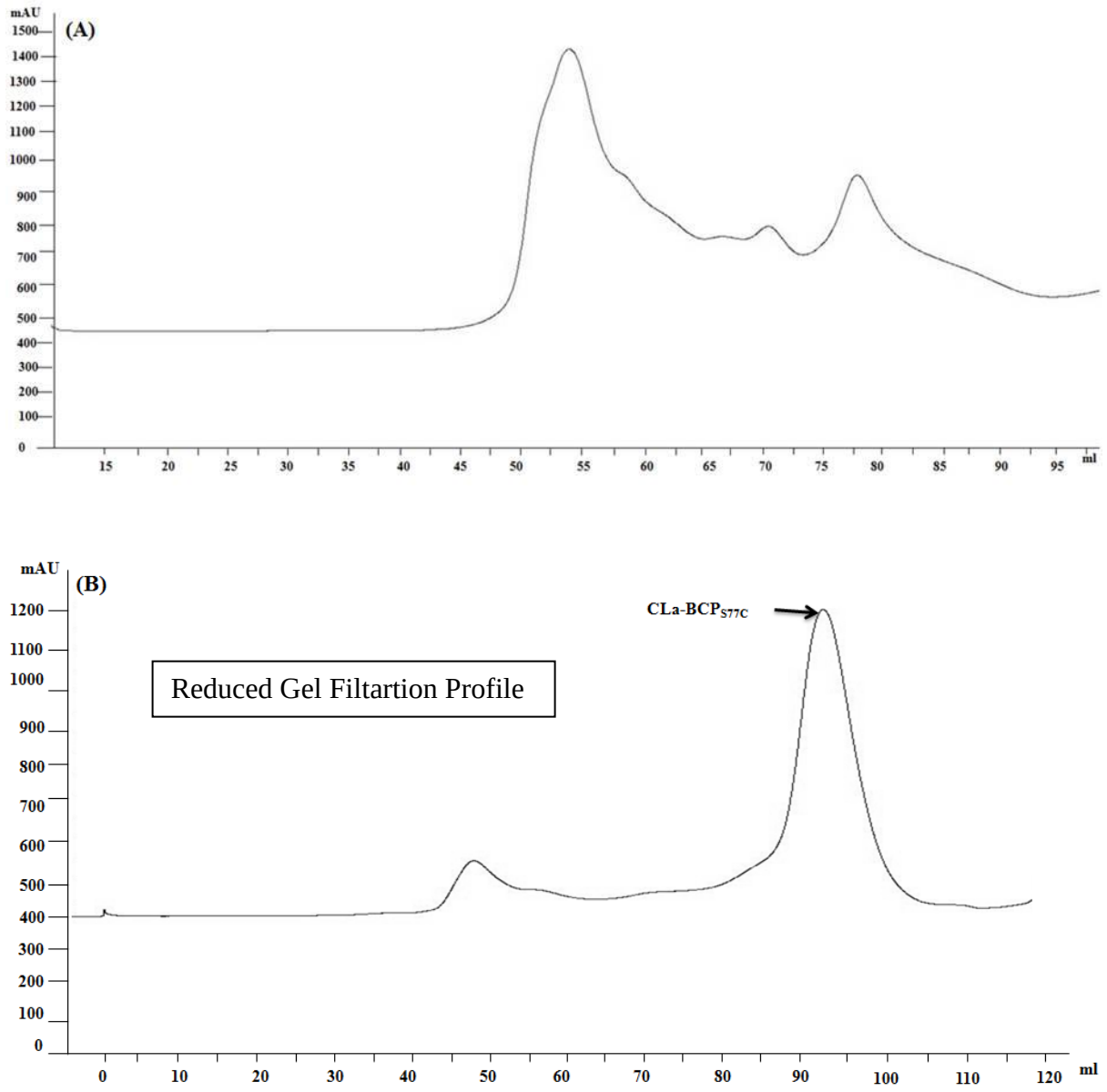

Figure 2.5: Gel filtration profile of CLa-BCP$_{S77C}$ in both normal and reduced condition. (A) Gel filtration in its native form showed merged peak at (45ml tailing peak till 90ml) depicting its aggregation behaviour. (B) In reduced condition, a single peak (90ml-100ml) showing the monomer condition of the protein in its reduced condition.

2.9.5 Amino acids sequence similarity search by NCBI-BLAST

The BLAST similarity search against the nr and pdb database showed the CLa-BCP belongs to Prx family. The sequence was found to contain putative conserved domain belonging to Thioredoxin-like super family (AhpC) (Fig 2.6). Since the wild type CLa-BCP contains a single cysteine residue, it can be referred to as a 1-Cys Prx. Sequence search was carried out using the BLAST search tool at the NCBI web site (http://www.ncbi.nlm.nih.gov/).

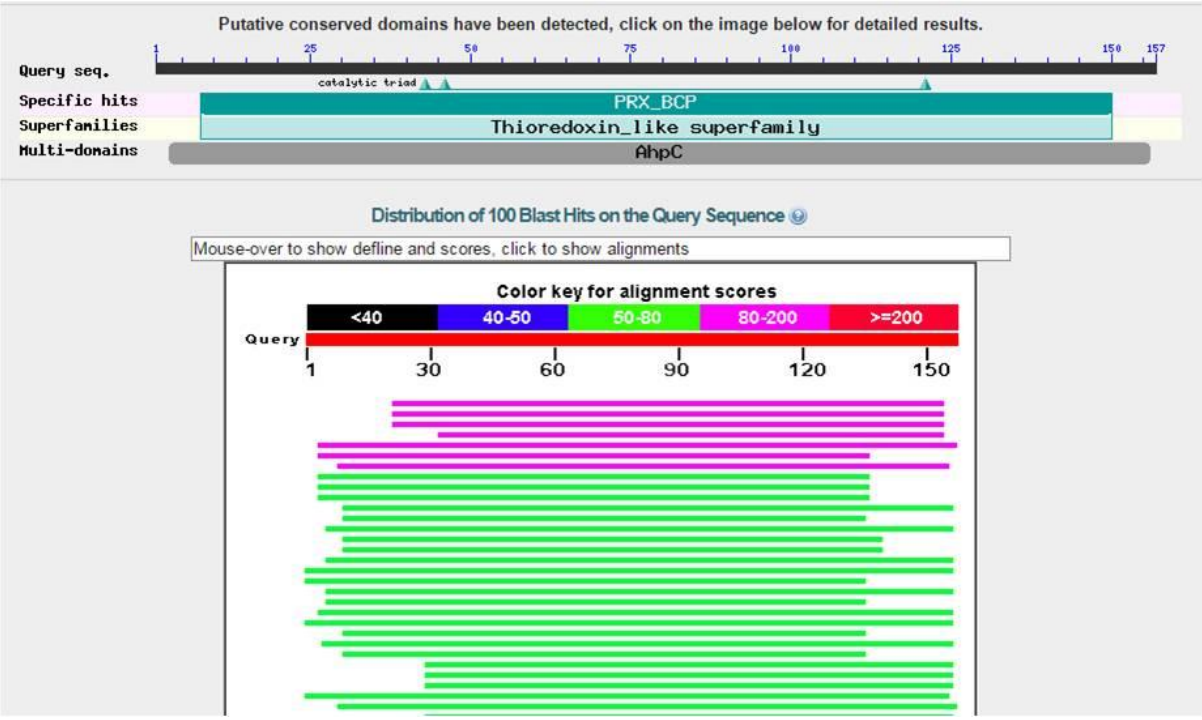

Figure 2.6: Sequence similarity search was done with the NCBI BLAST search program against Protein Database.

2.9.6 Homology search against PDB and Multiple sequence alignment with related bacterial Prxs

The BLAST result showed that CLa-BCP is highly similar to bacterial Bacterioferritin comigratory protein from 3GKK *Xanthomonas Campestris* Bacterioferritin Comigratory Protein, 3IXR *Xylella Fastidiosa* PrxsQ, and 3DRN Bcp1 from *Sulfolobus Sulfataricus* which are mainly known as plant pathogens against the PDB database. CLa-BCP shared 38% identity with 3GKK *Xanthomonas* bcp, *38% with* 3IXR PrxsQ and 39% identity with *Sulfolobus* bcp1.

Multiple sequence alignments were carried out using ClustalW Web server (http://www.ebi.ac.uk/Tools/msa/clustalw2/) taking default parameters. In general, multiple sequence alignment (MSA) showed maximum sequence identity ranging from (76%-55%) with Prxs (both 1 and 2-Cys) particularly to alkyl hydroperoxide reductase from variety of pathogenic bacteria. All of them possess conserved active site residue that in general are referred as peroxidatic cysteine residue at 46th position along with conserved catalytic triad (Y) Tyr, (P) Pro, (K) Lys (Fig 2.7). Beside the conserved catalytic triad, GCT motif more precisely known to have conserved PXXXTXXC motif is also present in other peroxiredoxins family of proteins. Phylogenetic analysis showed that it is closely related to BCPs (PRX)

from different organisms which includes *Candidatus* Liberibacter solanacearum (CLso) having 1-Cys while *helicobacter*, *campylobacter* and *caulobacter* known to have more than 2-Cys residue. CLa-BCP is phylogenetically slightly diverged from alkyl hydroperoxide reductase (AhpC/TSA) family (Fig. 2.8).

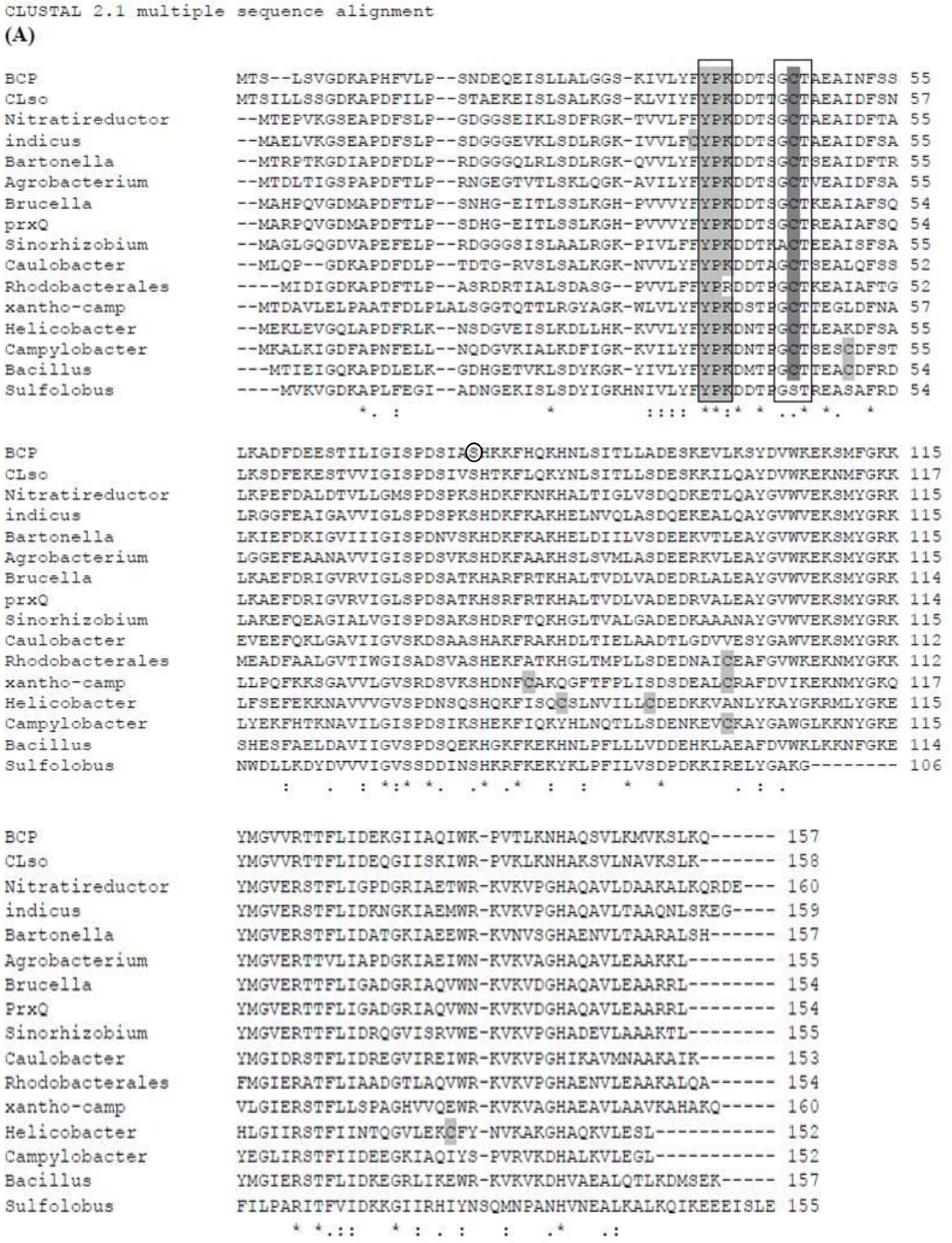

Figure 2.7: Multiple Sequence alignment of Cla-BCP and bacterial members of the peroxiredoxin subfamily. Catalytic triad (Tyr Y, Pro P and Lys K) and conserved peroxidatic cysteine are highlighted in dark grey color and non-conserved cysteine in light grey color.

Black rectangles point to residues resides at the catalytic site, including the peroxidatic cysteine at position 46 in CLa-BCP. Encircled serine residue represents the residue which has been mutated to cysteine in CLa-BCP$_{S77C}$. Organisms and their sequence accession numbers used are as follows: *Xanthomonas campestris* (ZP_06490734.1), *Candidatus* Liberibacter solanacearum (YP_004063129.1), *Agrobacterium tumefaciens* (NP_354814.1), *Nitratireductor aquibiodomus* (ZP_10235041.1), *Brucella melitensis* (NP_539966.1), *Bartonella schoenbuchensis* (CBI82261.1|), *Brucella sp*. NVSL 07-0026 (ZP_06792951.1), *Helicobacter pylori* (NP_222845.1), *Bacillus subtilis* (YP_054574.1), *Sinorhizobium meliloti* (NP_385847.1), *Caulobacter crescentus* CB15 (NP_420678.1), *Rhodobacterales* bacterium (ZP_05074732.1), *Campylobacter upsaliensis* (ZP_07893129.1), *Nitratireductor indicus* (ZP_11157137.1), *Sulfolobus Sulfataricus* (pdb|3DRN).

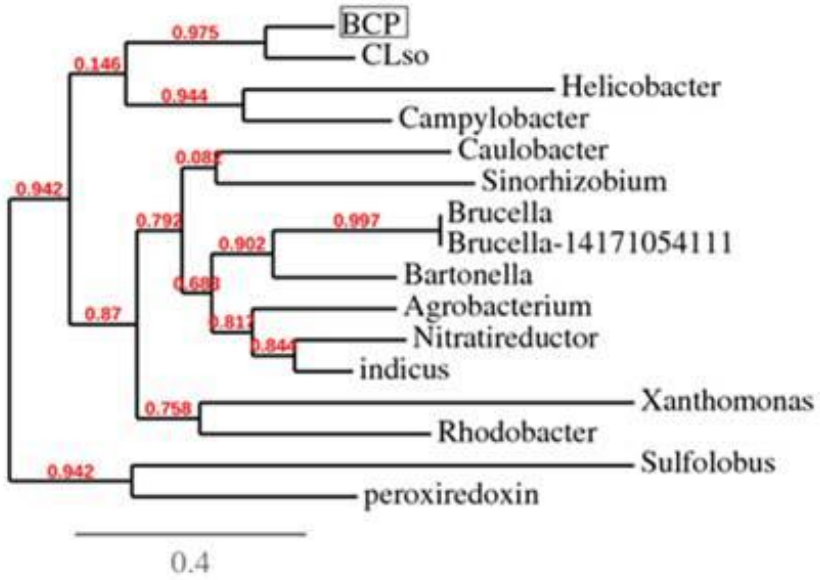

Figure 2.8: Phylogenetic tree of CLa-BCP with some closly related Prxs subfamily BCPs constructed by Phylogeny.fr programme. Tree constructed by the "maximum likelihood method" dividing them into different groups. The numbers indicate the confidence levels for the relationship of the paired sequences as determined through bootstrap statistical analysis.

Cloning, expression and purification of reductant partner Thioredoxin, TrxA

2.9.7 PCR amplification of CLa- TrxA gene from genomic DNA

Genomic DNA template was used to amplify the CLa-TrxA gene, using gene specific primers with restriction sites. A 324bp fragment was obtained for CLa-TrxA gene (Fig 2.9) which encodes for a small protein of 107 amino acids.

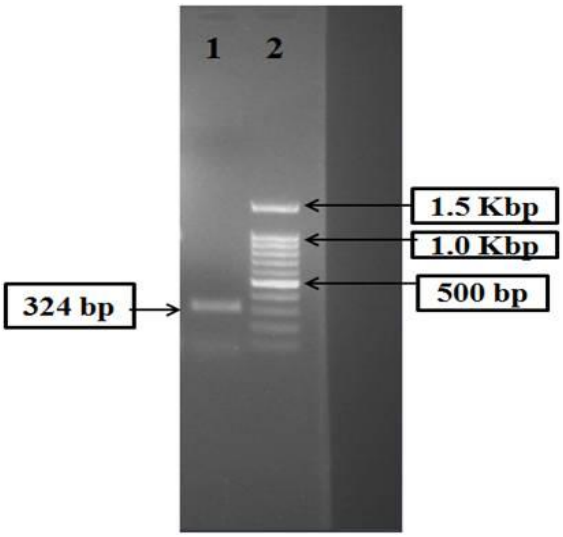

Figure 2.9: Agarose gel electrophoresis Lane1- PCR amplification of CLa- TrxA**,** Lane2- 100bp marker

2.9.8 Cloning confirmation

Directional cloning of CLa-TrxA gene was done by restriction digestion and ligation into in pET-TEV vector. The colonies obtained through antibiotic selection plates were verified for the presence of positive clones by PCR and restriction digestion (Fig 2.10).

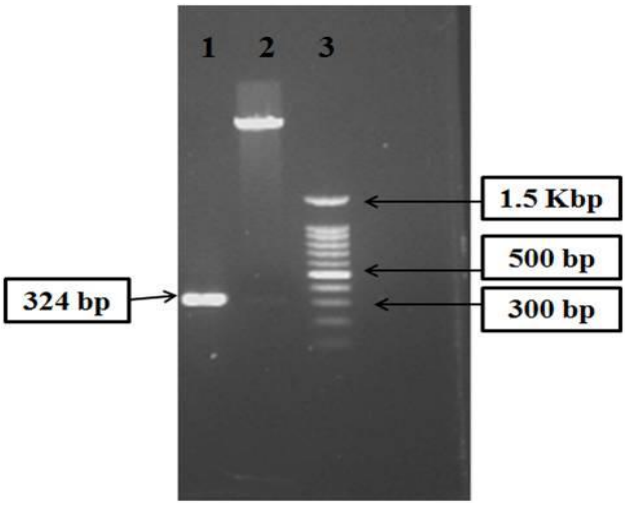

Figure 2.10: Agarose gel electrophoresis Lane1- PCR amplification of pET TEV - CLa-TrxA plasmid, Lane 2- restriction digestion from pET TEV - CLa- TrxA plasmid, Lane 3- DNA ladder

2.9.9 Recombinant protein over expression and purification of CLa- TrxA

The CLa-TrxA plasmid was transformed into *E.coli* BL-21(DE-3) expressing host cells. The protein was induced by 0.2mM IPTG and kept at 16 °C for 5h at 200 rpm. The purification of CLa-TrxA was achieved in two steps involving affinity Ni-NTA followed by gel filtration

chromatography. The purity was confirmed on a 15% SDS-PAGE gel. A single band corresponding to approximately 12.6 kDa in reducing condition was observed. The same protein showed a dimeric state (SDS band observed at ~25.2 kDa) under non-reducing SDS-PAGE, was showed to be in dimeric form (Fig. 2.11).

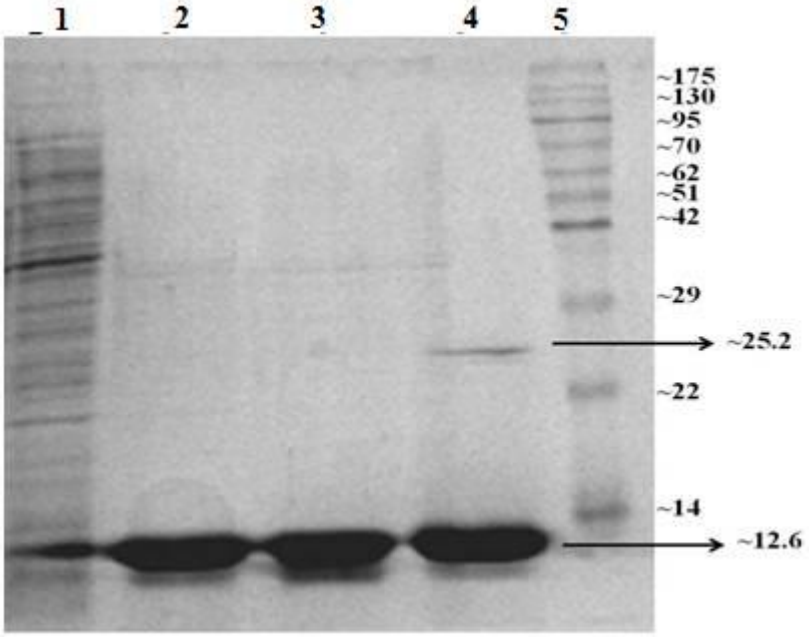

Figure 2.11: 15% SDS-PAGE reducing gel of recombinant CLa-TrxA **(**indicated by arrows). SDS-PAGE gel of protein purification of CLa-TrxA,(lane 4) in non-reducing condition confirming the presence of disulfide bond.

2.9.10 Determination of free thiol content of both Cla-BCP and CLa-BCP$_{S77C}$ protein

CLa-BCP was pre reduced with reducing agent βME followed by dialysis to ensure the removal of excess reducing reagent. Thus the estimation of thiol content was done for 1µM of reduced protein. Molar extinction coefficient (ε) of DTNB at 412nm is 14150 $M^{-1}cm^{-1}$, is defined as follows: ε=A/bc where A-absorbance, b-path length in cm and c-concentration in moles per litre. For calculation of free thiols group the dilution factor and volume used in reaction should be taken into consideration. Therefore, we have used the formula including all parameters.

Sulfhydryl concentration in µmole per ml= total reaction volume× 1L/1000ml × c [calculated from c=A/bε] present in the assay solution but original contribution by sample volume calculated as follows:

Concentration of free sulfhdryl present in sample used = Moles/reaction volume × 1000ml/1L

From the above formula, 350 X 10^{-5} M free sulfhydryl present in 1µM of reduced protein while there was no absorbance seen in case of oxidised form of protein. The same protocol was followed for CLa-BCP_{S77C} and it was 60.2 X 10^{-5} M free sulfhydryl present in 1µM of reduced CLa-BCP_{S77C} while there was no absorbance seen in case of oxidised form of protein. The natural reductant, Thioredoxin (TrxA) was also used to reduce the proteins. Both the proteins when pre-reduced with 5eq of Thioredoxin (TrxA), a natural reductant for Prxs proteins, 50 X 10^{-5} M free sulfhydryl present in 1µM of protein.

2.9.11 Peroxiredoxin activity assay with xylenol orange assay

The detoxification of peroxides by Prxs has been well established. Here we have used the easily detectable reagent for estimating the peroxide consumption, the ferrous xylenol reagent. This reagent gives absorbance at 560 nm when complex with peroxides [178]. The wild type CLa-BCP showed remarkable peroxiredoxin activity towards hydrogen peroxide (Fig. 2.12). When Prxs reacts with oxidizing agent like hydrogen peroxide the C_P group forms an intermediate termed as sulfenic acid (C_PSOH). Thus here we have employed the sufenic acid specific reagent; dimedone to inactivate the key peroxidatic residue C_PSOH. To our surprise, here in our case there was no effect of dimedone inactivation on CLa-BCP in DTT dependent peroxiredoxin activity (Fig. 2.12). The probable reason could be that DTT is sufficient to reduce the sulfenic acid into thiols for activity. Thus DTT could be used as an important reductant system explored for further peroxidase assay.

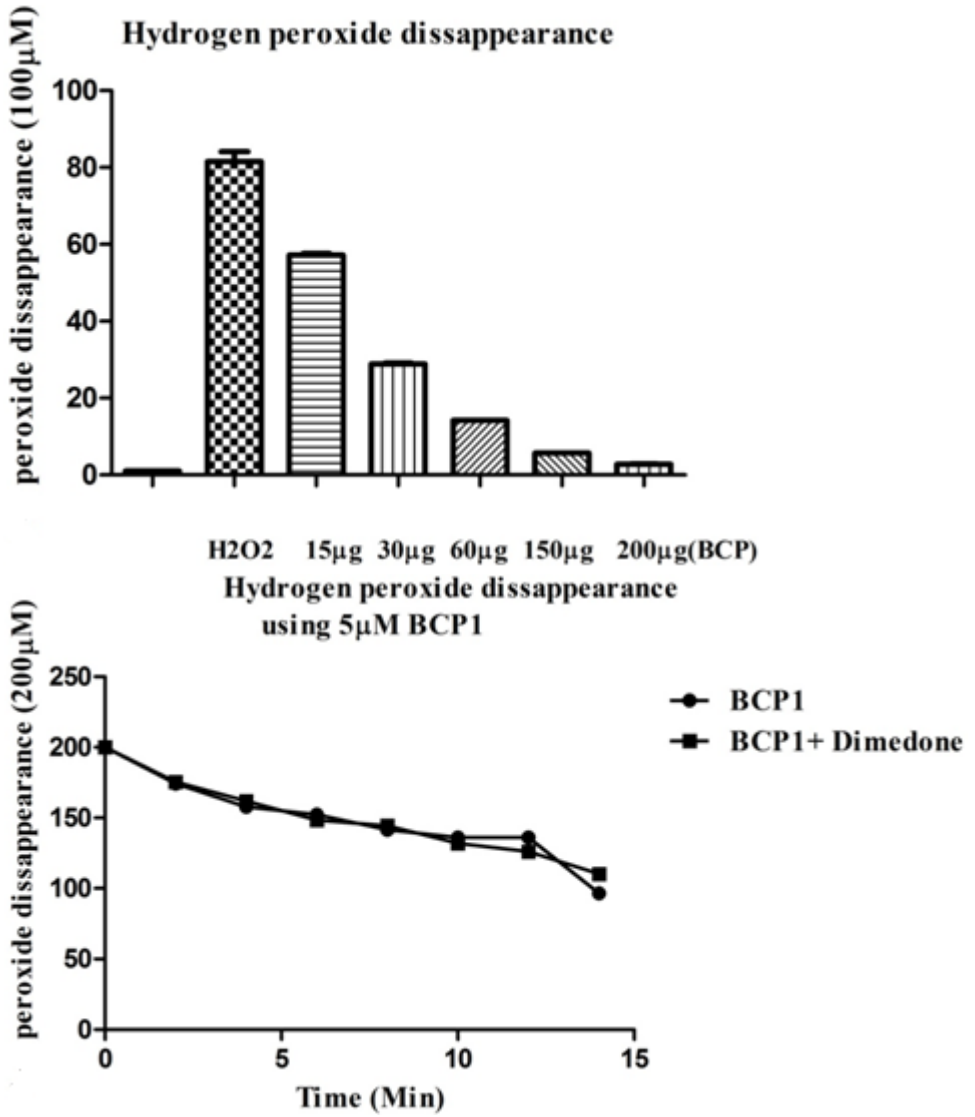

Figure 2.12: Peroxiredoxin activity ferrous xylenol assays for CLa-BCP (A) removal of H_2O_2 in DTT-dependent peroxidase assay by CLa-BCP, the remaining hydroperoxide content was measured using ferrous xylenol reagent and quantified in triplicate, and results are the mean +-S.D.U. (B) Dimedone inactivation of CLa-BCP, prior to the DTT-dependent peroxidase assay CLa-BCP protein treated with 1,000 eq of dimedone (closed squares) at room temperature for 30 min. The reactions were done in a mixture containing 200µM, 2mM DTT, and 5µM CLa-BCP at 37 °C. As a negative control, a peroxidase reaction was performed without CLa-BCP.

2.9.12 Peroxidase activity of purified CLa-BCP and its variant CLa-BCP$_{S77C}$

The peroxidase assay showed that both CLa-BCP and CLa-BCP$_{S77C}$ were able to catalyze peroxide-dependent DTT oxidation (Fig. 2.13 G). The effective concentrations for reductant and substrate were reaction to be carried out obtained after initial experiments with varying concentrations of both (Fig. 2.13 A-F). In high concentration of DTT, CLa-BCP showed considerable peroxidase activity towards varied organic hydroperoxides. The final assays

were performed with 10mM substrate concentration, keeping both protein and reductant DTT concentration constant (1µM and 2mM) respectively (Fig. 2.13 G). In case of CLa-BCP_{S77C} peroxidase activity with higher substrate concentration (mainly H_2O_2 and cumene-H_2O_2) got saturated in half time of the CLa-BCP. The endogenous electron donor for catalytic turnover of BCPs is not known but here in our study it can be turned over with non-physiological dithiothreitol thiol system.

(A) DTT Linked peroxidase assay of BCP1

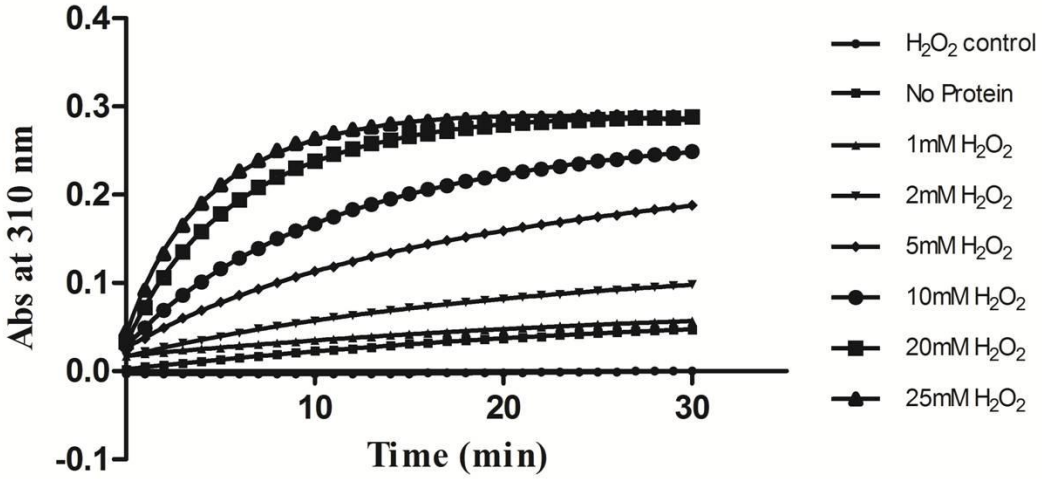

(B) Dtt Linked peroxidase assay of CLa-BCP

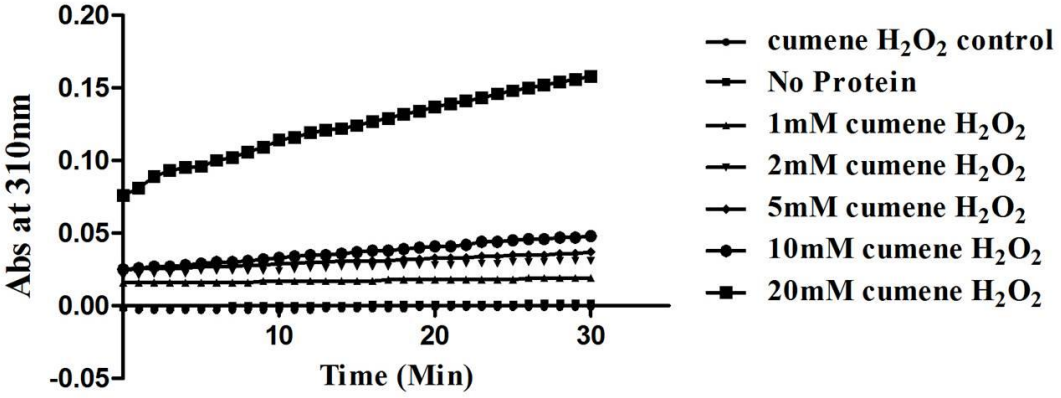

(C) DTT Linked Peroxidase assay of CLa-BCP

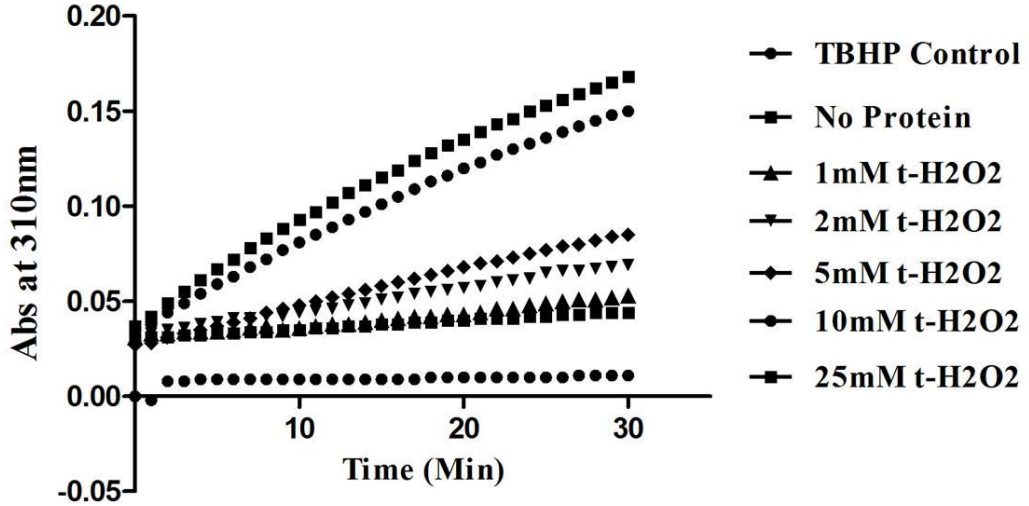

Dtt Linked peroxidase assay of CLa-BCP$_{S77C}$

(D)

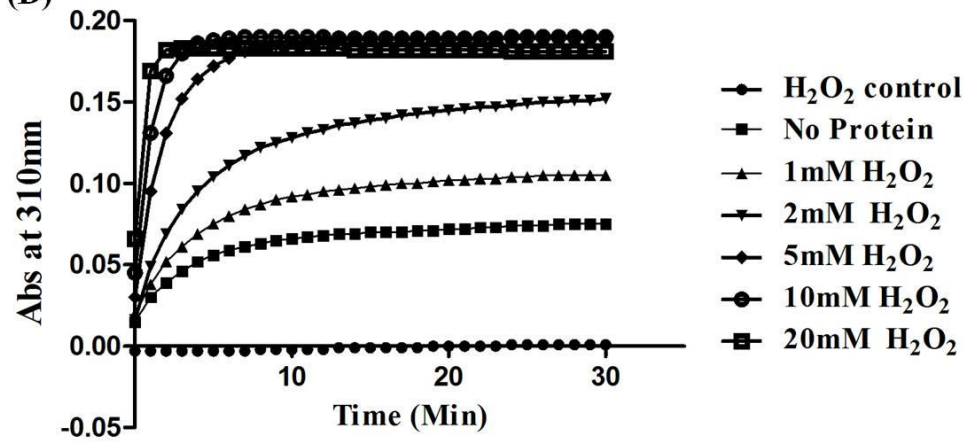

Dtt Linked peroxidase assay of CLa-BCP$_{S77C}$

(E)

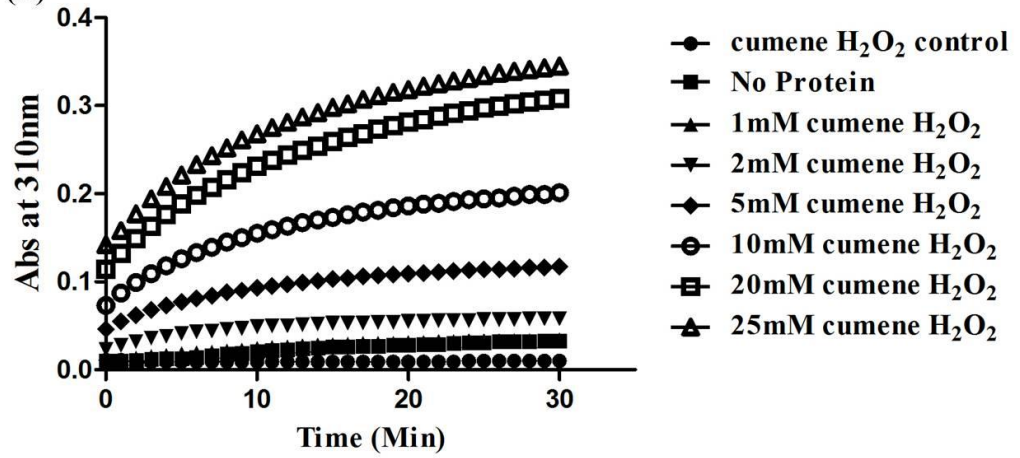

Dtt Linked peroxidase assay of CLa-BCP$_{S77C}$

(F)

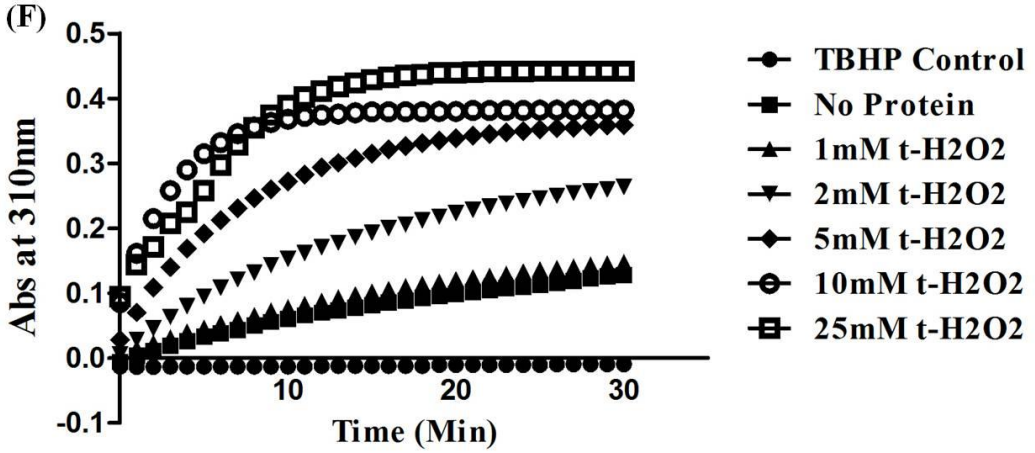

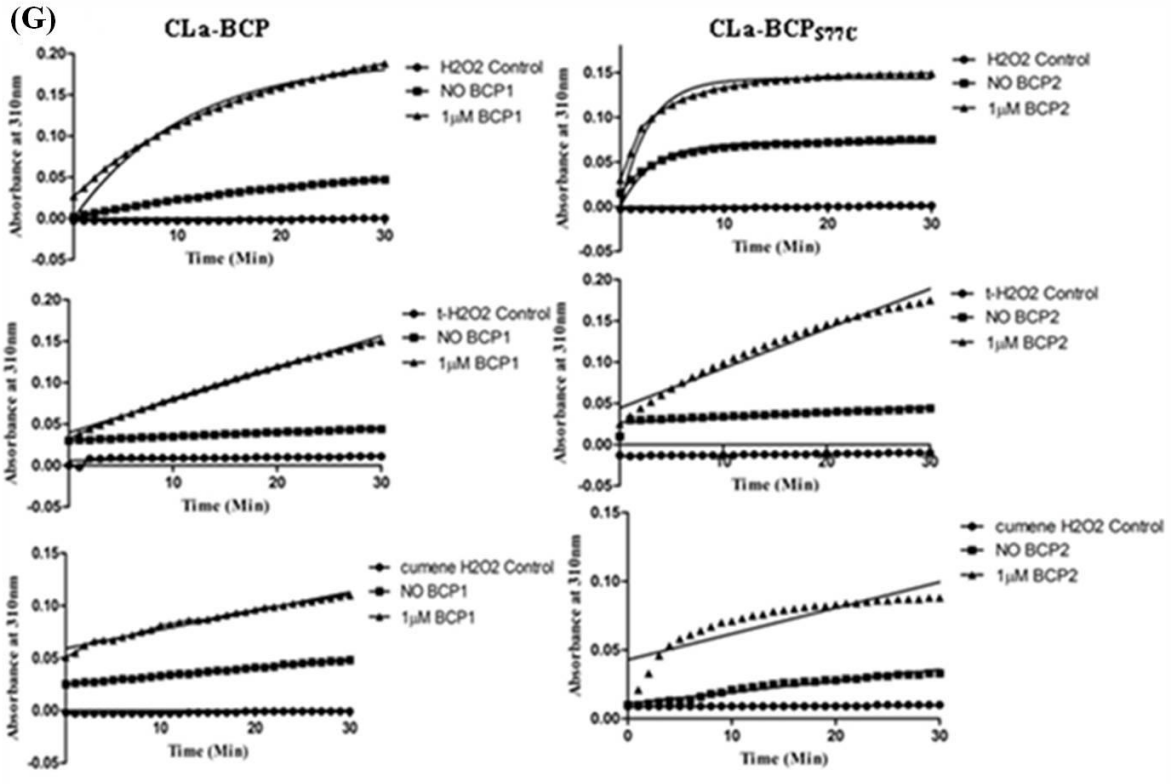

Figure 2.13: DTT linked peroxidase activities of purified protein. (A-F) DTT oxidation monitored with different concentration of substrates for both CLa-BCP and CLa-BCP_{S77C} in a course of 30 minutes. (G) Comparison panel, an absorbance time course at 310 nm (because of oxidized DTT) in the absence (closed circle) or the presence (closed triangle) of the protein shown, using proteins CLa-BCP (left column) and CLa-BCP_{S77C} (right column). The reaction mixture contained 20mM Tris-HCl (pH 8.8), 1 mM EDTA, 1μM pure CLa-BCP & CLa-BCP_{S77C}, 2mM DTT, and 10mM peroxide (hydrogen peroxide, cumene hydroperoxide, or tert-butyl-hydroperoxide) in a total volume of 1 ml at 37°C. The reaction was started by the addition of the substrate.

2.9.13 DNA protection activity from oxidative damage

The CLa-BCP and CLa-BCP_{S77C} were tested for DNA protection activity from oxidative damage by reactive oxygen species (ROS) using thiol-dependent metal catalyzed oxidation (MCO) system [195] and direct H_2O_2. The assay was carried out using supercoiled DNA. The supercoiled (SC) form was predominant then nicked circular (NC) when DNA was left untreated. In presence of H_2O_2, the linear form of DNA was observed and both SC and NC forms disappeared as a consequence of oxidative damage. An addition of CLa-BCP to the reactions increased the NC form along with SC and linear forms of DNA demonstrating the DNA protection activity (Fig. 2.14 A). In MCO system, the SC form was predominant then NC form when DNA was left untreated (lane 1, Fig. 2.14 B). The DNA was completely degraded when treated with thiols (DTT along with $FeCl_3$) in negative control (lane 2,

Fig.2.13 B). The clear DNA protection activity was observed in case of CLa-BCP as both SC and NC forms were found to be intact against generated hydroxyl radicals (lane 4, Fig. 2.13 B) similar to that of EDTA (positive control) in which both SC and NC form of DNA remained in intact from thus resisting oxidative nicking (lane 3, Fig.2.14 B). It has already been reported that Prxs and related proteins [142, 234, 309] shows a DNA-binding ability, interacts with DNA to protect it thus resulting in protection from oxidative nicking of DNA. The variant of CLa-BCP did not shown strong DNA protecting activity as NC form of DNA was predominant with marginal appearance of linear DNA (lane 5, Fig.2.14 B). Instead of DTT when ascorbate was used as a reducing agent, the wild-type enzyme and mutant were shown to have negligible effect in protecting the SC DNA (data not shown), confirming that ascorbate cannot acts as a reducing agent for both wild type and mutant proteins .

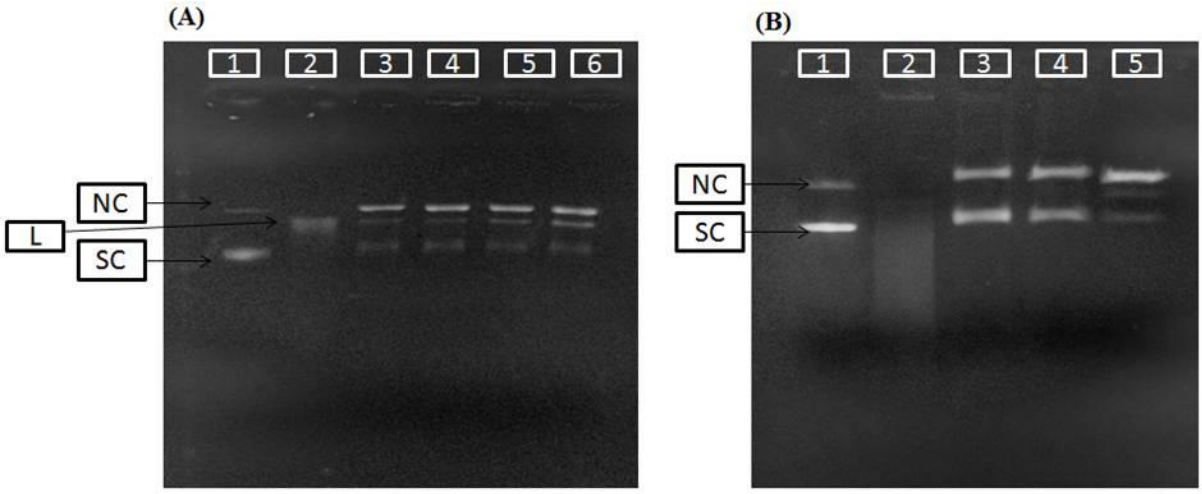

Fig 2.14 CLa-BCP and CLa-BCP_{S77C} (S77C) protect supercoiled plasmid DNA from nicking by H_2O_2. (A) Supercoiled (SC) pBR322 DNA (100 ng) (lane 1) was treated with 6 mM H_2O_2 for 30 min, resulting in linear (L) pBR322 (lane 2). Reactions were also done in the presence of 1 µM CLa-BCP (lane 3-4) and 1 µM CLa-BCP_{S77C} in its native (lane 5-6). (B) pBR322 supercoiled plasmid DNA (100ng) (lane 1) mixed with 5mM DTT and 20 µM $feCl_3$ results into complete degradation of DNA (lane2). Reactions carried out with 1 µM of CLa-BCP and CLa-BCP_{S77C} (lane 4 and 5), positive control (lane 3).The assay is a representative from three independent experiments.

2.9.14 Protection against Apoptosis

The protective effect of CLa-BCP and CLa-BCP_{S77C} on cell viability against H_2O_2-induced cell damage was assessed using MTT assay. As shown in (Fig.2.15 B), cell viability in non-treated cancerous cell line; MCF-7 cells were assigned as 100%, whereas in the H_2O_2-treated cells, the cell viability was reduced to 60%. However, both CLa-BCP and CLa-BCP_{S77C} could prevent the H_2O_2-induced cell damage at increasing concentrations from 0.1 to 10 µM. The

cell viability was increased from 60 to 90% in case of MCF-7 cell line. Almost a similar pattern of response was observed in normal cell line (COS7) (Fig.2.15 A). When challenged with H_2O_2, ~30-40% reduction in cell viability from positive control (buffer) was observed. While the cells when pre-treated with increased protein concentration was able to rescue the H_2O_2 mediated cell death.

In order to elucidate the antioxidant activity of CLa-BCP and CLa-BCP_{S77C}, the intracellular ROS scavenging activities were also determined. In case of C3H10t1/2 cells, although the untreated cells did not show any symptoms of oxidative stress, the relative fluorescent intensity was raised significantly in response to H_2O_2 ($p < 0.05$), indicative of oxidative stress. Interestingly, the cells pre-treated with 1 μM of CLa-BCP and CLa-BCP_{S77C} proteins followed by challenging with H_2O_2, the intensity was reduced significantly almost by 50% ($p < 0.001$ and $p < 0.01$) respectively as compared to H_2O_2 treated cells. The intracellular ROS scavenging activities of both the proteins were 2-fold as compared to positive control (Fig.2.15 C). In a similar pattern, in the presence of CLa-BCP and CLa-BCP_{S77C} the fluorescence intensity was reduced to almost 40% in response to those proteins in MCF-7 cells ($p < 0.01$ and $p < 0.001$) respectively (Fig.2.15 D). In brief, our results showed that the treatment of different concentrations of protein is able to rescue the hydrogen peroxide mediated cell killing. The DCF-DA dye assay showed the intercellular ROS scavenging activity of both CLa-BCP and CLa-BCP_{S77C} induced by H_2O_2 within cells. The protein exerted the antioxidant activity against radicals generated in MCO system and cell protective effect against H_2O_2-induced cell damage and apoptosis. To the best of our knowledge, the ROS scavenging activity within cells for 1-Cys Prxs especially BCPs is the first report of such activity and hence demands further in depth analysis.

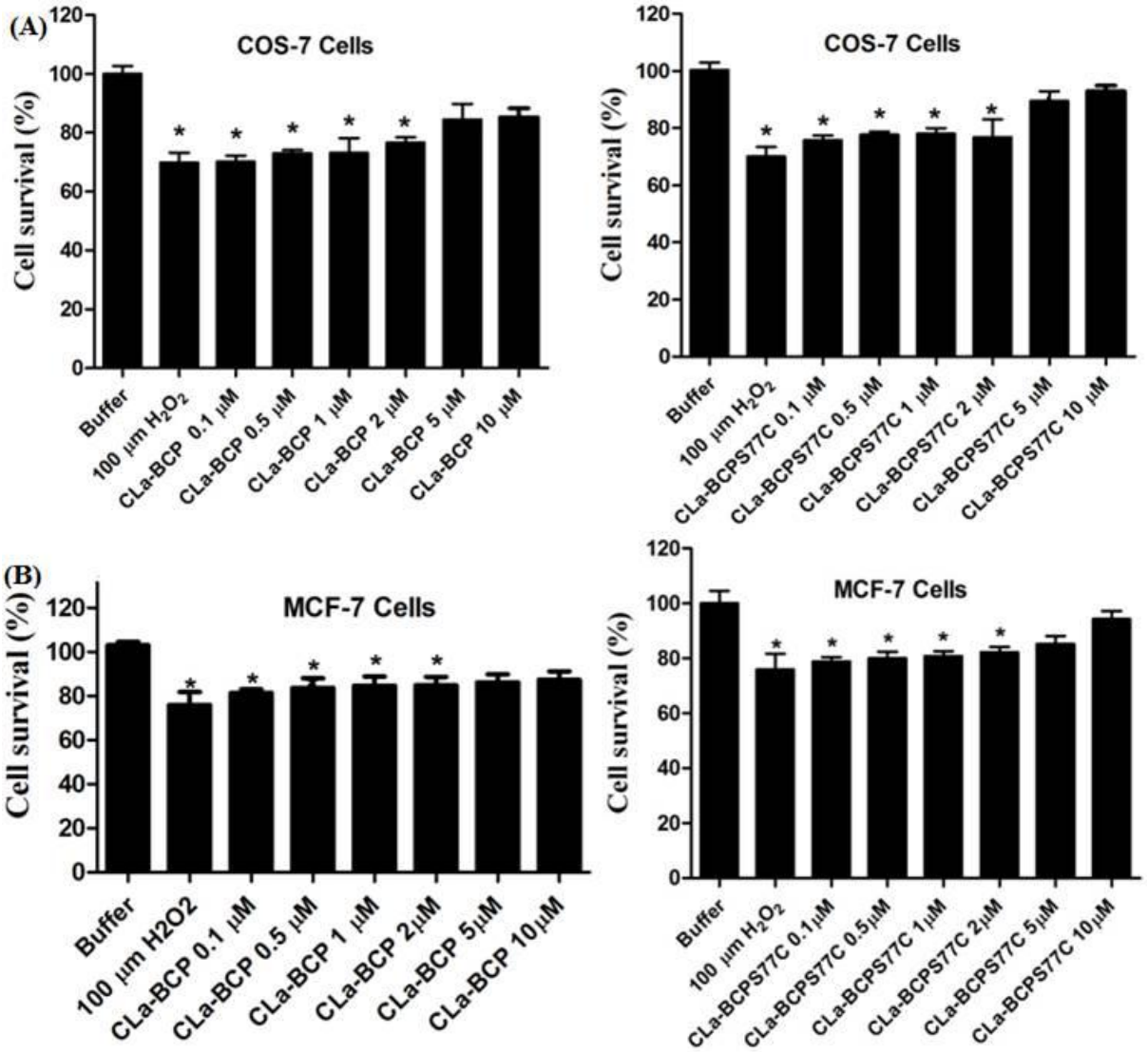
(A)
COS-7 Cells
Cell survival (%)
Buffer
100 μm H2O2
CLa-BCP 0.1 μM
CLa-BCP 0.5 μM
CLa-BCP 1 μM
CLa-BCP 2 μM
CLa-BCP 5 μM
CLa-BCP 10 μM
COS-7 Cells
Cell survival (%)
Buffer
100 μm H2O2
CLa-BCPS77C 0.1 μM
CLa-BCPS77C 0.5 μM
CLa-BCPS77C 1 μM
CLa-BCPS77C 2 μM
CLa-BCPS77C 5 μM
CLa-BCPS77C 10 μM
(B)
MCF-7 Cells
Cell survival (%)
Buffer
100 μm H2O2
CLa-BCP 0.1 μM
CLa-BCP 0.5 μM
CLa-BCP 1 μM
CLa-BCP 2μM
CLa-BCP 5μM
CLa-BCP 10μM
MCF-7 Cells
Cell survival (%)
Buffer
100 μm H2O2
CLa-BCPS77C 0.1μM
CLa-BCPS77C 0.5μM
CLa-BCPS77C 1μM
CLa-BCPS77C 2μM
CLa-BCPS77C 5μM
CLa-BCPS77C 10μM

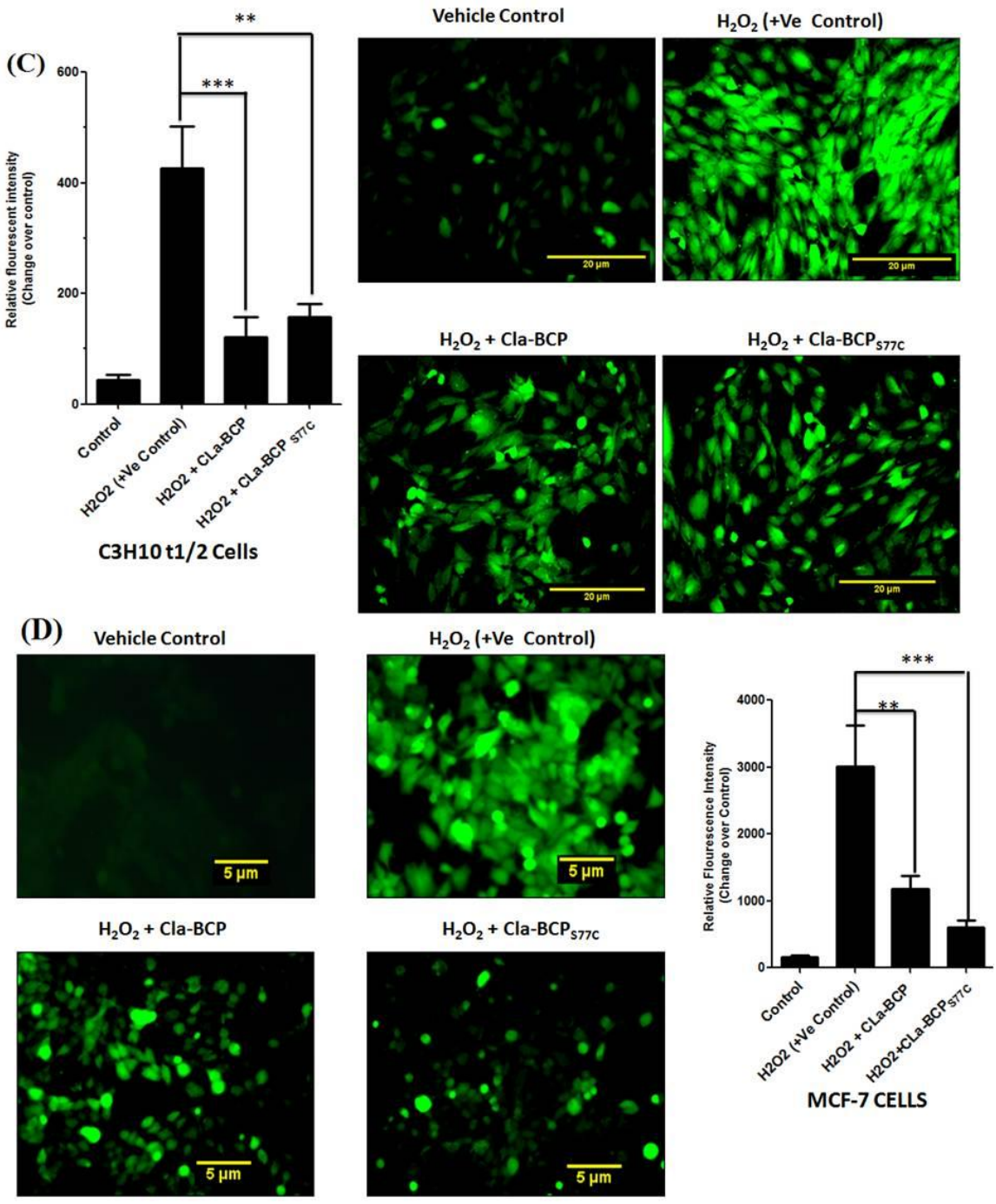

Fig 2.15 CLa-BCP and CLa-BCP_{S77C} protection against H_2O_2 mediated cell killing. (A, B) COS-7 cells and MCF7 cells ($1x10^6$ cells) were plated in 96-well plate for 16 h and then induced with 100µM H_2O_2 for 24 h with or without various concentrations of CLa-BCP and CLa-BCP_{S77C}. Cell viability was evaluated by MTT assay. Histograms indicate the sum of cells analyzed in presence of buffer and different concentration of protein. (C, D) Both the C3H10t1/2 and MCF-7 cells (1×10^5 cells) were seeded in 48-well plates for 16h and cells treated with 1µM of protein subsequently treated with 100µM of H_2O_2 after 30 min. DCFH-DA at a concentration of 5µg/ml) was added to the cells. Images were quantified using image-J software (NIH, USA). Results are the mean of SEM of three independent experiments.

2.10 CONCLUSION

In conclusions, a 1-Cys peroxyredoxin (CLa-BCP) having C_PSH /sulfenic acid cysteine (C-47) was characterized from CLA. It lacked the resolving cysteine (C_RSH). The bacterial system has evolved its antioxidant system, as a result of oxidative stress thiol peroxidase, peroxiredoxins (Prxs) to play a critical role in its viability. A 474bp CLa-BCP, a 1-Cys Prx protein was amplified and cloned in modified pet28C vector ie. pET-TEV vector. NCBI-BLAST search of the deduced amino acid showed presence of a thioredoxin like domain belonging to thioredxin like superfamily. CLa-BCP exhibits a significant sequence similarity with alkyl hydroperoxide reductase from various pathogenic and plant symbiotic bacteria.

The introduction of non-conserved resolving cysteine results into substantial change in the property of the protein. First, the variant form CLa-BCP_{S77C} was shown to be dimeric in nature secondly quite stable in its reduced form. The purification profile of CLa-BCP showed oligomeric property of the protein though having only single cysteine. Literature reports that 1-Cys Prx from human Prx-VI, 1-Cys Prx from *Mycobacterium*, 1-Cys Prx from *Aeropyrum pernix K1* [54, 174, 343] have shown oligomer formation. More studies needs to be done to authenticate the oligomerisation behaviour of CLa-BCP.

The DTNB assay showed that protein has free thiols only in its reduced form and proteins exhibits thiol dependent reduction as shown by using natural reductant thioredoxin (TrxA). As the natural partner for BCPs are still unknown, we have evaluated the catalytic activities of CLa-BCP and its variant CLa-BCP_{S77C} using a second system in which DTT is used to reduce the putative disulfide bond formed in their reactions with peroxides. In this assay, the peroxidase activity of both the protein was evaluated using varied peroxide substrates i.e. hydrogen peroxide, cumene H_2O_2 and t-butyl H_2O_2.

The protein showed peroxidase activity against varied substrates using DTT as non-physiological electron donor. The enzymatic activity increased as the protein concentration was increased and was saturable (not shown). The detoxification activity using xylenol orange showed that CLa-BCP was much more effective even at its lower concentration. It is well known that overoxidation of Prx provokes their inactivation but here in our case, after dimedone inactivation. It has been proposed that oxidize C_PSOH residue (sulfenic intermediate) could be easily revert back to its thiol form in the presence of DTT or DTT could easily reduced the sulfenic acid in Cys-46. Thus DTT could be potent reductant for CLa-BCP imparting its peroxidase as well as peroxide scavenging activity.

After peroxidase activity we wanted to determine whether CLa-BCP would protect supercoiled DNA from oxidative nicking by hydroxyl radicals, as reported for Prxs from different organisms [21, 30, 40, 41]. A lot has already been discussed about the risk associated with the oxidative damage to DNA, like as a potential indicator of cancer risk. The reaction of H_2O_2 with DNA results into predominant lesion in DNA is due to strand break, or some because of oxidation of bases. Appearance of faint linear DNA indicates that hydroxyl ions have been generated from UV-photolysis of H_2O_2 as a result of which DNA strand scission occurs. Hydroxyl radical is one of the most reactive radical known, and capable of abstracting hydrogen atoms from biological molecules, including thiols, foremost to the formation of sulphur radicals proficient to combine with oxygen to generate oxysulfur radicals, a quantity of which damage biological molecules [209]. These $HO^{\cdot}$ radicals are formed by monovalent reduction of H_2O_2 by a reduced metal such as Fe(II) [162, 163]. It is believed that the $HO^{\cdot}$ radicals that attack DNA are formed directly on the DNA surface by ferrous atoms complexes with the phosphodiester backbone rather than free in solution. The results of the assay showed that super coiled DNA was the predominant species in reactions lacking both H_2O_2 and CLa-BCP. *In-vitro* DNA binding studies showed that this protein can protect super coiled DNA from oxidative damage. The protective effect could be due to protein's physical shielding or exclusion of H_2O_2 from the nucleic acid. In case of MCO system, the clear protection was seen the probable reason could be that CLa-BCP may have chelated trace iron ions thereby reducing Fenton reaction followed by consequential oxidative damage to the DNA. From collective studies from other cited results, the data suggest that CLa-BCP protects DNA through its DNA binding and Prx activity. The whole chemistry behind the protective effect of protein towards super coiled DNA from oxidative damage needs elaborate studies. Nonetheless results are in observance with preceding work showing that 1-Cys and 2-Cys Prx's can protect DNA from oxidative damage.

It has been observed that normally when cells are exposed to H_2O_2 externally above the critical concentration. They exhibit their own anti-oxidative property by expressing related scavenging proteins. Thus in our study we make sure that cells were challenged with that concentration of H_2O_2 above which, cells will either leads to apoptosis or necrosis. For the same reason here we have used 100µM of H_2O_2 for inducing stress into cells. It has been elucidated through the *in-vitro* MTT assay that both CLa-BCP and CLa-BCP_{S77C} played an important defensive role against H_2O_2 induced cell killing effectively. It has been cited that peroxiredoxin know to have effective scavenging property towards peroxide and generated radicals thus our second target to know the *in-vitro* antioxidant property of both CLa-BCP and

CLa-BCP_{S77C}. In order to elucidate the antioxidative property of both the proteins, the DCF-DA has been used for detecting ROS generation inside the cells. In our case, it has been observed that in case of positive control (H_2O_2), an external stimulus cells responded efficiently by ROS generation. There was substantial decrement in the ROS level when cells were pre treated with proteins which concludes that beside rescuing peroxide mediating cell killing this protein is potent scavenger of ROS, thereby decreasing the effectiveness of H_2O_2.

3. BIOPHYSICAL CHARACTERIZATION OF CLA-BCP AND CLA-BCP$_{S77C}$, *IN-SILICO* ANALYSIS OF GENE AND PRELIMINARY CRYSTALLOGRAPHIC ANALYSIS OF CLA-BCP.

3.1. INTRODUCTION

BCPs constitute a group of antioxidant enzymes belonging to the Prx family, which are widely distributed in bacteria, plants, and fungi. The BCP subfamily initially assigned as the C group [146], the most diversified member. The members known so far in BCPs differ in their oligomerisation behaviour depending upon the locality of the resolving cysteine, C_R. Predominantly they exists as monomers but known to form dimers. They could be A-type and B-type dimers with either 1-Cys or 2-Cys mechanisms, on the basis of two separate sites for the C_R. With reference to their nomenclature, the BCP subfamily is being further divided into an α-group, with the conserved C_pXXXXC_R motif (as in case of 2-Cys Prxs), and a β-group without C_R reprsenting 1-Cys Prxs [384] . However with the upcoming sequences this nomenclature does not hold true in all the cases or for classifying the entire subfamily. The common step shared in catalytic mechanism by all Prxs is the involvement of an active peroxidatic Cysteine (Cp) thiolate attacking the peroxide substrate. But the resolution of recycling of the sulfenic acid back to a thiol is what classifies them further into three distinct enzyme groups. It can be typical 2-Cys whereby Cp and C_R forms intermolecular disulfide bond and keep the protein in its reduced form for another round of catalysis. It could be atypical, where intramolecular disulfide bond formation occurs in between Cp and C_R. Whereas in case of 1-Cys Prxs, resolution of active Cysteine is still an open puzzle, as they do not harbour resolving Cysteine. Very little information is available about the molecules which can acts as electron donors. Though some of them have been implicated for their role in reduction of peroxidatic active Cys which includes glutathione, lipoic acid, cyclophilin, and ascorbate and DTT [225, 243, 260, 266]. The basic chemical reaction employed by both the Prxs i.e. 1-Cys and 2-Cys, on reacting with hydrogen peroxide is the formation of sulfenic acid intermediate. These sulfenic acids have reactivity toward thiols to form disulfides, and under highly oxidizing condition, Cp may become over oxidized to sulfinic or sulfonic acid [188]. The over-oxidized form partly mimics the reduced state [87]. A commonly used reagent to detect the presence of a sulfenic acid, is dimedone, a nucleophilic reagent that attacks the sulfenate sulfur, displacing hydroxide and forming a thiol adduct. Another electrophilic reagent 7-chloro-4-nitrobenzo-2-oxa-1,3-diazole (NBD-Cl) had several

impending improvements over the nucleophilic reagents as NBD-adduct can be detected spectrophotometrically [32].

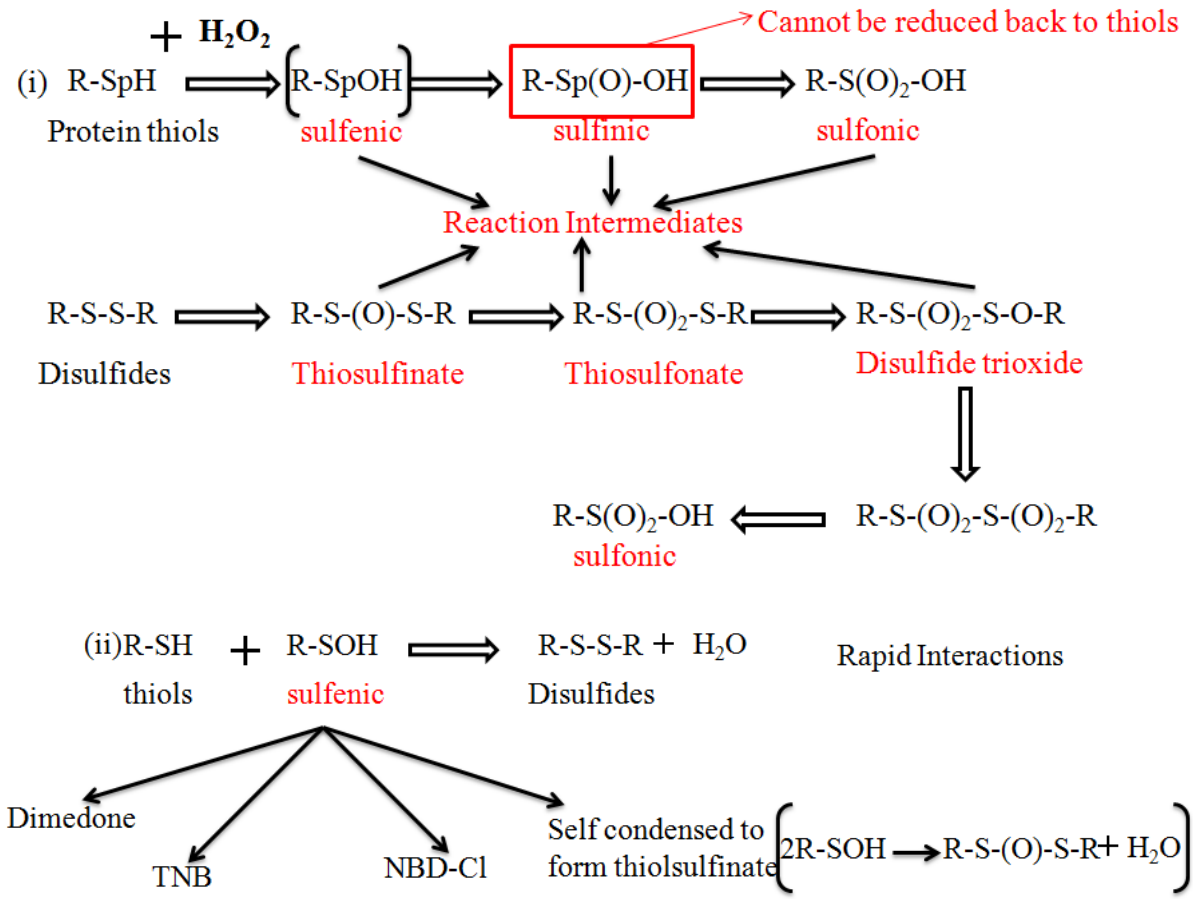

An overview of reaction intermediates formed during oxidation and overoxidation process.

The crystals of protein were grown utilizing most popular method i.e. vapour diffusion method, either by hanging or sitting drops when crystallization are considered. Many physical or chemical variables and processes may affect the growth and quality of protein crystals [120, 250]. The establishment of diffusive transport conditions by growth under microgravity [250] or in gels [111] can improve crystals. Microseed matrix-screening combined with random screens (rMMS) is a significant recent breakthrough in protein crystallization [336]. Glycerol appears to be more effective when coupled with alternative and complementary methods that can similarly reduce excessive nucleation [381]. The growth of protein crystals in agarose [305] or silica gels [73, 311] is an established technique. As noted previously, agarose showed quite a lot of benefits for the crystallization experiment [305, 311] and may facilitate cryogenic cooling [416].

Here in this chapter we have made an attempt to analyse gene sequence comprehensively by means of several bioinformatics tools. We wanted to decipher the catalytic mechanism employed by CLa-BCP that lacks resolving cysteine residue. We have studied reduction-

oxidation dependent conformational changes of protein via biophysical techniques like circular dichroism and intrinsic fluorescence. We initiated crystallographic studies of BCP in order to establish the structural and functional relationship of peroxiredoxins in context to their biochemical and biophysical properties. We have performed CLa-BCP preliminary crystallographic setups and found that addition of low percentage of agarose results into better diffracting crystals, procedure adopted from Kumar P. et.al [213] with little modification.

3.2. MATERIALS AND METHODS

3.2.1 Materials

Hydrogen peroxide purchased from Rankem. NBD-Cl (7-chloro-4-nitrobenzo-2-oxa-1, 3-diazole), Dimedone (5, 5-dimethyl-1, 3 cyclohexanedione) and NEM (N-Ethylmaleimide) were purchased from Sigma Aldrich. Amicon ultra concentrator, Millex syringe filters were from Millipore Corporation, Billerica, MA. Dialysis membrane with 3500 Da cutoff was from Pierce, Rockford, USA. For crystallization experiments, buffer components obtained from Sigma and polyethylene glycols obtained from Fluka were used. Crystal Screen 1, 2 and Index screens in 96-well Cryschem plates from Hampton Research (Aliso Viejo, California, USA).

3.2.2 Circular Dichorism Studies

Circular dichroism (CD) is observed when optically active matter absorbs left and right handed circularly polarized light slightly different. Proteins encompass several chromophores responsible for CD signals. The far UV region (240-180 nm) CD spectrum correlates to peptide bond incorporation, perhaps considered to find out usual secondary structural elements for example α-helix and β-sheet. For analysis of secondary structure content and effect of oxidizing agent, CLa-BCP and CLa-BCP_{S77C} both in the reduced form dissolved in 0.02M potassium phosphate buffer, pH 8 was subjected to CD using Chirascan™ CD Spectrometer (Applied Photophysics, UK). Both CLa-BCP and CLa-BCP_{S77C} were analyzed after treatment with 1.2eq of hydrogen peroxide at room temperature for 10 min. The CD spectra were generated using a 0.1-cm path length cuvette. The CD data were expressed in terms of mean residue ellipticity. The assays were carried out at RT; spectra were presented as an average of three scans recorded from 190 to 240 nm. CD spectroscopy studies at different temperature of CLa-BCP were also performed for knowing the conformational stability of protein also.

3.2.3 Fluorescence Spectroscopy of CLa-BCP and CLa-BCP$_{S77C}$

The tryptophan fluorescence study was performed to examine the redox state-dependent conformational transitions in CLa-BCP and CLa-BCP$_{S77C}$. Purified protein (50μg mL^{-1}) in 0.02M phosphate buffer, pH 8.0 filtered through 0.45 μm Millex syringe filter was used. Protein was excited at 280 nm and emission wavelength spectra were recorded at 290–400 nm using Fluorolog®-3 spectrofluorometer Jobin Yvon Inc (USA) at constant temperature (25 °C). Emission slits were at 5 nm and quartz cuvette of 1 cm path length was used. The samples were reduced with 2 mM DTT and oxidized with 10mM H_2O_2. An appropriate blank with 2 mM DTT was subtracted to the reduced CLa-BCP and CLa-BCP$_{S77C}$ spectrums. Effect of pH was also analyzed by incubating proteins CLa-BCP and CLa-BCP$_{S77C}$ with citrate borate buffer ranging from pH 3-9.

The unfolding of the proteins was carried out at a range of Urea (2-8M). Blanks were prepared for each data point and further subtracted from the fluorescence of the protein sample. Modification studies has also been carried out using N-Ethylmaleimide (NEM) an alkylating reagent and NBD-Cl (7-chloro-4-nitrobenzo-2-oxa-1, 3-diazole), Dimedone (5, 5-dimethyl-1, 3 cyclohexanedione) thiol modifying sulfenic acid reagents.

3.2.4 Chemical modification study of CLa-BCP

To known the reactivity of functional cysteine residue and formation of Cys-SOH as a reaction intermediate, experiments with wild type CLa-BCP and mutant CLa-BCP$_{S77C}$ labelled with NBD chloride (a sulfenic acid modifying agent) were carried out by modifying the previously described protocols [64, 89, 260]. The proteins were pre-treated with DTT (10 mM) overnight in reaction buffer (20mM potassium phosphate buffer pH 8.0) having DTPA to avoid metal-catalyzed progressions. After removing excess DTT through dialysis; reduced proteins were treated with 10 equimolar NBD-Cl or 1,000 equimolar of dimedone. Similarly for oxidation process, both proteins were treated with 10mM of H_2O_2 through dialysis at 4 °C. The excess H_2O_2 was removed through dialysis exchanged with buffer having no H_2O_2 for about three hours. Then the subsequent oxidized samples were reacted with 10 eq of NBD-Cl or 1,000 eq of dimedone.

3.2.5 Preliminary crystallographic analysis

3.2.5.1 Protein Crystallization

For CLa-BCP crystallization, the purified protein sample contained CLa-BCP at 10 mg ml^{-1}; 20mM Tris-Cl pH 8.8 concentrated using an Amicon Ultra concentrator (5 kDa molecular-

weight cutoff, Millipore). The purified CLa-BCP was set for initial crystallization trials via the sitting-drop vapour-diffusion method using Hampton crystal screens in 96-well Cryschem plates from Hampton Research (Aliso Viejo, California, USA). In sitting drop method, protein and the reservoir solution were used in 2:1 ratio and equilibrated against 50 µl of the reservoir solution.

3.2.5.2 Measurement and analysis of diffraction data

Crystals were cryoprotected by immersion in 10% ethylene glycol and preserved in a cryogenic N2-gas stream (~100 K) during diffraction experiments. Cryo-stabilization of the crystals was done with low percentage of glycerol. Diffraction data were collected in our in-house facility at MCU (Macromolecular Crystallography Unit) at IIT Roorkee. Diffraction Data was obtained with a MAR 345 imaging-plate system using Cu *K*α radiation generated by a Bruker-Nonius Microstar H rotating-anode generator operated at 45 kV and 60 mA and equipped with Helios optics. Diffraction images and intensities were processed and scaled using the *HKL*-2000 suite [291]. We tried solving the initial phases by using MolRep and Phaser of programs of CCP4i. We also tried using auto-rickshaw, the server for automated structure determination. SCALA package of CCP4 suite was used for scaling the data and the presence of the screw axis was also confirmed by POINTLESS in the CCP4 suite [393].

3.2.6 Gene Analysis

3.2.6.1 Multiple Sequence alignment (MSA)

Multiple sequence alignment with known peroxiredoxin from pathogenic microorganism on the basis of "nr BLAST" has already been discussed in chapter 2. Here secondary structure analysis using multiple sequence alignment with known subclasses of Prxs protein was carried out. MSA with known Prxs structures further enhanced by esprit 3.0 [312].

3.2.6.2 Phylogenetic analysis

For phylogenetic tree generation, sequences were submitted to open access Phylogeny.fr online server (http://www.phylogeny.fr). Upon execution the programs connects various programs and reconstruct a phylogenetic tree. In "default" mode it uses Muscle (v3.7) program for multiple alignment, Gblock (v0.91b) algorithm for removing the ambiguous region in the alignment [80] phylum program (v3.1/3.0 aLRT) for phylogeny analysis using the maximum likelihood method and TreeDyn (v198.3) for constructing the tree.

3.2.6.3 Signal peptide Prediction

Prediction of N-terminal signal peptides were done through various programmes signalP 3.0, Phobius, Signal-CF and Signal-BLAST [28, 61, 184].

3.2.6.4 Structure modeling

Structural modeling of CLa-BCP was done using different online software programs like Swiss Model [16], **Phyre2** (**P**rotein **H**omology/AnalogY **R**ecognition **Engine)** server [187], and Robetta full-chain protein structure prediction server (http://robetta.bakerlab.org/) which provide both *ab-initio* and comparative models of protein domains [189]. These robetta models are built from structures detected and aligned by HHSEARCH, SPARKS and RAPTOR. The best model was selected using PROCHECK program available on Structure Analysis and Verification Server (SAVES v4) server after evaluating the stereo-chemical quality using 1XVW as a template structure.

3.2.7 Interaction with H_2O_2 substrate through docking study

In order to understand the catalytic mechanism of CLa-BCP with substrate (hydrogen peroxide), we docked the substrate (H_2O_2) into the active site of CLa-BCP. AutoDock Vina 1.0.2 was used for docking in this work [383]. The docking parameters used for Vina were kept to their default values. However, the x,y and z coordinated of grid centre were 43.658, 21.604, 10.445 and the size of the docking grid was 5.25Å×5.25Å×6.75Å, which encompassed the hydrogen peroxide binding site of peroxiredoxin (C207S) from *Aeropyrum pernix* K1 (pdb id 3A2V). The 100 independent GA runs from AD4 were processed by means of the built-in clustering analysis with a 2.0 Å cutoff. The six best poses were obtained, out of which pose6 showing the RMSD value of

Mode	affinity (kcal/mol)	dist from best mode rmsd l.b.	rmsd u.b
1	-1.4	0.000	0.000
2	-1.4	0.269	1.473
3	-1.3	0.995	1.903
4	-1.3	1.062	1.166
5	-1.1	1.594	2.041
6	-1.0	1.658	1.853

3.3 RESULTS AND DISCUSSION

3.3.1 Circular Dichorism studies of both CLa-BCP and CLa-BCP$_{S77C}$

Circular dichroism technique can be benefited in favour of studying conformational stability of proteins in diverse environment, here in our case; we have performed Far-UV CD (wavelength range from 240-190) analysis in the presence of reducing and oxidizing agent. The data obtained was analyzed using the web based DichroWeb software [389] and the neuronal network program CDSSTR. The structures of related Prxs proteins possess α/β structure. BCPs has been reclassified by Wakita et.al., 2007 [384] into α and β-group having characteristic conserved C_PXXXXC_R motif and no C_R respectively. The CD study of reduced CLa-BCP showed negative peak at 198 nm showing predominance of β-sheets (27.9 %) having 10.8% α-helical content and 26.3% turns depicting that it belongs to β-group (Fig. 3.1 A). While mutant CLa-BCP_{S77C} in its reduced form showed negative peaks at 208 nm and 223 nm having 25% of α-helical shifting of β structure towards α- helical conformation in its reduced form with 24.8% turns (Fig. 3.1 B). This structural change could be due to the presence of another Cysteine in mutant CLa-BCP_{S77C}. Sequence analysis showed that positioning of introduced Cysteine if we consider it as a resolving Cysteine is more closely related to *Xanthomonas campestris* [229] belonging to subfamily of "atypical 2-Cys Prxs". But here in our case biochemically it forms intermolecular disulfide bond which is unique to typical 2-Cys Prx. It could be intermolecular disulfide bond formation between resolving Cysteine instead of in between C_PSH and C_RSH. More studies have to done to decipher that mutant follows atypical or typical mechanism or novel mechanism to detoxify peroxide substrates. Initial purification experiments discussed in chapter 2 observed that CLa-BCP_{S77C} protein in its native form tends to aggregates and degrades gradually, while it is quite stable in its reduced form. This observation could be due to stable conformational change as seen in case of CD spectra as well. An additional CD experiments have been done with H_2O_2 treatments. The stable conformation of CLa-BCP and CLa-BCP_{S77C} in its reduced form is seen whereas a decrease in ellipticity has been observed in case of oxidized condition (Fig. 3.1 A, B) implicates destabilization of the proteins. In oxidizing condition the structural content of CLa-BCP was 6.8% α-helical, 36.6% β-sheets and 22.7% turns, while CLa-BCP_{S77C} shown to have 16% α-helical and 32% β-sheets and 22.7% turns.

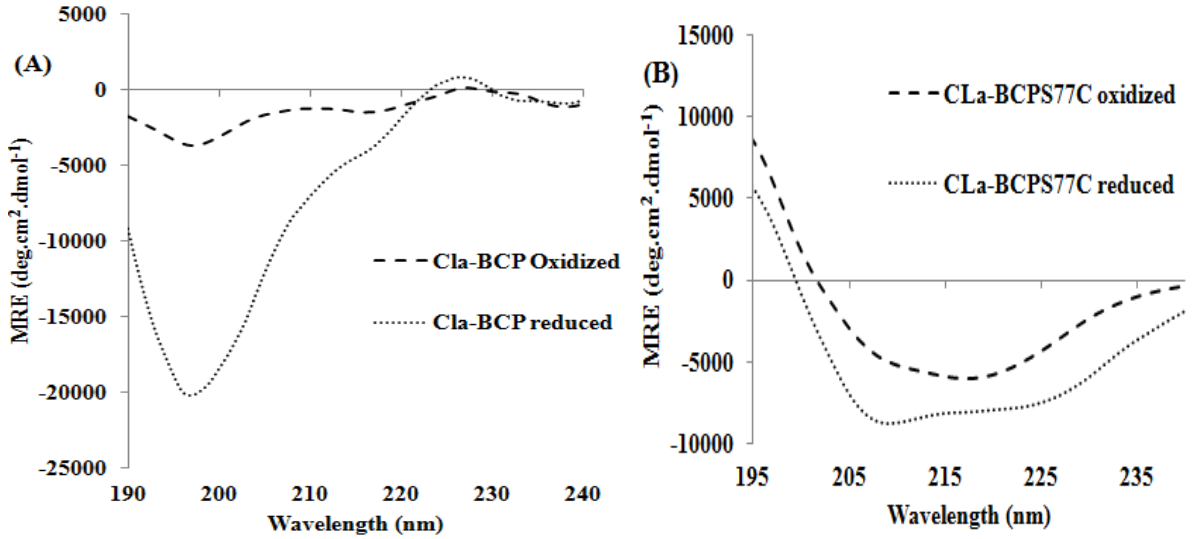

Figure 3.1: Far-UV CD studies of CLa-BCP and CLa-BCP$_{S77C}$, in reducing and oxidizing conditions. (A) CD spectra of wild type showing negative peak at around 198nm (B) while mutant showed two negative peaks at 208 nm and 223 nm decreased ellipticity in oxidizing condition.

The effect of temperature was carried out with wild type CLa-BCP across a range of temperature (40-100 °C). At higher temperature the helical content from 10.8% to 20.7% whereas the β-sheets is ~27% to 26.6 % (Fig. 3.2). It suggests that at higher temperature the random coil transition into α helical content occurs while % of β-sheets more or less remains same. Similar results have been observed in case of Sso1120 protein from *Sulfolobus solfataricus* where CD spectra recorded at 100 °C. It showed an increase of only 20% of disordered region demonstrating that protein to some extent maintains its secondary structure still at higher temperature [233]. During protein refolding from higher temperature to RT the % of α helix was 12.1% and 29.2% of β-sheets but with decreased ellipticity summarized in (table 3.1). We were unable to do analysis of temperature effect on CLa-BCP$_{S77C}$ as with increasing temperature it tends to aggregates (data not shown).

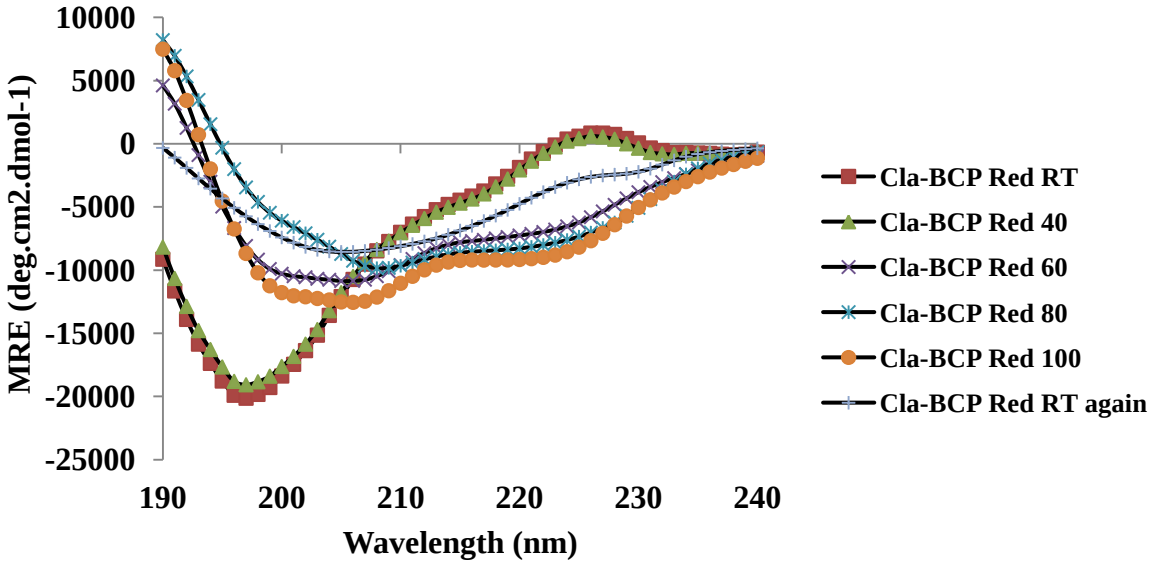

Figure 3.2: Far-UV CD studies of CLa-BCP at different temperature, CD spectra of wild type showing negative peak at around 198nm while at higher temperature negative peaks at 208 nm and 223 nm with decreased ellipticity.

Table 3.1 Temperature analysis of wild type protein CLa-BCP.

Temperature	Alpha helix	Beta sheets
RT	10.8 α	27.9 β
40	11.4 α	27.7 β
60	13.4 α	26 β
80	15.9 α	26.6 β
100	20.7α	18.7 β
RT again	12.1α	29.2 β

For redox changes, both proteins were over oxidized with H_2O_2 subsequently reduced with 2mM DTT and changes were recorded as CD spectra. There was a substantial conformational change seen due to over oxidation which has been reverting back by reduction with DTT treatment (Fig. 3.3). In sum, in over oxidized condition CLa-BCP possesses 20% of α helix, 41% of β-sheets having 11% β turns with 28% unordered region. While CLa-BCP_{S77C} possesses 22% of α helix, 35% of β-sheets having 14% β turn with 28% unordered region.

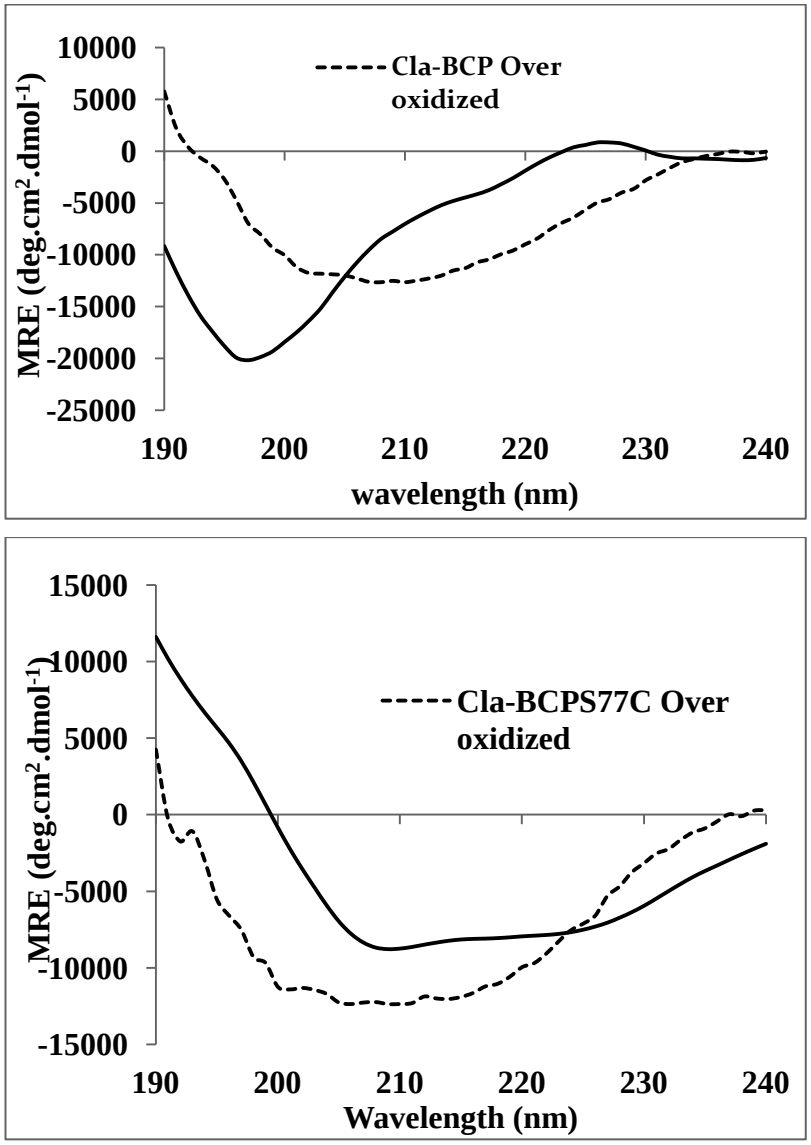

Figure 3.3: Far-UV CD studies of over oxidized CLa-BCP and CLa-BCP$_{S77C}$.

3.3.2 Fluorescence Spectroscopy of CLa-BCP and CLa-BCP$_{S77C}$

Fluorescence spectra of Prxs are well defined from human PrxV, *Mycobacterium tuberculosis* AhpE and closely related chloroplast 2-Cys Prx from barley exploited the possible benefit of measuring Trp fluorescence during oxidation [157, 207, 370]. The spectra were dominated by tryptophan emission with a maximum at 341 nm due to exposed Trp106 and Trp136. When CLa-BCP was exposed to H_2O_2 (10 mM), decreased intrinsic fluorescence intensity was seen with no shift in maximum emission (340 nm). This change reverted back upon reduction with 2mM DTT and results into two-fold enhance in emission with a little shift to 344.5 nm (Fig. 3.4 A) as seen in case bacterial AhpCs [157]. From sequence analysis with known Ahpc it has been seen that Trp residues are strictly conserved (Fig. 3.8 C). The data suggest conformational changes occurred at active site. The Trp136 which is distant from the active

site present in loop region between α5 and β9 could potentially sense local conformational changes around the C_P thiolate during substrate binding (Fig. 3.4 G). The conformational changes that occur at active site will be later discussed in docking section of this chapter.

The fluorescence spectrum of CLa-BCP_{S77C} having emission maxima at 347.5 nm, oxidized CLa-BCP_{S77C} exhibited a maximum emission at 350.5 nm a slight 3nm red shift, suggesting presence of free thiols. The reduction of CLa-BCP_{S77C} resulted in a two-fold increase in emission (Fig. 3.4 B) suggesting disulphuric bridge split after reduction as reported [74].

Some reports of 2-Cys Prxs have shown that during catalytic cycles, key Cys residues undergo over oxidation, which would be anticipated to lead to structural and functional changes [171, 197, 261]. Likewise, in our case, CLa-BCP was found to be over oxidized by H_2O_2 treatment (Fig. 3.4 A), but there was no substantial conformational change after over oxidation, which is to some extent different from the case of 2-Cys Prxs. In case of modification studies with thiol alkylating and sulfenic acid trapping reagent (NEM and NBD-Cl), fluorescence intensity was not changed (data not shown). These data suggests that the oxidation of the single peroxidatic Cys residue is required for change in fluorescence intensity for both the proteins. Moreover, when pre-reduced CLa-BCP and CLa-BCP_{S77C} were treated with an excess of H_2O_2 (10 mM), initially there was a quick decrease followed by a slower increase in protein fluorescence intensity (Fig. 3.4 A, B). These changes were hindered by pre-treatment of the enzyme with NEM and NBD-Cl in excess (data not shown), implying the involvement of the cysteine residue in the process. Secondly following the H_2O_2-dependent over oxidation of the sulfenic acid of the oxidized enzyme (C_P-SOH) to sulfinic acid (C_P-SO_2H) was dependable for the fluorescence upturn.

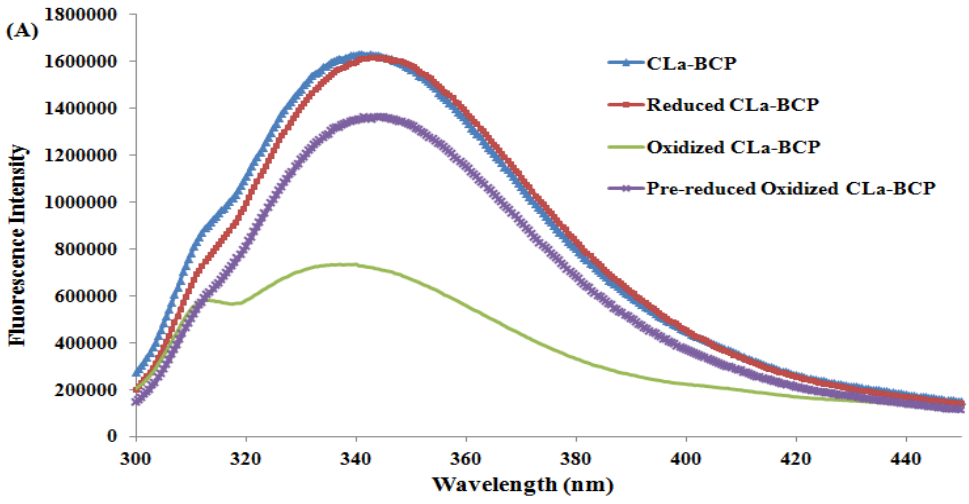

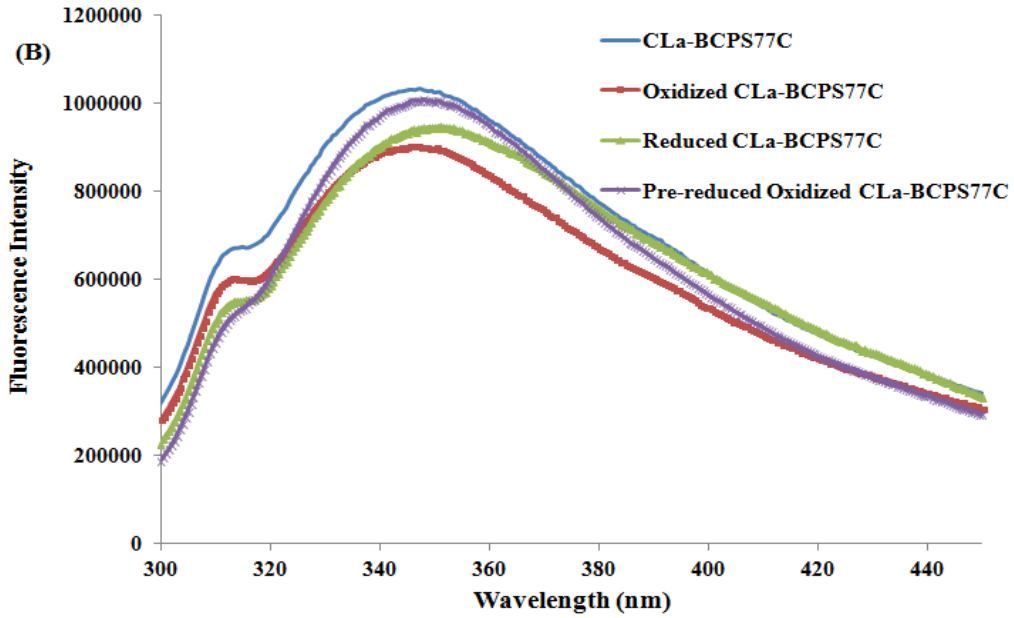

The effect of different pH showed stable conformational change of CLa-BCP and CLa-BCP_{S77C} in range of pH 6, 8 and 9 with more or less static emission maxima (Fig. 3.4 C, D). The effect of denaturant was almost same. There was gradual increase in intensity with a shift from 340 nm to ~362 nm in the presence of increasing concentration of urea, suggesting the gradual unfolding of the protein consistent with the tryptophan residues accessibility (Fig. 3.4 E and F).

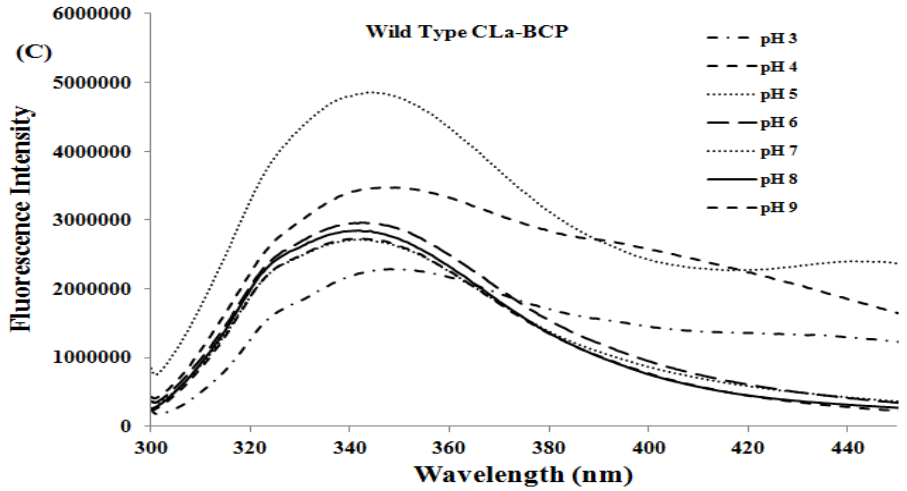

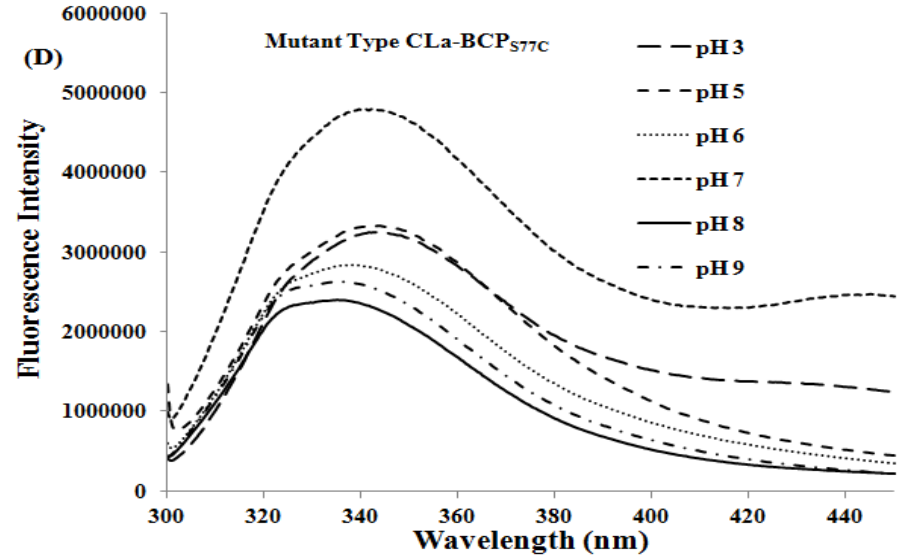
(D)
Mutant Type CLa-BCP$_{S77C}$
pH 3
pH 5
pH 6
pH 7
pH 8
pH 9
Fluorescence Intensity
Wavelength (nm)
6000000
5000000
4000000
3000000
2000000
1000000
0
300
320
340
360
380
400
420
440

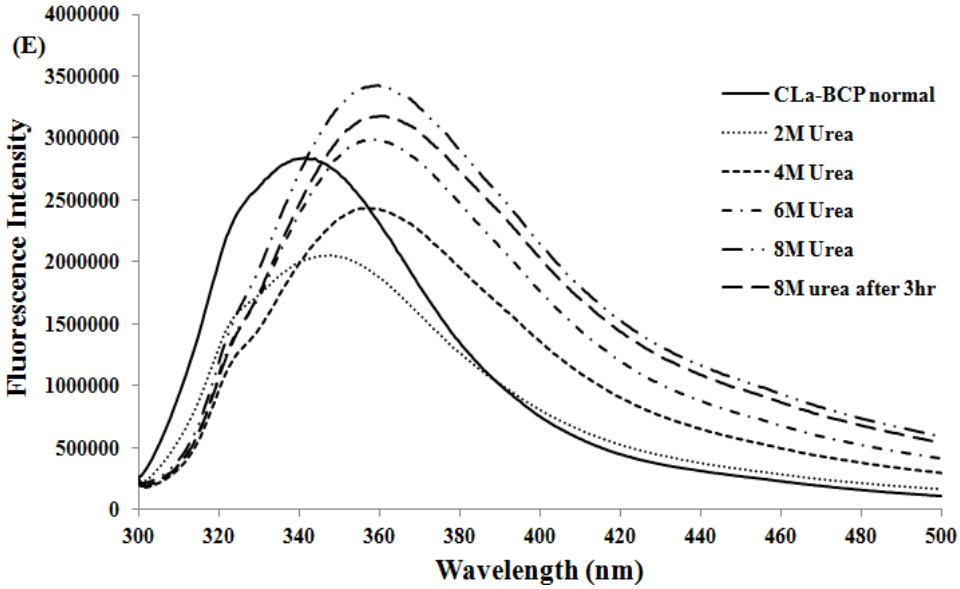
(E)
CLa-BCP normal
2M Urea
4M Urea
6M Urea
8M Urea
8M urea after 3hr
Fluorescence Intensity
Wavelength (nm)
4000000
3500000
3000000
2500000
2000000
1500000
1000000
500000
0
300
320
340
360
380
400
420
440
460
480
500

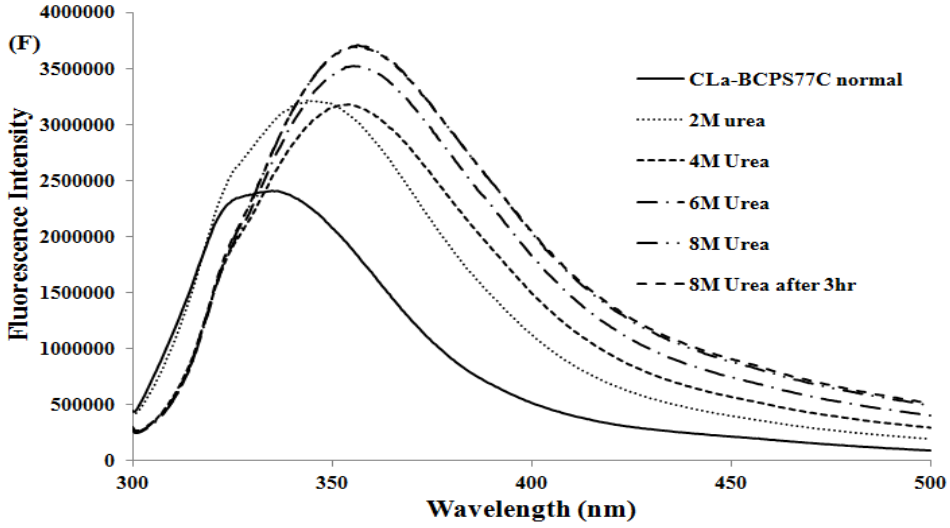
(F)
CLa-BCPS77C normal
2M urea
4M Urea
6M Urea
8M Urea
8M Urea after 3hr
Fluorescence Intensity
Wavelength (nm)
4000000
3500000
3000000
2500000
2000000
1500000
1000000
500000
0
300
350
400
450
500

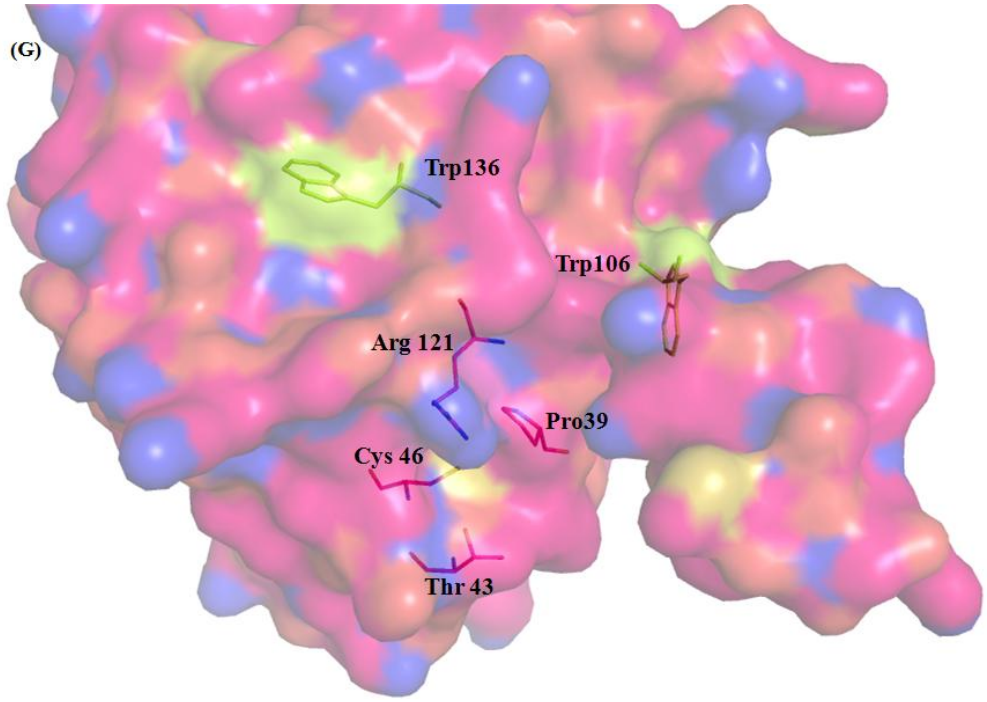

Figure 3.4: Fluorescence emission spectra of the purified protein under native, reduced, oxidized and denatured conditions. (A, B) Effect of DTT (reducing reagent) and H_2O_2 (oxidizing reagent) on the intrinsic fluorescence of both CLa-BCP and CLa-BCP_{S77C}. (C), (D) Fluorescence spectra in the presence of CLa-BCP and CLa-BCP_{S77C} respectively in a range of pH 3-9. (E), (F) Fluorescence spectra in the presence of denaturant Urea for CLa-BCP and CLa-BCP_{S77C} respectively. (G) Surface view of CLa-BCP model showing accessible Trp106 and Trp136 is shown in lemon colour. The other neighbouring residues of Trp136 (Pro39, Thr43, Cys46, and Arg121) are also involve in oxidation of CLa-BCP.

3.3.3 Chemical modification of key residue

The functional cysteine assay was carried out using NBD-Cl, an electrophilic reagent as a trapping agent for Cys-SOH which gives characteristic spectral peak at 347nm for thiol adduct (Cys-S(O)-NBD) and 422 nm for thioether linked adduct (Cys-S-NBD)[89]. NBD-labelled pre-reduced CLa-BCP showed an absorbance maximum from 344-349 nm a signal characteristic of NBD adducts of sulfenic acid R-SOH (R-S (O)-NBD). It evidently signifies the trapping and detection of approximately stochiometric amounts of SOH at Cys 46, the only Cys in wild type protein (Fig. 3.5 A). The absorbance maximum at 420-450 nm for CLa-BCP could be due to formation of sulhydryl adducts. When protein was not pre reduced with DTT and oxidized with peroxide treatment overnight, the predominant peak was at 347nm clearly indicates the formation of sulfenic acid intermediate (Fig. 3.5 B) as reported earlier also [89] . On the other hand, reduced CLa-BCP_{S77C} with or without peroxide treatment showed one peak around 420-450 nm after reaction with NBD chloride (Fig. 3.5 C). It could

be due to formation of thioether linked NBD adduct or lack of SOH formation in case of CLa-BCP$_{S77C}$. Instead a signal indicative for NBD-modified thiols (R-S-NBD) was to a large extent satisfied in the oxidized spectra, confirming the loss of the thiolate species (RS^-) upon reaction with peroxide. The results illustrated that the catalytic cysteine residue was oxidized to sulfenic acid upon peroxide addition in case of wild type protein. Beside that when the modified CLa-BCP run on SDS-PAGE, bands of higher molecular weight seen when treated with NBD-Cl (lane 3 and 5 (Fig. 3.5 D)). The probable reason could be formation of different reaction intermediates upon exposure with hydrogen peroxide or protein undergoes oligomerisation in oxidizing condition.

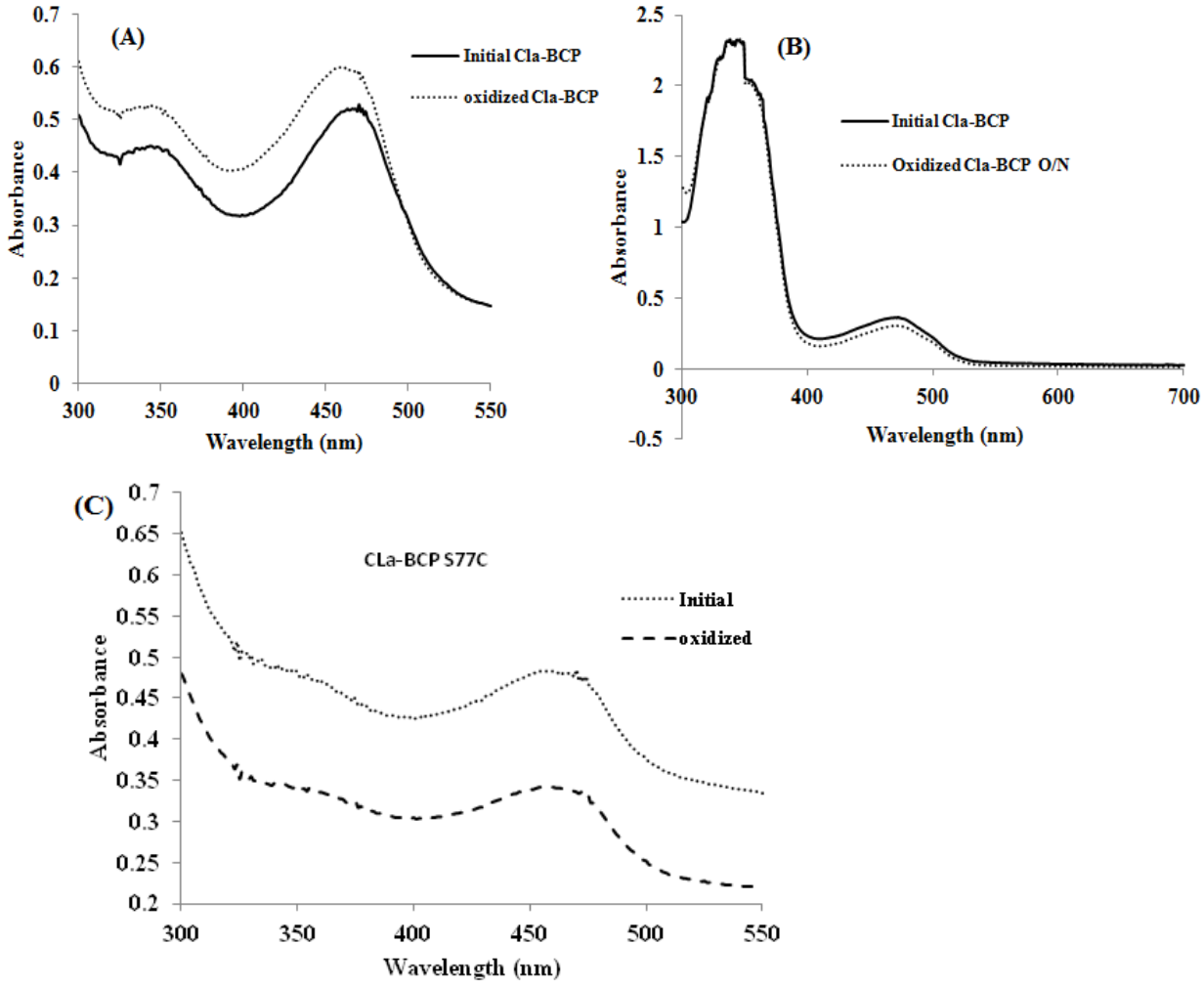

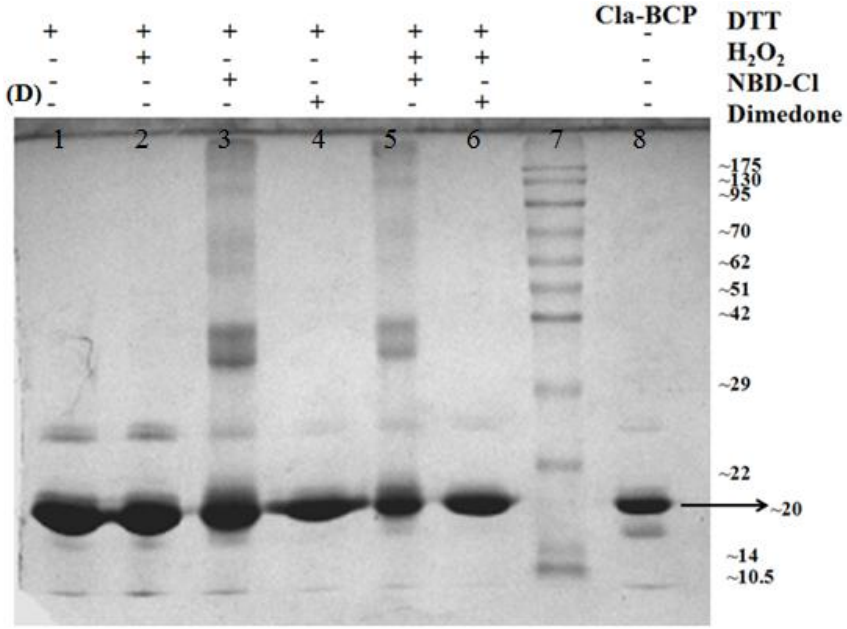

Figure 3.5: Analysis of the oxidation state of Cysteine residues from CLa-BCP and the mutants S77C by the NBD-Cl assay. (A, B) Pre-reduced wild type when treated with H_2O_2 and oxidized wild type protein without pre-treatment with DTT respectively. (C) Mutant type treated with H_2O_2. Sulfhydryl and sulfenic acid adducts peak at 420nmand 347 nm, respectively, with alike extinction coefficients. (D) SDS-PAGE of treated sample followed by NBD-Cl treatment in which (lane 3 and 5) either reduced or oxidized showed higher molecular weight bands.

3.3.4 Crystallization of CLa-BCP

The preliminary crystal growth forms were checked and hits achieved in the screens were subsequently optimized to obtain improved quality crystals. Small crystals were obtained in the presence of granular precipitate using 25% (w/v) polyethylene glycol 3350 (PEG 3350) but different buffers 0.1 M Bis-Tris pH 5.5, 0.1 M Bis-Tris pH 6.5, 0.1 M Bis-Tris pH 7.5; 0.2 M NaCl and 0.1 M HEPES pH 7.5 (condition were from Index solution screens) in one week (Fig. 3.6 A). Considerable improvement has been achieved by setting crystal tray using all buffers in which hits came along with 10 mM DTT using hint from Horta et.al. [154]. Further crystal shape and size has been improved by using condition of Choi et.al. [59] with little modification like keeping the same buffer 0.1M Citrate pH 5.5 with and without 100 mM NaCl having 20% PEG 6000/3350 along with 10 mM DTT (Fig. 3.6 B). They produced diffused Bragg diffraction when mounted in capillaries. A quick (<10 s) immersion of the crystals into a sample of the reservoir solution of 10-20 % (v/v) ethylene glycol firstly separated like layers of some bark trees and produced a low-resolution (3.5 Å) diffraction pattern (Fig. 3.6 B). Many other approaches to cryostabilization were tried but resulted in inferior or no diffraction. By means of adding additives and changing the key variables we

could not able to improve the crystal quality. At best, poor-quality inter grown sea urchin like crystals were obtained from 0.1 M Bis-Tris or HEPES pH 5.5–8.0, 0.2M NaCl, 20% (w/v) PEG 3350, 6000 at 294 K and 5% glycerol (Fig. 3.6 C). A significant improvement observed in crystal properties when we have incorporated 0.1 % (w/v) agarose to the reservoir solution before combining it with the protein sample. Crystals grown in the presence of agarose took more than 4 days and were eventually larger and better shaped (Fig. 3.6 D) compared with crystals grown without agarose. The best crystals grew at 293.15 K in these conditions i.e. 0.1M HEPES pH 7.5 and 0.1M Citrate pH 5.5 (buffers), 100mM NaCl, 10mM DTT having 20–25 % (w/v) PEG 6000/ 3350 and 0.1 % (w/v) agarose. We also saw decreased number of inter grown crystals or crystals with surface defects. Moreover, crystals grown with the aid of agarose remained physically intact even during serial transfer into solutions. Samples of the reservoir solution supplemented with increasing concentrations of glycerol (5-10%) followed by low % of ethylene glycol and flash-freezing by direct immersion in liquid nitrogen.

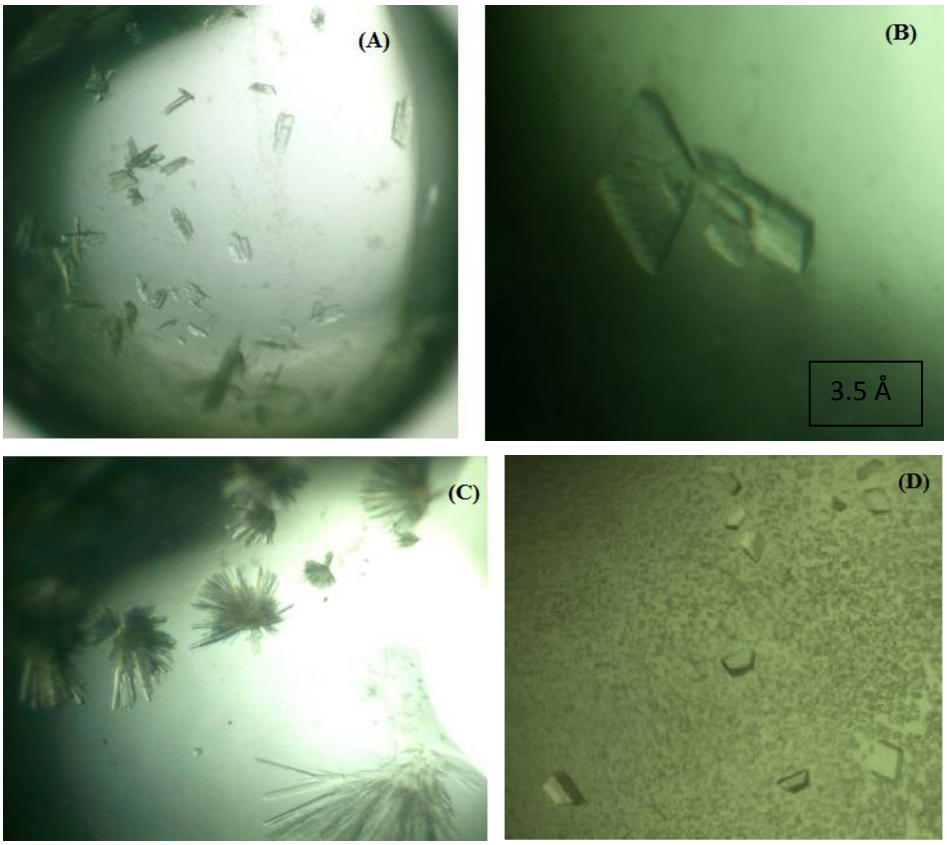

Figure 3.6: Crystal obtained in different crystal conditions. (A) Crystals were grown in 0.1 M Bis Tris pH 7.5; 0.2 M NaCl with 25% (w/v) PEG 3350. (B) crystals were grown in 0.1M Citrate pH 5.5, 100 mM NaCl, 20% PEG PEG 3350 along with 10 mM DTT. (C) Crystals from HEPES pH 8.0, 20% (w/v) PEG 3350 and 5% glycerol at 294 K. (D) Good improved better diffracting crystal were obtained in 0.1M Bis-Tris pH 7.5, 0.2M NaCl, 10mM DTT, 20% PEG6000 having 0.1% agarose.

Initially CLa-BCP crystals were not diffracting properly even in the presence of 0.05% agorose. The same crystal when picked up and annealing was done (twice), diffraction was

still not proper. However, the spots were getting better which could be due to annealing. The same crystal after annealing was put back in a solution containing 4% ethylene glycol and reservoir solution (0.1M Bis-Tris pH 7.5, 0.2M NaCl, 10mM DTT, 20% PEG6000 with 0.1% agarose) when mount for diffraction with exposure time of 5 mins. This time crystal gave a very good diffraction pattern (Fig. 3.7). Therefore, there were two possibilities for better diffraction of CLa-BCP crystals; first was very low percentage of ethylene glycol and second was annealing.

The frozen crystal diffracted X-rays from the Cu rotating-anode generator to 2.2 Å resolution. Analysis of crystal symmetry and recorded diffraction patterns indicated that the CLa-BCP crystal belongs to monoclinic space group type C2 with unit-cell parameters a = 92.22 b = 151.94, c = 139.50 Å, α= γ=90°, β= 108.71 other crystallographic data summarized in table 3.2.

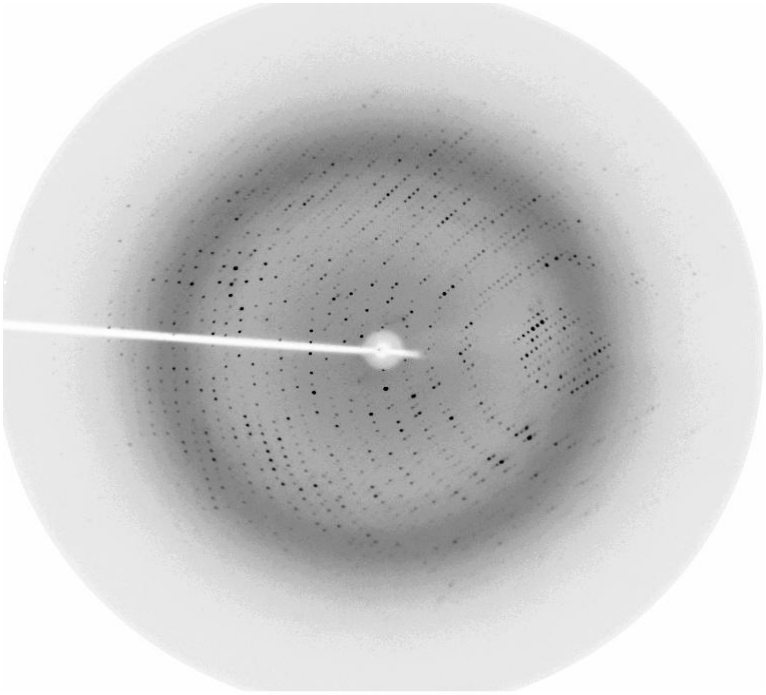

Figure 3.7: The diffraction pattern of CLa-BCP crystal obtained in 0.1% agarose condition.

Table 3.2 Data integration statistics for CLa-BCP

Crystallographic data	

Space group	C2
Wavelength	1.54179
Resolution (Last shell)	50-2.21(2.25-2.21)
Cell dimensions	
a (Å)	92.22
b (Å)	151.94
c (Å)	139.50
α	90˚
β	90˚
γ	108.71˚
Total reflections	258057
Unique reflections	86444 (1863)
Completeness (%) (Last shell)	95.5 (41.5)
Rsym(%)a (Last Shell)	0.115 (0.471)
I/ σ (Last shell)	11.06 (1.46)
Multiplicity (Last shell)	3.0 (1.7)
V_M ($Å^3$ Da^{-1})	3.04 (59.57% solvent)

3.3.5 Multiple sequence alignment and Phylogenetic analysis

Comparative sequence analysis was done individually with three major groups which include 1-Cys Prxs, atypical 2-Cys and alkylhydroperoxide reductase (AhpC) for knowing the relatedness of CLa-BCP to these groups. It has been observed with all classes the PXXXT/SXXC motif was strictly conserved with key residue "Cys" in all classes of peroxiredoxins. The maximum sequence similarity was observed with alkylhydroperoxide reductase (AhpC) subfamily. Subsequently phylogenetic tree was constructed from CLa-BCP MSA with different subclasses of Prxs. The CLa-BCP was having significant similarity with 1-Cys Prxs but not closely related with any of the known bacterial 1-Cys Prxs (Fig. 3.8 A). The sequence similarity and conservation was very less with known atypical 2-Cys Prxs protein (Fig. 3.8 B). The maximum sequence conservation was seen in case of AhpC family members, which implicates that CLa-BCP emerged as a new subfamily of bacterial AhpCs, a reductase protein first discovered in *Salmonella typhimurium* [167]. Candidatus genus was clustered in one group with maximum similarity, plant symbiotic and pathogenic bacteria were clustered in another group (Fig. 3.8 C).

(A) CLUSTAL O(1.2.1) multiple sequence alignment

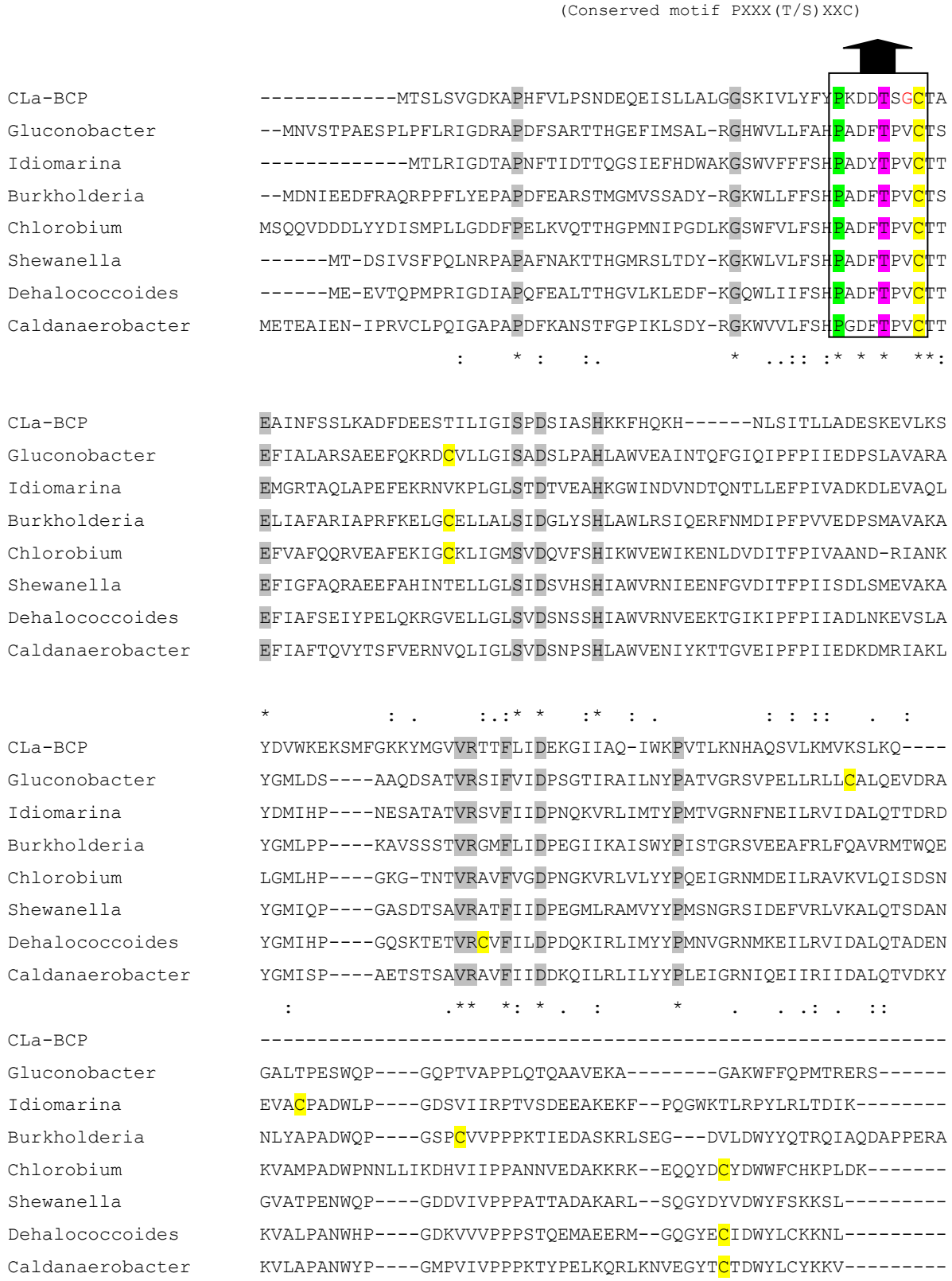

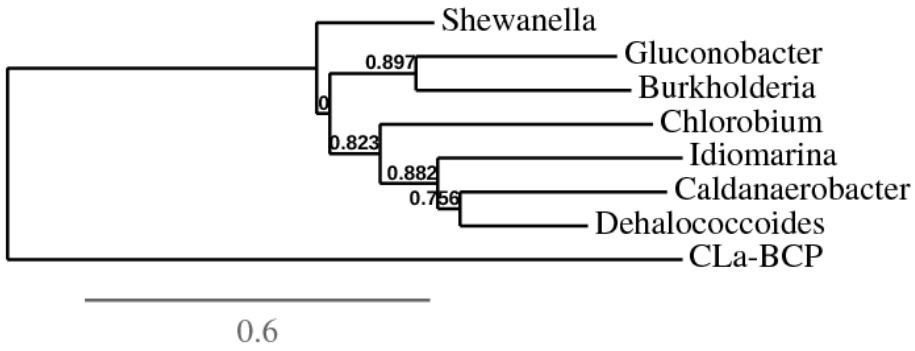

(B) CLUSTAL O(1.2.1) multiple sequence alignment

(Conserved motif PXXX(T/S)XXC)

```
CLa-BCP                ---------------MTSLSVGDKAPHFVLPSNDEQEISLLALGGSKIVLYFYPKDDTSG
Streptococcus          ---MVTFLGNPVSFTGKQLQVGDKALDFSLTTTDLSKKSLADFDGKKKVLSVVPSIDTGI
Enterobacteriaceae     MSQTVHFQGNPVTVANSIPQAGSKAQTFTLVAKDLSDVTLGQFAGKRKVLNIFPSIDTGV
Mycobacterium          -MAQITLRGNAINTVGELPAVGSPAPAFTLTGGDLGVISSDQFRGKSVLLNIFPSVDTPV
Haemophilus            --MTVTLAGNPIEVGGHFPQVGEIVENFILVGNDLADVALNDFASKRKVLNIFPSIDTGV
Bacillus               -MAEITFKGGPVTLVGQEVKVGDQAPDFTVLTNSLEEKSLADMKGKVTIISVIPSIDTGV
Clostridium            --MKVKFKGKEVTLEGTEIKVGDTFPDFVAVNSSLEPVMLKN-TNRVRVFLAVPSVDTPV
Lactococcus            MPMNITSHGEKIATL--NPPISGDAPDFELTDLKGNKIKLS-KLEKPVLISVFPDINTRV
Lactobacillus          --MKITFKGKEVKLIGTPPAVGEEMPNFAVLNKNNQEFTKSDLLGKFSLISVVPDINTPV
Pediococcus            --MEVLRGGEKVELVGNPPMIGEQLPKFKVFTGDGEKVKTRDLLGKPLLISVVPDLNTPV
                                                 .     *     .              ::   *. :*

CLa-BCP                CTAEAINFSSLKADFDEESTILIGISPDSIASHKKFHQKHNLSITLLADESK--EVLKSY
Streptococcus          CSTQTRRFNEELAGLDNTV--VLTVSMDLPFAQKRWCGAEGLDNAIMLSDYFDHSFGRDY
Enterobacteriaceae     CAASVRKFNQLATEIDNTV--VLCISADLPFAQSRFCGAEGLNNVITLSTFRNAEFLQAY
Mycobacterium          CATSVRTFDERAAAS-GAT--VLXVSKDLPFAQKRFCGAEGTENVMPASAFRD-SFGEDY
Haemophilus            CATSVRKFNQQAAKLSNTI--VLCISADLPFAQARFCGAEGIENAKTVSTFRNHALHSQL
Bacillus               CDAQTRRFNEEAAKLGDVN--VYTISADLPFAQARWCGANGIDKVETLSDHRDMSFGEAF
Clostridium            CDLEVKTFNARASEIDGVS--IYTISMDLPFAQSRWCGAEGIKNVTTLSDYRDRAFGKNT
Lactococcus            CSLQTKHFNLEAAKHSEID--FLSISNNTADEQKNWCATEGVDMTILADDG---TFGKAY
Lactobacillus          CSIQTKTFNKTMDKFPEIN--FLTISTNTVEDQQTWCAAEDVKNMQLMSDK-NFSFGKAT
Pediococcus            CSMQTKKFNQETDQYSDIR--FVTISNNMPKDQVAWCANEGVKNMEVLSDH-ELSFGYEM
                       *  ..  *.           .  :* :    :  :   .  .     .      .

CLa-BCP                DVWKEKSMFGKKYMGVVRTTFLIDEKGIIAQ--IWKPVTLKNHAQSVLKMVKSLKQ-
Streptococcus          ALLINE------WHLLARAVFVLDTDNTIRYVEYVDNINSEPNFEAAIAAAKAL---
Enterobacteriaceae     GVAIAD---GPLKGLAARAVVVIDENDNVIFSQLVDEITTEPDYEAALAVLKA----
Mycobacterium          GVTIAD---GPMAGLLARAIVVIGADGNVAYTELVPEIAQEPNYEAALAALGATSGS
Haemophilus            GVDIQT---GPLAGLTSRAVIVLDEQNNVLHSQLVEEIKEEPNYEAALAVLA-----
Bacillus               GVYIKE------LRLLARSVFVLDENGKVVYAEYVSEATNHPNYEKPIEAAKALVK-
Clostridium            GTYIKE------LGLLARAVFVVDSSNKVTYANYLEEVSGYPNYDEVLQAAQAAK--
Lactococcus            GLILNG---GPLEGRLARSVFVV-KNGQIVYSEVLSELSDEPNYEKALAATK-----
Lactobacillus          GLLI------PESGILARSVWVLDPNGKILYRELVDEITHEPNYDAVLNELKQLH--
Pediococcus            NLYI------PNAGYLARSIFIVDADGKIIYREIVPEIHDEPDYQAALDFINKM---
                                        *:  ::  .  :            . :  :
```

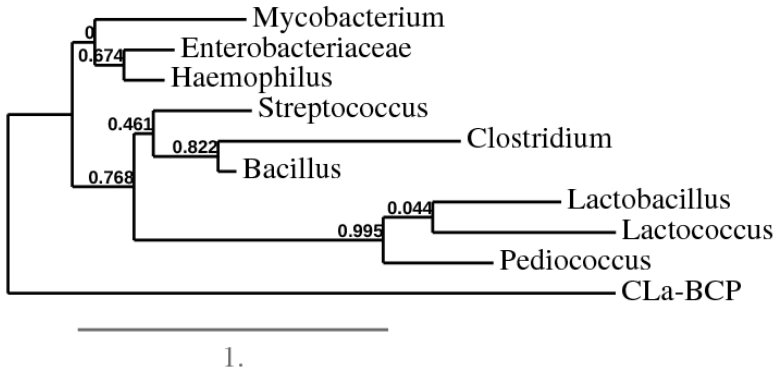

(C) CLUSTAL O(1.2.1) multiple sequence alignment

```
                                                    (Conserved motif PXXX(T/S)XXC)

CLa-BCP             --MTSLSVGDKAPHFVLPSNDEQEISLLALGGSKIVLYFYPKDDTSGCTAEAINFSSLKA
Candidatus          MTSILLSSGDKAPDFILPSTAEKEISLSALKGSKLVIYFYPKDDTTGCTAEAIDFSNLKS
Ag.                 --MTDLAIGDNAPDFTLPRNGSGDVTLSSLKGKAVVLYFYPKDDTSGCTAQAIDFSAMGG
Agrobacterium       --MTDLTIGGTAPDFTLPRNGEGTVTLSKLQGKAVILYFYPKDDTSGCTAEAIDFSALGG
Rhizobium           --MTDLTIGGPAPDFTLPRNLEGTVTLSKLQGKAVVLYFYPKDDTSGCTAEAIDFSALGG
Nitratireductor     --MTEPVKGSEAPDFSLPGDGGSEIKLSDFRGKTVVLFFYPKDDTSGCTAEAIDFTALKP
Ochrobactrum        --MAHPQVGDPAPDFTLPSDN-GEISLSSLRGKPVVIYFYPKDDTSGCTKEAIAFSQLKP
Sinorhizobium       --MAGLRQGDVAPEFELPREGGGTISLAALRGGPVVLFFYPKDDTKGCTQEAISFSALKE
vitis               --MAELSIGDMAPDFTLPRDGGGTVSLSSFKGKQVVVYFYPKDDTSGCTVEATSFTSLTP
                            *  **.* **      :.*  : *  ::::*******.*** :*  *: :

CLa-BCP             DFDEESTILIGISPDSIASHKKFHQKHNLSITLLADESKEVLKSYDVWKEKSMFGKKYMG
Candidatus          DFEKESTVVIGISPDSIVSHTKFLQKYNLSITLLSDESKKILQAYDVWKEKNMFGKKYMG
Ag.                 DFEAANAVVIGISPDSVKSHDKFAAKHSLSVMLASDEERKVLEAYGVWKEKSMYGKKYMG
Agrobacterium       EFEAANAVVIGISPDSVKSHDKFAAKHALSVMLAADEEKKVVEAYGVWKEKSMYGKKYMG
Rhizobium           EFEAANTVVIGISPDSVKSHDKFAAKHSLSVMLASDEERKVLEAYGVWKEKSMYGKKYMG
Nitratireductor     EFDALDTVLLGMSPDSPKSHDKFKNKHALTIGLVSDQDKETLQAYGVWVEKSMYGRKYMG
Ochrobactrum        EFDKIGARVIGLSPDSATKHAKFRKKHDLTVDLAADEDRVALEAYGVWVEKNMYGRKYMG
Sinorhizobium       EFQSAGIMLIGISPDSAKSHDRFTRKHGLTVALASDEDKAVASAYGVWVEKSMYGRKYMG
vitis               EFESSGAVIIGISPDTVKSHDKFVAKHGLAVMLGSDEEKTTLEAYGVWKEKSMYGKTYMG
                    :*:     ::*:***:  .* :*  *: *:: * :*:.:   .:* ** **.*:*:.***

CLa-BCP             VVRTTFLIDEKGIIAQIWKPVTLKNHAQSVLKMVKSLKQ---
Candidatus          VVRTTFLIDEQGIISKIWRPVKLKNHAKSVLNAVKSLK----
Ag.                 VERTTYLVSPDGKIVQIWNKVKVPGHAQAVLDTIKAL-----
Agrobacterium       VERTTFLIAPDGKIAEVWNKVKVAGHAQAVLEAVKKL-----
Rhizobium           VERTTFLVGPDGKIAEIWNKVKVAGHAQAVLDAAKKL-----
Nitratireductor     VERSTFLIGPDGRIAETWRKVKVPGHAQAVLDAAKALKQRDE
Ochrobactrum        VERTTFLIDAQGKIAQVWNKVKVDGHADAVLEAARAL-----
Sinorhizobium       VERTTFLIDRQGVISRVWEKVKVPGHADEVLAAAKAI-----
vitis               VERSTFLIDADGRIAGVWRKVKVPGHAEAVLQAVKDKAA---
                    * *:*:*:  .* *   *. *.:  **. **   :
```

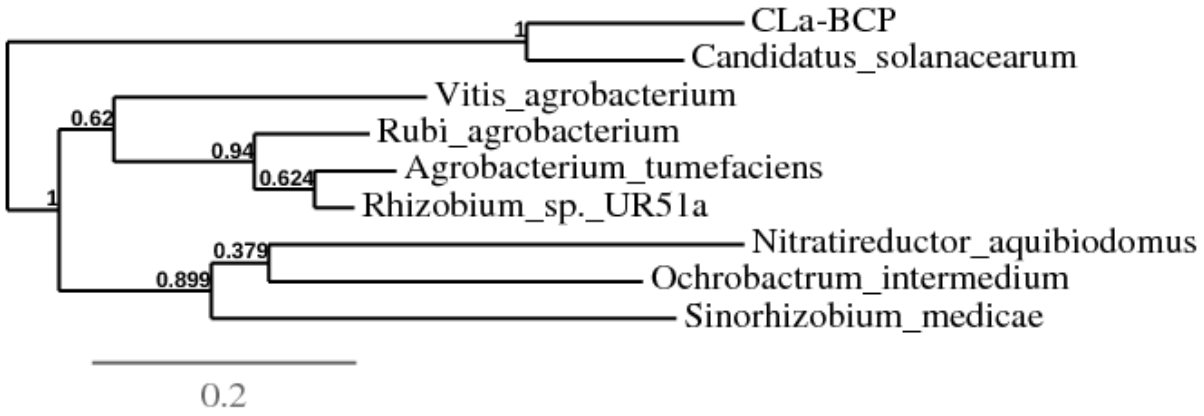

Figure 3.8: Multiple sequence alignment using Clustal omega with different subclasses of Prxs and Phylogenetic tree constructed using *Phylogeny.fr* online server. (A, B, C) The highly conserved motif represented by rectangle with highlighted catalytic residues, proline (P) green, threonine (T) magenta and including peroxidatic residue Cysteine (C) in yellow. The most conserved residues were highlighted in grey colour from 1-Cys prx, atypical 2-Cys prx and AhpC reductase family respectively.

The MSA with known pdb structures of Prxs protein was further improved by esprit3.0 server and showed conserved thioredoxin fold region and conservation of sequences structurally (Fig. 3.9).

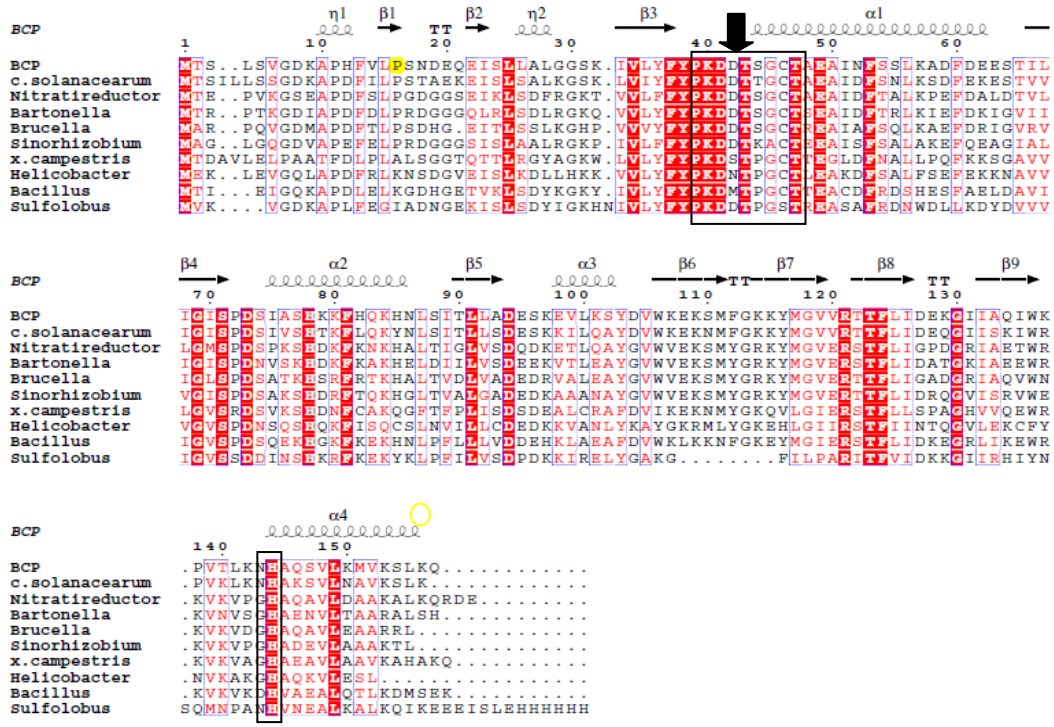

Figure 3.9: The MSA with structural conservation among known Prxs structures. The bold arrow indicates the catalytic motif site that forms a Cp loop generally present in Alpha helix region. Arg (R) highlighted from loop region preceded by β sheet interacts with peroxidatic Cys (Cp) residue.

3.3.6 Signal peptide Prediction

CLa-BCP protein sequence showed no signal peptide at the N-terminal end as predicted by different server. Here the result shown predicted from SignalP 4.1 server (Fig. 3.10).

```
# SignalP-4.0 gram+ predictions
# Measure  Position  Value  Cutoff  signal peptide?
  max. C     51      0.119
  max. Y      1      0.130
  max. S      1      0.171
  mean S      1-0    0.000
      D       1-0    0.079    0.450  NO
Name=tmp_signalp_seq    SP='NO' D=0.079 D-cutoff=0.450 Networks=SignalP-TM
```

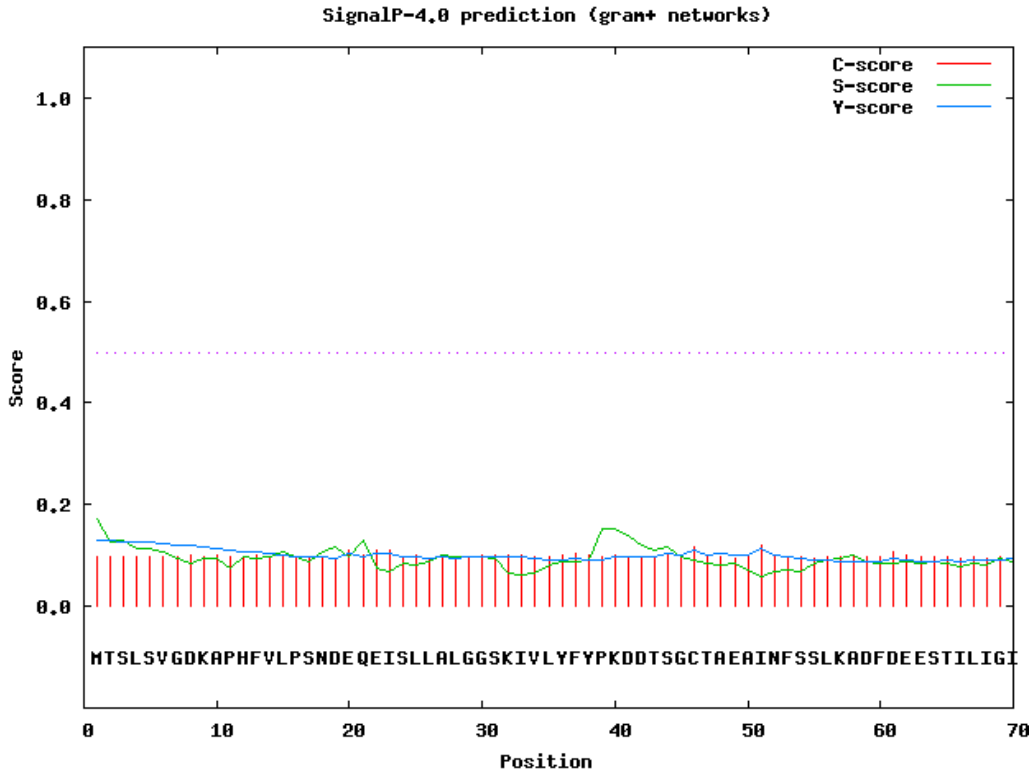

Figure 3.10: prediction of signal sequence by SignalP server in CLa-BCP sequence.

3.3.7 Prediction and evaluation of three-dimensional structure of CLa-BCP

The three-dimensional model of CLa-BCP was build using the crystal structure of *M.tuberculosis* AhpE (1XVW), a 1-Cys as a template (Fig. 3.11 A). The predicted model showed two chains (Fig 3.11 B). Stereo chemical evaluation of CLa-BCP model was done through PROCHECK program which show that 88.7% of residues fall within the most favored, 11.3% allowed regions in Ramachandran plot and 0.0% in disallowed regions for model. Similar to other members of the Prx family, the predicted model of CLa-BCP has characteristic Thioredoxin fold. The overall Thioredoxin fold consists of central β twist (cradle) formed by anti -parallel β5, β4, β3, β8, β2 and β1 with a backbone support of α2-α3-α5 helix (Fig. 3.11C). The catalytic peroxidatic Cys (C_P) is located in the α2 helix with other active site motif residues threonine (T) and proline (P) forming active C_P loop (Fig. 3.11 D).

Structural superimposition of predicted model shows significant conformational changes in loop region of C-terminal motif and loop region near α3 will be discussed further. The predicted structure showed 9 β-sheets flanked by large 3α-helices and 2 small α-helices with large loop region. It can be correlates with CD data of CLa-BCP which showed predominance of β-sheet structure.

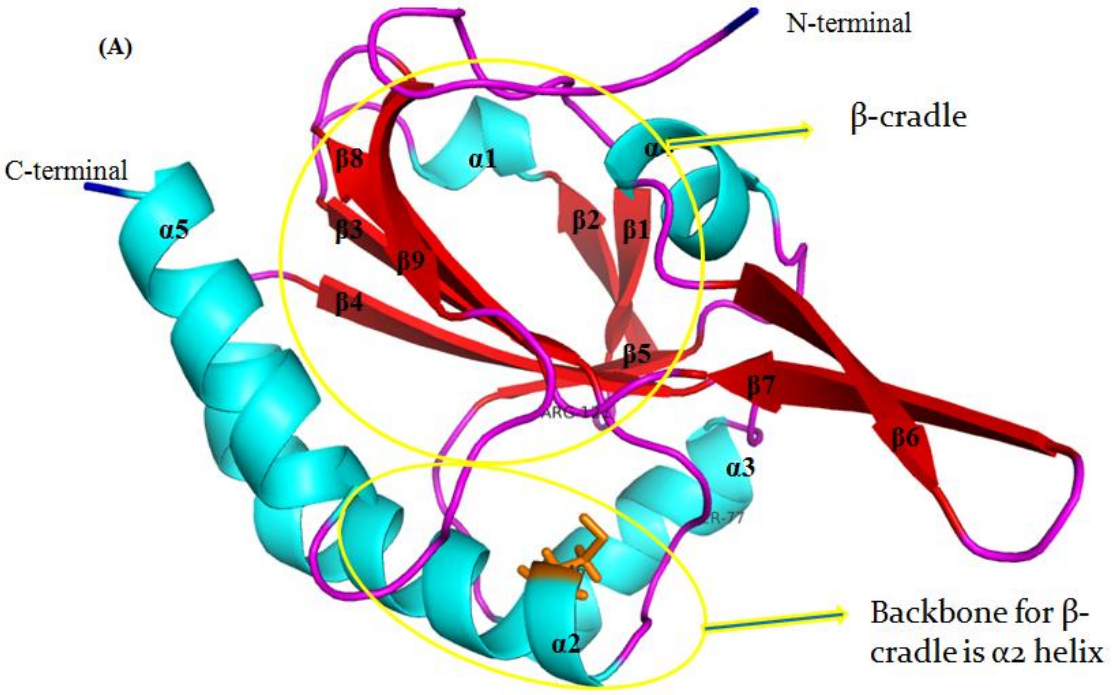

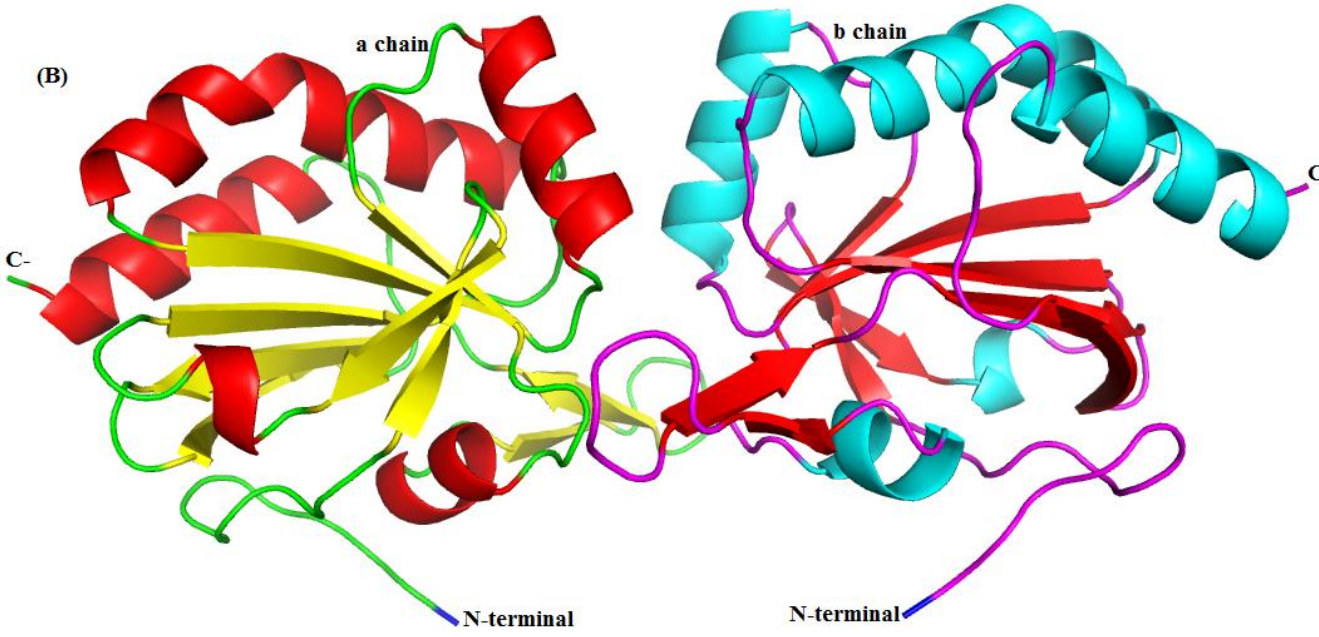

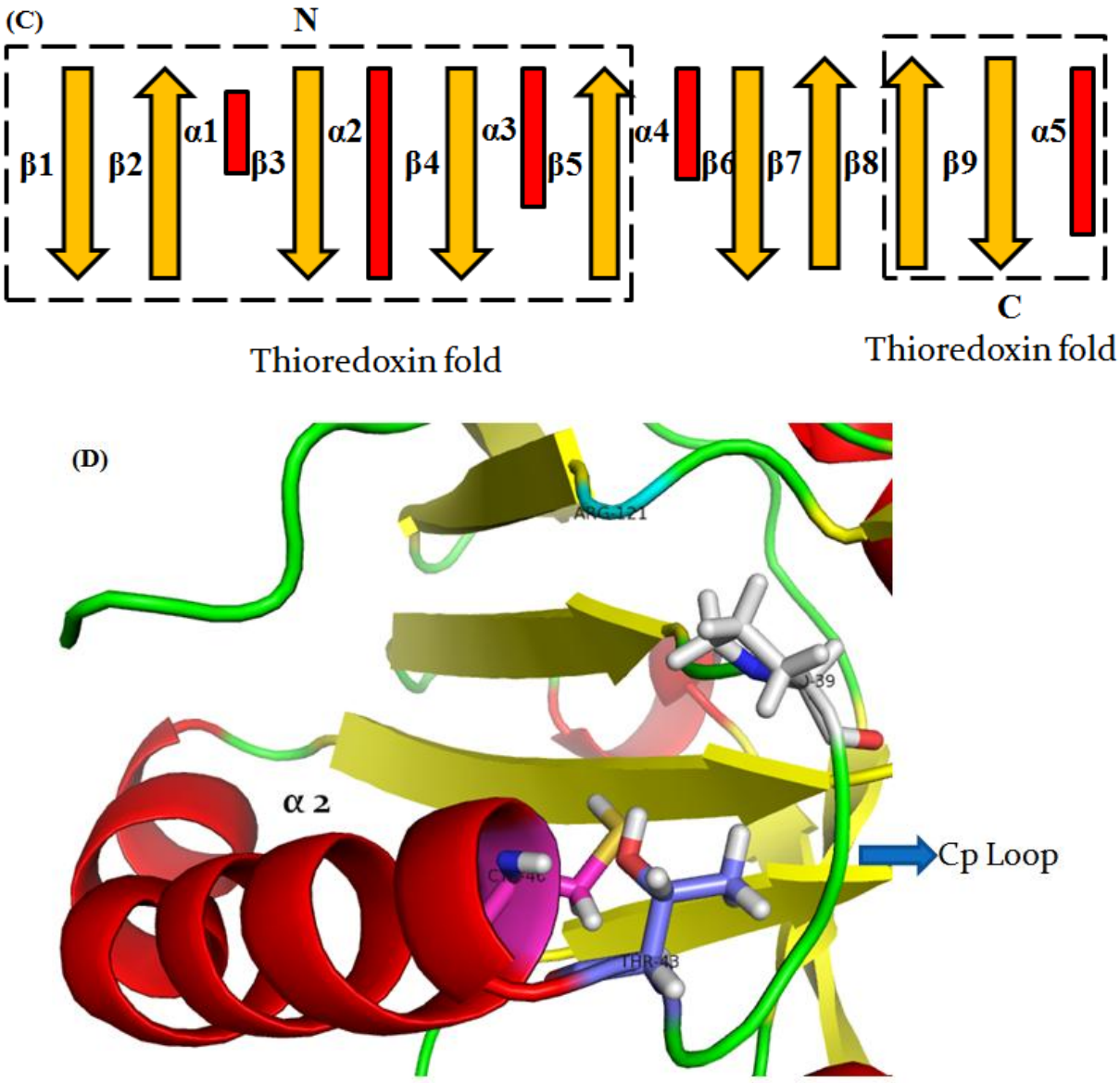

Figure 3.11: Predicted 3-D model of CLa-BCP. (A, B) represents monomeric and dimeric molecule, the peroxidatic catalytic Cys residue shown in orange sticks. (C) The overall topology present in CLa-BCP predicted model. (D) The conserved motif residues (PXXXTXXC) Thr 43, Pro 39 and Arg 121 (loop residues) along with key residue Cys 46 present in α2 helix are shown as sticks in blue, white, cyan and pink colour respectively. The universally conserved motif forms Cp loop which involves in catalytic activity of Prxs. The figures were made from pymol visualization tool.

By introduction of Cysteine residue at 77th position which is present in α3 position results into formation of intermolecular disulfide bond formation as shown through biochemical experiments. Here we have predicted the structure by mutating the S77 residue into Cysteine, structurally it have been seen that Cys77 from a chain forming interaction within 3.6 Å distance with another Cys77 from b chain (Fig. 3.12). Instead of forming disulfide bond in between Cp and Cr (resolving Cysteine) here in our predicted structure the most favourable

bond formation could be in-between mutated Cys77-Cys77` residue i.e. in between two resolving cysteine. More detailed study has to be carried to validate the role of introduced cysteine that it could act as resolving Cysteine or not and which catalytic pathway it follows atypical or typical 2-Cys.

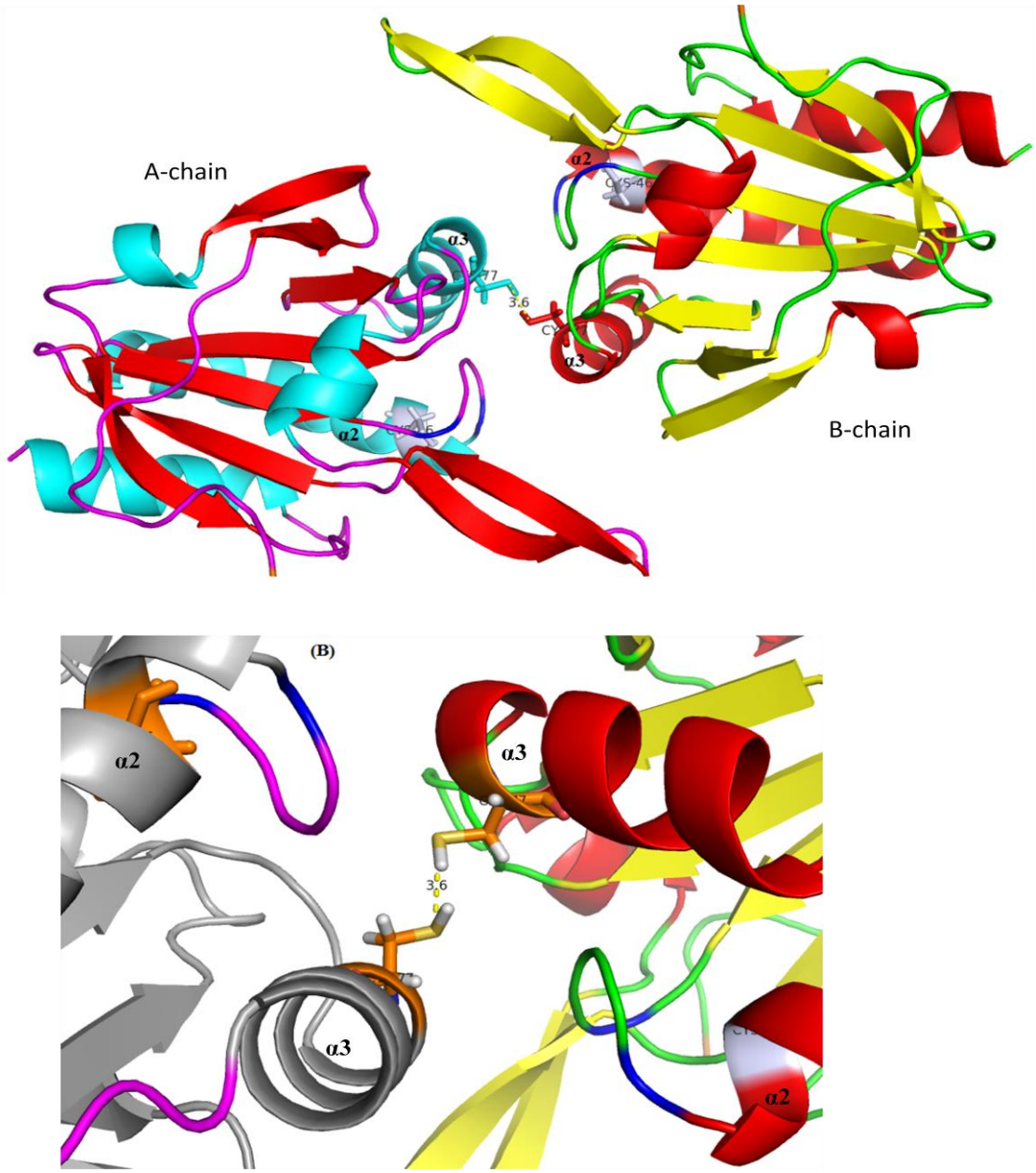

Figure 3.12: Predicted CLa-BCP model with mutated S77C residues at α3 position. (A) The disulfide interaction showed in between both the chains. (B) The closest view of interaction of introduced Cys residue within 3.6Å distances.

3.3.8 Interaction of CLa-BCP model with substrate H_2O_2

The Prxs catalytic reaction follows the basic S_N2 displacement reaction as described in standard organic chemistry textbook (McMurry 2004) [249]. The reaction involves addition of two hydrogen ions (H+) and two electrons to H_2O_2 to produce two H_2O molecules:

$$2e^- + 2H^+ + H_2O_2 \longrightarrow 2H_2O$$

S_N2 reaction is a nucleophilic bimolecular substitution reaction where a nucleophile (electron rich) attacks an electrophile (electron deficient) to form a nucleophile-electrophile bond and break the bond between the electrophile and the leaving group. Prxs follows the same basic reaction termed as peroxidation step in which sulfur atom of peroxidative Cys (Cp) residue acts as a nucleophile and O_A atom of peroxide acts as the electrophile; and O_B atom of the hydroxide (or alkoxide) acts as the leaving group. The reaction involves formation of stable catalytic covalent intermediates like sulfenic acid intermediate (SpOH) (Jencks 1969)[173].

$$H_2O_2 + RS_PH \longrightarrow RS_POH + H_2O \text{ (peroxidation step)}$$

In order to attack the substrate like H_2O_2, the SpOH moiety of the peroxidatic Cys (Cp) residue undergoes a conformational change and moves out of the fully folded active site pocket. This step involves local unfolding of helix.

In case of 2-cys Prxs, this reaction has an additional step where the resolving cysteine group reacts with these intermediates and forms a disulfide bond.

$$RS_POH + R'SH \longrightarrow RS_PSR' + H_2O \text{ (resolution step)}$$

For another round of catalysis, the protein needs to unlock its LU conformation and break the disulfide bond. This breaking of disulfide bond involves thiols which reduces the disulfide bond as a result of which RSpH becomes free to react with incoming peroxide molecules. This step is known as the recycling step. These protein thiols could be thioredoxin-thioredoxin reductase, glutaredoxin-glutaredoxin reductase or non-physiological reductant partners such as DTT, ascorbate etc which will act as electron donors.

To decipher the catalytic mechanism, we need to study the conformational change that occurs in the active site in the presence of the peroxide molecule. These conformational changes along with the changes in the nearby environment are important during the catalysis. Through various ligand-bound Prx structures, many research groups detailed the interactions studies such as hydrogen bonding at the active site and gained insight into the catalytic power of the Prxs [2, 92, 131, 227, 229, 271, 343, 349].

3.3.8.1 Comparison of CLa-BCP with 1-Cys Prxs

The comparison of CLa-BCP sequence with the other known 1-Cys Prxs from RCSB PBD, showed maximum similarity of 30% but with very high E-value which implicates the sequence alignment is insignificant (Fig. 3.13 A, B). However the structural alignment of these Prxs with CLa-BCP shows that these proteins share a similar canonical thioredoxin fold (consists of an antiparallel beta sheet intermediate between alpha helices) and the active site residues are highly conserved. Thus despite of low sequence similarity, CLa-BCP possesses the same structural fold as other known 1-cys Prxs (Fig. 3.13 C).

(A)

Chain A, Thioredoxin Peroxidase B From Red Blood Cells	54.7	54.7	82%	1e-09	32%	1QMV_A
Chain A, Crystal Structure Of Ahpe From Mycrobacterium Tuberculosis, A 1-Cys Peroxiredoxin	53.9	53.9	89%	1e-09	26%	1XXU_A
Chain A, Oxidation Of Archaeal Peroxiredoxin Involves A Hypervalent Sulfur Intermediate	55.5	55.5	80%	1e-09	28%	2ZCT_A
Chain A, Crystal Structure Of Archaeal Peroxiredoxin, Thioredoxin Peroxidase From Aeropyrum Pernix K1 (Sulfinic Acid Form)	55.1	55.1	80%	2e-09	28%	2E2M_A
Chain A, Crystal Structure Of An Archaeal Peroxiredoxin From The Aerobic Hyperthermophilic Crenarchaeon Aeropyrum Pernix K1	54.3	54.3	80%	3e-09	28%	2CV4_A
Chain A, Crystal Structure Of Human Peroxiredoxin 4 (Thioredoxin Peroxidase)	52.4	52.4	86%	9e-09	27%	2PN8_A
Chain A, Crystal Structure Of Peroxiredoxin Prx4 From Pseudosciaena Crocea	52.8	52.8	73%	9e-09	31%	3QPM_A
Chain A, Crystal Structure Of Human Peroxiredoxin 4(thioredoxin Peroxidase) With Mesna	52.8	52.8	86%	1e-08	27%	4RQX_A
Chain A, Crystal Structure Of Human Peroxiredoxin Iv C51a Mutant In Reduced Form	52.4	52.4	73%	2e-08	30%	3TJF_A
Chain A, Crystal Structure Of Human Peroxiredoxin Iv C245a Mutant In Reduced Form	52.4	52.4	73%	2e-08	30%	3TJK_A
Chain A, Crystal Structure Of N-terminally Truncated Peroxiredoxin 4 From M. Musculus	51.6	51.6	86%	2e-08	26%	3VWV_A
Chain A, Crystal Structure Of Full-Length Human Peroxiredoxin 4 In The Reduced Form	52.0	52.0	73%	2e-08	30%	3TKP_A
Chain A, Crystal Structure Of Wild-Type Human Peroxiredoxin Iv	52.4	52.4	73%	2e-08	30%	3TJB_A
Chain A, Crystal Structure Of Full-Length Human Peroxiredoxin 4 With T118e Mutation	51.6	51.6	73%	3e-08	30%	3TKR_A
Chain A, Crystal Structure Of Peroxiredoxin 4 From M. Musculus	51.6	51.6	86%	3e-08	26%	3VWU_A
Chain A, 1-Cys Peroxidoxin From Plasmodium Yoelli	50.8	50.8	78%	4e-08	30%	1XCC_A
Chain A, Escherichia Coli Thiol Peroxidase (Tpx) Resolving Cysteine To Serine Mutant (C95s) With An Intermolecular Disulfide Bond	49.3	49.3	94%	6e-08	27%	3HVX_A
Chain A, Crystal Structure Of Ahpe From Mycobacterium Tuberculosis, A 1-Cys Peroxiredoxin	49.3	49.3	89%	7e-08	25%	1XVW_A
Chain A, Horf6 A Novel Human Peroxidase Enzyme	32.7	32.7	98%	0.085	26%	1PRX_A

(B)

```
CLa-BCP     ----------MTSLSVGDKAPHFVLPSN--DEQEISLLALGGSK-IVLYFYPKDDTSGCT 47
1prx        ---------MPGGLLLGDVAPNFEANTT--VGRIRFHDFLGDSW-GILFSHPRDFTPVCT 48
1xiy        MKENDLIPNVKVMIDVRNMNNISDTDGSPNDFTSIDTHELFNNKKILLISLPGAFTPTCS 60
1xcc        -----------MGYHLGATFPNFTAKASGIDGDFELYKYIENSW-AILFSHPNDFTPVCT 48
1xxu        ------------MLNVGATAPDFTLRDQ--NQQLVTLRGYRGAKNVLLVFFPLAFTGICQ 46
                           :                         .    :*   *   *  *

CLa-BCP     AEAINFSSLKADFDEESTILIGISPDSIASHKKFHQ----------KHNLSITLLADESK 97
1prx        TELGRAAKLAPEFAKRNVKLIALSIDSVEDHLAWSKDINAYNSEEPTEKLPFPIIDDRNR 108
1xiy        TKMIPGYEEEYDYFIKENNFDDIYCITNNDIYVLKSWFKS------MDIKKIKYISDGNS 114
1xcc        TELAELGKMHEDFLKLNCKLIGFSCNSKESHDKWIEDIKYYG---KLNKWEIPIVCDESR 105
1xxu        GELDQLRDHLPEFENDDSAALAISVGPPPTHKIWAT----------QSGFTFPLLSDFWP 96
             :     .   ::   .     :   .                        :  : *

CLa-BCP     EVLKSYDVWKEKSMFGKKYMGVVRTTFLID-EKGIIAQIWKPVTLKNHAQSVLKMVKSLK 156
1prx        ELAILLGMLDPAEKDEKGMPVTARVVFVFGPDKKLKLSILYPATTGRNFDEILRVVISLQ 168
1xiy        SFTDSMNMLVDKSNFEMG---MRPWRFVAIVENNILVKMFQEKDKQHNIQTDPYDISTVN 171
1xcc        ELANKLKIMDEQEKDITGLPLTCRCLFFISPEKKIKATVLYPATTGRNAHEILRVLKSLQ 165
1xxu        HGAVSQAYGVFNEQAG----IANRGTFVVDRSGIIRFAEMKQPGEVRDQRLWTDALAALT 152
                        .             *.   .  :           ..       : ::
```

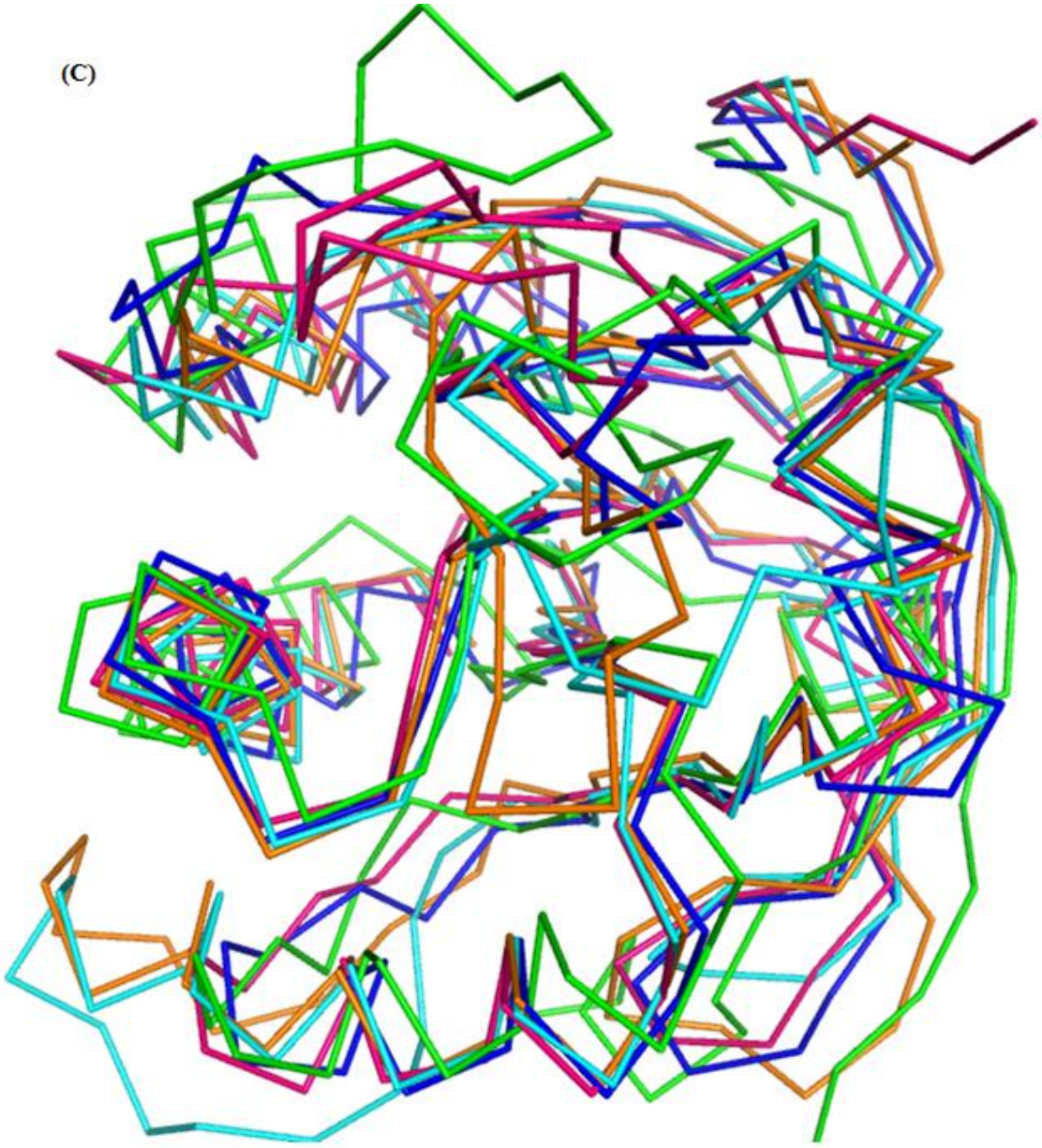

Figure 3.13 Comparison of CLa-BCP with 1-Cys Prxs. (A) BLAST results shows the similarity with 1-Cys prx highlighted in square box. (B) Sequence alignment of CLa-BCP with 1XXU (AhpE from Mycobacterium tuberculosis), 1XCC (1-Cys from Plasmodium yoelli), 1PRX (novel human peroxidase HORF6) and 1XIY (1-Cys from Plasmodium falciparum). (C) Structural alignment of CLa-BCP (magenta) with 1PRX (cyan), 1XXU (blue), 1XCC (orange) and 1XIY (green) possessing same fold. Figure of structure are drawn using PyMol visualization tool.

3.3.8.2 Comparison of CLa-BCP with other known Prxs

The previous studies reports that the active site of Prxs is composed of residues Pro, Lys, Thr, Cys, Glu and Arg. It was found that these residues are highly conserved sequentially as well as structurally (Fig. 3.14). The CLa-BCP sequence is more similar to other known 2-Cys Prxs from RCSB PBD than 1-Cys Prxs. The active site residues like Pro, Lys, Thr, Cys, and Arg are highly conserved among all the Prxs. The presence of this conserved motif region across

all known Prxs subfamilies reflecting the importance of these residues and in catalytic efficacy as well. Thus catalytic machinery of Prxs is much more sensitive to the assemblage of these residues.

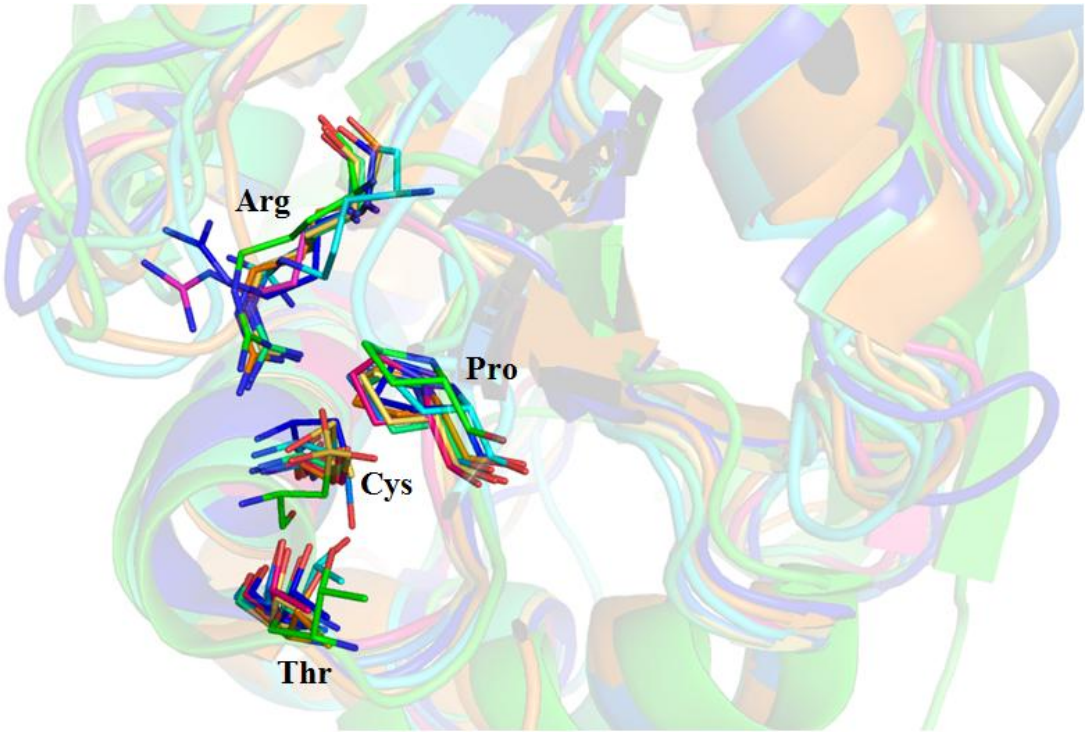

Figure 3.14 Comparison of CLa-BCP with other known Prxs. Structure superimposition of CLa-BCP (magenta) with 1PRX (cyan), 1XXU (blue), 1XCC (orange), 1XIY (green), 3GKM (golden yellow), 3DRN (lime green) having same conserved residues at active site. Figure drawn using PyMol visualization tool.

The CLa-BCP sequence is more similar to other known 2-Cys Prxs from RCSB PBD than 1-Cys Prxs. The active site region of CLa-BCP has a putative reactive loop with residues Thr43, Lys40, Pro39 and Arg121 stabilizing the interaction of the substrate H_2O_2 with sulfur atom of peroxidatic Cys46 residue (S_P). These residues (Pro39, Thr43 and C_P) belong to the conserved PXXXTXXC_P sequence motif region of Prxs (Fig. 3.8 A, Band C). This strictly conserved region is preceded by "YPK" motif which constitutes the Cp catalytic loop (Fig. 3.15). This loop region undergoes conformational change during the catalysis, the structural changes have been observed in the already known FF and LU Prxs structures.

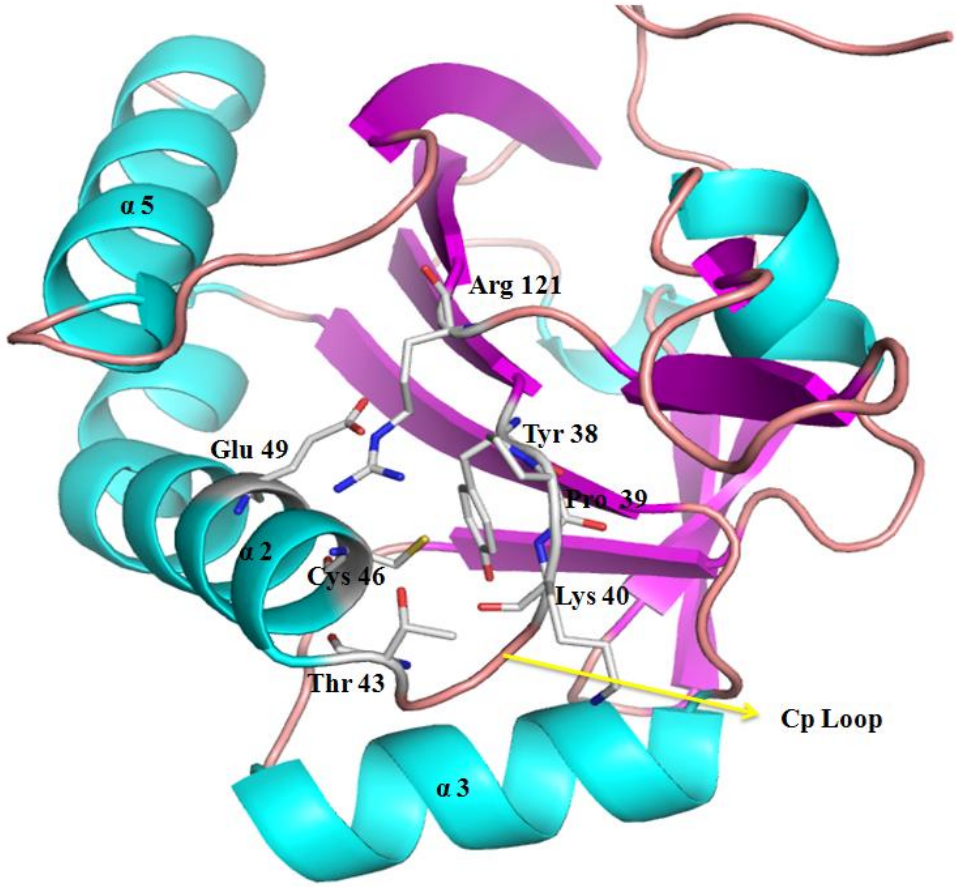

Figure 3.15 The active C_P loop in CLa-BCP model. The α-helices (cyan) and β-sheets (magenta) are labelled according to the common fold of all Prxs. The crucial residues like C_P residue (white) (coloured by atom, oxygen = red, nitrogen=blue, sulfur = yellow) are shown as sticks. The residues at active site interacting with peroxidative active Cys46 are Thr43, Tyr38, Pro39, and Lys40 (from conserved YPK motif) and Arg121 from C-terminal constitute the C_P loop. Figure drawn using PyMol visualization tool.

From known FF and LU structures literature have cited some of the members from eukaryotic subfamily, are particularly sensitive to inactivation like *Hs*PrxI and *Hs*PrxII [407], whereas others, such as *St*AhpC, are robust [400]. It has been shown to be structural difference due to the conserved "YF" motif at C-terminus. This YF motif groups on the opposite region of the active site pocket beside the first turn of helix α2. The presence of YF motif thus known to hinder the local unfolding of Cp loops after substrate binding and makes the enzyme sensitive. As of engineered Prxs, *Schistosoma mansoni* [324] showed that the deletion of C-terminal helix made an enzyme from sensitive to robust. Second region in addition to YF motif has also been identified from higher eukaryotic organisms was GGLG sequence loop. Though the function impart by these YF and GGLG motif not been completely characterized. But it has been shown that point mutations within the C-terminal of sensitive Prxs are enough to disrupt packing of the C-terminal helix [208] implicating their role in overoxidation pathways. During overoxidation, some eukaryotic Prxs are susceptible and tends to form

higher irreversible overoxidized species like SpO_2H (sulfinic) and SpO_3H (sulfonic) which can no longer be revert back to thiols by the "normal" catalytic cycle.

The alignment of structures having more that 29% similarity shows that the Prxs structures (pdb id 1E2Y, 4K1F, 3ZVJ and 3ZTL) are composed of a GGLG motif, which has not been observed in our model. This GGLG motif has been elucidated to be involved in overoxidation [400] in eukaryotes and in some parasitic bacteria *Helicobacter pylori*, *Yersinia pestis*, *Chlamydia pneumonia.* Moreover its absence in bacterial Prxs and CLa-BCP clearly indicates that they are less prone to overoxidation (Fig. 3.16 A, B).

(A)

```
CLUSTAL 2.1 multiple sequence alignment
CLa-BCP         ----------------------------------MTSLSVGDKAPHFVLPSND---EQ 21
3GKM|           -------------------------SNAMT------DAVLELPAATFDLPLSLSG---GT 26(38%)
3IXR|           --------------MGSSHHHHHHSSGLVPRGSHMNIGDTLNHSLLNHPLMLSG---ST 42(38%)
3DRN|           ------------------------------------MVKVGDKAPLFEGIADN---GE 19(39%)
2YWN|A          ------------------------------------GHMVEIGELAPDFELPDTE--LKK 22(35%)
3HJP|           ------------------------------------MVEIGEKAPEIELVDTD--LKK 20(33%)
4GQC|           ----------------------------------MKGLVELGEKAPDFTLPNQD--FEP 23(33%)
2CX3|           ----------------------------------XKGLVELGEKAPDFTLPNQD--FEP 23(32%)
1E2Y|           --------------XSCGAAK--------------------LNHPAPEFDDXALXPNGTF 26(33%)
3ZTL|           MRGSHHHHHHGMASMTGGQQMGRDLYDDDDKDRWGSTMVLLPNRPAPEFKGQAVI-NGEF 59(34%)
4K1F|           --------------MSCGNAK--------------------INSPAPSFEEVALMPNGSF 26(29%)
3ZVJ|           MRGSHHHHHHGMASMTGGQQMGRDLYDDDDK---GSTMVLLPNRPAPEFKGQAVI-NGEF 56(34%)
3A2V|           ----------------------------------PGSIPLIGERFPEMEVTTDHG--VI 23(28%)

CLa-BCP         EISLLALGGSK-IVLYFYPKDDTSGCTAEAINFSSLKADFDEESTILIGISPDSIASHKK 80
3GKM|           QTTLRAHAGHW-LVIYFYPKDSTPGSTTEGLDFNALLPEFDKAGAKILGVSRDSVKSHDN 85
3IXR|           CKTLSDYTNQW-LVLYFYPKDNTPGSSTEGLEFNLLLPQFEQINATVLGVSRDSVKSHDS 101
3DRN|           KISLSDYIGKHNIVLYFYPKDDTPGSTREASAFRDNWDLLKDYDVVVIGVSSDDINSHKR 79
2YWN|A          VKL-SALKG-KVVVLAFYPAAFTQVCTKEMCTFRDSMAKFNQVNAVVLGISVDPPFSNKA 80
3HJP|           VKIPSDFKG-KVVVLAFYPAAFTSVSTKEMSTFRDSMAKFNEVNAVVIGISVDPPFSNKA 79
4GQC|           VNLYEVLKRGRPAVLIFFPAAFSPVCTKELCTFRDKMAQLEKANAEVLAISVDSPWCLKK 83
2CX3|           VNLYEVLKRGRPAVLIFFPAAFSPVCTKELCTFRDKXAQLEKANAEVLAISVDSPWCLKK 83
1E2Y|           KKVSLSSYKGKYVVLFFYPXDFTFVCPTEIIQFSDDAKRFAEINTEVISCSCDSEYSHLQ 86
3ZTL|           KEICLKDYRGKYVVLFFYPADFTFVCPTEIIAFSDQVEEFNSRNCQVIACSTDSQYSHLA 119
4K1F|           KKISLSSYKGKWVVLFFYPLDFTFVCPTEVIAFSDSVSRFNELNCEVLACSIDSEYAHLQ 86
3ZVJ|           KEICLKDYRGKYVVLFFYPADFTFVCPTEIIAFSDQVEEFNSRNCQVIACSTDSQYSHLA 116
3A2V|           KLPDHYVSQGKWFVLFSHPADFTPVCTTEFVSFARRYEDFQRLGVDLIGLSVDSVFSHIK 83
                            *:  .*   :  .. *   *      :   .  ::. * *   .

CLa-BCP         FHQKHN-------LSITLLADESKEVLKSYDVWKEKSMFGKK-YMGVVRTTFLIDEKGII 132
3GKM|           FSAKQG-------FAFPLVSDGDEALCRAFDVIKEKNMYGKQ-VLGIERSTFLLSPEGQV 137
3IXR|           FCAKQG-------FTFPLVSDSDAILCKAFDVIKEKTMYGRQ-VIGIERSTFLIGPTHRI 153
3DRN|           FKEKYK-------LPFILVSDPDK---------KIRELYGAKGFILPARITFVIDKKGII 123
2YWN|A          FKEHNK-------LNFTILSDYNREVVKKYNVAWEFPALPGY--VLAKRAVFVIDKEGKV 131
3HJP|           FKEQNK-------INFTIVSDFNREAVKAYGVAGELPILKGY--VLAKRSVFVIDKNGIV 130
4GQC|           FKDENR-------LAFNLLSDYNREVIKLYNVYHED--LKGL-KMVAKRAVFIVKPDGTV 133
2CX3|           FKDENR-------LAFNLLSDYNREVIKLYNVYHED--LKGL-KXVAKRAVFIVKPDGTV 133
1E2Y|           WTSVDRKKGGLGPXAIPXLADKTKAIARAYGVLDEDS-------GVAYRGVFIIDPNGKL 139
3ZTL|           WDNLDRKSGGLGHMKIPLLADRKQEISKAYGVFDEED-------GNAFRGLFIIDPNGIL 172
4K1F|           WTLQDRKKGGLGTMAIPILADKTKNIARSYGVLEESQ-------GVAYRGLFIIDPHGML 139
3ZVJ|           WDNLDRKSGGLGHMKIPLLADRKQEISKAYGVFDEED-------GNAFRGLFIIDPNGIL 169
3A2V|           WKEWIERHIG-VRIPFPIIADPQGTVARRLGLLHAES------ATHTVRGVFIVDARGVI 136
                :             :  ::*                          *  *::     :
```

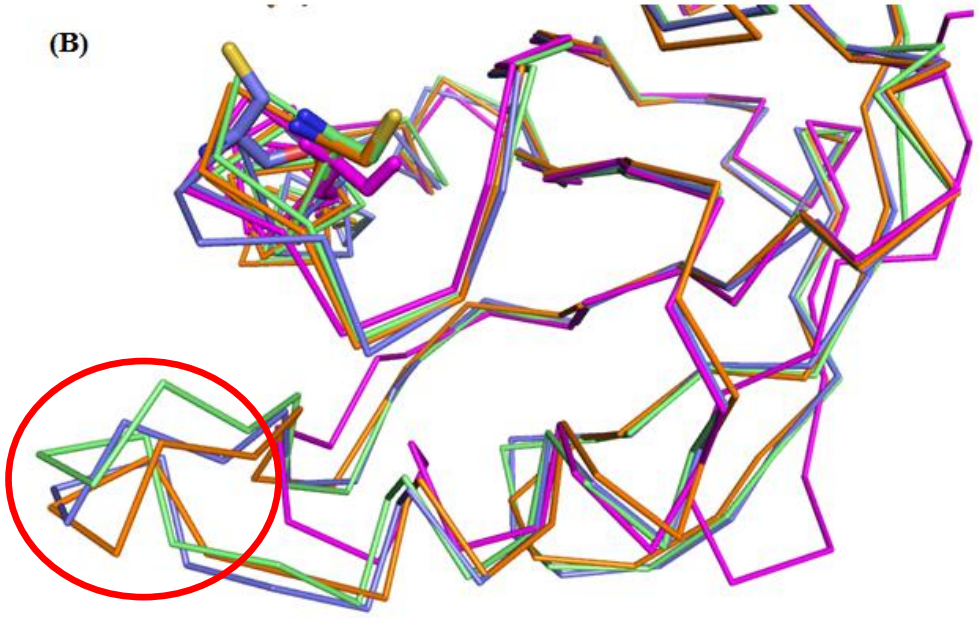

Figure 3.16 Comparison of the CLa-BCP model (A) Sequence alignment of CLa-BCP with known Prxs structures showed the absence of GGLG motif in most of the Prxs except 1E2Y (tryparedoxin peroxidase from *Crithidia fasiculata*), 3ZTL (peroxiredoxin1 from *Schistosoma mansoni*), 4K1F (tryparedoxin peroxidase from *Leishmania major*) and 3ZVJ (high molecular weight Prx from *Schistosoma mansoni*). (B) Superimposition of CLa-BCP (magenta) with 1E2Y (purple), 3ZTL (orange) and 4K1F (light green) showing GGLG motif encircled in red colour. Figure drawn using PyMol visualization tool.

3.3.8.3 Active site (H_2O_2 interaction with Gly, Thr, Cys, Arg and Tyr)

To identify the interaction of H2O2 with CLa-BCP, we compared our H2O2-docked-CLa-BCP structure with the two already known ligand bound structures of Prxs. The hydrogen peroxide bound structure of Peroxiredoxin (C207S) from *Aeropyrum pernix* K1 (PDB 3A2V) has 28% similarity while Human Pdrx5 (PDB 4MMM) complexed with 1,1'-BIPHENYL-3,4-DIOL (BP7) ligand has similarity almost same (Fig. 3.17).

```
CLa-BCP         ------MTSLSVGDKAPHFVLPSND--EQEISLLALGGSKIVLYFYPKDDTSGCTAEAIN 52
3a2v            -----PGSIPLIGERFPEMEVTTDHGVIKLPDHYVSQGKWFVLFSHPADFTPVCTTELVS 55
4mmm            HHHHHHSAPIKVGDAIPAVEVFEGEPGNKVNLAELFKGKKGVLFGVPGAFTPGCSKTHLP 60
                       :   :*:  * . :  ..   :        *.  **:  *   *. *:   :

CLa-BCP         -FSSLKADFDEESTILIG-ISPDSIASHKKFHQKHNLSITLLADESKEVLKSYDVWKEK- 109
3a2v            -FARRYEDFQRLGVDLIG-LSVDSVFSHIKWKEWIERHIGVRIPFPIIADPQGTVARRLG 113
4mmm            GFVEQAEALKAKGVQVVACLSVNDAFVTGEWGRAHKAEG---KVRLLADPTGAFGKETD 116
                 *       :.  .. ::. :* :.     :: .  :            .     . :.

CLa-BCP         SMFGKKYMGVVRTTFLIDEKGII-AQIWKPVTLKNHAQSVLKMVKSLKQ---------- 157
3a2v            LLHAESATHTVRGVFIVDARGVIRTMLYYPMELGRLVDEILRIVKALKLGDSLKRAVPAD 173
4mmm            LLLDDSLVSIFGNRRLKRFSMVVQDGIVKALNVEPDGTGLTCSL--------------- 160
                 :  ..    .    :     ::   :  .: :      :   :
```

Figure 3.17 Sequence alignment of CLa-BCP with ligand bound Prx structure.

We have assigned O_A and O_B for the two peroxide oxygen atoms; where O_A lies close to the C_P-thiolate and O_B is at the distal end and acts as leaving group. The positioning of O_A atom

(H_2O_2) is 3.3 Å away from S_p of CpSH (peroxidatic cysteine) residue. In the substrate-docked structure, the substrate molecule is fitted well in the active site as required for the peroxidatic "in-line S_N2 reaction" as described earlier. The active site is very well organized in stabilizing the transition state (Fig. 3.18).

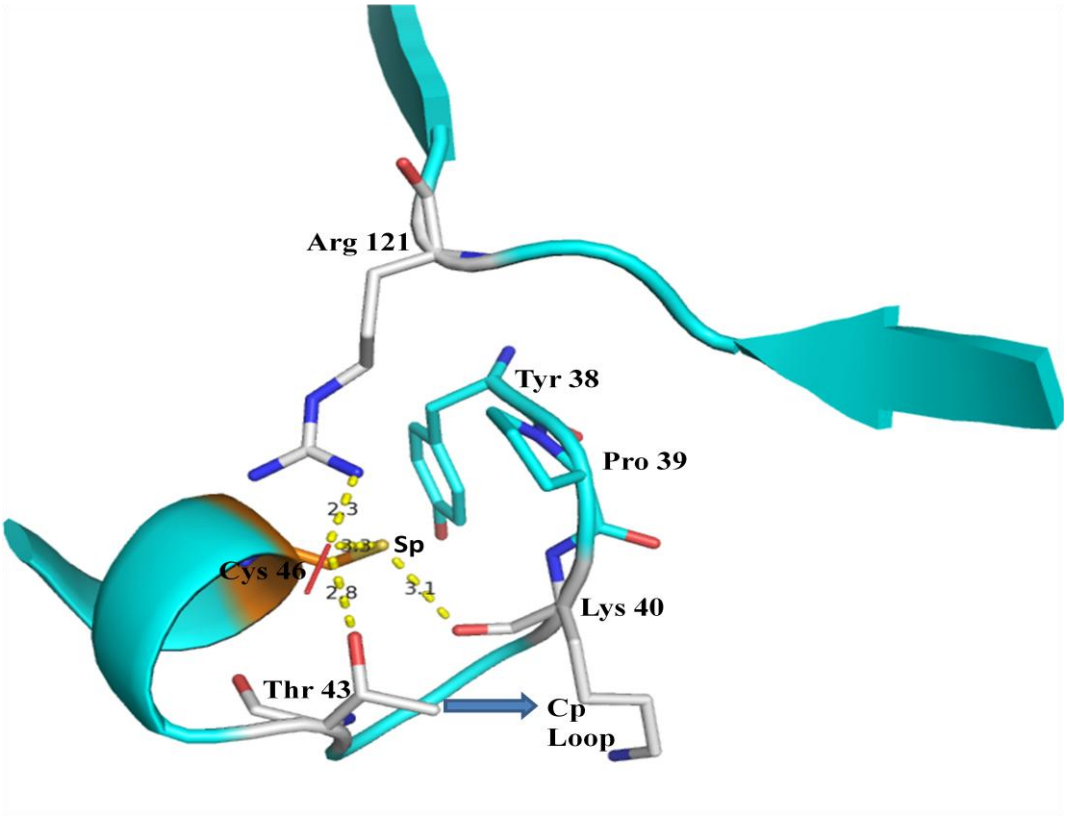

Figure 3.18 The active site of CLa-BCP.H_2O_2 structure. The distance of interacting catalytic residues with OA atom of H_2O_2 are Cys46 (3.3 Å) from α2, Thr43 (2.8Å), Lys40 (3.1 Å) and Arg121 (2.3 Å). Figure drawn using PyMol visualization tool.

When we overlaid our docked structure conformations with the known peroxide bound Prxs structure from *Aeropyrum pernix* (pdb id: 3A2V), it was observed that the positioning of NH1 atom from side chain of Arg121 residue around O_A atom from peroxide and Sp of peroxidatic cysteine residue is very similar. In 3A2V structure it has been observed that the polypeptide conformation around the active site was the same as that in the reduced form. In both 3A2V and 4MMM one of the oxygen atoms of the ligand interacted with C_P (S and N), Val (N), Thr (Oγ) and Arg (N), and other oxygen atom of ligand interact with Val (N). The surface has a positive electrostatic potential, which is brought by Arg126 side chain [271]. With the conformational change, Arg126 swings away from the Cp side chain, and His42 moves near to it. In case of modelled CLa-BCP structure, O_A of the hydrogen peroxide interacted with sulfur atom of the side chain Cp46 (distance of 3.3 Å) and NH-backbone atom (distance 3.4 Å) of Cp46. The other atoms like NH-backbone atom Gly45, (N,), the OG1 side chain atom of Thr43 and NH atom of side chain of Arg121 ($NH_{1,}$) are at a distance of 3.7 Å, 2.8 Å and 2.3

Å respectively. The O_B atom of hydrogen peroxide also interacts with the NH-backbone atom of Gly45 (N, 3.2 Å). Comparing these distances with the already known ligand-bound Prxs shows that H_2O_2 interacts in a similar fashion with the CLa-BCP as well (Fig. 3.19 A, B).

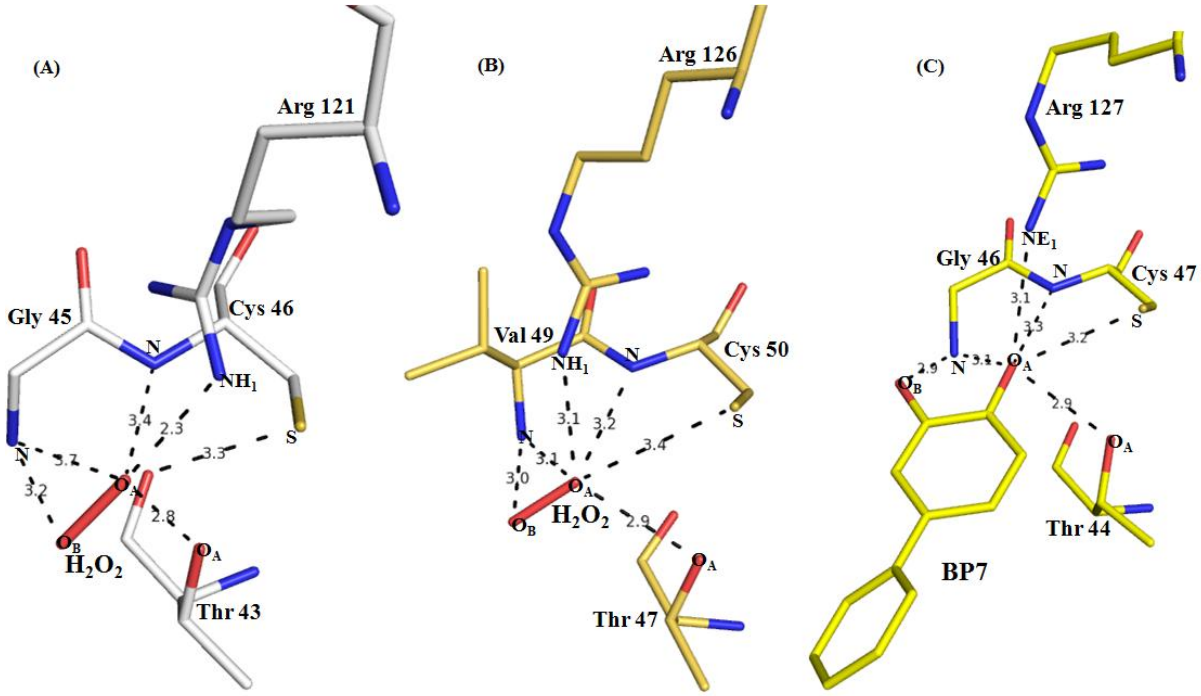

Figure 3.19 Residues representation of the CLa-BCP active site (white), 3A2V (golden) and 4MMM (yellow) structures with the bound ligand molecule. The oxygen atoms mimicking O_A and O_B of selected representative ligands are shown as red sticks. Hydrogen bonding (black dotted lines) important for ligand binding and the other interaction like S/N of Cys-O_A, OG1 of Thr-O_A, NH1 of Arg-O_A and N atom of Gly/Val with O_A and O_B of ligand/substrate are shown. The conserved four residues responsible for stabilization of the active site among Prxs are labeled. Figure drawn using PyMol visualization tool.

To gain more information about the Cys46 thiolate (Cp thiolate) stabilization we have compared our docked structure with ligand (benzoate) bound structure from human HsPrxV (pdb id: 4MMM) [2]. In case of human HsPrxV the Cp thiolate stabilization is facilitated through the conserved residues Thr44 and Arg127. The alcohol group of Thr44 is well placed to form a hydrogen bond with the thiolate ($^{d}O-S$ = 3 Å), which could limit the nucleophilicity of the sulfur. In our case the alcohol group of Thr43 is placed at a distance 2.8 Å (Fig 3.19 C).

3.3.8.4 Role of Arg121

In literature it was reported that the Arg residue close to Cp loop provides the positive electrostatic niche in oxidation step [271]. The surface has a positive electrostatic potential,

which is brought by Arg121 side chain. Moreover, the sulphur atom of Cys46 is in close interaction with the NH_1 atom of Arg121, which is responsible for the positive charge (Fig. 3.20).

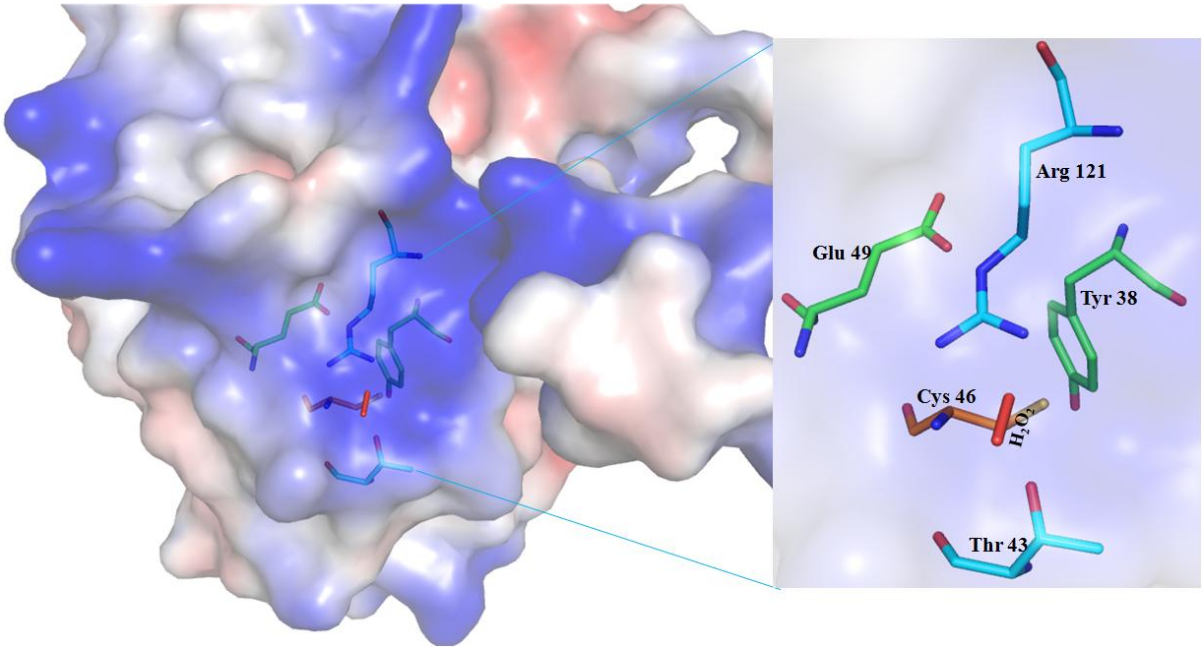

Figure 3.20 Surface of CLa-BCP active site. Blue and red indicate positive and negative electrostatic potential, respectively. Hydrogen peroxide molecule on the surface of peroxide-bound form is shown in right. Hydrogen peroxide and side chains of Cp46 and Arg121 are shown using stick models and contributing residues responsible for Arg121 activation and stabilisation showed in green colour. Figure drawn using PyMol visualization tool.

With the conformational change in *Aeropyrum pernix:* H_2O_2 bound structure, Arg126 swings away from the Cp side chain, and His42 moves near to it [271]. In the same manner here in our case Arg121 could also swings away but we have Tyr38 in place of His42. Mainly positively charged residues including His, Arg are found close to the active site cysteine [58]. It has been seen that some 1-Cys and 2-Cys Prx is likely to have tyrosine and tryptophan residue at His position. Thus, completely conserved Arg residue played a major contribution to the stabilization of the Cp (Cys46, CLa-BCP structure numbering) thiolate anion. Other 1-cys prx AhpE from *Mycobacterium* [227] showed that an arginine residue interacts by hydrogen bonding with Cp (~3.5 Å distant) allocating thiolate stabilization, an additional conserved trait among diverse Prxs. The charged Arg121 residue could be stabilized by forming hydrogen bond with Glu49 from α2 helix or conformational changes in backbone loop region of α5 and β9 (Fig. 3.21).

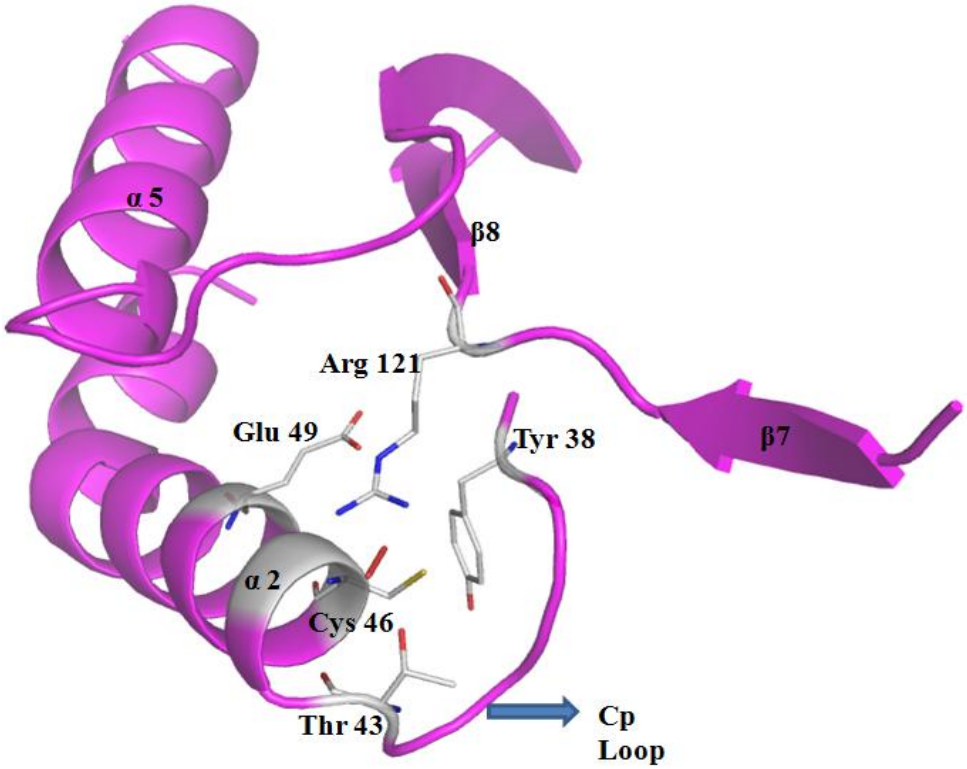

Figure 3.21 Structure of the active site and substrate-binding pocket of CLa-BCP. The H_2O_2 substrate and the four critical residues Thr43, Tyr38, Glu49, and Arg121 around the active site are drawn in stick form. The helices and sheets which are involve in oxidation and undergo conformational changes shown in magenta colour.

The identification of active site residues interaction with peroxide substrate proposes the putative role of these residues as already being discussed. First, the close proximity of active site is not only activating the C_P to be a potent nucleophile, but is also activating the peroxide to be attacked. Secondly, we can now noticeably propose the same roles for the three conserved residues around the C_P which have been embarked on them. The Thr residue orients itself via its Oγ and thereby activates the O_A atom of the incoming peroxide and could act as an acceptor molecule. The Arg residue stimulates both the C_P-thiolate and the O_A of the incoming substrate and its side chain could act as donors. There is one difference seen instead of conserved Gln/His residue, here in our case Tyr 38 and Lys40 from conserved YPK motif maximally stabilizing the transition state.

From the related known structure and literature we have observed that loop between alpha helix regions and between sheets have a strong role in peroxidation. From our predicted structure, the loop between α2 and β3 could be responsible for local unfolding of α2 when reacts with peroxide substrate. The longer loop between α5 and β9 could be for accommodating incoming protein or larger peroxide molecules along with small molecule thiols. The presence β-hairpin between α4 and β6 regulates the substrate channel accessibility

the similar structural conformation change seen in case of *X. campestris* structure (pdb id: 3GKN) (Fig. 3.22).

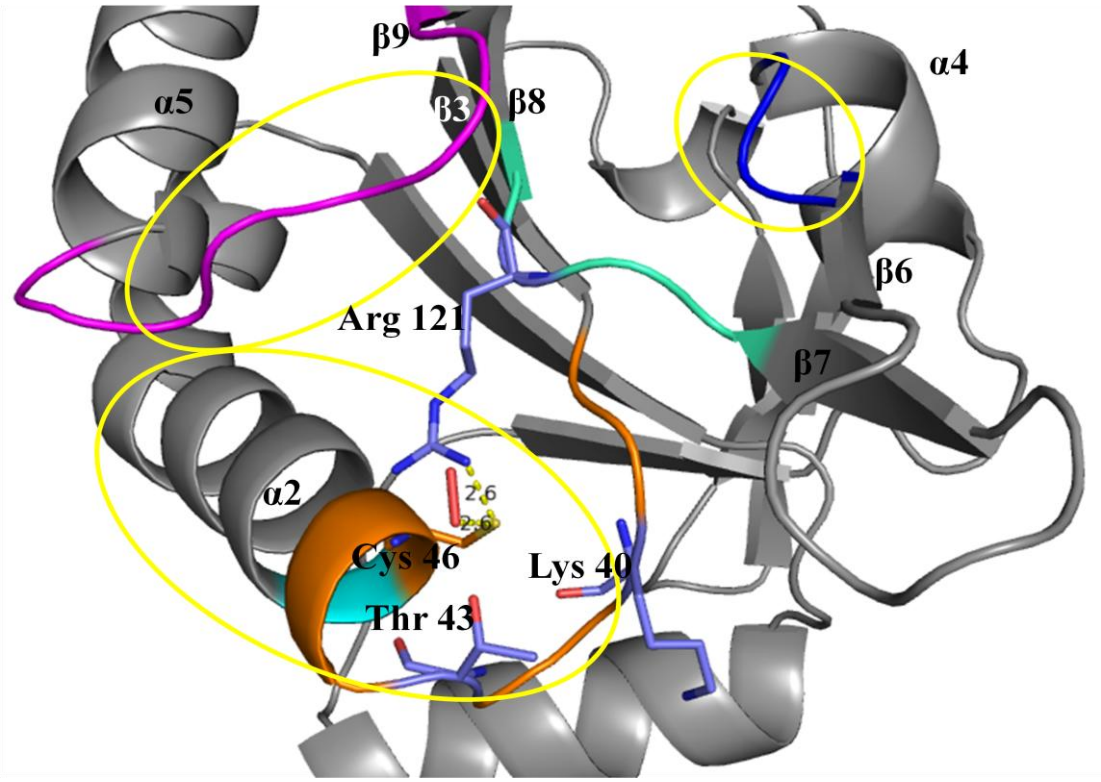

Figure 3.22 The significance of loop region present in CLa-BCP structure. For highlighting the loop the model showed in gray colour. The longer loop present in between α5-β9 (magenta) responsible for accommodation of charged Arg residue, the small loop between α4-β6 (blue) for substrate channelization, loop between β7-β8 (cyan) for Arg residue and the major reactive C_P loop (orange) are shown here.

3.9 CONCLUSIONS

In order to analyze the structural integrity of CLa-BCP and CLa-BCP $_{S77C}$ and to gather information about its stability, CD spectra were recorded at room temperature in the far-UV region. The maximum centred at 198 nm for CLa-BCP showing predominance of β-sheets whereas mutant CLa-BCP_{S77C} the broad minima centred at 208 and 223nm were indicative of the presence of both α and β secondary structure elements. BCPs classification by Wakita et.al, 2007 indicates that protein having C_PXXXXC_R motif or positioning of resolving cysteine 35bp towards C-terminal away from C_P possess both α/β structure arrangement. Whereas a protein having no CR predominantly falls under β –group. This statement holds true for CLa-BCP and mutant CLa-BCP_{S77C}, as introduction of Cys residue at 77^{th} position (~31bp) away from C_P showed both α and β secondary structure elements. Sequence

alignment also showed that positioning of introduced cysteine similar to *Xanthomonas campestris* which belongs to atypical 2-Cys Prx. Oxido-reduction changes also been observed in case of both CLa-BCP and CLa-BCP_{S77C}, decrease in ellipticity has been observed in case of oxidation. There was stable and substantial conformational changes seen when different temperature treatment is being given to CLa-BCP. The conformational changes could be due to random coil transition into α-helix at higher temperature, similar results were seen in case of atypical protein disulfide oxidoreductase from *Sulfolobus solfataricus* [233]. First time here we are showing conformational stability due to temperature variation. More studies needs to be carried out to authenticate this observation. We have carried out CD experiments with reduced form of protein because both the protein are quite stable in their reduced from as observed from purification experiments. Similar changes has been observed when protein over-oxidized, tends to stabilize their structure. This could be due to formation of stable higher intermediates which locks the protein and precluded from reacting with more incoming peroxide substrates.

Intrinsic fluorescence emission experiment of proteins by virtue of Trp residues, showed that both the Trp residues are exposed with maximum at 341 and 347.5 nm of CLa-BCP and CLa-BCP_{S77C} respectively. When exposed to peroxide treatment a decrease in fluorescence intensity was observed for both the proteins that but no appreciable shift in nm in case of CLa-BCP. This observation led to conclusion that CLa-BCP having a single Cys residue, thus named as 1-Cys Prx is quite different from 2-Cys Prx. These changes were reverted back by the DTT reducing agent which implicates that reversible sulfenic intermediate formation occurs which can be easily reverting back to thiols. In case of modification studies, one thing is clear that active site Cys residue undergoing changes lead to structural and functional changes.

From literature it has been reported that the functional Cys of 1-Cys prxs like TSA/AhpC, as in ORF6 and NADH peroxidase exists in the form of sulfenic acid (Cys-SOH) as a catalytic intermediate, which can be easily reduced to Cys-SH by DTT [58, 185, 293]. To investigate the possibility that the functional Cys-46 of BCP could exist in the form of sulfenic acid like those of ORF6 and NADH peroxidase, we reacted BCP with an electrophilic reagent, NBD-Cl, as a trapping agent for Cys-SOH. This reagent has been widely used over other sulfenic acid modifying agent like dimedone because of its capability to give characteristic spectral peak which can be detected spectrophotometrically. It react with Cys-S-OH and Cys-SH groups and form the corresponding thiol adducts, which have their own characteristic absorbance maxima (347 nm for Cys-S(O)-NBD and 422 nm for Cys-S-NBD) [89]. The

spectral analysis of NBD-Cl-treated CLa-BCP protein without DTT showed an absorbance maximum at 347 nm (Fig. 3.5 B), suggesting the existence of Cys-SOH in CLa-BCP. While NBD-Cl-treated mutant CLa-BCP_{S77C} showed a peak around 420-450 nm could be due to formation of thioether linked NBD adduct or lack of SOH formation in case of CLa-BCP_{S77C}. The NBD-Cl-treated CLa-BCP protein when run on SDS-PAGE showed higher bands which could be reaction intermediates or protein undergoes peroxide dependent oligomerisation.

On the basis of our results, we suggest the reaction machinery of CLa-BCP, involves Cysteine sulfenic acid (Cys-SOH) intermediates which catalyzes the reduction of peroxides. Further studies needs to be done for dissecting the reaction mechanism followed by CLa-BCP and to that of introduced one more Cys in CLa-BCP_{S77C}, that it follows which atypical or typical 2-Cys Prx mechanism. Here we are proposing that NBD-Cl reacted with a Cys-SOH should yield either a sulfoxide or sulfenate ester product depending on whether the sulphur or the oxygen of the Cys-SOH acts as the nucleophilic center. This basis could be further explored through mass spectrometry analysis which is most sensitive one to detect a difference of 1Da, thus can detect a difference of 16 amu between the thiol adduct, Cys-S-NBD, and the sulfenic acid adduct, Cys-S(O)-NBD (in case of oxidized form of protein).

The initial crystallization of CLa-BCP with crystal screens, we could not able to get crystal. Through several attempts here we have observed that crystal of CLa-BCP grows in the presence of DTT but sea-urchin like thus could not get diffracted well. But one concluding remark was that for CLa-BCP crystal formation is that, presence of DTT in reservoir buffer is much needed. A noteworthy perfection in crystal properties was attained by adding 0.1 % (w/v) agarose to the reservoir solution before mixing it with the protein. For getting better diffraction of obtained crystal the presence of very low percentage of ethylene glycol and annealing was of utmost importance.

From comparative sequence analysis of CLa-BCP it has been seen that, it is more closely related to that of alkylhydroperoxide reductase followed by 2-Cys Prxs instead of having only 1-Cys i.e. peroxidatic Cys at 46^{th} position. Multiple sequence alignment (MSA) was showed that CLa-BCP possess highly conserved PXXXT/SXXC motif. Phylogenetically CLa-BCP was clustered with plant symbiotic and pathogenic bacteria BCPs. MSA for knowing the structural similarity with other known Prxs further enhanced by Esprit server. It was observed though not having so much similarity in sequence the CLa-BCP do have significant structural similarity with characteristics common Thioredoxin fold.

To find out the molecular attributes answerable for the catalytic properties of CLa-BCP, a careful analysis has been done using predicted model, which was shown to have 88.7% of favoured residues checked through PROCHECK server. It was observed that CLa-BCP shares

a high level of structural similarity in the catalytic motif region with C-terminal residue especially Arginine. CLa-BCP model shown to have characteristic Thioredoxin fold consists of central β twist (cradle) formed by anti parallel β5, β4, β3, β8, β2 and β1 with a backbone support of α2-α3-α5 helix. Some small differences are also being observed in C-terminal consensus sequences i.e. GGLG sequence whose importance has been discussed in interaction studies with hydrogen peroxide substrate.

Through interaction studies via docking we could able to proposed that CLa-BCP also follows the basic S_N2 displacement reaction when reacts with H_2O_2. It was found that residues like Pro39, Lys40, Thr43, Cys46, and Arg121 at the active site are highly conserved both sequentially and structurally. This study showed that highly conserved "YPK" motif which not only constitutes the Cp catalytic loop but have remarkable impact on "Arg" and C_P thiolate stabilization. In literature it has been discussed that eukaryotic Prxs prone to overoxidation and the probable reason was the presence of YF and GGLG sequence loop at C-terminal. Through our interactive studies we have seen that CLa-BCP model does not have GGLG sequence loop thus could not be easily attacked by peroxide substrate to make it sensitive. The surface has a positive electrostatic potential due to the presence of active Arg121 residue is also being seen, and interacting residues responsible for activating Arg residue. In our model, instead of His residues as seen in most of the Prxs we have Tyr38 to do the role along with Glu49. The observe distance from O_A of the hydrogen peroxide in docked structure it was shown, that the active site is very well organized in CLa-BCP model for stabilizing the transition state. How the interaction takes place, and how the flipping of loop or conformational changes occurred in α2, α3 and α5 backbone. From known structures and their conformational changes occurred after interacting with ligands/substrates here we have managed to propose the significance of loop present in CLa-BCP structure.

SUMMARY

This thesis work intend to decipher the biochemical and biophysical properties of a peroxiredoxin protein, an antioxidant system from *Candidatus* Liberibacter asiaticus (CLa-BCP) which cause vicious citrus Huanlongbing disease in citrus plants. The present study

could be explored for developing new control strategies by obstructing antioxidant machinery of bacteria. The conclusions of the study are as follows:

- CLa-BCP exhibits a significant sequence similarity with alkyl hydroperoxide reductase from various pathogenic and plant symbiotic bacteria. It possess conserved PXXXTXXC motif as found in other peroxiredoxins family of proteins.
- 1-Cys peroxiredoxin (CLa-BCP) having single C_PSH /sulfenic acid cysteine (C-47), was successfully cloned, over-expressed and purified to its homogeneity. CLa-BCP shown to have concentration dependent oligomerisation behaviour.
- The introduction of non-conserved resolving cysteine at 77^{th} position, CLa-BCP_{S77C} variant results into significant change in the property of the protein. The variant form CLa-BCP_{S77C} is forming intermolecular disulfide bond thus shown to be dimeric in nature. The protein tends to aggregate in its native state while in reduced condition is quite stable.
- The free thiol content determination using DTNB reagent showed that, 1µM of reduced protein is having 350 X 10^{-5} M free sulfhydryl while there was no absorbance seen in case of oxidised form of protein. Both the proteins when pre-reduced with 5eq of Thioredoxin (TrxA), a natural reductant for Prxs proteins, 50 X 10^{-5} M free sulfhydryl present in 1µM of protein. In conclusion, protein has free thiols only in its reduced form and exhibits thiol dependent reduction demonstrated by using natural reductant thioredoxin (TrxA).
- From peroxiredoxin and peroxidase assays against varied substrates showed that CLa-BCP is much more effective even at its lower concentration using non-physiological electron donor DTT. Secondly, data represents that DTT could be potent reductant for CLa-BCP effective in reducing the sulfenic acid intermediate, C_PSOH forms during oxidation.
- Both CLa-BCP and CLa-BCP_{S77C} shows the protective effect through its DNA binding ability towards oxidative damage of DNA. On the basis of cell line based assays, both the proteins plays an important defensive role against H_2O_2 induced cell killing effectively. Both the protein possesses *in-vitro* antioxidative property turns out to be potent scavenger of ROS.
- Biophysical analysis by CD experiments shows that CLa-BCP is of predominance of β-sheets structure. While mutant CLa-BCP_{S77C} is indicative of the presence of both α and β secondary structure elements. CLa-BCP shown to possess conformational stability towards temperature variation. Both the proteins tend to stabilize their structure when over oxidized. Fluorescence experiments shows that reversible sulfenic

intermediate can be easily reverting back to thiols using DTT as a reducing agent which has been already observed in biochemical assays.

- From functional cysteine assay using NBD-Cl, an electrophilic reagent showed that Cys-46 of CLa-BCP could exist in the form of sulfenic acid (Cys-SOH) intermediate for catalyzing the reduction of peroxides. Protein undergoes peroxide dependent oligomerisation as showed in gel filtration experiments as well.
- For CLa-BCP crystallization presence of DTT and low percentage of agarose in reservoir buffer is required. For getting better diffraction of obtained crystal the presence of very low percentage of ethylene glycol and annealing is of utmost importance.
- CLa-BCP model have characteristic Thioredoxin fold consists of central β twist (cradle) formed by anti parallel β5, β4, β3, β8, β2 and β1 with a backbone support of α2-α3-α5 helix.
- Through interaction studies via docking it was found that residues like Pro39, Lys40, Thr43, Cys46, and Arg121 at the active site are highly conserved, very well organized and constitutes the catalytic Cp loop. By analyzing the active site geometry as well as hydrogen bonding arrangement that adds to substrate binding and catalysis, we give you an idea about the conserved Prx active site. This active site could activate both the C_p-thiolate and the peroxide substrate, to facilitate the reaction and best possibly coordinated to alleviate the transition state of the S_N2 displacement reaction. Tyr38 and Glu49 residues responsible for activating Arg residue instead of His as seen in most of the Prxs.
- Through comparative studies we have shown that CLa-BCP model does not have GGLG sequence loop thus could not be easily attacked by peroxide substrate to make it sensitive.

From literature understanding along with biochemical and *in-silico* studies revealed that the Prxs are not just indispensable as crucial antioxidant enzymes moreover they are required for cellular signaling regulation as well. The prevalent significance of these dual properties makes characterization of the Prxs essential for developing antimicrobials.

Future work

There are lot of things which remain unexplored during this thesis work and needs to be done there are some here summarized below:

- In future, kinetic parameters of CLa-BCP need to be measured against each substrate.

- Interaction studies of CLa-BCP and CLa-BCP_{S77C} with known reductant partner TrxA needs to be done through ITC experiments.
- The exact mechanism that CLa-BCP and CLa-BCP_{S77C} follows needs further exploration through MS studies and crystallographic analysis.
- A mutational study which includes mutating key residue (Cys-46) might perform to confirm the role exhibited by Cys-46 residue so far in relation to its peroxidase and protective activity.
- Lastly from the analysis and collective information from ligand bound structures of Prxs, we proposed that molecules which can mimic the substrate binding may results into effective competitive inhibitors for Prxs. Thus structure based drug designing by screening those molecules can be performed.

REFERENCES

1. Agrawal, H., Kumar, A., Bal, N. C., Siddiqi, M. I. and Arora, A. Ligand based virtual screening and biological evaluation of inhibitors of chorismate mutase (rv1885c) from mycobacterium tuberculosis h37rv. *Bioorganic & medicinal chemistry letters* 17(11):3053-3058 (2007).

2. Aguirre, C., Ten Brink, T., Guichou, J.-F., Cala, O. and Krimm, I. Comparing binding modes of analogous fragments using nmr in fragment-based drug design: Application to prdx5. *Plos One* (2014).

3. Akula, N., Zheng, H., Han, F. Q. and Wang, N. Discovery of novel seca inhibitors of *candidatus* liberibacter asiaticus by structure based design. *Bioorganic & medicinal chemistry letters* 21(14):4183-4188 (2011).

4. Akula, N., Zheng, H., Han, F. Q. and Wang, N. Discovery of novel seca inhibitors of *candidatus* liberibacter asiaticus by structure based design. *Bioorganic & medicinal chemistry letters* 21(14):4183-4188 (2012).

5. Albrecht, U. and Bowman, K. D. Gene expression in citrus sinensis (l.) osbeck following infection with the bacterial pathogen candidatus liberibacter asiaticus causing huanglongbing in florida. *Plant science* 175(3):291-306 (2008).

6. Alscher, R. G., Erturk, N. and Heath, L. S. Role of superoxide dismutases (sods) in controlling oxidative stress in plants. *Journal of experimental botany* 53(372):1331-1341 (2002).

7. Altschul, S. F., Madden, T. L., Schaffer, A. A., Zhang, J., Zhang, Z., Miller, W. and Lipman, D. J. Gapped blast and psi-blast: A new generation of protein database search programs. *Nucleic acids research* 25(17):3389-3402 (1997).

8. Anand, V., Dogra, N., Singh, S., Kumar, S. N., Jena, M. K., Malakar, D., Dang, A. K., Mishra, B. P., Mukhopadhyay, T. K., Kaushik, J. K. and Mohanty, A. K. Establishment and characterization of a buffalo (bubalus bubalis) mammary epithelial cell line. *Plos One* 7(7):e40469 (2012).

9. Andrews, S. C., Harrison, P. M. and Guest, J. R. A molecular analysis of the 53.3 minute region of the escherichia coli linkage map. *Journal of general microbiology* 137(2):361-367 (1991).

10. Anraku, Y. and Gennis, R. B. The aerobic respiratory chain of escherichia coli. *Trends in Biochemical Sciences* 12:262-266 (1987).

11. Antelmann, H., Engelmann, S., Schmid, R. and Hecker, M. General and oxidative stress responses in bacillus subtilis: Cloning, expression, and mutation of the alkyl hydroperoxide reductase operon. *Journal of bacteriology* 178(22):6571-6578 (1996).

12. Apel, K. and Hirt, H. Reactive oxygen species: Metabolism, oxidative stress, and signal transduction. *Annu Rev Plant Biol* 55:373-399 (2004).

13. Aran, M., Ferrero, D. S., Pagano, E. and Wolosiuk, R. A. Typical 2-cys peroxiredoxins–modulation by covalent transformations and noncovalent interactions. *FEBS journal* 276(9):2478-2493 (2009).

14. Argyrou, A. and Blanchard, J. S. Flavoprotein disulfide reductases: Advances in chemistry and function. *Progress in nucleic acid research and molecular biology* 78:89-142 (2004).

15. Armstrong-Buisseret, L., Cole, M. B. and Stewart, G. S. A homologue to the escherichia coli alkyl hydroperoxide reductase ahpc is induced by osmotic upshock in staphylococcus aureus. *Microbiology* 141(7):1655-1661 (1995).

16. Arnold, K., Bordoli, L., Kopp, J. r. and Schwede, T. The swiss-model workspace: A web-based environment for protein structure homology modelling. *Bioinformatics* 22(2):195-201 (2006).

17. Arora, A., Sairam, R. and Srivastava, G. Oxidative stress and antioxidative system in plants. *CURRENT SCIENCE-BANGALORE*- 82(10):1227-1238 (2002).

18. Asada, K. Production and scavenging of active oxygen in photosynthesis. *Photoinhibition* (1987).

19. Asana, R. D. The citrus dieback problem in relation to cultivation of citrus fruits in india. *Indian Journal of Horticulture* 15:283-286 (1958).

20. Atack, J. M., Harvey, P., Jones, M. A. and Kelly, D. J. The campylobacter jejuni thiol peroxidases tpx and bcp both contribute to aerotolerance and peroxide-mediated stress resistance but have distinct substrate specificities. *Journal of bacteriology* 190(15):5279-5290 (2008).

21. Aubert, B. and Quilici, S. Monitoring adult psyllas on yellow traps in reunion island. In: *Proc. 10th Conference of the International Organization of Citrus Virologists, Valencia,Spain*ed.^eds), p.^pp. 21, (1986).

22. Baier, M. and Dietz, K.-J. Primary structure and expression of plant homologues of animal and fungal thioredoxin-dependent peroxide reductases and bacterial alkyl hydroperoxide reductases. *Plant molecular biology* 31(3):553-564 (1996).

23. Baker, A., Payne, C. M., Briehl, M. M. and Powis, G. Thioredoxin, a gene found overexpressed in human cancer, inhibits apoptosis in vitro and in vivo. *Cancer Research* 57(22):5162-5167 (1997).

24. Baker, L. M. and Poole, L. B. Catalytic mechanism of thiol peroxidase from escherichia coli sulfenic acid formation and overoxidation of essential cys61. *Journal of Biological Chemistry* 278(11):9203-9211 (2003).

25. Baker, L. M., Raudonikiene, A., Hoffman, P. S. and Poole, L. B. Essential thioredoxin-dependent peroxiredoxin system from helicobacter pylori: Genetic and kinetic characterization. *Journal of bacteriology* 183(6):1961-1973 (2001).

26. Barriault, D., Plante, M.-M. l. and Sylvestre, M. Family shuffling of a targeted bpha region to engineer biphenyl dioxygenase. *Journal of bacteriology* 184(14):3794-3800 (2002).

27. Barriault, D. and Sylvestre, M. Evolution of the biphenyl dioxygenase bpha from burkholderia xenovorans lb400 by random mutagenesis of multiple sites in region iii. *Journal of Biological Chemistry* 279(46):47480-47488 (2004).

28. Bendtsen, J. D., Nielsen, H., von Heijne, G. and Brunak, S. Improved prediction of signal peptides: Signalp 3.0. *Journal of molecular biology* 340(4):783-795 (2004).

29. Berlett, B. S. and Stadtman, E. R. Protein oxidation in aging, disease, and oxidative stress. *Journal of Biological Chemistry* 272(33):20313-20316 (1997).

30. Bhattacharyya, A., Stilwagen, S., Reznik, G., Feil, H., Feil, W. S., Anderson, I., Bernal, A., D'Souza, M., Ivanova, N. and Kapatral, V. Draft sequencing and comparative genomics of xylella fastidiosa strains reveal novel biological insights. *Genome research* 12(10):1556-1563 (2002).

31. Bieger, B. and Essen, L.-O. Crystal structure of the catalytic core component of the alkylhydroperoxide reductase ahpf from escherichia coli. *Journal of molecular biology* 307(1):1-8 (2001).

32. Birkett, D. J., Price, N. C., Radda, G. K. and Salmon, A. G. The reactivity of sh groups with a fluorogenic reagent. *FEBS letters* 6(4):346-348 (1970).

33. Bora, H., Garg, S., Sen, P., Kumar, D., Kaur, P., Khan, R. H. and Sharma, Y. D. Plasmodium vivax tryptophan-rich antigen pvtrag33. 5 contains alpha helical structure and multidomain architecture. *Plos One* 6(1):e16294 (2011).

34. Bouffard, K. Greening found in 10 counties. *Citrus Ind* 87(1):5-26 (2006).

35. Bove, J. M. Huanglongbing: A destructive, newly-emerging, century-old disease of citrus. *Journal of plant pathology* 88(1):7-37 (2006).

36. Bové, J. M. Huanglongbing: A destructive, newly-emerging, century-old disease of citrus. *Journal of plant pathology*:7-37 (2006).

37. Bove, J. M. and Saglio, P. Stubborn and greening: A review. *IOCV, Riverside* (1974).

38. Bowler, C., Slooten, L., Vandenbranden, S., De Rycke, R., Botterman, J., Sybesma, C., Van Montagu, M. and Inzé, D. Manganese superoxide dismutase can reduce cellular damage mediated by oxygen radicals in transgenic plants. *The EMBO journal* 10(7):1723 (1991).

39. Brigelius-Flohe, R. Tissue-specific functions of individual glutathione peroxidases. *Free Radical Biology and Medicine* 27(9):951-965 (1999).

40. Bryk, R., Griffin, P. and Nathan, C. Peroxynitrite reductase activity of bacterial peroxiredoxins. *Nature* 407(6801):211-215 (2000).

41. Bryk, R., Lima, C., Erdjument-Bromage, H., Tempst, P. and Nathan, C. Metabolic enzymes of mycobacteria linked to antioxidant defense by a thioredoxin-like protein. *Science* 295(5557):1073-1077 (2002).

42. Bsat, N., Chen, L. and Helmann, J. D. Mutation of the bacillus subtilis alkyl hydroperoxide reductase (ahpcf) operon reveals compensatory interactions among hydrogen peroxide stress genes. *Journal of bacteriology* 178(22):6579-6586 (1996).

43. Budde, H. Antioxidant defense in trypanosoma brucei brucei; (2003).

44. Buettner, G. R. and Jurkiewicz, B. A. Ascorbate free radical as a marker of oxidative stress: An epr study. *Free Radical Biology and Medicine* 14(1):49-55 (1993).

45. Capoor, S. P. Decline of citrus trees in india. *Bull Nat Inst Sci India* 24:48-64 (1963).

46. Capoor, S. P., Rao, D. G. and Viswanath, S. M. Diaphorina citri kuway., a vector of the greening disease of citrus in india. *Indian J Agric Sci* 37:572-576 (1967).

47. Cha, M.-K., Kim, H.-K. and Kim, I.-H. Thioredoxin-linked" Thiol peroxidase" From periplasmic space of escherichia coli. *Journal of Biological Chemistry* 270(48):28635-28641 (1995).

48. Cha, M.-K., Kim, W.-C., Lim, C.-J., Kim, K. and Kim, I.-H. Escherichia coli periplasmic thiol peroxidase acts as lipid hydroperoxide peroxidase and the principal antioxidative function during anaerobic growth. *Journal of Biological Chemistry* 279(10):8769-8778 (2004).

49. Chae, H. Z., Chung, S. J. and Rhee, S. G. Thioredoxin-dependent peroxide reductase from yeast. *Journal of Biological Chemistry* 269(44):27670-27678 (1994).

50. Chae, H. Z., Kim, I. H., Kim, K. and Rhee, S. G. Cloning, sequencing, and mutation of thiol-specific antioxidant gene of saccharomyces cerevisiae. *Journal of Biological Chemistry* 268(22):16815-16821 (1993).

51. Chae, H. Z., Robison, K., Poole, L. B., Church, G., Storz, G. and Rhee, S. G. Cloning and sequencing of thiol-specific antioxidant from mammalian brain: Alkyl hydroperoxide reductase and thiol-specific antioxidant define a large family of antioxidant enzymes. *Proceedings of the National Academy of Sciences* 91(15):7017-7021 (1994).

52. Chang, J. W., Jeon, H. B., Lee, J. H., Yoo, J. S., Chun, J. S., Kim, J. H. and Yoo, Y. J. Augmented expression of peroxiredoxin I in lung cancer. *Biochemical and biophysical research communications* 289(2):507-512 (2001).

53. Chang, T.-S., Cho, C.-S., Park, S., Yu, S., Kang, S. W. and Rhee, S. G. Peroxiredoxin iii, a mitochondrion-specific peroxidase, regulates apoptotic signaling by mitochondria. *Journal of Biological Chemistry* 279(40):41975-41984 (2004).

54. Chauhan, R. and MANDE, S. Characterization of the mycobacterium tuberculosis h37rv alkyl hydroperoxidase ahpc points to the importance of ionic interactions in oligomerization and activity. *Biochem J* 354:209-215 (2001).

55. Chauhan, R. and Mande, S. Site-directed mutagenesis reveals a novel catalytic mechanism of mycobacterium tuberculosis alkylhydroperoxidase c. *Biochem J* 367:255-261 (2002).

56. Chen, J.-W., Dodia, C., Feinstein, S. I., Jain, M. K. and Fisher, A. B. 1-cys peroxiredoxin, a bifunctional enzyme with glutathione peroxidase and phospholipase a2 activities. *Journal of Biological Chemistry* 275(37):28421-28427 (2000).

57. Cheng, Q., Sandalova, T., Lindqvist, Y. and Arnér, E. S. Crystal structure and catalysis of the selenoprotein thioredoxin reductase 1. *Journal of Biological Chemistry* 284(6):3998-4008 (2009).

58. Choi, H.-J., Kang, S. W., Yang, C.-H., Rhee, S. G. and Ryu, S.-E. Crystal structure of a novel human peroxidase enzyme at 2.0 Å resolution. *Nature Structural & Molecular Biology* 5(5):400-406 (1998).

59. Choi, J., Choi, S., Choi, J., Cha, M.-K., Kim, I.-H. and Shin, W. Crystal structure of escherichia coli thiol peroxidase in the oxidized state insights into intramolecular disulfide

formation and substrate binding in atypical 2-cys peroxiredoxins. *Journal of Biological Chemistry* 278(49):49478-49486 (2003).

60. Choi, Y. O., Cheong, N. E., Lee, K. O., Jung, B. G., Hong, C. H., Jeong, J. H., Chi, Y. H., Kim, K., Cho, M. J. and Lee, S. Y. Cloning and expression of a new isotype of the peroxiredoxin gene of chinese cabbage and its comparison to 2cys-peroxiredoxin isolated from the same plant. *Biochemical and biophysical research communications* 258(3):768-771 (1999).

61. Chou, K. C. and Shen, H. B. Signal-cf: A subsite-coupled and window-fusing approach for predicting signal peptides. *Biochemical and biophysical research communications* 357(3):633-640 (2007).

62. Christman, M. F., Morgan, R. W., Jacobson, F. S. and Ames, B. N. Positive control of a regulon for defenses against oxidative stress and some heat-shock proteins in salmonella typhimurium. *Cell* 41(3):753-762 (1985).

63. Clarke, C. B. The cultivated oranges and lemons of india and ceylon. *Nature* 41:579-582 (1890).

64. Clarke, D. J., Mackay, C. L., Campopiano, D. J., Langridge-Smith, P. and Brown, A. R. Interrogating the molecular details of the peroxiredoxin activity of the escherichia coli bacterioferritin comigratory protein using high-resolution mass spectrometry. *Biochemistry* 48(18):3904-3914 (2009).

65. Clayton, R. K. Purified catalase from rhodopseudomonas spheroides. *Biochimica et biophysica acta* 36(1):40-47 (1959).

66. Coletta-Filho, H. D., Targon, M., Takita, M. A., De Negri, J. D., Pompeu Jr, J., Machado, M. A., Do Amaral, A. M. and Muller, G. W. First report of the causal agent of huanglongbing (candidatus liberibacter asiaticus) in brazil. *Plant Disease* 88(12):1382-1382 (2004).

67. Conrad, M., Jakupoglu, C., Moreno, S. G., Lippl, S., Banjac, A., Schneider, M., Beck, H., Hatzopoulos, A. K., Just, U. and Sinowatz, F. Essential role for mitochondrial thioredoxin reductase in hematopoiesis, heart development, and heart function. *Molecular and cellular biology* 24(21):9414-9423 (2004).

68. Conrad, M., Jakupoglu, C., Moreno, S. p. G., Lippl, S., Banjac, A., Schneider, M., Beck, H., Hatzopoulos, A. K., Just, U. and Sinowatz, F. Essential role for mitochondrial thioredoxin reductase in hematopoiesis, heart development, and heart function. *Molecular and cellular biology* 24(21):9414-9423 (2004).

69. Copley, S. D., Novak, W. R. and Babbitt, P. C. Divergence of function in the thioredoxin fold suprafamily: Evidence for evolution of peroxiredoxins from a thioredoxin-like ancestor. *Biochemistry* 43(44):13981-13995 (2004).

70. Cox, A., Winterbourn, C. and Hampton, M. Mitochondrial peroxiredoxin involvement in antioxidant defence and redox signalling. *Biochem J* 425:313-325 (2010).

71. Cox, A. G., Peskin, A. V., Paton, L. N., Winterbourn, C. C. and Hampton, M. B. Redox potential and peroxide reactivity of human peroxiredoxin 3. *Biochemistry* 48(27):6495-6501 (2009).

72. Coyne, S., Litomska, A., Chizzali, C., Khalil, M. N. A., Richter, K., Beerhues, L. and Hertweck, C. Control of plant defense mechanisms and fire blight pathogenesis through the regulation of 6-thioguanine biosynthesis in erwinia amylovora. *ChemBioChem* 15(3):373-376 (2014).

73. Cudney, R., Patel, S., Weisgraber, K., Newhouse, Y. and McPherson, A. Screening and optimization strategies for macromolecular crystal growth. *Acta Crystallographica Section D: Biological Crystallography* 50(4):414-423 (1994).

74. D'Ambrosio, K., Limauro, D., Pedone, E., Galdi, I., Pedone, C., Bartolucci, S. and De Simone, G. Insights into the catalytic mechanism of the bcp family: Functional and structural analysis of bcp1 from sulfolobus solfataricus. *Proteins: Structure, Function, and Bioinformatics* 76(4):995-1006 (2009).

75. D'Autréaux, B. and Toledano, M. B. Ros as signalling molecules: Mechanisms that generate specificity in ros homeostasis. *Nature Reviews Molecular Cell Biology* 8(10):813-824 (2007).

76. Dai, S., Saarinen, M., Ramaswamy, S., Meyer, Y., Jacquot, J.-P. and Eklund, H. Crystal structure ofarabidopsis thaliananadph dependent thioredoxin reductase at 2.5 ã… resolution. *Journal of molecular biology* 264(5):1044-1057 (1996).

77. Dat, J., Vandenabeele, S., Vranová, E., Van Montagu, M., Inzé, D. and Van Breusegem, F. Dual action of the active oxygen species during plant stress responses. *Cellular and Molecular Life Sciences CMLS* 57(5):779-795 (2000).

78. Denicola, A., Souza, J. M. and Radi, R. Diffusion of peroxynitrite across erythrocyte membranes. *Proceedings of the National Academy of Sciences* 95(7):3566-3571 (1998).

79. Deponte, M. and Becker, K. Biochemical characterization of toxoplasma gondii 1-cys peroxiredoxin 2 with mechanistic similarities to typical 2-cys prx. *Molecular and biochemical parasitology* 140(1):87-96 (2005).

80. Dereeper, A., Guignon, V., Blanc, G., Audic, S. p., Buffet, S., Chevenet, F. o., Dufayard, J. F., Guindon, S. p., Lefort, V. and Lescot, M. Phylogeny. Fr: Robust phylogenetic analysis for the non-specialist. *Nucleic acids research* 36(suppl 2):W465-W469 (2008).

81. Deretic, V., Philipp, W., Dhandayuthapani, S., Mudd, M., Curcic, R., Garbe, T., Heym, B., Via, L. and Cole, S. Mycobacterium tuberculosis is a natural mutant with an inactivated oxidative stress regulatory gene: Implications for sensitivity to isoniazid. *Molecular microbiology* 17(5):889-900 (1995).

82. Desikan, R., Hancock, J. and Neill, S. Reactive oxygen species as signalling molecules. *Antioxidants and reactive oxygen species in plants*:169-196 (2005).

83. Dhandayuthapani, S., Zhang, Y., Mudd, M. and Deretic, V. Oxidative stress response and its role in sensitivity to isoniazid in mycobacteria: Characterization and inducibility of ahpc by peroxides in mycobacterium smegmatis and lack of expression in m. Aurum and m. Tuberculosis. *Journal of bacteriology* 178(12):3641-3649 (1996).

84. Dietz, K.-J., Jacob, S., Oelze, M.-L., Laxa, M., Tognetti, V., de Miranda, S. M. N., Baier, M. and Finkemeier, I. The function of peroxiredoxins in plant organelle redox metabolism. *Journal of Experimental Botany* 57(8):1697-1709 (2006).

85. do Carmo Teixeira, D., Danet, J. L., Eveillard, S., Martins, E. C., de Jesus Junior, W. C., Yamamoto, P. T., Lopes, S. A., Bassanezi, R. B., Ayres, A. J. and Saillard, C. Citrus huanglongbing in sao paulo state, brazil: Pcr detection of the candidatus liberibacter species associated with the disease. *Molecular and cellular probes* 19(3):173-179 (2005).

86. Duan, Y., Zhou, L., Hall, D. G., Li, W., Doddapaneni, H., Lin, H., Liu, L., Vahling, C. M., Gabriel, D. W. and Williams, K. P. Complete genome sequence of citrus huanglongbing bacterium, 'candidatus liberibacter asiaticus' obtained through metagenomics. *Molecular Plant-Microbe Interactions* 22(8):1011-1020 (2009).

87. Echalier, A., Trivelli, X., Corbier, C., Rouhier, N., Walker, O., Tsan, P., Jacquot, J.-P., Aubry, A., Krimm, I. and Lancelin, J.-M. Crystal structure and solution nmr dynamics of a d (type ii) peroxiredoxin glutaredoxin and thioredoxin dependent: A new insight into the peroxiredoxin oligomerism. *Biochemistry* 44(6):1755-1767 (2005).

88. Eklund, H., Gleason, F. K. and Holmgren, A. Structural and functional relations among thioredoxins of different species. *Proteins: Structure, Function, and Bioinformatics* 11(1):13-28 (1991).

89. Ellis, H. R. and Poole, L. B. Novel application of 7-chloro-4-nitrobenzo-2-oxa-1, 3-diazole to identify cysteine sulfenic acid in the ahpc component of alkyl hydroperoxide reductase. *Biochemistry* 36(48):15013-15018 (1997).

90. Ellman, G. L. Tissue sulfhydryl groups. *Archives of biochemistry and biophysics* 82(1):70-77 (1959).

91. Erickson, A., Sarsam, R. and Fisher, A. J. Expression, purification and preliminary crystallographic analysis of mycobacterium tuberculosis cysq, a phosphatase involved in sulfur metabolism. *Acta Crystallographica Section F: Structural Biology Communications* 70(6):750-753 (2014).

92. Evrard, C., Smeets, A., Knoops, B. and Declercq, J.-P. Crystal structure of the c47s mutant of human peroxiredoxin 5. *Journal of Chemical Crystallography* 34(8):553-558 (2004).

93. Fahey, R. C., Brown, W. C., Adams, W. B. and Worsham, M. B. Occurrence of glutathione in bacteria. *Journal of Bacteriology* 133(3):1126-1129 (1978).

94. Fan, G. C., Cai, Z. J., Weng, Q. Y., Ke, C., Liu, B., Zhou, L. J. and Duan, Y. P. First report of a new host (pithecellobium lucidum benth.) of the citrus huanglongbing bacterium, candidatus liberibacter asiaticus. 2nd international. In: *Res. Conf. Huanglonbing.* (2011).

95. Fan, J., Chen, C., Yu, Q., Brlansky, R. H., Li, Z.-G. and Gmitter, F. G. Comparative itraq proteome and transcriptome analyses of sweet orange infected by "*Candidatus* liberibacter asiaticus". *Physiologia plantarum* 143(3):235-245 (2011).

96. Fernandes, A. P. and Holmgren, A. Glutaredoxins: Glutathione-dependent redox enzymes with functions far beyond a simple thioredoxin backup system. *Antioxidants and Redox Signaling* 6(1):63-74 (2004).

97. Ferrante, A. A., Augliera, J., Lewis, K. and Klibanov, A. M. Cloning of an organic solvent-resistance gene in escherichia coli: The unexpected role of alkylhydroperoxide reductase. *Proceedings of the National Academy of Sciences* 92(17):7617-7621 (1995).

98. Finkel, T. and Holbrook, N. J. Oxidants, oxidative stress and the biology of ageing. *Nature* 408(6809):239-247 (2000).

99. Fisher, A. B., Dodia, C., Manevich, Y., Chen, J.-W. and Feinstein, S. I. Phospholipid hydroperoxides are substrates for non-selenium glutathione peroxidase. *Journal of Biological Chemistry* 274(30):21326-21334 (1999).

100. Flohé, L. and Harris, J. R. Peroxiredoxin systems: Structures and functions: Springer (2007).

101. Flohé, L., Loschen, G., Günzler, W. A. and Eichele, E. Glutathione peroxidase, v. The kinetic mechanism. *Hoppe-Seyler´ s Zeitschrift für physiologische Chemie* 353(1):987-1000 (1972).

102. Fomenko, D. E. and Gladyshev, V. N. Identity and functions of cxxc-derived motifs. *Biochemistry* 42(38):11214-11225 (2003).

103. Foster, J., Ganatra, M., Kamal, I., Ware, J., Makarova, K., Ivanova, N., Bhattacharyya, A., Kapatral, V., Kumar, S. and Posfai, J. The wolbachia genome of brugia malayi: Endosymbiont evolution within a human pathogenic nematode. *PLoS biology* 3(4):e121 (2005).

104. Fridovich, I. Biological effects of the superoxide radical. *Archives of Biochemistry and Biophysics* 247(1):1-11 (1986).

105. Fucci, L., Oliver, C. N., Coon, M. J. and Stadtman, E. R. Inactivation of key metabolic enzymes by mixed-function oxidation reactions: Possible implication in protein turnover and ageing. *Proceedings of the National Academy of Sciences* 80(6):1521-1525 (1983).

106. Fujii, J. and Ikeda, Y. Advances in our understanding of peroxiredoxin, a multifunctional, mammalian redox protein. *Redox Report* 7(3):123-130 (2002).

107. Fujii, T., Fujii, J. and Taniguchi, N. Augmented expression of peroxiredoxin vi in rat lung and kidney after birth implies an antioxidative role. *European Journal of Biochemistry* 268(2):218-225 (2001).

108. Gadave, K. S., Panda, S., Singh, S., Kalra, S., Malakar, D., Mohanty, A. K. and Kaushik, J. K. Structural and functional insights into the catalytic inactivity of the major fraction of buffalo milk xanthine oxidoreductase. *Plos One* 9(1):e87618 (2014).

109. Gahloth, D., Selvakumar, P., Shee, C., Kumar, P. and Sharma, A. K. Cloning, sequence analysis and crystal structure determination of a miraculin-like protein from murraya koenigii. *Archives of biochemistry and biophysics* 494(1):15-22 (2010).

110. Gangwar, S., Baig, M. S., Shah, P., Biswas, S., Batra, S., Siddiqi, M. I. and Goyal, N. Identification of novel inhibitors of dipeptidylcarboxypeptidase of leishmania donovani via ligand-based virtual screening and biological evaluation. *Chemical biology & drug design* 79(2):149-156 (2012).

111. Garca-Ruiz, J. M., Novella, M. L., Moreno, R. and Gavira, J. A. Agarose as crystallization media for proteins: I: Transport processes. *Journal of Crystal Growth* 232(1):165-172 (2001).

112. Garnier, M. and Bove, J. M. Transmission of the organism associated with citrus greening disease from sweet orange to periwinkle by dodder. *Phytopathology* 73(10):1358-1363 (1983).

113. Garnier, M., Danel, N. and Bove, J. M. Aetiology of citrus greening disease. In: *Annales de l'Institut Pasteur/Microbiologie*ed.^eds), p.^pp. 169-179. Elsevier, (1984).

114. Gasdaska, J. R., Kirkpatrick, D. L., Montfort, W., Kuperus, M., Hill, S. R., Berggren, M. and Powis, G. Oxidative inactivation of thioredoxin as a cellular growth factor and protection by a cys 73 →ser mutation. *Biochemical pharmacology* 52(11):1741-1747 (1996).

115. Gasdaska, P. Y., Berggren, M. M., Berry, M. J. and Powis, G. Cloning, sequencing and functional expression of a novel human thioredoxin reductase. *FEBS letters* 442(1):105-111 (1999).

116. Gasdaska, P. Y., Gasdaska, J. R., Cochran, S. and Powis, G. Cloning and sequencing of a human thioredoxin reductase. *FEBS letters* 373(1):5-9 (1995).

117. Gasteiger, E., Gattiker, A., Hoogland, C., Ivanyi, I., Appel, R. D. and Bairoch, A. Expasy: The proteomics server for in-depth protein knowledge and analysis. *Nucleic acids research* 31(13):3784-3788 (2003).

118. Gerschman, R., Gilbert, D., Nye, S., Dwyer, P. and Fenn, W. Oxygen poisoning and x-irradiation: A mechanism in common. *Science See Saiensu* 119 (1954).

119. Gerschman, R., Gilbert, D. L., Nye, S. W., Dwyer, P. and Fenn, W. O. Oxygen poisoning and x-irradiation: A mechanism in common. *Science of Aging Knowledge Environment* 2005(17):cp1 (2005).

120. Giege, R. and Ducruix, A. An introduction to the crystallogenesis of biological macromolecules. *Crystallization of Nucleic Acids and Proteins A Practical Approach*:1-16 (1999).

121. Gopalan, G., He, Z., Balmer, Y., Romano, P., Gupta, R., Heroux, A., Buchanan, B. B., Swaminathan, K. and Luan, S. Structural analysis uncovers a role for redox in regulating fkbp13, an immunophilin of the chloroplast thylakoid lumen. *Proceedings of the National Academy of Sciences of the United States of America* 101(38):13945-13950 (2004).

122. Gopalan, G., He, Z., Battaile, K. P., Luan, S. and Swaminathan, K. Structural comparison of oxidized and reduced fkbp13 from arabidopsis thaliana. *Proteins: Structure, Function, and Bioinformatics* 65(4):789-795 (2006).

123. Gottwald, T. R., da Graca, J. V. and Bassanezi, R. B. Citrus huanglongbing: The pathogen and its impact. *Plant Health Progress* 6 (2007).

124. Graca, J. V. d. Citrus greening disease. *Annual Review of Phytopathology* 29(1):109-136 (1991).

125. Grafton-Cardwell, E. Asian citrus psyllid: UCANR Publications (2005).

126. Greenberg, J. T. and Demple, B. Overproduction of peroxide-scavenging enzymes in escherichia coli suppresses spontaneous mutagenesis and sensitivity to redox-cycling agents in oxyr-mutants. *The EMBO journal* 7(8):2611 (1988).

127. Halbert, S. E. Citrus greening/huanglongbing. *Pest Alert, Florida Department of Agriculture and Consumer Services, Division of Plant Industry, Gainesville, Florida* (2005).

128. Halbert, S. E. and Manjunath, K. L. Asian citrus psyllids (sternorrhyncha: Psyllidae) and greening disease of citrus: A literature review and assessment of risk in florida. *Florida Entomologist* 87(3):330-353 (2004).

129. Hall, A., Karplus, P. A. and Poole, L. B. Typical 2-cys peroxiredoxins–structures, mechanisms and functions. *FEBS journal* 276(9):2469-2477 (2009).

130. Hall, A., Nelson, K., Poole, L. B. and Karplus, P. A. Structure-based insights into the catalytic power and conformational dexterity of peroxiredoxins. *Antioxidants & redox signaling* 15(3):795-815 (2011).

131. Hall, A., Parsonage, D., Poole, L. B. and Karplus, P. A. Structural evidence that peroxiredoxin catalytic power is based on transition-state stabilization. *Journal of molecular biology* 402(1):194-209 (2010).

132. Hall, A., Sankaran, B., Poole, L. B. and Karplus, P. A. Structural changes common to catalysis in the tpx peroxiredoxin subfamily. *Journal of molecular biology* 393(4):867-881 (2009).

133. Halliwell, B. and Gutteridge, J. M. C. Free radicals in biology and medicine. *NY: Oxford University Pressâ€“1999â€“968 Ñ€* (1999).

134. Hammad, Y., Marechal, J., Cournoyer, B., Normand, P. and Domenach, A. M. Modification of the protein expression pattern induced in the nitrogen-fixing actinomycete frankia sp. Strain acn14a-tsr by root exudates of its symbiotic host alnus glutinosa and cloning of the sodf gene. *Canadian journal of microbiology* 47(6):541-547 (2001).

135. Hariprasad, G., Kaur, P., Srinivasan, A., Singh, T. P. and Kumar, M. Structural analysis of secretory phospholipase a2 from clonorchis sinensis: Therapeutic implications for hepatic fibrosis. *Journal of molecular modeling* 18(7):3139-3145 (2012).

136. Harman, D. Aging: A theory based on free radical and radiation chemistry: University of California Radiation Laboratory Berkeley, CA (1955).

137. Hartford, O. M. and Dowds, B. C. Isolation and characterization of a hydrogen peroxide resistant mutant of bacillus subtilis. *Microbiology* 140(2):297-304 (1994).

138. Held, P. An introduction to reactive oxygen species-measurement of ros in cells. *Biotech instruments* (2012).

139. Herbert, D. and Pinsent, J. Crystalline bacterial catalase. *Biochemical Journal* 43(2):193 (1948).

140. Herbig, A. F. and Helmann, J. D. Roles of metal ions and hydrogen peroxide in modulating the interaction of the bacillus subtilis perr peroxide regulon repressor with operator DNA. *Molecular microbiology* 41(4):849-859 (2001).

141. Heym, B., Stavropoulos, E., Honore, N., Domenech, P., Saint-Joanis, B., Wilson, T. M., Collins, D. M., Colston, M. J. and Cole, S. T. Effects of overexpression of the alkyl hydroperoxide reductase ahpc on the virulence and isoniazid resistance of mycobacterium tuberculosis. *Infection and immunity* 65(4):1395-1401 (1997).

142. Hicks, L. D., Raghavan, R., Battisti, J. M. and Minnick, M. F. A DNA-binding peroxiredoxin of coxiella burnetii is involved in countering oxidative stress during exponential-phase growth. *Journal of bacteriology* 192(8):2077-2084 (2010).

143. Higuchi, M., Yamamoto, Y., Poole, L. B., Shimada, M., Sato, Y., Takahashi, N. and Kamio, Y. Functions of two types of nadh oxidases in energy metabolism and oxidative stress of streptococcus mutans. *Journal of bacteriology* 181(19):5940-5947 (1999).

144. Hillas, P. J., del Alba, F. S., Oyarzabal, J., Wilks, A. and de Montellano, P. R. O. The ahpc and ahpd antioxidant defense system of mycobacterium tuberculosis. *Journal of Biological Chemistry* 275(25):18801-18809 (2000).

145. Hirt, R. P., MÃ¼ller, S., Embley, T. M. and Coombs, G. H. The diversity and evolution of thioredoxin reductase: New perspectives. *Trends in parasitology* 18(7):302-308 (2002).

146. Hofmann, B., Hecht, H.-J. and Flohé, L. Peroxiredoxins. *Biological chemistry* 383(3-4):347-364 (2002).

147. Holmgren, A. Thioredoxin. 6. The amino acid sequence of the protein from escherichia coli b. *European Journal of Biochemistry* 6(4):475-484 (1968).

148. Holmgren, A. Thioredoxin. *Annual review of biochemistry* 54(1):237-271 (1985).

149. Holmgren, A. Thioredoxin and glutaredoxin systems. *J Biol Chem* 264(24):13963-13966 (1989).

150. Holmgren, A. and Lu, J. Thioredoxin and thioredoxin reductase: Current research with special reference to human disease. *Biochemical and biophysical research communications* 396(1):120-124 (2010).

151. Holmgren, A. and Sengupta, R. The use of thiols by ribonucleotide reductase. *Free Radical Biology and Medicine* 49(11):1617-1628 (2010).

152. Horling, F., Konig, J. and Dietz, K.-J. Type ii peroxiredoxin c, a member of the peroxiredoxin family of arabidopsis thaliana: Its expression and activity in comparison with other peroxiredoxins. *Plant Physiology and Biochemistry* 40(6):491-499 (2002).

153. Horling, F., Lamkemeyer, P., Konig, J., Finkemeier, I., Kandlbinder, A., Baier, M. and Dietz, K.-J. Divergent light-, ascorbate-, and oxidative stress-dependent regulation of expression of the peroxiredoxin gene family in arabidopsis. *Plant Physiology* 131(1):317-325 (2003).

154. Horta, B. B., de Oliveira, M. A., Discola, K. F., Cussiol, J. R. R. and Netto, L. E. S. Structural and biochemical characterization of peroxiredoxin qβ from xylella fastidiosa catalytic mechanism and high reactivity. *Journal of Biological Chemistry* 285(21):16051-16065 (2010).

155. Hoy, M. A., Jeyaprakash, A. and Nguyen, R. Long pcr is a sensitive method for detecting liberobacter asiaticum in parasitoids undergoing risk assessment in quarantine. *Biological Control* 22(3):278-287 (2001).

156. Hsiang, L. K. Yellow shoot of citrus. Symptomatology. Investigations in the cause of huanglongbing. Natural transmission and spread. General conclusions. *Acta Phytopathologica Sinica* 2:1-42 (1956).

157. Hugo, M., Turell, L., Manta, B., Botti, H., Monteiro, G., Netto, L. E. S., Alvarez, B., Radi, R. and Trujillo, M. Thiol and sulfenic acid oxidation of ahpe, the one-cysteine peroxiredoxin from mycobacterium tuberculosis: Kinetics, acidity constants, and conformational dynamics. *Biochemistry* 48(40):9416-9426 (2009).

158. Hugo, M., Van Laer, K., Reyes, A. M., Vertommen, D., Messens, J., Radi, R. and Trujillo, M. Mycothiol/mycoredoxin 1-dependent reduction of the peroxiredoxin ahpe from mycobacterium tuberculosis. *Journal of Biological Chemistry* 289(8):5228-5239 (2014).

159. Hung, T.-H., Hung, S.-C., Chen, C.-N., Hsu, M.-H. and Su, H.-J. Detection by pcr of candidatus liberibacter asiaticus, the bacterium causing citrus huanglongbing in vector psyllids: Application to the study of vector-pathogen relationships. *Plant Pathology* 53(1):96-102 (2004).

160. Hung, T.-H., Wu, M.-L. and Su, H.-J. Identification of the chinese box orange (severinia buxifolia) as an alternative host of the bacterium causing citrus huanglongbing. *European Journal of Plant Pathology* 107(2):183-189 (2001).

161. Hurd, T. R., Requejo, R., Filipovska, A., Brown, S., Prime, T. A., Robinson, A. J., Fearnley, I. M. and Murphy, M. P. Complex i within oxidatively stressed bovine heart mitochondria is glutathionylated on cys-531 and cys-704 of the 75-kda subunit potential role of cys residues in decreasing oxidative damage. *Journal of Biological Chemistry* 283(36):24801-24815 (2008).

162. Imlay, J. A., Chin, S. M. and Linn, S. Toxic DNA damage by hydrogen peroxide through the fenton reaction in vivo and in vitro. *Science* 240(4852):640-642 (1988).

163. Imlay, J. A. and Linn, S. DNA damage and oxygen radical toxicity. *Science* 240(4857):1302-1309 (1988).

164. Immenschuh, S., Baumgart-Vogt, E., Tan, M., Iwahara, S.-i., Ramadori, G. and Fahimi, H. D. Differential cellular and subcellular localization of heme-binding protein 23/peroxiredoxin i and heme oxygenase-1 in rat liver. *Journal of Histochemistry & Cytochemistry* 51(12):1621-1631 (2003).

165. Islam, Z., Kumar, A., Singh, S., Salmon, L. and Karthikeyan, S. Structural basis for competitive inhibition of 3, 4-dihydroxy-2-butanone-4-phosphate synthase from vibrio cholerae. *Journal of Biological Chemistry* 290(18):11293-11308 (2015).

166. Iwao-Koizumi, K., Matoba, R., Ueno, N., Kim, S. J., Ando, A., Miyoshi, Y., Maeda, E., Noguchi, S. and Kato, K. Prediction of docetaxel response in human breast cancer by gene expression profiling. *Journal of clinical oncology* 23(3):422-431 (2005).

167. Jacobson, F. S., Morgan, R., Christman, M. and Ames, B. An alkyl hydroperoxide reductase from salmonella typhimurium involved in the defense of DNA against oxidative damage. Purification and properties. *Journal of Biological Chemistry* 264(3):1488-1496 (1989).

168. Jagoueix, S., Bove, J.-m. and Garnier, M. The phloem-limited bacterium of greening disease of citrus is a member of the α subdivision of the proteobacteria. *International journal of systematic bacteriology* 44(3):379-386 (1994).

169. Jagoueix, S., Bove, J.-M. and Garnier, M. The phloem-limited bacterium of greening disease of citrus is a member of the α-subdivision of the *proteobacteria*. *International Journal of Systematic Bacteriology* 44(3):379-386 (1994).

170. Jagoueix, S., Bove, J. M. and Garnier, M. Pcr detection of the two â«candidatusâ» liberobacter species associated with greening disease of citrus. *Molecular and cellular probes* 10(1):43-50 (1996).

171. Jang, H. H., Lee, K. O., Chi, Y. H., Jung, B. G., Park, S. K., Park, J. H., Lee, J. R., Lee, S. S., Moon, J. C. and Yun, J. W. Two enzymes in one: Two yeast peroxiredoxins display oxidative stress-dependent switching from a peroxidase to a molecular chaperone function. *Cell* 117(5):625-635 (2004).

172. Janjanam, J., Singh, S., Choudhary, S., Pradeep, M. A., Kumar, S., Kumaresan, A., Das, S. K., Kaushik, J. K. and Mohanty, A. K. Molecular cloning, sequence characterization and heterologous expression of buffalo (bubalus bubalis) oviduct-specific glycoprotein in e. Coli. *Molecular biology reports* 39(12):10031-10043 (2012).

173. Jencks, W. P. Catalysis in chemistry and enzymology: Courier Corporation (1987).

174. Jeon, S.-J. and Ishikawa, K. Characterization of novel hexadecameric thioredoxin peroxidase from aeropyrum pernix k1. *Journal of Biological Chemistry* 278(26):24174-24180 (2003).

175. Jeong, J. S., Kwon, S. J., Kang, S. W., Rhee, S. G. and Kim, K. Purification and characterization of a second type thioredoxin peroxidase (type ii tpx) from saccharomyces cerevisiae. *Biochemistry* 38(2):776-783 (1999).

176. Jeong, W., Cha, M.-K. and Kim, I.-H. Thioredoxin-dependent hydroperoxide peroxidase activity of bacterioferritin comigratory protein (bcp) as a new member of the thiol-specific antioxidant protein (tsa)/alkyl hydroperoxide peroxidase c (ahpc) family. *Journal of Biological Chemistry* 275(4):2924-2930 (2000).

177. Jeong, W., Yoon, H. W., Lee, S.-R. and Rhee, S. G. Identification and characterization of trp14, a thioredoxin-related protein of 14 kda new insights into the specificity of thioredoxin function. *Journal of Biological Chemistry* 279(5):3142-3150 (2004).

178. Jiang, Z.-Y., Hunt, J. V. and Wolff, S. P. Ferrous ion oxidation in the presence of xylenol orange for detection of lipid hydroperoxide in low density lipoprotein. *Analytical biochemistry* 202(2):384-389 (1992).

179. Jiménez, A., Johansson, C., Ljung, J., Sagemark, J., Berndt, K. D., Ren, B., Tibbelin, G., Ladenstein, R., Kieselbach, T. and Holmgren, A. Human spermatid-specific thioredoxin-1 (sptrx-1) is a two-domain protein with oxidizing activity. *FEBS letters* 530(1):79-84 (2002).

180. Jin, D.-Y., Chae, H. Z., Rhee, S. G. and Jeang, K.-T. Regulatory role for a novel human thioredoxin peroxidase in nf-κb activation. *Journal of Biological Chemistry* 272(49):30952-30961 (1997).

181. Jiratchariyakul, W., Beerhues, L., Mahady, G. B., Kummalue, T. and Vongsakul, M. Botanicals in dietary supplements. *Evidence-Based Complementary and Alternative Medicine* 2013 (2013).

182. Johnson, N., McKenzie, R. and Fletcher, H. The bcp gene in the bcp-reca-vima-vime-vimf operon is important in oxidative stress resistance in porphyromonas gingivalis w83. *Molecular oral microbiology* 26(1):62-77 (2011).

183. JORNOT, L., PETERSEN, H. and JUNOD, A. Hydrogen peroxide-induced DNA damage is independent of nuclear calcium but dependent on redox-active ions. *Biochem J* 335:85-94 (1998).

184. Kall, L., Krogh, A. and Sonnhammer, E. A combined transmembrane topology and signal peptide prediction method. *Journal of molecular biology* 338(5):1027-1036 (2004).

185. Kang, S. W., Baines, I. C. and Rhee, S. G. Characterization of a mammalian peroxiredoxin that contains one conserved cysteine. *Journal of Biological Chemistry* 273(11):6303-6311 (1998).

186. Karplus, P. A. and Hall, A. Structural survey of the peroxiredoxins. In: *Peroxiredoxin systems*ed.), pp. 41-60. Springer, (2007).

187. Kelley, L. A. and Sternberg, M. J. E. Protein structure prediction on the web: A case study using the phyre server. *Nature protocols* 4(3):363-371 (2009).

188. Kice, J. L. Mechanisms and reactivity in reactions of organic oxyacids of sulfur and their anhydrides. *Advances in Physical Organic Chemistry* 17:65-181 (1981).

189. Kim, D. E., Chivian, D. and Baker, D. Protein structure prediction and analysis using the robetta server. *Nucleic acids research* 32(suppl 2):W526-W531 (2004).

190. Kim, H.-K., Kim, S.-J., Lee, J.-W., Lee, J.-W., Cha, M.-K. and Kim, I.-H. Identification of promoter in the 5′-flanking region of the e. Coli thioredoxin-linked thiol peroxidase gene: Evidence for the existence of oxygen-related transcriptional regulatory protein. *Biochemical and biophysical research communications* 221(3):641-646 (1996).

191. Kim, H., Lee, T.-H., Park, E. S., Suh, J. M., Park, S. J., Chung, H. K., Kwon, O.-Y., Kim, Y. K., Ro, H. K. and Shong, M. Role of peroxiredoxins in regulating intracellular hydrogen peroxide and hydrogen peroxide-induced apoptosis in thyroid cells. *Journal of Biological Chemistry* 275(24):18266-18270 (2000).

192. Kim, J.-S., Sagaram, U. S., Burns, J. K., Li, J.-L. and Wang, N. Response of sweet orange (citrus sinensis) to'candidatus liberibacter asiaticus' infection: Microscopy and microarray analyses. *Phytopathology* 99(1):50-57 (2009).

193. Kim, K., Kim, I., Lee, K.-Y., Rhee, S. and Stadtman, E. The isolation and purification of a specific" Protector" Protein which inhibits enzyme inactivation by a thiol/fe (iii)/o2 mixed-function oxidation system. *Journal of Biological Chemistry* 263(10):4704-4711 (1988).

194. Kim, K., Rhee, S. G. and Stadtman, E. Nonenzymatic cleavage of proteins by reactive oxygen species generated by dithiothreitol and iron. *Journal of Biological Chemistry* 260(29):15394-15397 (1985).

195. Kim, K., Rhee, S. G. and Stadtman, E. R. Nonenzymatic cleavage of proteins by reactive oxygen species generated by dithiothreitol and iron. *Journal of Biological Chemistry* 260(29):15394-15397 (1985).

196. Kim, S. J., Han, Y. H., Kim, I. H. and Kim, H. K. Involvement of arca and fnr in expression of escherichia coli thiol peroxidase gene. *IUBMB life* 48(2):215-218 (1999).

197. Kim, S. Y., Jang, H. H., Lee, J. R., Sung, N. R., Lee, H. B., Lee, D. H., Park, D.-J., Kang, C. H., Chung, W. S. and Lim, C. O. Oligomerization and chaperone activity of a plant 2-cys peroxiredoxin in response to oxidative stress. *Plant Science* 177(3):227-232 (2009).

198. King, K. Y., Horenstein, J. A. and Caparon, M. G. Aerotolerance and peroxide resistance in peroxidase and perr mutants of streptococcus pyogenes. *Journal of bacteriology* 182(19):5290-5299 (2000).

199. Kinnula, V., Lehtonen, S., Sormunen, R., Kaarteenaho-Wiik, R., Kang, S., Rhee, S. and Soini, Y. Overexpression of peroxiredoxins i, ii, iii, v, and vi in malignant mesothelioma. *The Journal of pathology* 196(3):316-323 (2002).

200. Kitano, K., Niimura, Y., Nishiyama, Y. and Miki, K. Stimulation of peroxidase activity by decamerization related to ionic strength: Ahpc protein from amphibacillus xylanus. *Journal of biochemistry* 126(2):313-319 (1999).

201. Klundt, T., Bocola, M., Lutge, M., Beuerle, T., Liu, B. and Beerhues, L. A single amino acid substitution converts benzophenone synthase into phenylpyrone synthase. *Journal of Biological Chemistry* 284(45):30957-30964 (2009).

202. Knoops, B., Clippe, A., Bogard, C., Arsalane, K., Wattiez, R., Hermans, C., Duconseille, E., Falmagne, P. and Bernard, A. Cloning and characterization of aoeb166, a novel mammalian antioxidant enzyme of the peroxiredoxin family. *Journal of Biological Chemistry* 274(43):30451-30458 (1999).

203. Knoops, B., Loumaye, E. and Van Der Eecken, V. Evolution of the peroxiredoxins. In: *Peroxiredoxin systems*ed.), pp. 27-40. Springer, (2007).

204. Kohler, A. C., Gae, D. D., Richley, M. A., Stoll, S., Gunn, A., Lim, S., Martin, S. S., Doukov, T. I., Britt, R. D., Ames, J. B. and Fisher, A. J. Structural basis for hydration dynamics in radical stabilization of bilin reductase mutants. *Biochemistry* 49(29):6206-6218 (2010).

205. Koizumi, M., Prommintara, M., Linwattana, G. and Kaisuwan, T. Field evaluation of citrus cultivars for greening disease resistance in thailand. In: *Proceedings of the 12th international conference organ citrus virology. New Delhi, India: International Organization of Citrus Virologists, University of California, Riversid* pp. 27, (1993).

206. Kong, W., Shiota, S., Shi, Y., Nakayama, H. and Nakayama, K. A novel peroxiredoxin of the plant sedum lineare is a homologue of escherichia coli bacterioferritin co-migratory protein (bcp). *Biochem J* 351:107-114 (2000).

207. Konig, J., Lotte, K., Plessow, R., Brockhinke, A., Baier, M. and Dietz, K.-J. Reaction mechanism of plant 2-cys peroxiredoxin role of the c terminus and the quaternary structure. *Journal of Biological Chemistry* 278(27):24409-24420 (2003).

208. Koo, K. H., Lee, S., Jeong, S. Y., Kim, E. T., Kim, H. J., Kim, K., Song, K. and Chae, H. Z. Regulation of thioredoxin peroxidase activity by c-terminal truncation. *Archives of biochemistry and biophysics* 397(2):312-318 (2002).

209. Korycka-Dahl, M. and Richardson, T. Photogeneration of superoxide anion in serum of bovine milk and in model systems containing riboflavin and amino acids. *Journal of Dairy Science* 61(4):400-407 (1978).

210. Korytowski, W., Pilas, B., Sarna, T. and Kalyanaraman, B. Photoinduced generation of hydrogen peroxide and hydroxyl radicals in melanins. *Photochemistry and photobiology* 45(2):185-190 (1987).

211. Kovtun, Y., Chiu, W.-L., Tena, G. and Sheen, J. Functional analysis of oxidative stress-activated mitogen-activated protein kinase cascade in plants. *Proceedings of the national academy of sciences* 97(6):2940-2945 (2000).

212. Krone, F. A., Westphal, G., Meyer, H. E. and Schwenn, J. D. Paps-reductase of escherichia coli: Correlating the n-terminal amino acid sequence with the DNA of gene cys h. *FEBS letters* 260(1):6-9 (1990).

213. Kumar, P., Gomez-Gil, L., Mohammadi, M., Sylvestre, M., Eltis, L. D. and Bolin, J. T. Anaerobic crystallization and initial x-ray diffraction data of biphenyl 2, 3-dioxygenase from burkholderia xenovorans lb400: Addition of agarose improved the quality of the crystals. *Acta Crystallographica Section F: Structural Biology and Crystallization Communications* 67(1):59-63 (2010).

214. Kumar, P., Singh, M., Gautam, R. and Karthikeyan, S. Potential anti-bacterial drug target: Structural characterization of 3, 4-dihydroxy-2-butanone-4-phosphate synthase from salmonella typhimurium lt2. *Proteins: Structure, Function, and Bioinformatics* 78(16):3292-3303 (2010).

215. Kumar, P., Singh, M. and Karthikeyan, S. Crystal structure analysis of icosahedral lumazine synthase from salmonella typhimurium, an antibacterial drug target. *Acta Crystallographica Section D: Biological Crystallography* 67(2):131-139 (2011).

216. Kumar, S., Ahmad, E., Mansuri, M. S., Kumar, S., Jain, R., Khan, R. H. and Gourinath, S. Crystal structure and trimer-monomer transition of n-terminal domain of ehcabp1 from entamoeba histolytica. *Biophysical journal* 98(12):2933-2942 (2010).

217. Kumar Singh, N., S Hasan, S., Kumar, J., Raj, I., A Pathan, A., Parmar, A., Shakil, S., Gourinath, S. and Madamwar, D. Crystal structure and interaction of phycocyanin with î²-secretase: A putative therapy for alzheimerâ€™s disease. *CNS & Neurological Disorders-Drug Targets (Formerly Current Drug Targets-CNS & Neurological Disorders)* 13(4):691-698 (2015).

218. Kuriyan, J., Krishna, T. S. R., Wong, L., Guenther, B., Pahler, A., Williams, C. H. and Model, P. Convergent evolution of similar function in 2 structurally divergent enzymes. *Nature* 352(6331):172-174. (1991).

219. Ladenstein, R., Epp, O., Bartels, K., Jones, A., Huber, R. and Wendel, A. Structure analysis and molecular model of the selenoenzyme glutathione peroxidase at 2.8 å resolution. *Journal of Molecular Biology* 134(2):199-218 (1979).

220. Laemmli, U. K. and Favre, M. Maturation of the head of bacteriophage t4: I. DNA packaging events. *Journal of molecular biology* 80(4):575-599 (1973).

221. Lafleche, D. and Bove, J. M. Mycoplasmes dans les agrumes atteints de â€œgreeningâ€, de â€œstubbornâ€ ou de maladies similaires. *Fruits* 25(6):455-465 (1970).

222. Laloi, C., Rayapuram, N., Chartier, Y., Grienenberger, J.-M., Bonnard, G. and Meyer, Y. Identification and characterization of a mitochondrial thioredoxin system in plants. *Proceedings of the National Academy of Sciences* 98(24):14144-14149 (2001).

223. Laurent, T. C., Moore, E. C. and Reichard, P. Enzymatic synthesis of deoxyribonucleotides iv. Isolation and characterization of thioredoxin, the hydrogen donor from escherichia coli b. *Journal of Biological Chemistry* 239(10):3436-3444 (1964).

224. Lee, J.-W. and Helmann, J. D. The perr transcription factor senses h2o2 by metal-catalysed histidine oxidation. *Nature* 440(7082):363-367 (2006).

225. Lee, S. P., Hwang, Y. S., Kim, Y. J., Kwon, K.-S., Kim, H. J., Kim, K. and Chae, H. Z. Cyclophilin a binds to peroxiredoxins and activates its peroxidase activity. *Journal of Biological Chemistry* 276(32):29826-29832 (2001).

226. Lemaire, S., Collin, V., Keryer, E., Quesada, A. and Miginiac-Maslow, M. Characterization of thioredoxin y, a new type of thioredoxin identified in the genome of chlamydomonas reinhardtii. *FEBS letters* 543(1):87-92 (2003).

227. Li, S., Peterson, N. A., Kim, M.-Y., Kim, C.-Y., Hung, L.-W., Yu, M., Lekin, T., Segelke, B. W., Lott, J. S. and Baker, E. N. Crystal structure of ahpe from mycobacterium tuberculosis, a 1-cys peroxiredoxin. *Journal of molecular biology* 346(4):1035-1046 (2005).

228. Li, W., Hartung, J. S. and Levy, L. Quantitative real-time pcr for detection and identification of candidatus liberibacter species associated with citrus huanglongbing. *Journal of microbiological methods* 66(1):104-115 (2006).

229. Liao, S.-J., Yang, C.-Y., Chin, K.-H., Wang, A. H.-J. and Chou, S.-H. Insights into the alkyl peroxide reduction pathway of< i> xanthomonas campestris bacterioferritin comigratory protein from the trapped intermediate–ligand complex structures. *Journal of molecular biology* 390(5):951-966 (2009).

230. Liefting, L. W., Perez-Egusquiza, Z. C., Clover, G. R. G. and Anderson, J. A. D. A new'candidatus liberibacter'species in solanum tuberosum in new zealand. *Plant Disease* 92(10):1474-1474 (2008).

231. Lillig, C. H., Berndt, C. and Holmgren, A. Glutaredoxin systems. *Biochimica et Biophysica Acta (BBA)-General Subjects* 1780(11):1304-1317 (2008).

232. Lillig, C. H. and Holmgren, A. Thioredoxin and related molecules-from biology to health and disease. *Antioxidants & redox signaling* 9(1):25-47 (2007).

233. Limauro, D., De Simone, G., Pirone, L., Bartolucci, S., D'Ambrosio, K. and Pedone, E. Sulfolobus solfataricus thiol redox puzzle: Characterization of an atypical protein disulfide oxidoreductase. *Extremophiles* 18(2):219-228 (2014).

234. Limauro, D., Pedone, E., Pirone, L. and Bartolucci, S. Identification and characterization of 1-cys peroxiredoxin from sulfolobus solfataricus and its involvement in the response to oxidative stress. *Febs Journal* 273(4):721-731 (2006).

235. Link, A. J., Robison, K. and Church, G. M. Comparing the predicted and observed properties of proteins encoded in the genome of escherichia coli k-12. *Electrophoresis* 18(8):1259-1313 (1997).

236. Liu, R., Zhang, P., Pu, X., Xing, X., Chen, J. and Deng, X. Analysis of a prophage gene frequency revealed population variation of'candidatus liberibacter asiaticus' from two citrus-growing provinces in china. *Plant disease* 95(4):431-435 (2011).

237. Logan, C. and Mayhew, S. G. Cloning, overexpression, and characterization of peroxiredoxin and nadh peroxiredoxin reductase from thermus aquaticus. *Journal of Biological Chemistry* 275(39):30019-30028 (2000).

238. Loprasert, S., Atichartpongkun, S., Whangsuk, W. and Mongkolsuk, S. Isolation and analysis of the xanthomonas alkyl hydroperoxide reductase gene and the peroxide sensor regulator genes ahpc and ahpf-oxyr-orfx. *Journal of bacteriology* 179(12):3944-3949 (1997).

239. Lu, J. and Holmgren, A. Selenoproteins. *Journal of Biological Chemistry* 284(2):723-727 (2009).

240. Lu, J. and Holmgren, A. The thioredoxin antioxidant system. *Free Radical Biology and Medicine* 66:75-87 (2014).

241. Lubos, E., Loscalzo, J. and Handy, D. E. Glutathione peroxidase-1 in health and disease: From molecular mechanisms to therapeutic opportunities. *Antioxidants & redox signaling* 15(7):1957-1997 (1997).

242. Lundström, A. M. and Bölin, I. A 26 kda protein of helicobacter pylori shows alkyl hydroperoxide reductase (ahpc) activity and the mono-cistronic transcription of the gene is affected by ph. *Microbial pathogenesis* 29(5):257-266 (2000).

243. Manevich, Y., Feinstein, S. and Fisher, A. Activation of the antioxidant enzyme 1-cys peroxiredoxin requires glutathionylation mediated by heterodimerization with πgst. *Proceedings of the National Academy of Sciences of the United States of America* 101(11):3780-3785 (2004).

244. Manta, B., Hugo, M. n., Ortiz, C., Ferrer-Sueta, G., Trujillo, M. and Denicola, A. The peroxidase and peroxynitrite reductase activity of human erythrocyte peroxiredoxin 2. *Archives of biochemistry and biophysics* 484(2):146-154 (2009).

245. Matsui, M., Oshima, M., Oshima, H., Takaku, K., Maruyama, T., Yodoi, J. and Taketo, M. M. Early embryonic lethality caused by targeted disruption of the mouse thioredoxin gene. *Developmental biology* 178(1):179-185 (1996).

246. May, J. M., Cobb, C. E., Mendiratta, S., Hill, K. E. and Burk, R. F. Reduction of the ascorbyl free radical to ascorbate by thioredoxin reductase. *Journal of Biological Chemistry* 273(36):23039-23045 (1998).

247. McClean, A. P. D. and Oberholzer, P. C. J. Citrus psylla, a vector of the greening disease of sweet orange. *South African Journal of Agricultural Science* 8(1):297-298 (1965).

248. McClean, A. P. D. and Oberholzer, P. C. J. Greening disease of the sweet orange: Evidence that it is caused by a transmissible virus. *South African journal of agricultural science* 8(1):253-275. (1965).

249. McMurry, J. Organic chemistry, thomson learning. *Inc United States* (2004).

250. McPherson, A. Crystallization of biological macromolecules. (1999).

251. Meyer, Y., Vignols, F. and Reichheld, J. P. Classification of plant thioredoxins by sequence similarity and intron position. *Methods in enzymology* 347:394-402 (2002).

252. Michaud, J. P. Natural mortality of asian citrus psyllid (homoptera: Psyllidae) in central florida. *Biological Control* 29(2):260-269 (2004).

253. Mieyal, J. J., Gallogly, M. M., Qanungo, S., Sabens, E. A. and Shelton, M. D. Molecular mechanisms and clinical implications of reversible protein s-glutathionylation. *Antioxidants & redox signaling* 10(11):1941-1988 (2008).

254. Mills, E. M., Takeda, K., Yu, Z.-X., Ferrans, V., Katagiri, Y., Jiang, H., Lavigne, M. C., Leto, T. L. and Guroff, G. Nerve growth factor treatment prevents the increase in superoxide produced by epidermal growth factor in pc12 cells. *Journal of Biological Chemistry* 273(35):22165-22168 (1998).

255. Mittler, R., Herr, E. H., Orvar, B. L., Van Camp, W., Willekens, H., Inzé, D. and Ellis, B. E. Transgenic tobacco plants with reduced capability to detoxify reactive oxygen intermediates are hyperresponsive to pathogen infection. *Proceedings of the National Academy of Sciences* 96(24):14165-14170 (1999).

256. Mohammadi, M. and Sylvestre, M. Resolving the profile of metabolites generated during oxidation of dibenzofuran and chlorodibenzofurans by the biphenyl catabolic pathway enzymes. *Chemistry & biology* 12(7):835-846 (2005).

257. Møller, I. M., Jensen, P. E. and Hansson, A. Oxidative modifications to cellular components in plants. *Annu Rev Plant Biol* 58:459-481 (2007).

258. Mongkolsuk, S., Loprasert, S., Whangsuk, W., Fuangthong, M. and Atichartpongkun, S. Characterization of transcription organization and analysis of unique expression patterns of an alkyl hydroperoxide reductase c gene (ahpc) and the peroxide regulator operon ahpf-oxyr-orfx from xanthomonas campestris pv. Phaseoli. *Journal of bacteriology* 179(12):3950-3955 (1997).

259. Mongkolsuk, S., Whangsuk, W., Vattanaviboon, P., Loprasert, S. and Fuangthong, M. A xanthomonas alkyl hydroperoxide reductase subunit c (ahpc) mutant showed an altered peroxide stress response and complex regulation of the compensatory response of peroxide detoxification enzymes. *Journal of bacteriology* 182(23):6845-6849 (2000).

260. Monteiro, G., Horta, B. B., Pimenta, D. C., Augusto, O. and Netto, L. E. S. Reduction of 1-cys peroxiredoxins by ascorbate changes the thiol-specific antioxidant paradigm, revealing another function of vitamin c. *Proceedings of the National Academy of Sciences* 104(12):4886-4891 (2007).

261. Moon, J. C., Hah, Y.-S., Kim, W. Y., Jung, B. G., Jang, H. H., Lee, J. R., Kim, S. Y., Lee, Y. M., Jeon, M. G. and Kim, C. W. Oxidative stress-dependent structural and functional switching of a human 2-cys peroxiredoxin isotype ii that enhances hela cell resistance to h2o2-induced cell death. *Journal of Biological Chemistry* 280(31):28775-28784 (2005).

262. Moore, E. C., Reichard, P. and Thelander, L. Enzymatic synthesis of deoxyribonucleotides v. Purification and properties of thioredoxin reductase from escherichia coli b. *Journal of Biological Chemistry* 239(10):3445-3452 (1964).

263. Mosmann, T. Rapid colorimetric assay for cellular growth and survival: Application to proliferation and cytotoxicity assays. *Journal of immunological methods* 65(1):55-63 (1983).

264. Muller, F. Chemistry and biochemistry of flavoenzymes. (1992).

265. Muller, F. L., Lustgarten, M. S., Jang, Y., Richardson, A. and Van Remmen, H. Trends in oxidative aging theories. *Free Radical Biology and Medicine* 43(4):477-503 (2007).

266. Muller, S. Redox and antioxidant systems of the malaria parasite plasmodium falciparum. *Molecular microbiology* 53(5):1291-1305 (2004).

267. Murray, R. G. E. and Schleifer, K. H. Taxonomic notes: A proposal for recording the properties of putative taxa of procaryotes. *International journal of systematic bacteriology* 44(1):174-176 (1994).

268. Mustacich, D. and Powis, G. Thioredoxin reductase. *Biochem J* 346:1-8 (2000).

269. Nagpal, I., Raj, I., Subbarao, N. and Gourinath, S. Virtual screening, identification and in vitro testing of novel inhibitors of o-acetyl-l-serine sulfhydrylase of entamoeba histolytica. *Plos One* 7(2):e30305 (2012).

270. Nagy, N., Malik, G., Fisher, A. B. and Das, D. K. Targeted disruption of peroxiredoxin 6 gene renders the heart vulnerable to ischemia-reperfusion injury. *American Journal of Physiology-Heart and Circulatory Physiology* 291(6):H2636-H2640 (2006).

271. Nakamura, T., Kado, Y., Yamaguchi, T., Matsumura, H., Ishikawa, K. and Inoue, T. Crystal structure of peroxiredoxin from aeropyrum pernix k1 complexed with its substrate, hydrogen peroxide. *Journal of biochemistry* 147(1):109-115 (2010).

272. Neidhardt, F. C., Vaughn, V., Phillips, T. and Bloch, P. L. Gene-protein index of escherichia coli k-12. *Microbiological reviews* 47(2):231 (1983).

273. Neill, S., Bright, J., Desikan, R., Hancock, J., Harrison, J. and Wilson, I. Nitric oxide evolution and perception. *Journal of Experimental Botany* 59(1):25-35 (2008).

274. Neill, S. J., Desikan, R. and Hancock, J. T. Nitric oxide signalling in plants. *New Phytologist* 159(1):11-35 (2003).

275. Neumann, C. A., Krause, D. S., Carman, C. V., Das, S., Dubey, D. P., Abraham, J. L., Bronson, R. T., Fujiwara, Y., Orkin, S. H. and Van Etten, R. A. Essential role for the peroxiredoxin prdx1 in erythrocyte antioxidant defence and tumour suppression. *Nature* 424(6948):561-565 (2003).

276. Newton, G. L., Arnold, K., Price, M. S., Sherrill, C., Delcardayre, S. B., Aharonowitz, Y., Cohen, G., Davies, J., Fahey, R. C. and Davis, C. Distribution of thiols in microorganisms: Mycothiol is a major thiol in most actinomycetes. *Journal of bacteriology* 178(7):1990-1995 (1996).

277. Niimura, Y., Nishiyama, Y., Saito, D., Tsuji, H., Hidaka, M., Miyaji, T., Watanabe, T. and Massey, V. A hydrogen peroxide-forming nadh oxidase that functions as an alkyl hydroperoxide reductase in amphibacillus xylanus. *Journal of bacteriology* 182(18):5046-5051 (2000).

278. Niimura, Y., Poole, L. B. and Massey, V. Amphibacillus xylanus nadh oxidase and salmonella typhimurium alkyl-hydroperoxide reductase flavoprotein components show extremely high scavenging activity for both alkyl hydroperoxide and hydrogen peroxide in the presence of s. Typhimurium alkyl-hydroperoxide reductase 22-kda protein component. *Journal of Biological Chemistry* 270(43):25645-25650 (1995).

279. Nishiyama, A., Matsui, M., Iwata, S., Hirota, K., Masutani, H., Nakamura, H., Takagi, Y., Sono, H., Gon, Y. and Yodoi, J. Identification of thioredoxin-binding protein-2/vitamin d3 up-regulated protein 1 as a negative regulator of thioredoxin function and expression. *Journal of Biological Chemistry* 274(31):21645-21650 (1999).

280. Nishiyama, Y., Massey, V., Takeda, K., Kawasaki, S., Sato, J., Watanabe, T. and Niimura, Y. Hydrogen peroxide-forming nadh oxidase belonging to the peroxiredoxin oxidoreductase family: Existence and physiological role in bacteria. *Journal of bacteriology* 183(8):2431-2438 (2001).

281. Noguera-Mazon, V., Krimm, I., Walker, O. and Lancelin, J.-M. Protein–protein interactions within peroxiredoxin systems. *Photosynthesis research* 89(2-3):277-290 (2006).

282. Noguera-Mazon, V. r., Lemoine, J. r. m., Walker, O., Rouhier, N., Salvador, A., Jacquot, J.-P., Lancelin, J.-M. and Krimm, I. Glutathionylation induces the dissociation of 1-cys d-peroxiredoxin non-covalent homodimer. *Journal of Biological Chemistry* 281(42):31736-31742 (2006).

283. Noh, D.-Y., Ahn, S.-J., Lee, R.-A., Kim, S.-W., Park, I.-A. and Chae, H.-Z. Overexpression of peroxiredoxin in human breast cancer. *Anticancer research* 21(3B):2085-2090 (2000).

284. Nonn, L., Williams, R. R., Erickson, R. P. and Powis, G. The absence of mitochondrial thioredoxin 2 causes massive apoptosis, exencephaly, and early embryonic lethality in homozygous mice. *Molecular and cellular biology* 23(3):916-922 (2003).

285. Novoselov, V., Baryshnikova, L., Yanin, V., Amelina, S. and Fesenko, E. The influence of peroxyredoxin vi on incised-wound healing in rats. In: *Doklady Biochemistry and Biophysics*e pp. 326-327. Springer, (2003).

286. Novoselov, V., Peshenko, I., Evdokimov, V., Kamzalov, S., Novoselov, S., Nikolaev, I., Bystrova, M. and Fesenko, E. [properties of the catalytic center of a secretory 28kda protein (1-cys peroxiredoxin) from rat olfactory epithelium]. *Biofizika* 43(4):610-616 (1997).

287. Ogusucu, R., Rettori, D., Munhoz, D. C., Netto, L. E. S. and Augusto, O. Reactions of yeast thioredoxin peroxidases i and ii with hydrogen peroxide and peroxynitrite: Rate constants by competitive kinetics. *Free Radical Biology and Medicine* 42(3):326-334 (2007).

288. Oláhová, M., Taylor, S. R., Khazaipoul, S., Wang, J., Morgan, B. A., Matsumoto, K., Blackwell, T. K. and Veal, E. A. A redox-sensitive peroxiredoxin that is important for longevity has tissue-and stress-specific roles in stress resistance. *Proceedings of the National Academy of Sciences* 105(50):19839-19844 (2008).

289. Olczak, A. A., Olson, J. W. and Maier, R. J. Oxidative-stress resistance mutants of helicobacter pylori. *Journal of bacteriology* 184(12):3186-3193 (2002).

290. Oliveira, M. A., Guimaraes, B. G., Cussiol, J. R. R., Medrano, F. J., Gozzo, F. C. and Netto, L. E. S. Structural insights into enzyme-substrate interaction and characterization of enzymatic intermediates of organic hydroperoxide resistance protein from xylella fastidiosa. *Journal of molecular biology* 359(2):433-445 (2006).

291. Otwinowski, Z., Minor, W. and W Jr, C. C. Processing of x-ray diffraction data collected in oscillation mode. (1997).

292. Papp, L. V., Lu, J., Holmgren, A. and Khanna, K. K. From selenium to selenoproteins: Synthesis, identity, and their role in human health. *Antioxidants & redox signaling* 9(7):775-806 (2007).

293. Parsonage, D., Miller, H., Ross, P. R. and Claiborne, A. Purification and analysis of streptococcal nadh peroxidase expressed in e. Coli. *J Biol Chem* 268:3161-3167 (1995).

294. Passardi, F., Theiler, G., Zamocky, M., Cosio, C., Rouhier, N., Teixera, F., Margis-Pinheiro, M., Ioannidis, V., Penel, C. and Falquet, L. Peroxibase: The peroxidase database. *Phytochemistry* 68(12):1605-1611 (2007).

295. Pauly, N., Pucciariello, C., Mandon, K., Innocenti, G., Jamet, A., Baudouin, E., Hérouart, D., Frendo, P. and Puppo, A. Reactive oxygen and nitrogen species and glutathione: Key players in the legume–rhizobium symbiosis. *Journal of experimental botany* 57(8):1769-1776 (2006).

296. Pei, Z.-M., Murata, Y., Benning, G., Thomine, S., Klüsener, B., Allen, G. J., Grill, E. and Schroeder, J. I. Calcium channels activated by hydrogen peroxide mediate abscisic acid signalling in guard cells. *Nature* 406(6797):731-734 (2000).

297. Peltier, J.-B., Emanuelsson, O., Kalume, D. E., Ytterberg, J., Friso, G., Rudella, A., Liberles, D. A., Söderberg, L., Roepstorff, P. and von Heijne, G. Central functions of the lumenal and peripheral thylakoid proteome of arabidopsis determined by experimentation and genome-wide prediction. *The Plant Cell Online* 14(1):211-236 (2002).

298. Penna, C., Mancardi, D., Tullio, F. and Pagliaro, P. Postconditioning and intermittent bradykinin induced cardioprotection require cyclooxygenase activation and prostacyclin release during reperfusion. *Basic research in cardiology* 103(4):368-377 (2008).

299. Peshenko, I., Novoselov, V., Evdokimov, V., Nikolaev, Y. V., Kamzalov, S., Shuvaeva, T., Lipkin, V. and Fesenko, E. Identification of a 28 kda secretory protein from rat olfactory epithelium as a thiol-specific antioxidant. *Free Radical Biology and Medicine* 25(6):654-659 (1998).

300. Peshenko, I., Novoselov, V., Evdokimov, V., Nikolaev, Y. V., Shuvaeva, T., Lipkin, V. and Fesenko, E. Novel 28-kda secretory protein from rat olfactory epithelium. *FEBS letters* 381(1):12-14 (1996).

301. Polyak, K., Xia, Y., Zweier, J. L., Kinzler, K. W. and Vogelstein, B. A model for p53-induced apoptosis. *Nature* 389(6648):300-305 (1997).

302. Poole, L. B. Bacterial defenses against oxidants: Mechanistic features of cysteine-based peroxidases and their flavoprotein reductases. *Archives of biochemistry and biophysics* 433(1):240-254 (2005).

303. Poole, L. B. and Ellis, H. R. Flavin-dependent alkyl hydroperoxide reductase from salmonella typhimurium. 1. Purification and enzymatic activities of overexpressed ahpf and ahpc proteins. *Biochemistry* 35(1):56-64 (1996).

304. Poole, L. B., Higuchi, M., Shimada, M., Li Calzi, M. and Kamio, Y. Streptococcus mutans h2o2-forming nadh oxidase is an alkyl hydroperoxide reductase protein. *Free Radical Biology and Medicine* 28(1):108-120 (2000).

305. Provost, K. and Robert, M.-C. Application of gel growth to hanging drop technique. *Journal of crystal growth* 110(1):258-264 (1991).

306. Pullman, M. E., Penefsky, H. S., Datta, A. and Racker, E. Partial resolution of the enzymes catalyzing oxidative phosphorylation i. Purification and properties of soluble, dinitrophenol-stimulated adenosine triphosphatase. *Journal of Biological Chemistry* 235(11):3322-3329 (1960).

307. Rae, D. J., Liang, W. G., Watson, D. M., Beattie, G. A. C. and Huang, M. D. Evaluation of petroleum spray oils for control of the asian citrus psylla, diaphorina citri (kuwayama)(hemiptera: Psyllidae), in china. *International Journal of Pest Management* 43(1):71-75 (1997).

308. Reynolds, C. M., Meyer, J. and Poole, L. B. An nadh-dependent bacterial thioredoxin reductase-like protein in conjunction with a glutaredoxin homologue form a unique peroxiredoxin (ahpc) reducing system in clostridium pasteurianum. *Biochemistry* 41(6):1990-2001 (2002).

309. Rho, B.-S., Hung, L.-W., Holton, J. M., Vigil, D., Kim, S.-I., Park, M. S., Terwilliger, T. C. and Pedelacq, J.-D. Functional and structural characterization of a thiol peroxidase from mycobacterium tuberculosis. *Journal of molecular biology* 361(5):850-863 (2006).

310. Riddles, P. W., Blakeley, R. L. and Zerner, B. Ellman's reagent: 5, 5-dithiobis (2-nitrobenzoic acid) -a reexamination. *Analytical biochemistry* 94(1):75-81 (1979).

311. Robert, M. C. and Lefaucheux, F. Crystal growth in gels: Principle and applications. *Journal of Crystal Growth* 90(1):358-367 (1988).

312. Robert, X. and Gouet, P. Deciphering key features in protein structures with the new endscript server. *Nucleic acids research* 42(W1):W320-W324 (2014).

313. Roberts, B. R., Wood, Z. A., Jönsson, T. J., Poole, L. B. and Karplus, P. A. Oxidized and synchrotron cleaved structures of the disulfide redox center in the n-terminal domain of salmonella typhimurium ahpf. *Protein science* 14(9):2414-2420 (2005).

314. Rocha, E. R., Owens, G. and Smith, C. J. The redox-sensitive transcriptional activator oxyr regulates the peroxide response regulon in the obligate anaerobebacteroides fragilis. *Journal of bacteriology* 182(18):5059-5069 (2000).

315. Rocha, E. R. and Smith, C. J. Role of the alkyl hydroperoxide reductase (ahpcf) gene in oxidative stress defense of the obligate anaerobe bacteroides fragilis. *Journal of bacteriology* 181(18):5701-5710 (1999).

316. Rocha, E. R., Tzianabos, A. O. and Smith, C. J. Thioredoxin reductase is essential for thiol/disulfide redox control and oxidative stress survival of the anaerobe bacteroides fragilis. *Journal of bacteriology* 189(22):8015-8023 (2007).

317. Rogers, M. E. and Timmer, L. W. Florida citrus pest management guide. *University of Florida, IFAS Ext ENY-601* (2006).

318. Rollet-Labelle, E., Grange, M.-J., Elbim, C., Marquetty, C., Gougerot-Pocidalo, M.-A. and Pasquier, C. Hydroxyl radical as a potential intracellular mediator of polymorphonuclear neutrophil apoptosis. *Free Radical Biology and Medicine* 24(4):563-572 (1998).

319. Rosenkranz, A. R., Schmaldienst, S., Stuhlmeier, K. M., Chen, W., Knapp, W. and Zlabinger, G. J. A microplate assay for the detection of oxidative products using 2, 7-dichlorofluorescin-diacetate. *Journal of immunological methods* 156(1):39-45 (1992).

320. Ruch, W., Cooper, P. H. and Baggiolini, M. Assay of h 2 o 2 production by macrophages and neutrophils with homovanillic acid and horse-radish peroxidase. *Journal of immunological methods* 63(3):347-357 (1983).

321. Sadek, C. M., Damdimopoulos, A. E., Pelto-Huikko, M., Gustafsson, J.-Å., Spyrou, G. and Miranda-Vizuete, A. Sptrx-2, a fusion protein composed of one thioredoxin and three tandemly repeated ndp-kinase domains is expressed in human testis germ cells. *Genes to Cells* 6(12):1077-1090 (2001).

322. Sahrawy, M., Hecht, V., Lopez-Jaramillo, J., Chueca, A., Chartier, Y. and Meyer, Y. Intron position as an evolutionary marker of thioredoxins and thioredoxin domains. *Journal of molecular evolution* 42(4):422-431 (1996).

323. Sarma, G. N., Nickel, C., Rahlfs, S., Fischer, M., Becker, K. and Karplus, P. A. Crystal structure of a novel plasmodium falciparum 1-cys peroxiredoxin. *Journal of molecular biology* 346(4):1021-1034 (2005).

324. Sayed, A. A. and Williams, D. L. Biochemical characterization of 2-cys peroxiredoxins from schistosoma mansoni. *Journal of Biological Chemistry* 279(25):26159-26166 (2004).

325. Scandalios, J. Oxidative stress: Molecular perception and transduction of signals triggering antioxidant gene defenses. *Brazilian Journal of Medical and Biological Research* 38(7):995-1014 (2005).

326. Schonbaum, G. R., Chance, B. and Boyer, P. D. The enzymes , vol. In: e pp. 13Academic Press, New York, (1976).

327. Seaver, L. C. and Imlay, J. A. Alkyl hydroperoxide reductase is the primary scavenger of endogenous hydrogen peroxide in escherichia coli. *Journal of Bacteriology* 183(24):7173-7181 (2001).

328. Sechler, A., Schuenzel, E. L., Cooke, P., Donnua, S., Thaveechai, N., Postnikova, E., Stone, A. L., Schneider, W. L., Damsteegt, V. D. and Schaad, N. W. Cultivation of 'candidatus liberibacter asiaticus', 'ca. L. Africanus', and 'ca. L. Americanus' associated with huanglongbing. *Phytopathology* 99(5):480-486 (2009).

329. Selvakumar, P., Gahloth, D., Tomar, P. P. S., Sharma, N. and Sharma, A. K. Molecular evolution of miraculin-like proteins in soybean kunitz super-family. *Journal of molecular evolution* 73(5-6):369-379 (2011).

330. Selvakumar, P., Sharma, N., Tomar, P. P. S., Kumar, P. and Sharma, A. K. Structural insights into the aggregation behavior of murraya koenigii miraculinâ€like protein below ph 7.5. *Proteins: Structure, Function, and Bioinformatics* 82(5):830-840 (2014).

331. Sen, C. K. and Packer, L. Antioxidant and redox regulation of gene transcription. *The FASEB journal* 10(7):709-720 (1996).

332. Serata, M., Iino, T., Yasuda, E. and Sako, T. Roles of thioredoxin and thioredoxin reductase in the resistance to oxidative stress in lactobacillus casei. *Microbiology* 158(Pt 4):953-962 (2012).

333. Sharma, P., Dube, D., Singh, A., Mishra, B., Singh, N., Sinha, M., Dey, S., Kaur, P., Mitra, D. K. and Sharma, S. Structural basis of recognition of pathogen-associated molecular patterns and inhibition of proinflammatory cytokines by camel peptidoglycan recognition protein. *Journal of Biological Chemistry* 286(18):16208-16217 (2011).

334. Sharma, P., Dube, D., Sinha, M., Mishra, B., Dey, S., Mal, G., Pathak, K. M. L., Kaur, P., Sharma, S. and Singh, T. P. Multiligand specificity of pathogen-associated molecular pattern-binding site in peptidoglycan recognition protein. *Journal of Biological Chemistry* 286(36):31723-31730 (2011).

335. Sharma, P., Jha, A. B., Dubey, R. S. and Pessarakli, M. Reactive oxygen species, oxidative damage, and antioxidative defense mechanism in plants under stressful conditions. *Journal of Botany* 2012 (2012).

336. Shaw Stewart, P. D., Kolek, S. A., Briggs, R. A., Chayen, N. E. and Baldock, P. F. M. Random microseeding: A theoretical and practical exploration of seed stability and seeding techniques for successful protein crystallization. *Crystal Growth & Design* 11(8):3432-3441 (2011).

337. Shee, C., Islam, A., Ahmad, F. and Sharma, A. K. Structure-function studies of murraya koenigii trypsin inhibitor revealed a stable core beta sheet structure surrounded by α-helices with a possible role for α-helix in inhibitory function. *International journal of biological macromolecules* 41(4):410-414 (2007).

338. Shee, C. and Sharma, A. K. Purification and characterization of a trypsin inhibitor from seeds of murraya koenigii. *Journal of enzyme inhibition and medicinal chemistry* 22(1):115-120 (2007).

339. Sherman, D. R., Mdluli, K., Hickey, M. J., Arain, T. M., Morris, S. L., Barry, C. E. and Stover, C. K. Compensatory ahpc gene expression in isoniazid-resistant mycobacterium tuberculosis. *Science* 272(5268):1641-1643 (1996).

340. Shi, J., Vlamis-Gardikas, A., Åslund, F., Holmgren, A. and Rosen, B. P. Reactivity of glutaredoxins 1, 2, and 3 fromescherichia coli shows that glutaredoxin 2 is the primary hydrogen donor to arsc-catalyzed arsenate reduction. *Journal of Biological Chemistry* 274(51):36039-36042 (1999).

341. Sies, H. Strategies of antioxidant defense. In: *Ejb reviews 1993*ed.), pp. 101-107. Springer, (1994).

342. Singh, A., Selvakumar, P., Saraswat, A., Tomar, P. P., Mishra, M., Singh, P. K. and Sharma, A. K. Characterization and cloning of an 11s globulin with hemagglutination activity from murraya paniculata. *Protein and peptide letters* (2015).

343. Smeets, A., Loumaye, E. o., Clippe, A., Rees, J. F. o., Knoops, B. and Declercq, J. P. The crystal structure of the c45s mutant of annelid arenicola marina peroxiredoxin 6 supports its assignment to the mechanistically typical 2-cys subfamily without any formation of toroidâ€shaped decamers. *Protein Science* 17(4):700-710 (2008).

344. Smith, A. D., Guidry, C. A., Morris, V. C. and Levander, O. A. Aurothioglucose inhibits murine thioredoxin reductase activity in vivo. *The Journal of nutrition* 129(1):194-198 (1999).

345. Springer, B., Master, S., Sander, P., Zahrt, T., McFalone, M., Song, J., Papavinasasundaram, K., Colston, M., Boettger, E. and Deretic, V. Silencing of oxidative stress response in mycobacterium tuberculosis: Expression patterns of ahpc in virulent and avirulent strains and effect ofahpc inactivation. *Infection and immunity* 69(10):5967-5973 (2001).

346. Sridharamurthy, M., Kovach, A., Zhao, Y., Zhu, J.-K., Xu, H. E., Swaminathan, K. and Melcher, K. H2o2 inhibits aba-signaling protein phosphatase hab1. *Plos One* 9(12):e113643 (2014).

347. Srivastava, V., Gupta, S. P., Siddiqi, M. I. and Mishra, B. N. Molecular docking studies on quinazoline antifolate derivatives as human thymidylate synthase inhibitors. *Bioinformation* 4(8):357 (2010).

348. Stadtman, E. R. Protein oxidation and aging. *Science* 257(5074):1220-1224 (1992).

349. Stehr, M., Hecht, H. J., Jager, T., Flohe, L. and Singh, M. Structure of the inactive variant c60s of mycobacterium tuberculosis thiol peroxidase. *Acta Crystallographica Section D: Biological Crystallography* 62(5):563-567 (2006).

350. Sticher, L., Mauch-Mani, B., Metraux and Jp. Systemic acquired resistance. *Annual review of phytopathology* 35(1):235-270 (1997).

351. Stoll, S., Gunn, A., Brynda, M., Sughrue, W., Kohler, A. C., Ozarowski, A., Fisher, A. J., Lagarias, J. C. and Britt, R. D. Structure of the biliverdin radical intermediate in phycocyanobilin: Ferredoxin oxidoreductase identified by high-field epr and dft. *Journal of the American Chemical Society* 131(5):1986-1995 (2009).

352. Stork, T., Laxa, M., Dietz, M. S. and Dietz, K.-J. Functional characterisation of the peroxiredoxin gene family members of synechococcus elongatus pcc 7942. *Archives of microbiology* 191(2):141-151 (2009).

353. Storz, G., Christman, M. F., Sies, H. and Ames, B. N. Spontaneous mutagenesis and oxidative damage to DNA in salmonella typhimurium. *Proceedings of the National Academy of Sciences* 84(24):8917-8921 (1987).

354. Storz, G. and Imlayt, J. A. Oxidative stress. *Current opinion in microbiology* 2(2):188-194 (1999).

355. Storz, G., Jacobson, F., Tartaglia, L., Morgan, R., Silveira, L. and Ames, B. An alkyl hydroperoxide reductase induced by oxidative stress in salmonella typhimurium and escherichia coli: Genetic characterization and cloning of ahp. *Journal of bacteriology* 171(4):2049-2055 (1989).

356. Swain, D. K., Kushwah, M. S., Kaur, M., Patbandha, T. K., Mohanty, A. K. and Dang, A. K. Formation of net, phagocytic activity, surface architecture, apoptosis and expression of toll like receptors 2 and 4 (tlr2 and tlr4) in neutrophils of mastitic cows. *Veterinary research communications* 38(3):209-219 (2014).

357. Sweetlove, L., Heazlewood, J., Herald, V., Holtzapffel, R., Day, D., Leaver, C. and Millar, A. The impact of oxidative stress on arabidopsis mitochondria. *The Plant Journal* 32(6):891-904 (2002).

358. Tanaka, K., Pracyk, J. B., Takeda, K., Yu, Z.-X., Ferrans, V. J., Deshpande, S. S., Ozaki, M., Hwang, P. M., Lowenstein, C. J. and Irani, K. Expression of id1 results in apoptosis of cardiac myocytes through a redox-dependent mechanism. *Journal of Biological Chemistry* 273(40):25922-25928 (1998).

359. Tao, K. Subcellular localization and in vivo oxidation–reduction kinetics of thiol peroxidase in escherichia coli. *FEMS microbiology letters* 289(1):41-45 (2008).

360. Tarpey, M. M., Wink, D. A. and Grisham, M. B. Methods for detection of reactive metabolites of oxygen and nitrogen: In vitro and in vivo considerations. *American Journal of Physiology-Regulatory, Integrative and Comparative Physiology* 286(3):R431-R444 (2004).

361. Tartaglia, L., Storz, G., Brodsky, M. H., Lai, A. and Ames, B. N. Alkyl hydroperoxide reductase from salmonella typhimurium. Sequence and homology to thioredoxin reductase and other flavoprotein disulfide oxidoreductases. *Journal of Biological Chemistry* 265(18):10535-10540 (1990).

362. Tartaglia, L. A., Storz, G. and Ames, B. N. Identification and molecular analysis of oxyr-regulated promoters important for the bacterial adaptation to oxidative stress. *Journal of molecular biology* 210(4):709-719 (1989).

363. Taylor, N. L., Day, D. A. and Millar, A. H. Environmental stress causes oxidative damage to plant mitochondria leading to inhibition of glycine decarboxylase. *Journal of Biological Chemistry* 277(45):42663-42668 (2002).

364. Telfer, A., Dhami, S., Bishop, S. M., Phillips, D. and Barber, J. . Beta.-carotene quenches singlet oxygen formed by isolated photosystem ii reaction centers. *Biochemistry* 33(48):14469-14474 (1994).

365. Tomb, J.-F., White, O., Kerlavage, A. R., Clayton, R. A., Sutton, G. G., Fleischmann, R. D., Ketchum, K. A., Klenk, H. P., Gill, S. and Dougherty, B. A. The complete genome sequence of the gastric pathogen helicobacter pylori. *Nature* 388(6642):539-547 (1997).

366. Toomey, D. and Mayhew, S. G. Purification and characterisation of nadh oxidase from thermus aquaticus yt1 and evidence that it functions in a peroxide-reduction system. *European Journal of Biochemistry* 251(3):935-945 (1998).

367. Torres, M. A., Dangl, J. L. and Jones, J. D. Arabidopsis gp91phox homologues atrbohd and atrbohf are required for accumulation of reactive oxygen intermediates in the plant defense response. *Proceedings of the National Academy of Sciences* 99(1):517-522 (2002).

368. Trivedi, P. and Wang, N. Characterization of salicylate hydroxylase of â candidatus liberibacter asiaticus-? and its role in plant defense suppression. In: *Phytopathology* pp. S127-S127. AMER PHYTOPATHOLOGICAL SOC 3340 PILOT KNOB ROAD, ST PAUL, MN 55121 USA, (2010).

369. Trivedi, P. and Wang, N. Modulation of plant defense responses by salicylate hydroxylase of a candidatus liberibacter asiaticus and its implication on canker pathogen

xanthomonas citri subsp. Citri in huanglongbing-infected plants. In: *Abstr.) Phytopathology* pp. S4, (2014).

370. Trujillo, M., Clippe, A., Manta, B., Ferrer-Sueta, G., Smeets, A., Declercq, J.-P., Knoops, B. and Radi, R. Pre-steady state kinetic characterization of human peroxiredoxin 5: Taking advantage of trp84 fluorescence increase upon oxidation. *Archives of biochemistry and biophysics* 467(1):95-106 (2007).

371. Trujillo, M., Ferrer-Sueta, G., Thomson, L., Flohe, L. and Radi, R. Kinetics of peroxiredoxins and their role in the decomposition of peroxynitrite. In: *Peroxiredoxin systems*ed.), pp. 83-113. Springer, (2007).

372. Tsai, C. H., Su, H. J., Liao, Y. C. and Hung, T. H. First report of the causal agent of huanglongbing (candidatus liberibacter asiaticus-) infecting kumquat in taiwan. *Plant Disease* 90(10):1360-1360 (2006).

373. Tsukuda, S., Gomi, K., Yamamoto, H. and Akimitsu, K. Characterization of cdnas encoding two distinct miraculin-like proteins and stress-related modulation of the corresponding mrnas in *citrus jambhiri* lush. *Plant molecular biology* 60(1):125-136 (2006).

374. Uziel, O., Borovok, I., Schreiber, R., Cohen, G. and Aharonowitz, Y. Transcriptional regulation of the staphylococcus aureus thioredoxin and thioredoxin reductase genes in response to oxygen and disulfide stress. *Journal of bacteriology* 186(2):326-334 (2004).

375. Vahling, C. M., Duan, Y. and Lin, H. Characterization of an atp translocase identified in the destructive plant pathogen "*Candidatus* liberibacter asiaticus". *Journal of bacteriology* 192(3):834-840 (2010).

376. Valko, M., Leibfritz, D., Moncol, J., Cronin, M. T., Mazur, M. and Telser, J. Free radicals and antioxidants in normal physiological functions and human disease. *The international journal of biochemistry & cell biology* 39(1):44-84 (2007).

377. Van Loon, L. C., Bakker, P. and Pieterse, C. M. J. Systemic resistance induced by rhizosphere bacteria. *Annual review of phytopathology* 36(1):453-483 (1998).

378. Van Wees, S. and Glazebrook, J. Loss of non-host resistance of arabidopsis nahg to pseudomonas syringae pv. Phaseolicola is due to degradation products of salicylic acid. *The Plant Journal* 33(4):733-742 (2003).

379. Varma, A., Ahlawat, Y. S., Chakraborty, N. K., Garnier, M. and Bove, J.-M. Detection of greening blo by electron microscopy, DNA hybridization in citrus leaves with and without mottle from various regions in india. In: *Proc 12th Conf IOCV, Riverside, California* pp. 280-285, (1993).

380. Vasudeva, R. S. and Capoor, S. P. Citrus decline in bombay states. *FAO Plant Protection Bulletin* 6:91 (1958).

381. Vera, L., Czarny, B., Georgiadis, D., Dive, V. and Stura, E. A. Practical use of glycerol in protein crystallization. *Crystal Growth & Design* 11(7):2755-2762 (2011).

382. Vergauwen, B., Pauwels, F., Jacquemotte, F., Meyer, T. E., Cusanovich, M. A., Bartsch, R. G. and Van Beeumen, J. J. Characterization of glutathione amide reductase from chromatium gracile identification of a novel thiol peroxidase (prx/grx) fueled by glutathione amide redox cycling. *Journal of Biological Chemistry* 276(24):20890-20897 (2001).

383. Vina, A. Improving the speed and accuracy of docking with a new scoring function, efficient optimization, and multithreading trott, oleg; olson, arthur j. *Journal of Computational Chemistry* 31(2):455-461 (2010).

384. Wakita, M., Masuda, S., Motohashi, K., Hisabori, T., Ohta, H. and Takamiya, K.-i. The significance of type ii and prxq peroxiredoxins for antioxidative stress response in the purple bacterium rhodobacter sphaeroides. *Journal of Biological Chemistry* 282(38):27792-27801 (2007).

385. Waksman, G., Krishna, T. S. R., Williams, C. H. and Kuriyan, J. Crystal structure of escherichia coli thioredoxin reductase refined at 2 å. Resolution: Implication for a large conformational change during catalysis. *Journal of molecular biology* 236(3):800-816 (1994).

386. Walter, A. J., Hall, D. G. and Duan, Y. P. Low incidence of'candidatus liberibacter asiaticus' in murraya paniculata and associated diaphorina citri. *Plant Disease* 96(6):827-832 (2012).

387. Wang, G., Hong, Y., Johnson, M. K. and Maier, R. J. Lipid peroxidation as a source of oxidative damage in helicobacter pylori: Protective roles of peroxiredoxins. *Biochimica et Biophysica Acta (BBA)-General Subjects* 1760(11):1596-1603 (2006).

388. Wang, G., Olczak, A. A., Walton, J. P. and Maier, R. J. Contribution of the helicobacter pylori thiol peroxidase bacterioferritin comigratory protein to oxidative stress resistance and host colonization. *Infection and immunity* 73(1):378-384 (2005).

389. Whitmore, L. and Wallace, B. A. Dichroweb, an online server for protein secondary structure analyses from circular dichroism spectroscopic data. *Nucleic acids research* 32(suppl 2):W668-W673 (2004).

390. Williams, C. H., Arscott, L. D., Muller, S., Lennon, B. W., Ludwig, M. L., Wang, P. F., Veine, D. M., Becker, K. and Schirmer, R. H. Thioredoxin reductase. *European Journal of Biochemistry* 267(20):6110-6117 (2000).

391. Wilson, T., de Lisle, G. W., Marcinkeviciene, J. A., Blanchardand, J. S. and Collins, D. M. Antisense rna to ahpc, an oxidative stress defence gene involved in isoniazid resistance, indicates that ahpc of mycobacterium bovis has virulence properties. *Microbiology* 144(10):2687-2695 (1998).

392. Wilson, T. M. and Collins, D. M. Ahpc, a gene involved in isoniazid resistance of the mycobacterium tuberculosis complex. *Molecular microbiology* 19(5):1025-1034 (1996).

393. Winn, M. D., Ballard, C. C., Cowtan, K. D., Dodson, E. J., Emsley, P., Evans, P. R., Keegan, R. M., Krissinel, E. B., Leslie, A. G. W. and McCoy, A. Overview of the ccp4 suite and current developments. *Acta Crystallographica Section D: Biological Crystallography* 67(4):235-242 (2011).

394. Winterbourn, C. C. Reconciling the chemistry and biology of reactive oxygen species. *Nature chemical biology* 4(5):278-286 (2008).

395. Witte, S., Villalba, M., Bi, K., Liu, Y., Isakov, N. and Altman, A. Inhibition of the c-jun n-terminal kinase/ap-1 and nf-κb pathways by picot, a novel protein kinase c-interacting protein with a thioredoxin homology domain. *Journal of Biological Chemistry* 275(3):1902-1909 (2000).

396. Wojtaszek, P. Nitric oxide in plants: To no or not to no. *Phytochemistry* 54(1):1-4 (2000).

397. Wong, C.-M., Chun, A. C. S., Kok, K. H., Zhou, Y., Fung, P. C. W., Kung, H.-F., Jeang, K.-T. and Jin, D.-Y. Characterization of human and mouse peroxiredoxin iv: Evidence for inhibition by prx-iv of epidermal growth factor-and p53-induced reactive oxygen species. *Antioxidants and Redox Signaling* 2(3):507-518 (2000).

398. Wonsey, D. R., Zeller, K. I. and Dang, C. V. The c-myc target gene prdx3 is required for mitochondrial homeostasis and neoplastic transformation. *Proceedings of the National Academy of Sciences* 99(10):6649-6654 (2002).

399. Wood, Z. A., Poole, L. B., Hantgan, R. R. and Karplus, P. A. Dimers to doughnuts: Redox-sensitive oligomerization of 2-cysteine peroxiredoxins. *Biochemistry* 41(17):5493-5504 (2002).

400. Wood, Z. A., Poole, L. B. and Karplus, P. A. Peroxiredoxin evolution and the regulation of hydrogen peroxide signaling. *Science* 300(5619):650-653 (2003).

401. Wood, Z. A., Schröder, E., Robin Harris, J. and Poole, L. B. Structure, mechanism and regulation of peroxiredoxins. *Trends in biochemical sciences* 28(1):32-40 (2003).

402. Wu, Y.-Z., Manevich, Y., Baldwin, J. L., Dodia, C., Yu, K., Feinstein, S. I. and Fisher, A. B. Interaction of surfactant protein a with peroxiredoxin 6 regulates phospholipase a2 activity. *Journal of Biological Chemistry* 281(11):7515-7525 (2006).

403. Xiudong, Y. and You-Jin, J. Antioxidant activity and cell protective effect of loliolide isolated from sargassum ringgoldianum subsp. Coreanum. *Algae* 26(2):201-208 (2011).

404. Yamasaki, H. The no world for plants: Achieving balance in an open system. *Plant, Cell & Environment* 28(1):78-84 (2005).

405. Yanagawa, T., Ishikawa, T., Ishii, T., Tabuchi, K., Iwasa, S., Bannai, S., Omura, K., Suzuki, H. and Yoshida, H. Peroxiredoxin i expression in human thyroid tumors. *Cancer letters* 145(1):127-132 (1999).

406. Yanagawa, T., Iwasa, S., Ishii, T., Tabuchi, K., Yusa, H., Onizawa, K., Omura, K., Harada, H., Suzuki, H. and Yoshida, H. Peroxiredoxin i expression in oral cancer: A potential new tumor marker. *Cancer letters* 156(1):27-35 (2000).

407. Yang, K.-S., Kang, S. W., Woo, H. A., Hwang, S. C., Chae, H. Z., Kim, K. and Rhee, S. G. Inactivation of human peroxiredoxin i during catalysis as the result of the oxidation of the catalytic site cysteine to cysteine-sulfinic acid. *Journal of Biological Chemistry* 277(41):38029-38036 (2002).

408. Yeo, W.-S., Lee, S. J., Lee, J. R. and Kim, K. P. Nitrosative protein tyrosine modifications: Biochemistry and functional significance. *BMB rep* 41(3):194-203 (2008).

409. Zhang, M., Guo, Y., Powell, C. A., Doud, M. S., Yang, C. and Duan, Y. Effective antibiotics against candidatus liberibacter asiaticus in hlb-affected citrus plants identified via the graft-based evaluation. *Plos One* 9(11):e111032 (2014).

410. Zhang, M., Powell, C. A., Zhou, L., He, Z., Stover, E. and Duan, Y. Chemical compounds effective against the citrus huanglongbing bacterium'candidatus liberibacter asiaticus' in planta. *Phytopathology* 101(9):1097-1103 (2011).

411. Zhao, W., Fan, G.-C., Zhang, Z.-G., Bandyopadhyay, A., Zhou, X. and Kranias, E. G. Protection of peroxiredoxin ii on oxidative stress-induced cardiomyocyte death and apoptosis. *Basic research in cardiology* 104(4):377-389 (2009).

412. Zhao, X. Y. Citrus yellow shoot disease (huanglongbing) in china-a review. In: *Proceedings of the international society of citriculture, November 9-12, 1981, Tokyo, Japan. Vol. 1*. pp. 466-469. International Society of Citriculture, (1982).

413. Zhong, L., Arner, E. S. J. and Holmgren, A. Structure and mechanism of mammalian thioredoxin reductase: The active site is a redox-active selenolthiol/selenenylsulfide formed from the conserved cysteine-selenocysteine sequence. *Proceedings of the National Academy of Sciences* 97(11):5854-5859 (2000).

414. Zhou, M., Diwu, Z., Panchuk-Voloshina, N. and Haugland, R. P. A stable nonfluorescent derivative of resorufin for the fluorometric determination of trace hydrogen peroxide: Applications in detecting the activity of phagocyte nadph oxidase and other oxidases. *Analytical biochemistry* 253(2):162-168 (1997).

415. Zhou, Y., Wan, X.-Y., Wang, H.-L., Yan, Z.-Y., De Hou, Y. and Jin, D.-Y. Bacterial scavengase p20 is structurally and functionally related to peroxiredoxins. *Biochemical and biophysical research communications* 233(3):848-852 (1997).

416. Zhu, D. W., Lorber, B., Sauter, C., Ng, J. D., Benas, P., Le Grimellec, C. and Giege, R. Growth kinetics, diffraction properties and effect of agarose on the stability of a novel crystal form of thermus thermophilus aspartyl-trna synthetase-1. *Acta Crystallographica Section D: Biological Crystallography* 57(4):552-558 (2001).

APPENDIX

CHARACTERIZATION AND CLONING OF AN 11S GLOBULIN WITH HEMAGGLUTINATION ACTIVITY FROM *MURRAYA PANICULATA*

A1 Introduction

Plant seed proteins play an important role in human and animal nutrition by providing the major share of dietary proteins and are categorised as storage, structural and biologically active proteins. Globulins are large globular proteins that constitute an indispensible part of the plant seed due to their ability to act as nutrient source for emerging embryos during seed germination [39]. The seed storage proteins of different species have been studied in detail from the turn of the century, when Osborne in 1924 classified them into four groups on the basis of their extraction and solubility characteristics: albumins, globulins, glutenins, and prolamins [34]. In addition to the role of globulins as seed storage proteins, they have been shown to have secondary activities such as protease inhibitor activity, insecticidal activity, chitin-binding [9] and lectin-like activity [21]. Globulins have also been implicated to play a defensive role in plant pathogenesis [33]. Many seed storage proteins have also been found to have regulatory roles for example amandin from almonds [1], 11S globulins from Amaranthus [40], dehydrin like protein from cauliflower, arabidopsis and lupin [40], basic 7S proteins from soybean [25] etc. A family of antimicrobial peptides is produced by processing of a 7S globulin protein in *Macadamia integrifolia* kernels [29]. Globulins belonging to the class 11S are the most prevalent forms and identified as the major food allergen [2]. Globulins are oligomeric proteins in which each subunit of the protein consists of a heavy, acidic (α) chain and a light , basic (β) chain, which are processed from a precursor peptide possessing a hydrophobic amino-terminal leader peptide that is absent in the mature protein. A single disulfide bond is formed between the linked A and B chain regions of the resulting proglobulin. The globulins are the most widely distributed group of storage proteins; they are present not only in dicots but also in monocots and fern spores [41]. They can be divided into two groups based on their sedimentation coefficients (S 20.w): the 7S vicilin-type globulins and the 11S legumin-type globulins. Both groups show considerable variation in their structures, which results partly from post-translational processing. In addition, both have nutritional significance in that they are deficient in cysteine and methionine, although 11S globulins generally contain slightly higher levels of these amino acids. Because of their abundance and economic importance, seed storage proteins were among the earliest of all

proteins to be characterized. The Cupin superfamily was identified by Dunwell [13] and has the most functionally diverse folding patterns described to date, comprising both enzymatic and nonenzymatic members. These include helix-turn-helix transcription factors, AraC type transcription factor, oxalate decarboxylase, auxin-binding protein, globulins, etc. Many proteins of this superfamily have functions and chemical properties with a great influence on plant physiology; like related oxalate oxidase is involved in pathogen activities and germin-like proteins, apoplastic, glycoproteins are remarkably protease resistant because of their cupin fold. According to [14, 15] the cupin domain comprises two conserved motifs, each corresponding to two β strands, separated by a less conserved region composed of another two β strands with an intervening variable loop. The characteristic conserved sequence in motif 1 and 2 is G(X)5 HXH (X)3,4 E(X)6 G and $P(X)_4H(X)_3N$ respectively where (X is any amino acid). These core β-strands in cupin family members are denoted as βC-βH, in analogy with the notation first used for viral capsid proteins and subsequently adapted for application to the jelly-roll β-barrels of phaseolin [28] and canavalin [23]. The identification of metal binding residues in cupin proteins was first accomplished with the structure of germin, a Mn^{2+} containing oxalate oxidase in plants. The Mn^{2+} in germin was coordinated in a tetrad with three histidine residues and one glutamate site [46]. The Cupin superfamily is very large with diverse functions like cupins are involved in enzymatic activities such as oxalate oxidase, decarboxylase, dioxygenases, etc. Also, lignin processing is highly dependent on oxidases and peroxidases (cupins). A related class of cupins is the auxin binding proteins, which do not show catalytic activity but work as signal transducers in plant cells.

Murraya paniculata is a tropical, evergreen plant, which is grown as an ornamental tree or hedge belongs to rutaceae family. Murraya bears small orange to red fruit resembling kumquats. The crude ethanolic extract of leaves of *Murraya paniculata* has antidiarrhoeal [38], antinceptive [36], *antioxidative* and anti-inflammatory activities. In many parts of Asia, the twigs are chewed and used as a natural toothbrush. The shrub's astringent qualities [17] have been used to treat bleeding wounds and dysentery, joint pain and body ache. *M. paniculata* is most preferable host of psyllids as confirmed by field observation and laboratory studies but yet not clear that whether it will serve as substitute host for Liberibacters [19, 43, 49]. Some reports [20] mentioned that it might be able to serve as reservoir host for CLAs. In present study, we report isolation; purification, characterization and gene cloning of globulin protein from *M. paniculata* seeds. The present study demonstrated that M. *paniculata* globulin (MPG) belongs to 11S globulin seed storage family and possesses a characteristic *bi-cupin* motif and a putative metal binding pocket.

A2 Materials and methods

A2.1 Materials

Buffers, acids or bases, and salts were purchased from Sigma-Aldrich Corporation, St. Louis, MO USA; BioRad Laboratories, Hercules, California, USA; Himedia Laboratories India Private Limited, Mumbai, India; Merck Limited, Worli, Mumbai, India. Hiload superdex 200 16/60 columns and HMW Calibration kit were obtained from GE Healthcare, AB Uppsala, Sweden. Amicon ultra concentrator, PVDF (Polyvinylidene Fluoride) membrane and millex syringe filters were from Millipore Corporation, Billerica, MA. Dialysis membrane with 3500 Da cutoff was from Pierce, Rockford, USA. Dry seeds of *M. paniculata* were obtained from IIT premises. The dry cotyledons were milled with a mortar and pestle.

A2.2 Purification of MPG

The mature, dry seeds of *M. paniculata*, were used for the purification of the protein. The seed extract obtained after soaking and grounding of mature seeds (20 g) overnight in 0.05M of Tris-HCl , was filtered and centrifuged for 30 min at 18000 × g. The clear supernatant obtained after centrifugation was subjected to pre-equilibrated (with 0.05M Tris, pH 8.0) affinity Cibacron Blue 3GA column (Sigma). The desired protein was eluted with a step gradient of NaCl in same buffer (0.1, 0.3, 0.5, and 1M). The desalted protein was concentrated to 10 mg/mL using 10kDa cutoff membrane (Amicon Ultra 15). The concentrated protein sample was gel-filtered on a pre-equilibrated HiLoad 16/60 Superdex 200 (GE Healthcare) with 0.05M Tris-HCl buffer, pH 8.0.The size-exclusion column was calibrated with gel filtration HMW calibration kit containing thyroglobulin, (669 kDa), ferritin (440 kDa), aldolase (158 kDa), conalbumin (75 kDa) and ovalbumin (44 kDa) for construction of the standard curve and estimation of molecular weight of the purified protein. Protein concentration was estimated by standard dye-binding method using bovine serum albumin as standard [3].

A2.3 Native and SDS-PAGE analysis of MPG

SDS-PAGE analysis of MPG was performed according to Laemmli [26] under reducing and non-reducing conditions. The relative molecular mass of MPG was estimated from a 12% SDS-PAGE. The purified MPG was analysed for subunit composition on SDS and native-PAGE in various conditions. In SDS-PAGE, the heated and non heated protein samples were analysed using sample buffer having both SDS and βME, only SDS, only βME and neither SDS nor βME. On native PAGE, heated and non heated protein samples were analysed

where sample buffer contained both SDS and βME ,only SDS, only βME and neither SDS nor βME. The heat treatment at 95 °C for 5 min has been given to MPG.

A2.4 Amino acid sequencing of MPG

The N-terminal amino acid sequencing of acidic and basic subunits of MPG was performed by Edman degradation on an automated protein sequencer (model PROCISE 491 cLCs) at the protein sequencing facility of IMTECH Chandigarh, INDIA.

For internal sequencing, the Coomassie blue-stained protein bands were excised from the corresponding SDS polyacrylamide gels and destained with methanol: acetic acid solution without the dye for approximately 6 h, changing destaining solution 3-4 times. Mass spectrometric analysis of the purified protein was performed on 4800 plus MALDI TOF/TOF mass spectrometer (Applied Biosystems/MDS SCIEX) at NBRI Lucknow, INDIA. Peptides, fragmented to generate MS/MS spectra were used for protein identification through MASCOT search and *de novo* sequencing of the peptides. Sample preparation protocol for protein identification through MS/MS was followed as reported [42].

A2.5 Chemical modification of trypsin digested protein by SPITC for De novo sequence

When a protein is novel or having some amino acid variation in protein sequence of known proteins than sequencing of the protein is only method to identify the sequence of peptides. Unidentified protein band was chemically modified at its N-terminal by SPITC derivatization and processed for mass spectrometric analysis. A solid phase derivatization method of tryptic peptides was used to prepare N-terminus sulphonated peptides. C18 µZipTip (Millipore) was used as solid support and was equilibrated with 50% acetonitrile containing 1% TFA by slow aspiration and de-aspiration cycles. It was further equilibrated with 0.1% TFA. The finally equilibrated tips were used to bind the peptides (dissolved in same solution 0.1% TFA) with a minimum of 15 cycles and washed with deionised autoclaved water. Further, bound peptides were treated with 4-Sulfophenyl isothiocyanate (2.55 mg/ml in 50 mM Tris-HCL buffer, pH 8.2) by carefully aspiration of the solution so that the presence of air bubbles in between of solution and peptides are avoided. Filled ZipTip is ejected in to a 1.5 ml eppendorf tube containing 50µl of the same SPITC solution. Tube was caped and kept at 50ºC for 2 hour. ZipTip was again washed with 0.1% TFA and eluted in 20 µl of 80% ACN containing 0.5% TFA. Eluted sample was lyophilised completely, re-suspended in 5µl of 50% ACN containing 0.5% TFA solution and analyzed on MALDI platform following . DOI: 10.1002/rcm.1280.

A2.6 Hemagglutination assay

The hemagglutination activity (H.U.) of purified protein MPG and its basic subunit alone was tested against human erythrocytes by standard serial dilution technique in a multi-well Microtiter plate as described earlier [27] with little modification. Blood samples (1 mL volume) of different blood types (A, B, O) were taken in centrifuge tubes containing 6 % EDTA as anticoagulant in 3 mL of phosphate buffer saline (PBS), pH 7.2. The mixture was then centrifuged at 1000 × g for 5 min at 4 °C. Supernatant was discarded and the cell pellet was diluted and resuspended in 10 mL of PBS buffer. Dilution and centrifugation steps were repeated until the supernatant was clear. Finally, erythrocytes were resuspended in PBS buffer to make a 3 % (v/v) blood suspension. Then, 50 µL of 3 % suspension of human red blood cells were treated with 50 µL of (between 10 µg mL^{-1} and 100 µg mL^{-1}) protein sample. The agglutination reaction was assessed after 1 h incubation at 37 °C. BSA was used as a negative control for the assay. Erythrocytes Cells were finally observed under 277 fluorescent microscope (Axiovert 25; Zeiss, Germany) using 20X magnification.

A2.7 Far-UV CD and intrinsic fluorescence studies

For analysis of secondary structure content, purified MPG dissolved in 0.02M potassium phosphate buffer, pH 8 was subjected to CD using Chirascan™ CD Spectrometer (Applied Photophysics,UK) [31, 48]. To record spectra, 0.2 mg/mL protein was used in 1 mm quartz cell under constant nitrogen purge. CD spectra was collected between 190 to 240 nm in 0.1 nm wavelength steps at an average time of 3.0 s at 25 °C .Three data sets were recorded and then average CD spectra were used for analysis. The CD data were expressed in terms of mean residue ellipticity. The data obtained was analyzed using the web based DichroWeb software [45] and the neuronal network program CDSSTR. Effect of temperature (20 °C to 100 °C) on the secondary structure content of MPG was examined. Effect of pH was also analyzed by incubation of purified MPG with different buffers (pH 2–3, glycine-HCl; pH 4–5, sodium acetate; pH 6–8, phosphate; pH 9, borate and pH 10–11, Glycine-NaOH) at 25°C followed by the far-UV CD measurements.

For studying the unfolding of native protein and effect of various chemical denaturants, fluorescence studies were carried out using urea, guanidine hydrochloride (GuHCl), SDS and dithiothreitol (DTT). Purified protein (50 µg/mL) in 0.02M phosphate buffer, pH 8.0 filtered through 0.45 µm Millex syringe filter was used. Protein was excited at 280 nm and emission

wavelength spectra were recorded at 290–400 nm using Fluorolog®-3 spectrofluorometer Jobin Yvon Inc (USA) at constant temperature (25 °C). Emission slits were at 5 nm and quartz cuvette of 1 cm path length was used. Fluorescence measurements were also performed to study the effect of pH on MPG. The protein samples were incubated overnight with urea (0.05 to 5M) or GuHCl (0.05 to 5M), 2 h with DTT (0.001 to 0.01M) and 2 h in the pH range from 2 to 11 at room temperature.

A2.8 Cloning and bioinformatic analysis of MPG

Total RNA was extracted from the mature leaves of plant and reverse transcribed for cDNA synthesis. The reaction was carried out in two steps: cDNA synthesis and PCR amplification. First amplification was done with forward primer designed on the basis of the signal sequence of citrin, as obtained *de-novo* sequence of purified MPG through mascot search showed higher similarity to that of citrin protein, and poly A-tail as the reverse primer without any success in getting desired results. Therefore, the reverse primer was designed from the internal sequence, obtained after *de novo* sequencing, towards the carboxy-terminal of the protein. Thus, signal sequence of citrin and N-terminal sequences of the 21 kDa basic subunit were used for designing of forward primers and a *de novo* sequence towards the C-terminal end was used as reverse primer. The nucleotide sequences of forward and reverse primers respectively, are: (1) MPF 5’- ATGGCTTCTTCTTCTTTGCTCTG -3'-23bp, (2) MP21F 5’-GCTTCGAGGAAACTATCTGTACAATGAA-3’-28bp, (3) REVMP 5'-TTGAATGATATCCACTCC -3' -18bp. The amplified product was cloned in to a pGEMT-easy vector.

Deduced amino acid sequence of cloned MPG was used as an input for BLAST search to retrieve the homologous sequences from NCBI database (http://www.ncbi.nlm.nih.gov/). Sequence search was made against the ‘nr’ database. Multiple sequence alignment of these sequences was done with the Clustalw program using the default parameters. For phylogenetic tree genration, sequences were submitted in the *Phylogeny.fr* online server (http://www.phylogeny.fr) which aligns the sequences with Muscle (v3.7) to the highest accuracy. Gblock (v0.91b) algorithm implemented in server further removes the ambiguous region in the alignment [11]. Finally, the phylogenetic tree was reconstructed by Phylum program (v3.0 a LRT) using the maximum likelihood method. Next the sequence after removing signal sequence was submitted to mGenThreader (http://bioinf.cs.ucl.ac.uk/psipred/) for the fold recognition. Both PSI-BLAST and mGenThreader returned hits with the x-ray structure of 11s globulin protein pdb id: 2E9QA,

3QAC, 2EVX, 3KGL, 3KSC having similarity of almost 40-50%. From the cloned sequence, model has been generated using **Phyre2** (**P**rotein **H**omology/AnalogY **R**ecognition **Engine)** server [22]. Homology models of MPG were generated by comparative modeling method implemented in program MODBASE [35]. MODBASE server uses input sequence alignment with related template structure, and generates a refined 3-dimensional homology model of the query sequence. The best model of MPG was selected on the basis of the lowest DOPE score. Stereochemistry of the selected model was checked by SAVES (http://nihserver.mbi.ucla.edu/SAVES/). Steric clash in structure/models, characterized by unphysical overlap of the newly positioned side-chain atoms with other side-chain and backbone atoms, is one of the prevalent artifacts in homology modeling. These steric clashes were further removed by energy-minimization of the homology models on Swiss PDBViewer (SPDBV) version4.1 that uses Gromos96 force field to compute energy and execute energy minimization. This energy-minimized model was further validated by SAVES.

A3 Results

A3.1 Purification and amino acid sequencing of MPG

The purification of MPG was accomplished in two steps using affinity and size-exclusion chromatography. The protein was bound onto the affinity column and was eluted with a salt (NaCl) gradient. Almost pure protein was eluted at 0.1 M NaCl. It was further purified on a gel filtration column and the target protein eluted in a major peak at an elution volume of 60 mL in 0.05M Tris- HCl buffer, pH 8. The relative molecular mass and purity of MPG was analysed on a 12% SDS-PAGE under reducing condition. The SDS-PAGE analysis revealed the hetrodimeric nature of MPG with apparent molecular mass of two major subunits found to be ~35 kDa and ~21 kDa referred as higher acidic (α) and lower basic (β) subunits respectively (Fig. A1, A).

The oligomerization state of MPG was analyzed on a gel filtration column. The analysis on gel filtration column showed that elution volume for MPG corresponded to ~150 kDa when compared with gel filtration molecular weight standards (Fig. A1, B) which implicates it to be exists in a trimeric form. Fractions of the major peak containing pure protein were pooled and concentrated to about 20 mg mL^{-1}.

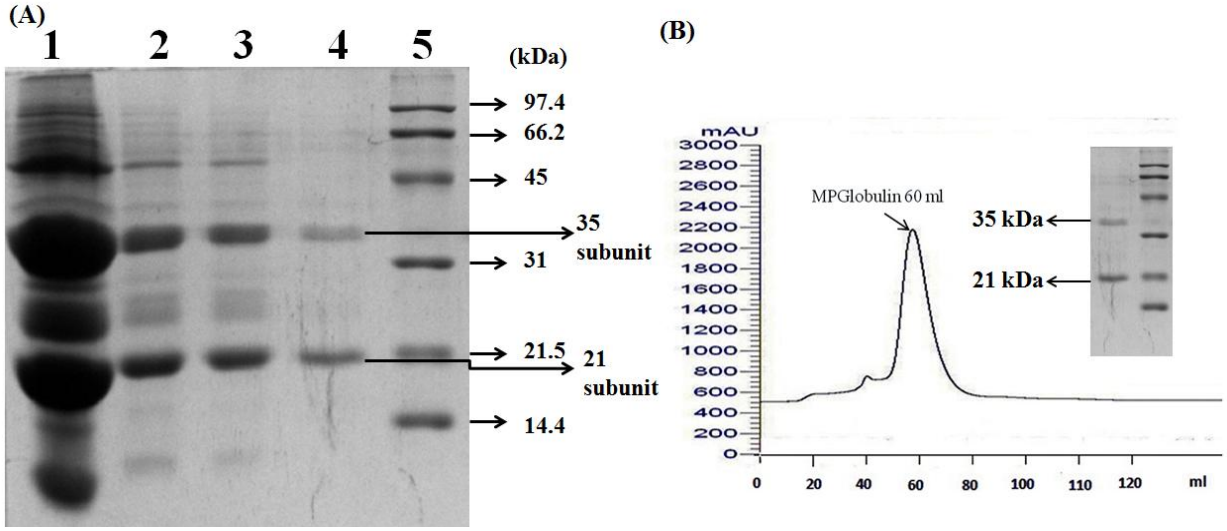

Figure A1. The purification and PAGE analysis of MPG. A) A 12% reducing SDS-PAGE analysis of purification on Cibacron Blue 3GA affinity column: Lane 1, crude extract after extraction from seeds; Lane 2, flow through (FT) from column ; Lane 3, wash fraction ; Lane 4, 0.1M NaCl eluted fraction; Lane 5, molecular weight marker. B) Size-exclusion chromatography profile, where major peak corresponds to ~150kDa.

The estimated yield of purified MPG protein was about 6mg.g^{-1} of seeds (data not shown). Interestingly, it was observed that the acidic subunit (α) in the heterodimer degrades after one week (data not shown) despite using protease inhibitor cocktail whereas the 21 kDa basic subunit is very stable. There is no report of degradation of acidic subunit in literature, however, in vivo as well as in vitro limited proteolysis produces several high-molecular-mass fragments from both the 7S and 11S globulin subunits [16] and [27] have been reported.

Attempts to separate and purify two subunits under native and denaturing conditions did not succeed except in the presence of both SDS and βME under denaturing conditions. The purified MPG was analysed on native and 12% SDS-PAGE in various conditions. The heated and non heated protein samples were analysed using sample buffer having only SDS, only βME, both SDS and βME and no SDS or βME. In SDS-PAGE, the addition of both βME and SDS in sample buffer led to the complete dissociation of MPG into polypeptides of ~35 kDa and ~21 kDa (lane 2-3) (Fig. A1, C). Under non-reducing conditions (in presence of SDS but no βME (lane 4-5); in absence of both βME and SDS (lane 8-9) in sample buffer, a major band of ~56 kDa with minor bands at ~42 kDa and ~35 kDa were observed. In case of reducing condition without SDS in sample buffer (lane 6-7), an increase in intensity for bands corresponding to the two subunits 35 kDa and 21 kDa was observed with slight decreased intensities of the 56 kDa and 42 kDa bands.

In native PAGE, heated and non heated protein samples were analyzed where sample buffer contained no SDS or βME, only βME, only SDS, and both SDS and βME. In case of native PAGE, only one band was observed in the absence of βME and SDS (lane 1-2) and even in the presence of βME but without SDS (lane 3-4). However MPG tends to get apart in the presence of SDS (lane 5-6) and SDS and βME (lane 7-8) (Fig. A1, D).

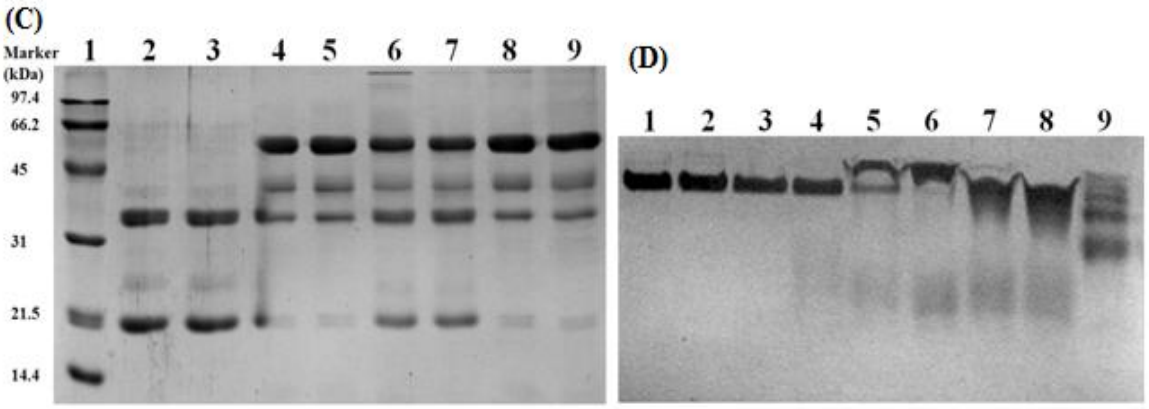

Figure A1. C) A 12% SDS-PAGE profile in different conditions: Lane 1, molecular weight marker; Lane 2-3, non heated and heated purified protein respectively in the presence of reducing agent and SDS; Lane 4-5, non heated and heated purified protein respectively in the absence of βME but with SDS; Lane 6-7, non heated and heated purified protein respectively in the presence of reducing agent βME but no SDS; Lane 8-9, non heated and heated purified protein respectively in the absence of both reducing agent and SDS. D) Native-PAGE analysis of MPG: Lane 1-2, non heated and heated purified protein respectively in the absence of both reducing agent and SDS; Lane 3-4, non heated and heated purified protein respectively in the presence of reducing agent only; Lane 5-6, non heated and heated purified protein respectively in the presence of SDS only; Lane 7-8, non heated and heated purified protein respectively in the presence of reducing agent and SDS.

Purified MPG was electro blotted onto PVDF membrane from reducing SDS-PAGE gel and N-terminal sequence of the globulin was determined. The N-terminal sequence determined for acidic subunit was ITREEE/RQQXQQ and for basic subunit was GIEETLXTM/TM/KL. The partial internal sequencing using mass spectrometry was performed. *De novo* amino acid sequence of internal peptide of the subunits constituting MPG was obtained (KEL/ITVFTPGAR and AFNVNVI/LVI/LQR) after chemical modification of the peptide (Fig A2, A). Mascot search was performed against obtained internal sequence and the results (Fig A2, B) showed higher similarity to that of Citrin, an 11S seed storage protein.

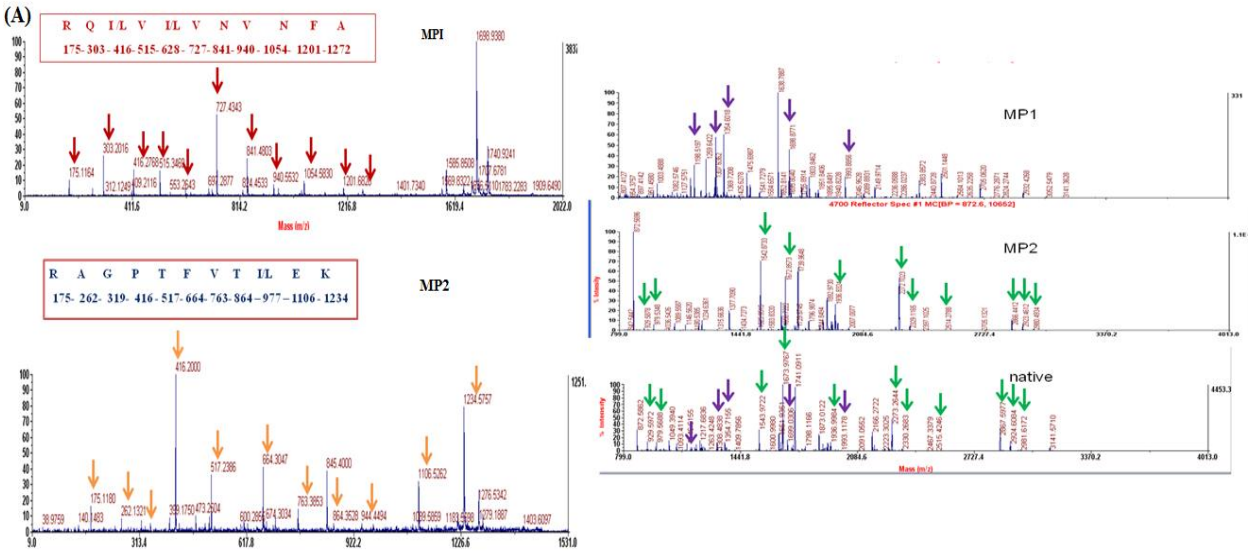

(B)

gi|1061408 **Mass:** 55426 **Score:** 247 **Matches:** 5(1) **Sequences:** 5(1)

citrin [Citrus sinensis]

Check to include this hit in error tolerant search

Query	Observed	Mr(expt)	Mr(calc)	Delta	Miss	Score	Expect	Rank	Unique	Peptide
11	1377.7097	1376.7024	1376.7201	-0.0176	1	27	1.6e+02	1	U	R.AGNRGLEWISFK.T
14	1542.8732	1541.8659	1541.9042	-0.0383	1	40	7.6	1	U	R.VTTVNRFNLPILR.D
22	1672.8578	1671.8505	1671.8944	-0.0439	0	56	0.21	1	U	R.GLPLDVIQNSFQVSR.D
25	1739.9650	1738.9577	1739.0094	-0.0517	1	80	0.00067	1	U	R.EGQLIVVPQGFAVVKR.A
39	1935.8381	1934.8308	1934.9156	-0.0848	0	46	1.5	1	U	R.MQIVAENGENVFDGQIR.E + Oxidation (M)

Figure A2 (A) Mass spectra showing peaks of both reduced subunit as well showed the similar peaks in native form of protein suggesting that it synthesized as a precursor protein then proteolytically cleaved after disulfide bond formation.(B) Mascot search showed higher similarity to that of Citrin from *citrin sinensis*.

A3.2 Hemagglutination Activity of MPG

Hemagglutination activity was detected in seed extracts of *M. paniculata* and it was measured on purified MPG and stable basic subunit using human erythrocytes from three blood groups (A, B, O). Purified MPG protein and its basic subunit as well showed lattice formation of the erythrocytes of all the blood groups (Fig. A3). Absence of such activity for BSA used as a negative control confirmed that MPG was indeed responsible for the hemagglutination activity.

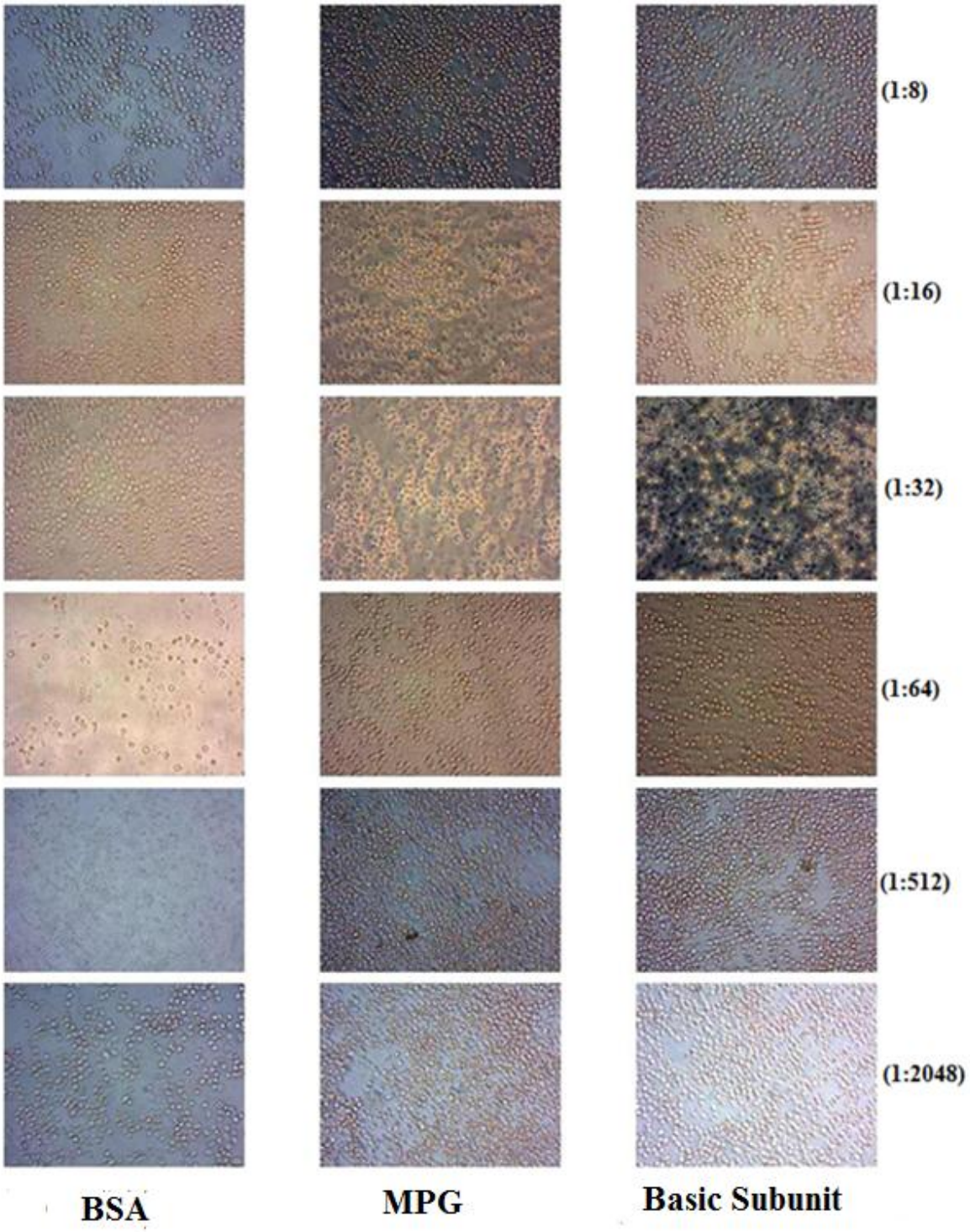

Figure A3. Hemagglutination Activity of MPG. Purified protein containing both subunits and only basic subunit with maximum dilution showed lattice formation of the erythrocytes of all the blood group. BSA is taken as a negative control. Right panel showed dilution used for experiment.

A3.3 Far-UV CD and intrinsic fluorescence studies

Far-UV (190-240nm) CD spectroscopy studies were performed for secondary structure analysis and conformational stability of protein at different temperature and pH (Fig. A4, A). CD spectra of native protein showed maximal negative mean residual ellipticities [θ] near 210 nm characteristic for 11S globulin proteins. CDSSTR yielded a structural content of 27 % β sheets and 18 % α helix with an equal percentage of β turns and random coil. Nevertheless, an increase in β sheets (31 %) and α helix (27 %) was noted at higher temperatures showing subtle conformational changes (Fig. A4,A). The CD spectra of MPG revealed a predominance of α helical structure (31 %) as compared to β sheets (25 %) at higher pH with no considerable change in β turns and random coils (Fig. A4, B).

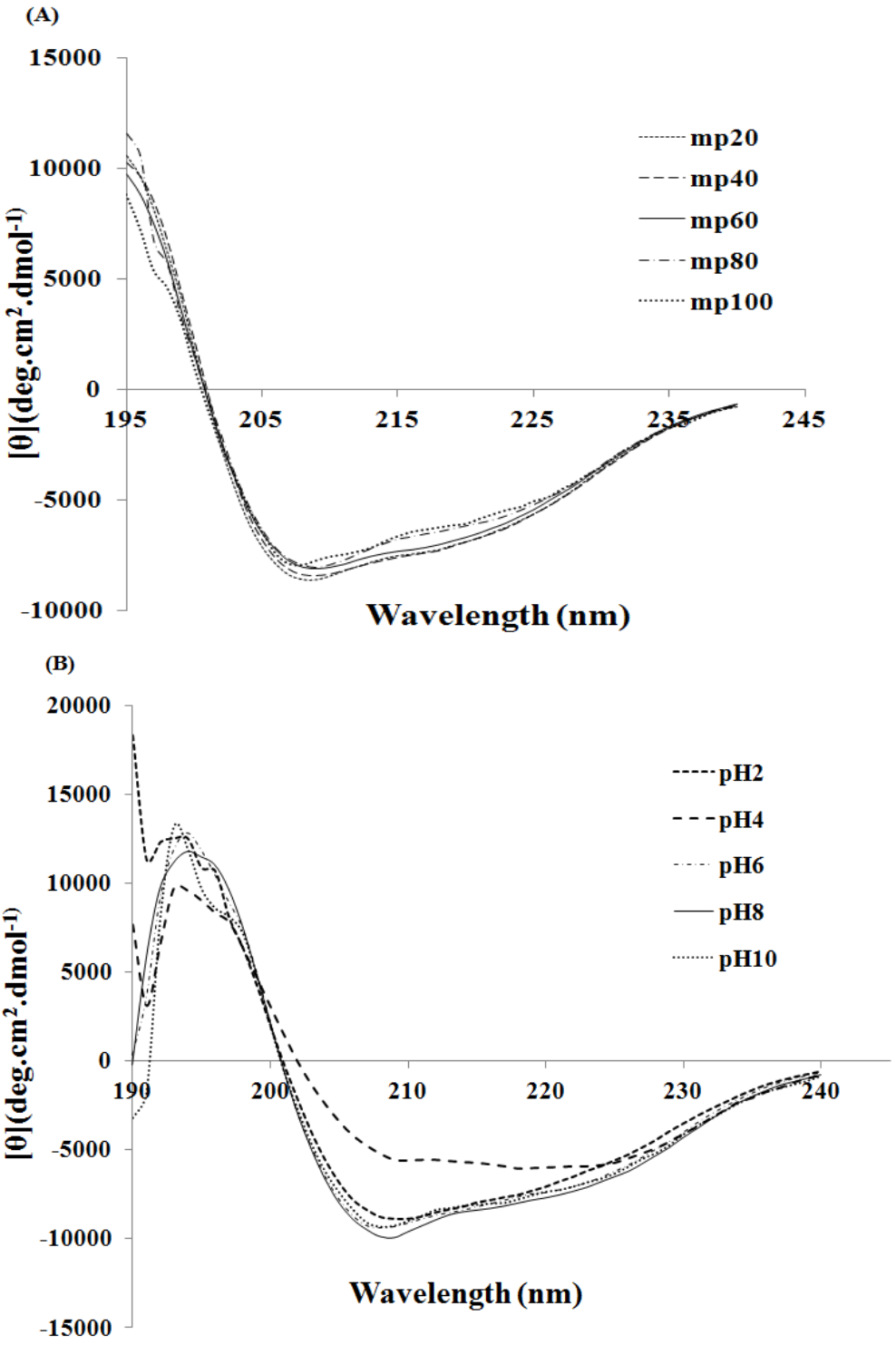

Figure A4. Far UV CD analysis of MPG. A) CD spectra of the protein at concentrations of 0.2 mg/mL, in 20 mM potassium phosphate buffer, pH 8.0 at different temperatures. B) CD spectra of MPG in different pH conditions.

The conformational stability of MPG in different conditions was examined by fluorescence measurements. Fluorescence emission spectra of native MPG protein showed emission λmax was 330 nm. The behaviour of MPG at different pH indicated that the protein is

conformationally stable in the pH range of 5 to 10 (Fig A5, A). The spectra at lower pH showed distinct decrease in the fluorescence emission intensity and redshift (15 nm at pH 2) was observed. However, there was no significant change in respect to intensity and shift in wavelength observed in the presence of NaCl up to IM (Fig A5, B).

The effect of reducing agents DTT and βME were carried out at different concentrations. A small shift of 10 nm from that of native protein was observed in 0.01M DTT. A decrease in the fluorescence emission intensity with increasing DTT concentration was observed (Fig A5, C). A slight decrease in fluorescence intensity at λmax for MPG was observed in case of βME (Fig A5, D). It appears that although *β*ME treatment may potentially break disulfide bonds in 11S, overall conformational structure of 11S is not significantly altered because of involvement of noncovalent interactions (hydrophobic interactions and salt bridges) in stabilizing the protein. However, the progressive decrease of fluorescence intensity which is consistent with unfolding was more intensive with SDS even at lower concentration (10 mM) (Fig A5, E).

To study the conformational unfolding of the native protein, protein denaturant such as guanidinium chloride (GuHCl) and urea were used. A red shift was observed and the λ_{max} of protein in 5M GuHCl and urea was 355nm and 360 nm respectively (Fig A5, F, G), is a characteristic of fully exposed tryptophan residues in presence of denaturants. There was an abrupt but significant increase in fluorescence intensity at λ_{max} was observed even at lower concentration of urea It could be due to the existence of folding intermediate(s) of 11S (Fig A5, G). The percentage of protein denaturation (% *D*) was determined by eq 1: (%*D*) = (I_0 - I_1)/ (I_0) ×100. In eq 1, *I*o and *I*1 are the fluorescence intensities of native and denatured protein, respectively. The % *D* was measured after incubation of globulins with a denaturant for overnight (A1.Table1).

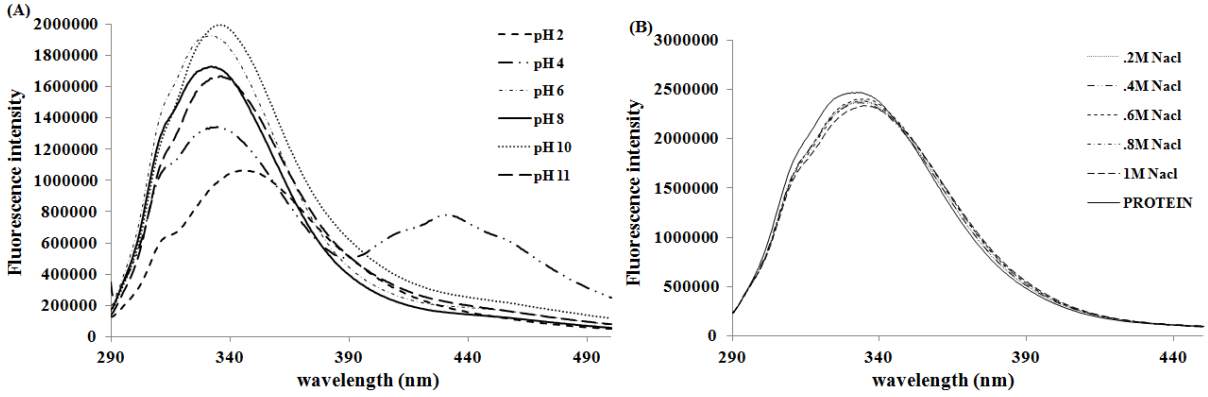

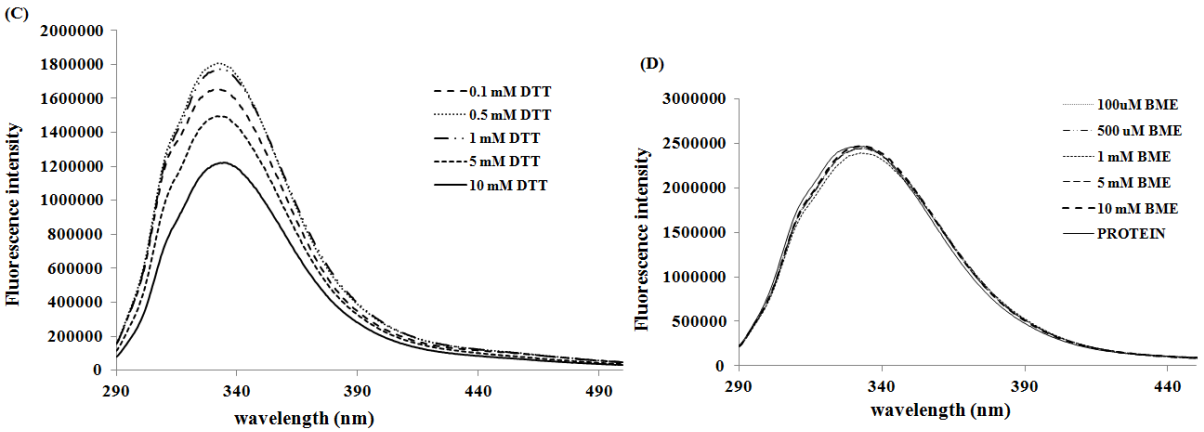
(C)
Fluorescence intensity
wavelength (nm)
0.1 mM DTT
0.5 mM DTT
1 mM DTT
5 mM DTT
10 mM DTT
(D)
Fluorescence intensity
wavelength (nm)
100uM BME
500 uM BME
1 mM BME
5 mM BME
10 mM BME
PROTEIN

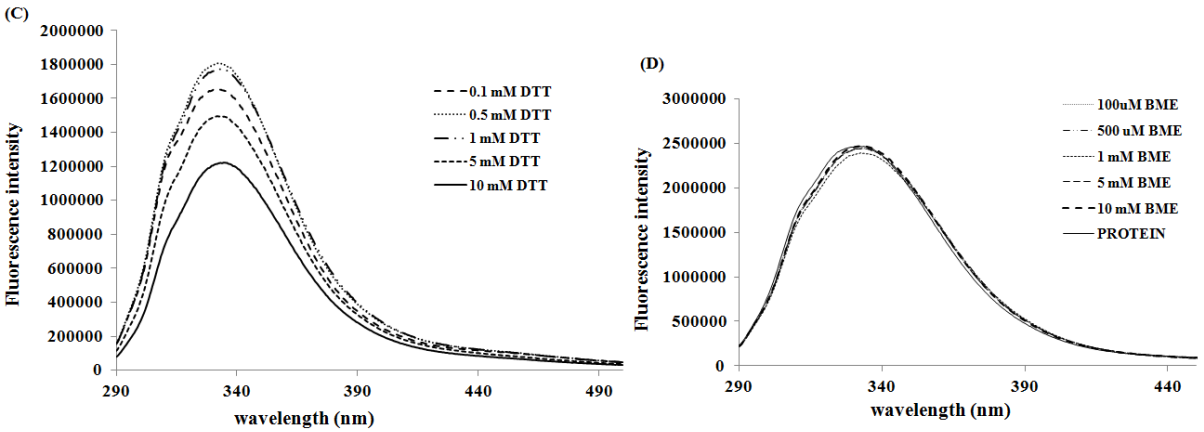
(C)
Fluorescence intensity
wavelength (nm)
0.1 mM DTT
0.5 mM DTT
1 mM DTT
5 mM DTT
10 mM DTT
(D)
Fluorescence intensity
wavelength (nm)
100uM BME
500 uM BME
1 mM BME
5 mM BME
10 mM BME
PROTEIN

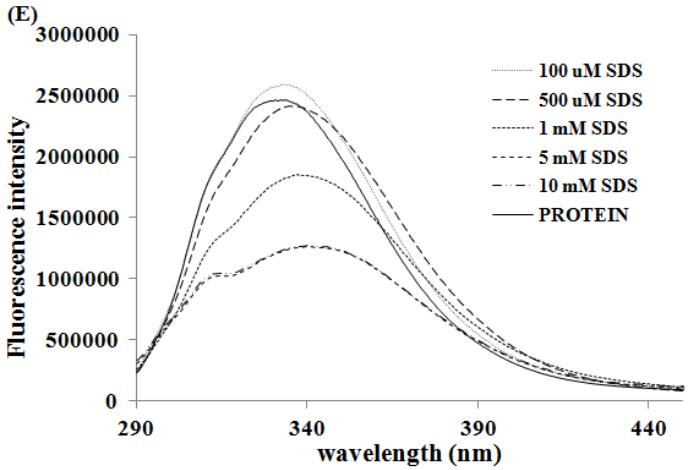
(E)
Fluorescence intensity
wavelength (nm)
100 uM SDS
500 uM SDS
1 mM SDS
5 mM SDS
10 mM SDS
PROTEIN

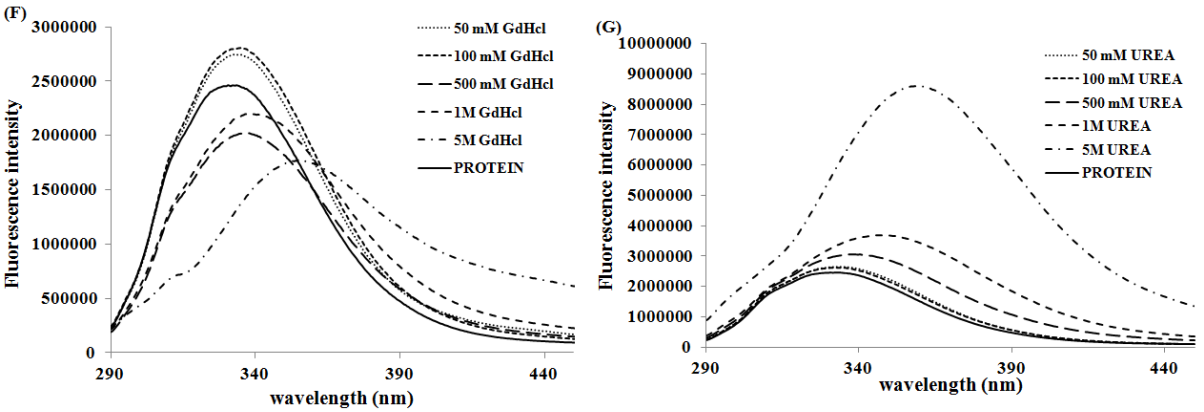
(F)
Fluorescence intensity
wavelength (nm)
50 mM GdHcl
100 mM GdHcl
500 mM GdHcl
1M GdHcl
5M GdHcl
PROTEIN
(G)
Fluorescence intensity
wavelength (nm)
50 mM UREA
100 mM UREA
500 mM UREA
1M UREA
5M UREA
PROTEIN

Figure A5. Fluorescence emission spectra of the purified protein (50µg/mL) in 20 mM phosphate buffer, pH 8.0 under native and denatured conditions. (A) Effect of pH on the intrinsic fluorescence of MPGlobulin. (B) Spectra in the absence and in the presence of increasing concentration of NaCl. (C), (D) Fluorescence spectra in the absence and in the presence of increasing concentration of DTT and βME respectively. (E) Fluorescence spectra in the absence and in the presence of increasing concentration of SDS. (F), (G) Fluorescence spectra in the absence and in the presence of increasing concentration of GuHCl and Urea respectively.

Table A1. Fluorescence Properties of MPGlobulin native protein

Denaturant	**Conc.of denaturant, M**	**%D**	**Shift, nm**
SDS	10×10^{-3}	49.4%	340
GdHcl	5	46.7%	355

Emission spectrum of native globulin has maximum at 333nm.

A3.3 Cloning and sequence analysis of MPG gene

The cDNA synthesis was accomplished using total RNA isolated from leaves of plant. Although globulin predominance in seeds is easily recognized, there is an aspect of these proteins in mature leaves as well [30]. The MPG gene was cloned in TA cloning vector (pGEMT-Easy) and sequenced. The 1425 bp long amplification product includes signal sequence and mature protein with sequence for ~22 amino acids at the C - terminal of 21 kDa basic subunit missing (Fig. A6, A). The partial gene sequence has been submitted to the NCBI gene bank database with accession no. **KJ508183**.

```
atggcgagcagcagcctgctgtgctttggcctgtgctttctggtgctgtttaacgcgtgc
 M  A  S  S  S  L  L  C  F  G  L  C  F  L  V  L  F  N  A  C
tttgcgcagattgaacaggtgaccggcattacccgcgaagaacgccagcagcgccagcag
 F  A  Q  I  E  Q  V  T  G ➡I  T  R  E  E  R  Q  Q  R  Q  Q
cgccagcgctttcagacccagtgcaactttcagaacctgaacgcgctggaaccgcagcag
 R  Q  R  F  Q  T  Q  C  N  F  Q  N  L  N  A  L  E  P  Q  Q
aaagtggaaagcgaagcgggcgtgaccgaattttgggatcagaacaacgaacagctgcag
 K  V  E  S  E  A  G  V  T  E  F  W  D  Q  N  N  E  Q  L  Q
tgcgcgaacgtggcggtgtttcgccatcgcattcagcagcgcggcctgctggtgccggcg
 C  A  N  V  A  V  F  R  H  R  I  Q  Q  R  G  L  L  V  P  A
tataccaacaccccggaaatttttatgtggtgcagggcagcggcattcatggcgcggtg
 Y  T  N  T  P  E  I  F  Y  V  V  Q  G  S  G  I  H  G  A  V
```

```
tttccgggctgcgcggaaacctatcaggatagccagcagcagagctttcagggcagc
 F  P  G  C  A  E  T  Y  Q  D  S  Q  Q  Q  Q  S  F  Q  G  S
cgcagccaggatcagcatcagaaagtgcgccagctgcgcgaaggcgatattattgcgctg
 R  S  Q  D  Q  H  Q  K  V  R  Q  L  R  E  G  D  I  I  A  L
ccggcgggcgcggcgcattggatttataacaacggccgcgatcagctggtgctggtggcg
 P  A  G  A  A  H  W  I  Y  N  N  G  R  D  Q  L  V  L  V  A
ctggtggatgtgggcaacagccagaaccagctggatcagtattttcgcaaattttatctg
 L  V  D  V  G  N  S  Q  N  Q  L  D  Q  Y  F  R  K  F  Y  L
ggcggcaacccgcagccggaactgcagggctatagccagagccagggcagccgcgatcag
 G  G  N  P  Q  P  E  L  Q  G  Y  S  Q  S  Q  G  S  R  D  Q
ggcagccagggcagcgaaggcggcgatcgcagccgccgcggcggcaacatttttagcggc
 G  S  Q  G  S  E  G  G  D  R  S  R  R  G  G  N  I  F  S  G
tttgatgaacgcctgctggcggaagcgtttaacgtgaacccggatgtgattaaacgcctg
 F  D  E  R  L  L  A  E  A  F  N  V  N  P  D  V  I  K  R  L
cagagcccgcagatgcagcgcggcattattgtgcgcgtggaagaagaactgcgcgtgctg
 Q  S  P  Q  M  Q  R  G  I  I  V  R  V  E  E  E  L  R  V  L
agcccgcagcgcggcggcgaacaggaagaagaatttcagggcaaagaaaccatggcgagc
 S  P  Q  R  G  G  E  Q  E  E  E  F  Q  G  K  E  T  M  A  S
cgcaaactgagcgtgcagggcgataacggcattgaagaaaccctgtgcaccatgaaactg
 R  K  L  S  V  Q  G  D  N ➡G  I  E  E  T  L  C  T  M  K  L
aaacagaacattaacgatccgagcgcggcggatgtgtataacccgcgcgcgggccgcgtg
 K  Q  N  I  N  D  P  S  A  A  D  V  Y  N  P  R  A  G  R  V
accaccgtgaaccgctttaacctgccgattctgcgctatctgcagctgagcgcggaaaaa
 T  T  V  N  R  F  N  L  P  I  L  R  Y  L  Q  L  S  A  E  K
ggcaacctgtatcagaacgcgctgaccgcgccgcattggaacctgaacgcgcatagcatt
 G  N  L  Y  Q  N  A  L  T  A  P  H  W  N  L  N  A  H  S  I
gtgtatattacccgcggcaacggccgcatgcagattgtggcggaaaacggcgaaaacgtg
 V  Y  I  T  R  G  N  G  R  M  Q  I  V  A  E  N  G  E  N  V
tttgatggccagattcgcgaaggccagctgattgtggtgccgcagggctttgcggtggtg
 F  D  G  Q  I  R  E  G  Q  L  I  V  V  P  Q  G  F  A  V  V
aaacgcgcgggcaaccgcggcctggaatggattagctttaaaaccaacgatgtggcgatg
 K  R  A  G  N  R  G  L  E  W  I  S  F  K  T  N  D  V  A  M
accagccagctggcgggccgcgcgagcgtgattcgcggcctgccgctggatgtgattcag
 T  S  Q  L  A  G  R  A  S  V  I  R  G  L  P  L  D  V  I  Q
aacagctttcaggtgagccgcgaagcgagcagcagcgcggtgtaa
 N  S  F  Q  V  S  R  E  A  S  S  S  A  V  -
```

Figure A6. A) Nucleotide and deduced amino acid sequence of MPG. The 474 amino acid sequences include signal sequence (underlined) and mature protein with ~22 amino acids missing at C-terminus. Arrow indicates the N - terminal sequence of acidic and basic subunits. Cys residues are underlined. Apart from the single Cys residue in the ~21-kDa peptide, an additional six are indicated in the 35-kDa peptide.

The N-terminal and internal sequencing results were supported from the partial gene sequence. The results confirmed that MPG belongs to the 11S seed storage family proteins. The analysis on "nr BLAST" of NCBI showed that all the sequences belonging to the 11S seed storage globulins possess *bi-Cupin* conserved domain, a characteristic feature of cupin-2 superfamily of 11S seed storage globulins (data not shown). Phylogenetic analysis revealed that MPG is more closely related to citrin 11S globulin from *Citrus sinensis cultivar valencia* which also belong to *the Rutaceae family* (Fig. A6). Secondary structure analysis using Multiple sequence alignment with known globulin crystal structures further enhanced by esprit 3.0 [37] (Fig. A6, B) showed conserved cupin motif region. The predicted MPG model from Phyre2, after energy minimization from SAVES server, has been shown to have 83.0% residues in most favored regions and only 1% in disallowed regions in the Ramachandran plot (data not shown). It showed β-barrel core at both N and C-terminal followed by extended α helix domain which is a characteristic feature of known globulins (Fig. A6, C).

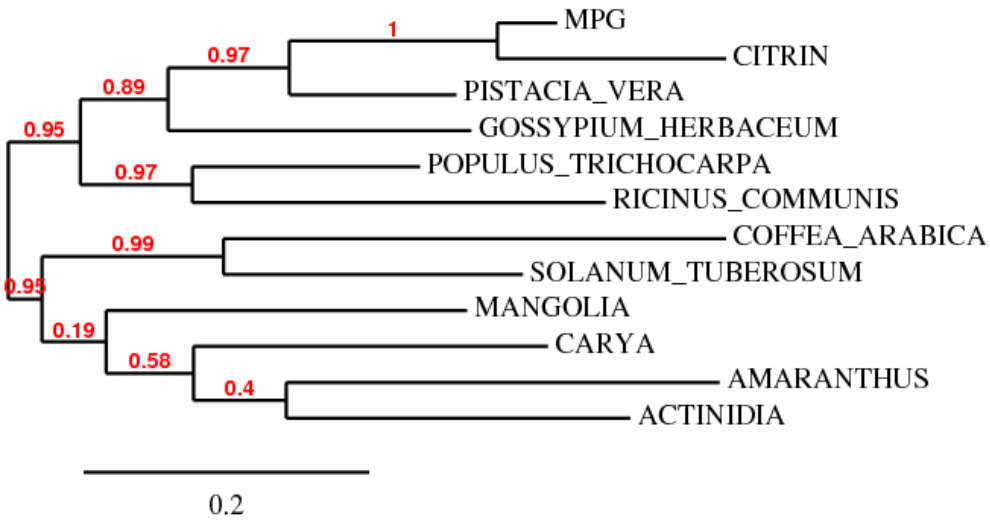

Figure. A6 Phylogenetic tree of MPG with some closly related 11S globulins constructed by Phylogeny.fr programme. Tree constructed by the maximum likelihood method dividing them into different groups. The numbers above and below the branch points indicate the confidence levels for the relationship of the paired sequences as determined by bootstrap statistical analysis.

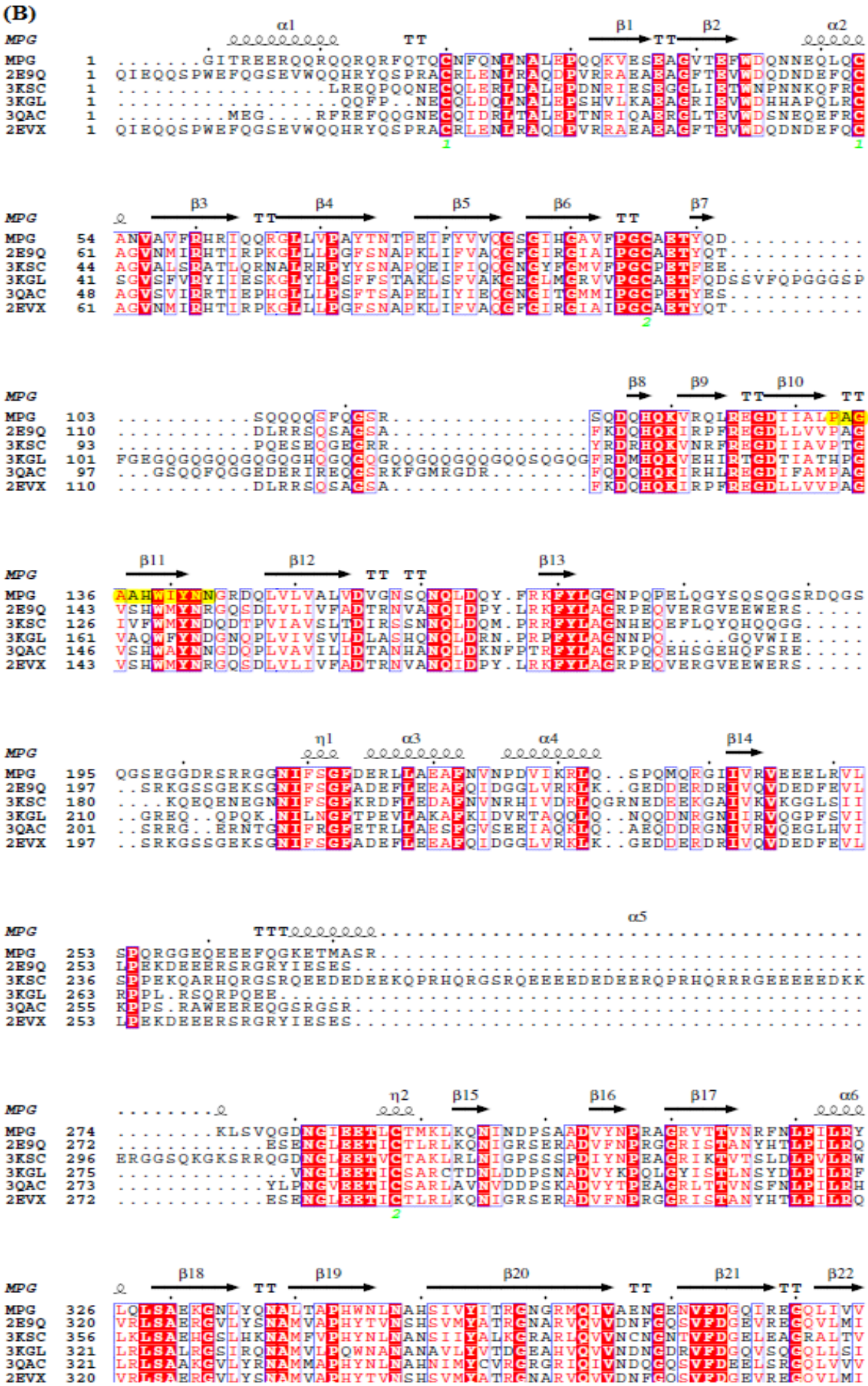
(B)
MPG
2E9Q
3KSC
3KGL
3QAC
2EVX

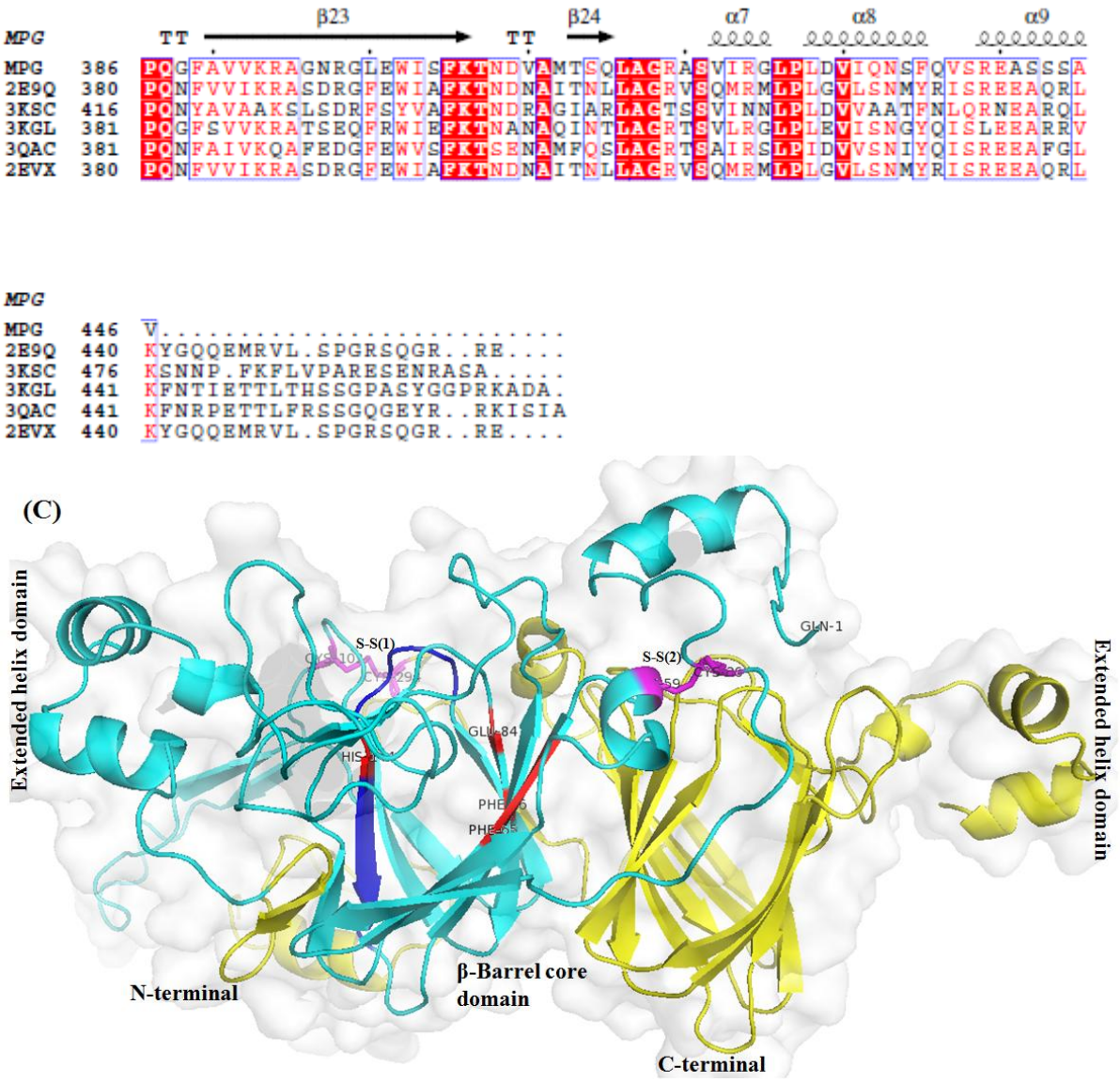

Figure A6. B) Multiple sequence alignment from Clustalw further improved in Espript server using know globulin structures 2E9Q (pro-11S pumpkin), 3KSC (*Pisum sativum L.*), 3KGL (*Brassica napus*), 3QAC (*Amaranthus hypochondriacus L.*) and 2EVX (pumpkin). Secondary structure was assigned according to the homology model of MPG. Conserved residues are highlighted in red. C) Predicted model having β-barrel core domain with extended alpha helix region with two disulphide bonds were observed in the model between C26-C59, C102-C294 (shown in magenta sticks).

MPG protein showed the characteristic cupin domain which has been modelled using Auxin Binding Protein1 (ABP1) from *Zea mays* (PDB id 1LR5) and found to have a metal binding site (Fig. A6, D). Histidine (H144) residue from characteristic motif P (X) 4H (X) 3N (where X is any amino acid) present on β strand of acidic subunit of the modelled structure coordinating with other four residues H67, E84, F86 and F65 on another β strands of N-terminal β-barrel core in a close proximity. It has been shown to have almost conserved residues involved in metal binding site to that of ABP1 protein (Fig. A7 A, B). Close to other

residues like A-78, Y-79, T-80, L-138, A-142 of the cupin motif region also involved in forming metal binding pocket as predicted from 3DLigandSite server [44] and shown to be putative metal binding protein (Fig. A6, E).

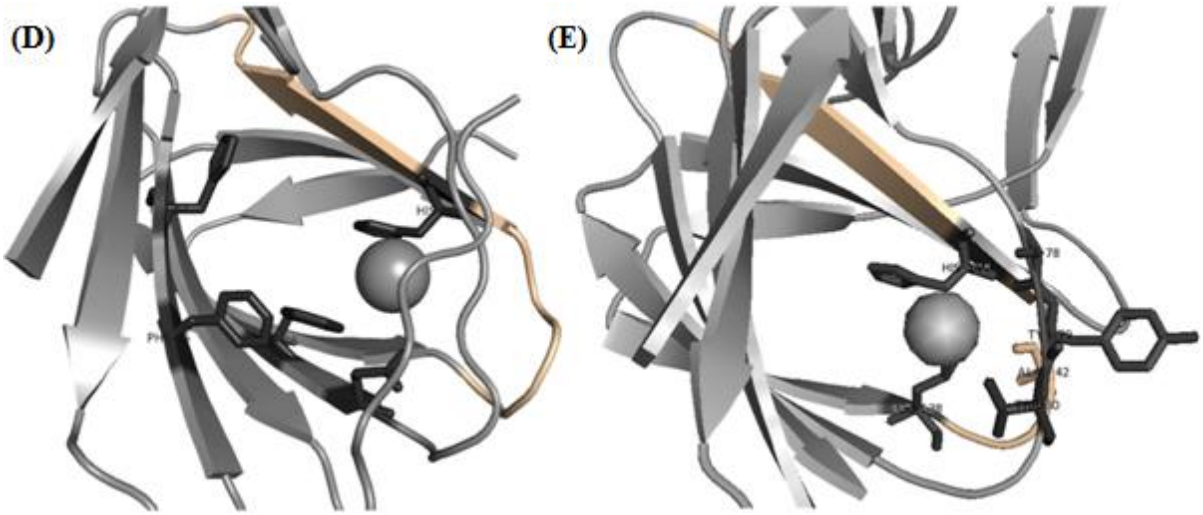

Figure A6. D) H144 of bi-cupin motif coordinating with other residues for metal binding pocket with some different residues highlighted on the basis of modelled ABP1 structure pdb id 1lr5. E) Conserved residue His-144 of cupin motif coordinating with other different residues, ALA-78, TYR-79, THR-80, LEU-138 and ALA-142 (cupin motif region) forming metal binding pocket on the basis of different known metal binding proteins, pdb ids 1Y3T, 2H0V, 2P17, 2PHD, 3BU7, 1H1M, 1H1I, 1JUH, 1GQG, 1GQH.

A

```
MPG             QIEQVTGITREERQQRQQRQRFQTQCNFQNLNALEPQQKVESEAGVTEFWDQNNEQLQCA 60
ABP1            ------SCVRDNSLVRDISQMPQSSYGIEGLSHITVAGALNHGMKEVEVWLQTIS--PGQ 52
                      . .*::   *:  *  *:. .::.*. :     ::     .*.* *. .

MPG             NVAVFRHRIQQRGLLVPAYTNTPEIFYVVQGSGIHGAVFPGCAETYQDSQQQQSFQGSRS 120
ABP1            RTPIHRH-------------SCEEVFTVLKG---KGTLLMGSSSLKYPGQPQE------- 89
                ...:.**             .  *:* *::*   :*::: *.:.    .* *:

MPG             QDQHQKVRQLREGDIIALPAGAAHWIYNNGRDQLVLVALVDVGNSQNQLDQYFRKFYLGG 180
ABP1            -------IPFFQNTTFSIPVNDPHQVWNSDE---------------------------- 113
                        : :.  :::*.. .* ::*...

MPG             NPQPELQGYSQSQGSRDQGSQGSEGGDRSRRGGNIFSGFDERLLAEAFNVNPDVIKRLQS 240
ABP1            ------------------------------------------------------------

MPG             PQMQRGIIVRVEEELRVLSPQRGGEQEEEFQGKETMASRKLSVQGDNGIEETLCTMKLKQ 300
ABP1            ----------HEDLQVL-------------------------------------------- 120
                          .*:*:**

MPG             NINDPSAADVYNPRAGRVTTVNRFNLPILRYLQLSAEKGNLYQNALTAPHWNLNAHSIVY 360
ABP1            ------------------------------------------------------VI 122
                                                                       *

MPG             ITRGNGRMQIVAENGENVFDGQIREGQLIVVPQGFAVVKRAGNRGLEWISFKTNDVAMTS 420
ABP1            ISRPPAKIFLYDDWS---------------MPHTAAVLK-------------------- 146
                *:*  .:: :  : .               :*:  **:*

MPG             QLAGRASVIRGLPLDVIQNSFQVSREASSSAV 452
ABP1            ----------FPFVWDEDCFEAAKEQL---- 163
                          :*:   ::.*:.::*
```

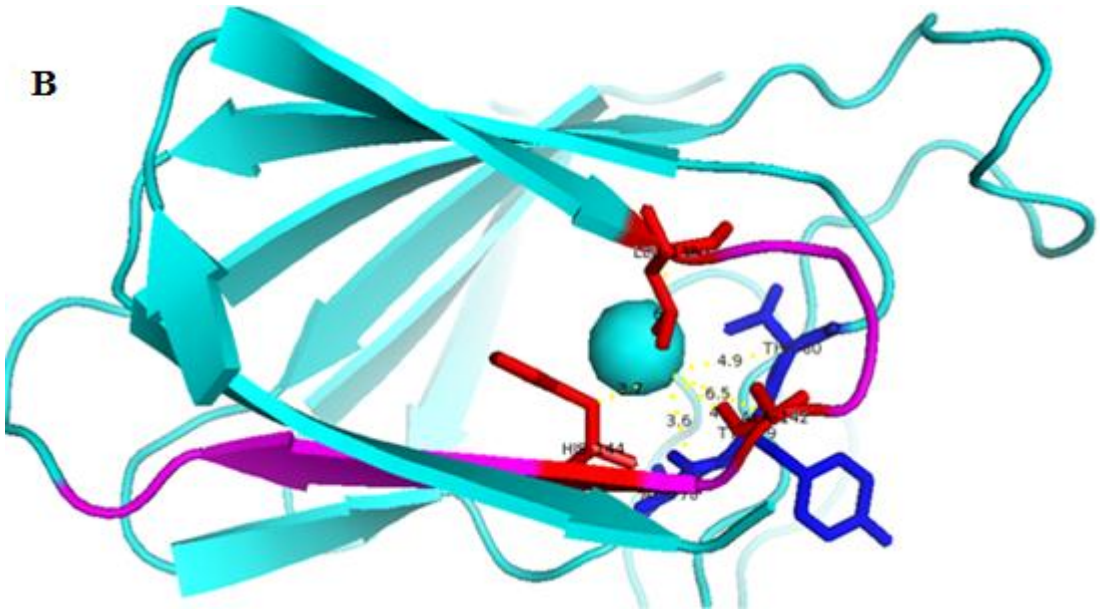

Figure A7. (A) Sequence alignment showed conserve residues involving in metal binding protein and underlined sequence is bi-cupin motif present in acidic subunit. (B) H144 of bi-cupin motif coordinating with other residues for metal binding pocket with some different residues highlighted in Red and Blue color on the basis of modelled ABP1 structure pdb id 1LR5 and alignment.

A4 Discussion

Murraya paniculata, a well known evergreen tropical plant grown mostly as hedge, has been shown to possess medicinal properties. In present study, we report purification, characterization and gene cloning of a globulin protein (MPG) with hemagglutination activity from *M. paniculata* seeds. The protein was purified in two steps by affinity and gel filtration chromatography. The heterodimeric nature of the protein was revealed on a reducing SDS-PAGE where two bands of ~35 and ~21 kDa were observed. Analysis of N-terminal and internal sequences of two polypeptides showed that the protein belongs to 11S globulin family. This was further confirmed after gene cloning and amino acid sequence analysis of MPG. The higher and lower molecular weight polypeptides were referred to as acidic (α) and basic (β) subunits respectively as in other 11S globulins isolated from oat [4], pea [5] and broad bean [47]. We have adopted the same nomenclature for MPG. The analysis of elution profile of MPG and standard molecular weight markers on gel filtration column revealed the oligomerization state of the protein. A major peak at an elution volume of 60 mL corresponded to be in range of ~150 kDa suggesting that three MPG heterodimers combine to form the trimeric native protein. The mature 11S globulin generally is hexameric but is initially assembled and transported through the secretory system as an intermediate trimer. Each subunit pair is synthesized as a precursor protein that is proteolytically cleaved after disulfide bond formation [16]. Although all attempts to separate and purify the subunits under native conditions failed, interestingly the ~35 kDa acidic subunit in heterodimer degrades after one week and complete degradation was observed in two weeks (data not shown) while basic ~21 kDa subunit remains stable. Therefore, all analysis was performed on a freshly purified MPG except for hemagglutination assay on basic subunit. The native and SDS-PAGE analysis of MPG in various conditions as described in 'Material and Methods' and 'Results' section demonstrated that the two are linked by inter-molecular disulfide bonds and strong secondary forces. The appearance of a major band at ~56 kDa in non-reducing conditions suggested that two subunits are linked through inter-molecular disulfide bonds. The amino acid sequence analysis and homology modelling of MPG confirmed the presence of one disulfide bond between two subunits. The predicted model of MPG shown to have seven cysteines out of which C26 and C59, C102 and C294 forming disulfide bonds in mature form of protein after cleavage of signal peptide (Fig. A8 A, B).

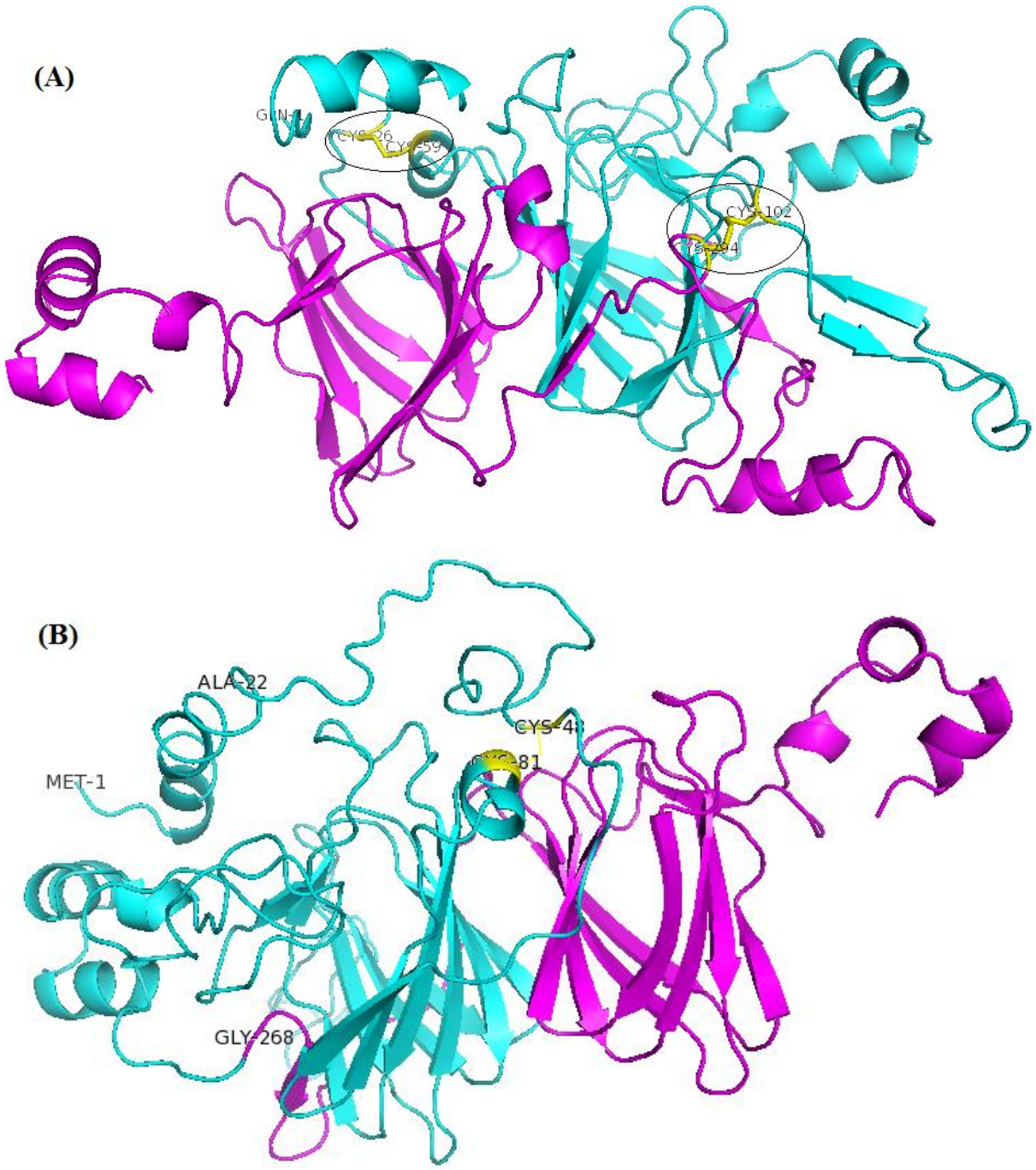

Figure A8. (A) From predicted model it has been showed that C26 and C59 within acidic subunit, C102 and C294 (between both subunit) participate in disulfide bridge formation in the processed protein after cleavage of signal peptide at residue GLN (Q) in mature protein. (B) Only one intra disulfide bond C48, C81 in case of precursor globulin protein.

Interestingly, the subunit bands at ~35 and ~21 kDa do not completely disappear on SDS-PAGE under non-reducing conditions. Likewise, the absence of SDS in sample buffer under reducing condition does not completely dissociate the two MPG subunits. A protein band at ~42 kDa was observed under non-reducing conditions in SDS-PAGE. This may be most probably due to either heterogeneity of subunits or self-association of 21 kDa subunits or

association of partially degraded 35 kDa and 21 kDa subunits. The native PAGE analysis of MPG showed similar results where the presence of both SDS and β-ME is required for subunit dissociation. There was some subunit dissociation was observed in presence of SDS alone in sample buffer but minimal effect was seen on heat-treated protein sample in presence of only β-ME. The two conclusions can be drawn from these results. One, the two subunits are held together not only by disulfide bond but some other noncovalent interactions also (hydrophobic interactions and salt bridges). These results were further validated through fluorescence studies (Fig A5 D) in presence of β-ME, where only minor alterations in conformation were observed. Two, could be due to the presence of heterogeneity of two chains in MPG. The heterogeneity has been reported for many globulins including buckwheat globulin which exists as a heterooligomer and is composed of a large number of polypeptides which might differ in molecular weight and relative concentrations [7]. The MPG and its basic subunit exhibited hemagglutination activity where lattice formation against erythrocytes was observed indicating its lectin like property. Other members of globulin family have shown the lectin like properties [10, 32]. The acidic subunit could not be tested for activity as the attempts to separate two subunits failed.

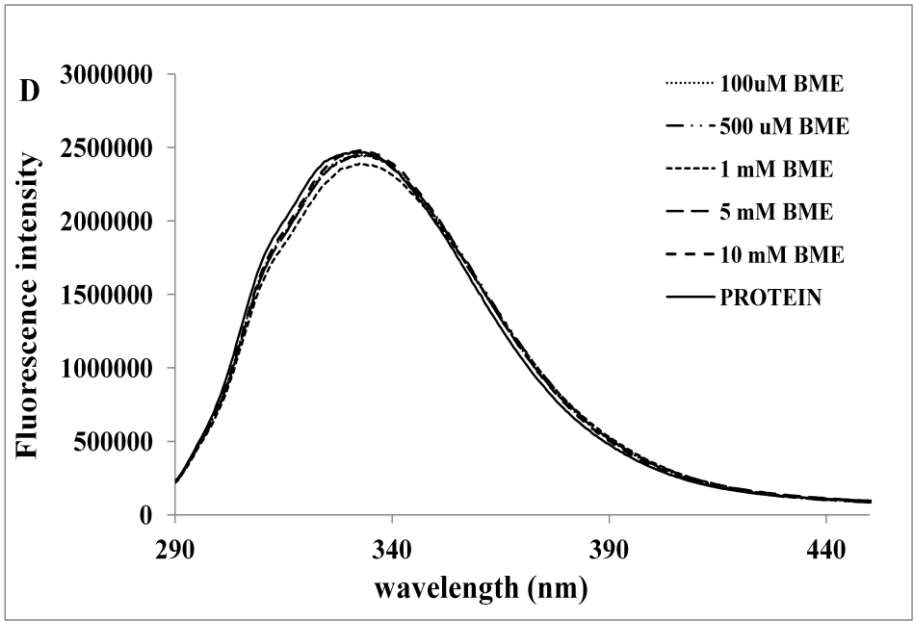

The CD analysis revealed that MPG protein is composed of both β-sheets and α- helices which is similar to the reported 11S globulin proteins [8, 50]. The predicted model of MPG demonstrated β-barrel core at both N and C-terminal followed by extended α helix domain which is a characteristic feature of known globulins. Although the MPG exhibited conformational stability over a broad range of pH and temperature, subtle conformational changes were observed at higher temperatures and pH. The CD spectra of MPG revealed a

predominance of α helical structure (31 %) as compared to β sheets (25 %) at higher pH (Fig. A4, B).

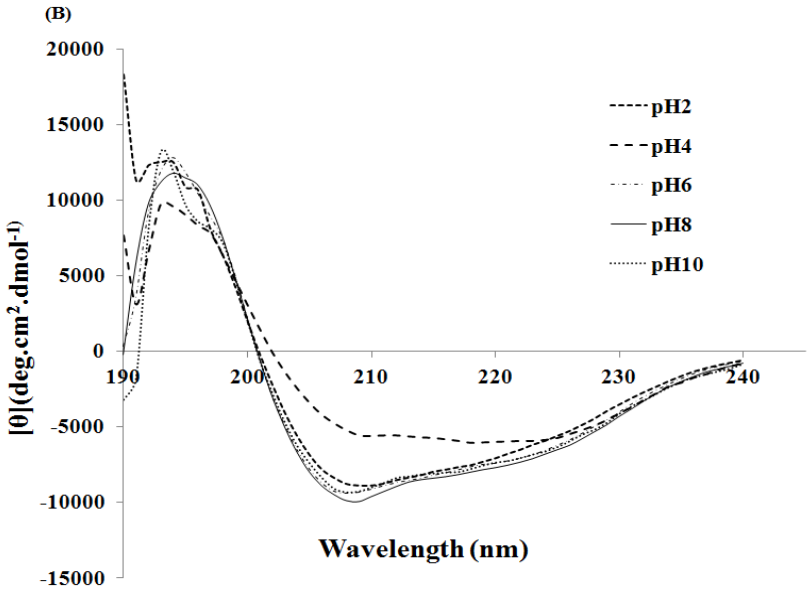

Tryptophan, among other aromatic amino acids, is quite sensitive to the change of the local environment and roughly acts as an indicator that correlate the extent of solvent exposure to the chromospheres [6]. With λmax 330 nm, MPG Fluorescence emission spectra is a characteristic emission profile of tryptophan residues in a relatively hydrophobic environment indicating that MPG is natively folded as observed earlier [12].

In case of βME, there were minor alterations in the microenvironments of tryptophan residues. It appears that although *β*ME treatment may potentially break disulfide bonds in 11S, overall conformational structure of 11S is not significantly altered because of involvement of noncovalent interactions (hydrophobic interactions and salt bridges) in stabilizing the protein.

While at lower SDS concentration, spectra showed decreasing fluorescence intensity and a shift reflecting gradual unfolding of this protein with SDS. Similar results for 11S globulin from Amaranthus globulin in presence of SDS have been reported denaturation achieved at low concentrations of SDS [18]. In the presence of denaturants there was a significant increase in tryptophan solvent accessibility and additional randomization of the tertiary structure. Instead, even at lower concentration of urea, an abrupt but significant increase in fluorescence intensity at λ_{max} was observed, could be due to the existence of folding intermediate(s) of 11S. Clearly, more studies are needed to determine the biochemical nature of these intermediates.

The mascot search (http://www.matrixscience.com/server.html) against the obtained internal sequence results (Fig. A2 A,B) showed similarity to plant globulin citrin from *Citrus Sinensis*

suggesting that the protein may belong to 11S globulin family. A partial gene of MPG was cloned on the basis of sequence similarity of internal sequences with the citrin. Phylogentic and amino acid sequence analysis confirmed that MPG is more closely related to citrin 11S globulin from *Citrus sinensis cultivar valencia* which also belong to the *Rutaceae* family. The bioinformatic analysis demonstrated that MPG possesses a conserved bicupin motif, a characteristic feature of 11S seed storage globulins. The predicted model analysis also points to a putative metal binding site in MPG. As it has been earlier, stated that MPG protein belongs to CITRIN family which is a solute carrier family 25, member 13 (citrin) [24]. Thus analysis indicated that MPG could be a solute carrier protein. It has been well documented that cupin fold is associated with several functions beside a marker for seed storage globulins.

A5 CONCLUSIONS

In conclusions, an 11S globulin was purified, characterized and cloned from *M. paniculata* seeds. The 11S MPG protein exists as a trimer with a molecular weight of ~150 kDa composed of heterodimers of 56 kDa. Secondary structure analysis revealed that the MPG is a β/α protein and retains conformation stability at a broad range of pH and temperature. Fluorescence studies revealed conformational changes at lower concentrations of denaturants and pH. MPG and its basic subunit exhibited hemagglutination activity that may transmit the unique ability to be acting as a lectin like protein. Phylogentic and amino acid sequence analysis confirmed that MPG is more closely related to citrin 11S globulin from *Citrus sinensis cultivar valencia* which also belong to the *Rutaceae* family. This paper presents evidence on the conservation of characteristic fold within the cupin superfamily, with a focus on the signification of the active- site ligands in the possible use of these proteins. Here along the basis of superimposing on ABP1 crystal structure and known iron and copper binding proteins from some other organism, we are proposing that beside a storage protein, it might have some ligand binding site. Further conclusion can be reached only from the crystal structure of the mature protein.

A6 References

1. Albillos, S. M., Menhart, N. and Fu, T.-J. Structural stability of amandin, a major allergen from almond (prunus dulcis), and its acidic and basic polypeptides. *Journal of agricultural and food chemistry* 57(11):4698-4705 (2009).

2. Beyer, K., Grishina, G., Bardina, L., Grishin, A. and Sampson, H. A. Identification of an 11s globulin as a major hazelnut food allergen in hazelnut-induced systemic reactions. *Journal of Allergy and Clinical Immunology* 110(3):517-523 (2002).

3. Bradford, M. M. A rapid and sensitive method for the quantitation of microgram quantities of protein utilizing the principle of protein-dye binding. *Analytical biochemistry* 72(1):248-254 (1976).

4. Brinegar, A. C. and Peterson, D. M. Separation and characterization of oat globulin polypeptides. *Archives of biochemistry and biophysics* 219(1):71-79 (1982).

5. Casey, R. Genetic variability in the structure of the α subunits of legumin from pisum-a two-dimensional gel electrophoresis study. *Heredity* 43(2):265-272 (1979).

6. Chen, J., Liu, B., Ji, N., Zhou, J., Bian, H.-j., Li, C.-y., Chen, F. and Bao, J.-k. A novel sialic acid-specific lectin from phaseolus coccineus seeds with potent antineoplastic and antifungal activities. *Phytomedicine* 16(4):352-360 (2009).

7. Choi, S.-M. and Ma, C.-Y. Extraction, purification and characterization of globulin from common buckwheat (fagopyrum esculentum moench) seeds. *Food research international* 39(9):974-981 (2006).

8. Clara Sze, K. W., Kshirsagar, H. H., Venkatachalam, M. and Sathe, S. K. A circular dichroism and fluorescence spectrometric assessment of effects of selected chemical denaturants on soybean (glycine max l.) storage proteins glycinin (11s) and β-conglycinin (7s). *J of Agricultural and Food Chemistry* 55(21):8745-8753 (2007).

9. Coelho, M. B., Macedo, M. L. R., Marangoni, S., Silva, D. S. d., Cesarino, I. and Mazzafera, P. Purification of legumin-like proteins from coffea arabica and coffea racemosa seeds and their insecticidal properties toward cowpea weevil (callosobruchus maculatus)(coleoptera: Bruchidae). *Journal of agricultural and food chemistry* 58(5):3050-3055 (2010).

10. Da Silva, C., Goes, A. and De Azevedo, R. Isolation and partial characterization of a lectin from bauhinia pentandra (bong) vog. *Ex Steua* 13(3):262-269 (2001).

11. Dereeper, A., Guignon, V., Blanc, G., Audic, S. p., Buffet, S., Chevenet, F. o., Dufayard, J. F., Guindon, S. p., Lefort, V. and Lescot, M. Phylogeny. Fr: Robust phylogenetic analysis for the non-specialist. *Nucleic acids research* 36(suppl 2):W465-W469 (2008).

12. Dufour, E., Hoa, G. H. B. and Haertle, T. High-pressure effects on β lactoglobulin interactions with ligands studied by fluorescence. *Biochimica et Biophysica Acta (BBA)-Protein Structure and Molecular Enzymology* 1206(2):166-172 (1994).

13. Dunwell, J. M. Cupins: A new superfamily of functionally diverse proteins that include germins and plant storage proteins. *Biotechnology and Genetic Engineering Reviews* 15(1):1-32 (1998).

14. Dunwell, J. M., Culham, A., Carter, C. E., Sosa-Aguirre, C. R. and Goodenough, P. W. Evolution of functional diversity in the cupin superfamily. *Trends in biochemical sciences* 26(12):740-746 (2001).

15. Dunwell, J. M., Khuri, S. and Gane, P. J. Microbial relatives of the seed storage proteins of higher plants: Conservation of structure and diversification of function during evolution of the cupin superfamily. *Microbiology and Molecular Biology Reviews* 64(1):153-179 (2000).

16. Gatehouse, J. A., Croy, R. R. D., Boulter, D. and Shewry, P. R. The synthesis and structure of pea storage proteins. *Critical Reviews in Plant Sciences* 1(4):287-314 (1984).

17. Gautam, M. K., Gangwar, M., Singh, A., Rao, C. V. and Goel, R. K. Invitro antioxidant properties of murraya paniculata (l.) leaves extract. *Inventi Rapid: Ethnopharmacology* (2012).

18. Gorinstein, S., Zemser, M. and Paredes-Lopez, O. Structural stability of globulins. *Journal of Agricultural and Food Chemistry* 44(1):100-105 (1996).

19. Hung, T.-H., Wu, M.-L. and Su, H.-J. Identification of the chinese box orange (severinia buxifolia) as an alternative host of the bacterium causing citrus huanglongbing. *European Journal of Plant Pathology* 107(2):183-189 (2001).

20. Islam, Z., Kumar, A., Singh, S., Salmon, L. and Karthikeyan, S. Structural basis for competitive inhibition of 3, 4-dihydroxy-2-butanone-4-phosphate synthase from vibrio cholerae. *Journal of Biological Chemistry* 290(18):11293-11308 (2015).

21. Jin, T., Albillos, S. M., Guo, F., Howard, A., Fu, T.-J., Kothary, M. H. and Zhang, Y.-Z. Crystal structure of prunin-1, a major component of the almond (prunus dulcis) allergen amandin. *Journal of agricultural and food chemistry* 57(18):8643-8651 (2009).

22. Kelley, L. A. and Sternberg, M. J. E. Protein structure prediction on the web: A case study using the phyre server. *Nature protocols* 4(3):363-371 (2009).

23. Ko, T. P., Day, J. and McPherson, A. The refined structure of canavalin from jack bean in two crystal forms at 2.1 and 2.0 Å resolution. *Acta Crystallographica Section D: Biological Crystallography* 56(4):411-420 (2000).

24. Kobayashi, K., Sinasac, D. S., Iijima, M., Boright, A. P., Begum, L., Lee, J. R., Yasuda, T., Ikeda, S., Hirano, R. and Terazono, H. The gene mutated in adult-onset type ii citrullinaemia encodes a putative mitochondrial carrier protein. *Nature genetics* 22(2):159-163 (1999).

25. Komatsu, S. and Hirano, H. Plant basic 7 s globulin-like proteins have insulin and insulin-like growth factor binding activity. *FEBS letters* 294(3):210-212 (1991).

26. Laemmli, U. K. Cleavage of structural proteins during the assembly of the head of bacteriophage t4. *Nature* 227(5259):680-685 (1970).

27. Langston-Unkefer, P. J. and Gade, W. A seed storage protein with possible self-affinity through lectin-like binding. *Plant physiology* 74(3):675-680 (1984).

28. Lawrence, M. C., Izard, T., Beuchat, M., Blagrove, R. J. and Colman, P. M. Structure of phaseolin at 2.2 Å resolution: Implications for a common vicilin/legumin structure and the

genetic engineering of seed storage proteins. *Journal of molecular biology* 238(5):748-776 (1994).

29. Marcus, J. P., Green, J. L., Goulter, K. C. and Manners, J. M. A family of antimicrobial peptides is produced by processing of a 7s globulin protein in macadamia integrifolia kernels. *The Plant Journal* 19(6):699-710 (1999).

30. Marraccini, P., Deshayes, A., Petiard, V. and Rogers, W. J. Molecular cloning of the complete 11s seed storage protein gene of coffea arabica and promoter analysis in transgenic tobacco plants. *Plant Physiology and Biochemistry* 37(4):273-282 (1999).

31. Matsuura, J. E. and Manning, M. C. Heat-induced gel formation of. Beta.-lactoglobulin: A study on the secondary and tertiary structure as followed by circular dichroism spectroscopy. *Journal of Agricultural and Food Chemistry* 42(8):1650-1656 (1994).

32. Moreira, R. D. A. and Perrone, J. o. C. Purification and partial characterization of a lectin from phaseolus vulgaris. *Plant Physiology* 59(5):783-787 (1977).

33. Moura, F. T., Oliveira, A. S., Macedo, L. L. P., Vianna, A. L. B. R., Andrade, L. B. S., Martins-Miranda, A. S., Oliveira, J. T. A., Santos, E. A. and de Sales, M. P. Effects of a chitin-binding vicilin from enterolobium contortisiliquum seeds on bean bruchid pests (callosobruchus maculatus and zabrotes subfasciatus) and phytopathogenic fungi (fusarium solani and colletrichum lindemuntianum). *Journal of agricultural and food chemistry* 55(2):260-266 (2007).

34. Osborne, T. B. The vegetable proteins: Longmans, Green and Company (1916).

35. Pieper, U., Eswar, N., Davis, F. P., Braberg, H., Madhusudhan, M. S., Rossi, A., Marti-Renom, M., Karchin, R., Webb, B. M. and Eramian, D. Modbase: A database of annotated comparative protein structure models and associated resources. *Nucleic acids research* 34(suppl 1):D291-D295 (2006).

36. Rahman, M. A., Hasanuzzaman, M., Uddin, N. and Shahid, I. Z. Antidiarrhoeal and anti-inflammatory activities of murraya paniculata (l.) jack. *Pharmacologyonline* (3):768-776 (2010).

37. Robert, X. and Gouet, P. Deciphering key features in protein structures with the new endscript server. *Nucleic acids research* 42(W1):W320-W324 (2014).

38. Sharker, S. M., Shahid, I. J. and Hasanuzzaman, M. Antinociceptive and bioactivity of leaves of murraya paniculata (l.) jack, rutaceae. *Revista Brasileira de Farmacognosia* 19(3):746-748 (2009).

39. Shotwell, M. A. and Larkins, B. A. The biochemistry and molecular biology of seed storage proteins. *The Biochemistry of plants: a comprehensive treatise (USA)* (1989).

40. Tandang-Silvas, M. R., Cabanos, C. S., Pena, L. D. C., De La Rosa, A. P. B., Osuna-Castro, J. A., Utsumi, S., Mikami, B. and Maruyama, N. Crystal structure of a major seed storage protein, 11s proglobulin, from amaranthus hypochondriacus: Insight into its physico-chemical properties. *Food chemistry* 135(2):819-826 (2012).

41. Templeman, T. S., DeMaggio, A. E. and Stetler, D. A. Biochemistry of fern spore germination: Globulin storage proteins in matteuccia struthiopteris l. *Plant physiology* 85(2):343-349 (1987).

42. Upadhyay, S. K., Mishra, M., Singh, H., Ranjan, A., Chandrashekar, K., Verma, P. C., Singh, P. K. and Tuli, R. Interaction of allium sativum leaf agglutinin with midgut brush border membrane vesicles proteins and its stability in helicoverpa armigera. *Proteomics* 10(24):4431-4440 (2010).

43. Walter, A. J., Hall, D. G. and Duan, Y. P. Low incidence of'candidatus liberibacter asiaticus' in murraya paniculata and associated diaphorina citri. *Plant Disease* 96(6):827-832 (2012).

44. Wass, M. N., Kelley, L. A. and Sternberg, M. J. E. 3dligandsite: Predicting ligand-binding sites using similar structures. *Nucleic acids research*:gkq406 (2010).

45. Whitmore, L. and Wallace, B. A. Dichroweb, an online server for protein secondary structure analyses from circular dichroism spectroscopic data. *Nucleic acids research* 32(suppl 2):W668-W673 (2004).

46. Woo, E.-J., Dunwell, J. M., Goodenough, P. W., Marvier, A. C. and Pickersgill, R. W. Germin is a manganese containing homohexamer with oxalate oxidase and superoxide dismutase activities. *Nature Structural & Molecular Biology* 7(11):1036-1040 (2000).

47. Wright, D. J. and Boulter, D. Purification and subunit structure of legumin of vicia faba l.(broad bean). *Biochem J* 141:413-418 (1974).

48. Zemser, M., Friedman, M., Katzhendler, J., Greene, L. L., Minsky, A. and Gorinstein, S. Relationship between functional properties and structure of ovalbumin. *Journal of protein chemistry* 13(2):261-274 (1994).

49. Zhang, M., Guo, Y., Powell, C. A., Doud, M. S., Yang, C. and Duan, Y. Effective antibiotics against candidatus liberibacter asiaticus in hlb-affected citrus plants identified via the graft-based evaluation. *Plos One* 9(11):e111032 (2014).

50. Zirwer, D., Gast, K., Welfle, H., Schlesier, B. and Schwenke, K. D. Secondary structure of globulins from plant seeds: A re-evaluation from circular dichroism measurements. *International Journal of Biological Macromolecules* 7(2):105-108 (1985).